Encapsulated Metal Ions: Mononuclear and Binuclear Complexes of Schiff-Base Macrocycles and Cryptands

Thesis

"ENCAPSULATED METAL IONS: MONONUCLEAR AND BINUCLEAR COMPLEXES OF SCHIFF-BASE MACROCYCLES AND CRYPTANDS."

A Thesis Submitted for the Degree

of

Doctor of Philosophy

by

Mary Josephine Hunter, B.A.

Faculty of Science

The Open University, Milton Keynes.

December 1990

Date of submission: 7 January 1991

Date of award: 8 March 1991

ProQuest LLC.
789 East Eisenhower Parkway
P.O. Box 1346
Ann Arbor, MI 48106 – 1346

DECLARATION

The work described in this thesis was carried out in the Department of Chemistry, The Queen's University of Belfast, on behalf of the Open University, Milton Keynes, between November 1987 and November 1990. The work has not been submitted for any other degree and is the original work of the author, except where acknowledged by reference.

M. J. Hunter.

December 1990.

ACKNOWLEDGEMENTS

I would like to thank my supervisor Dr. Jane Nelson for her enthusiasm and encouragement throughout the last three years. I am indebted to Dr. Vickie Mc Kee, Dr. M.G.B.Drew and Dr. J. Malone for the X-ray structural analyses on complexes prepared during the course of this work. I would also like to thank Dr. Charlie Harding for guidance on the use of the faraday balance and Dr. Malachy Mc Cann for carrying out the electrochemical studies.

My thanks are due to the Queen's University of Belfast for the use of the facilities in the Department of Chemistry where this research was carried out. In particular, I thank the analytical services for elemental analyses.

The award of a higher degrees studentship by the Open University is gratefully acknowledged.

CONTENTS

CHAPTER 5 - RESULTS AND DISCUSSION 3Bp R3Bp 3Bm R3Bm

ABSTRACT

Schiff-base condensation of 2,6-diacetylpyridine with diamines on Pb(II) afforded complexes of binucleating [2+2] macrocyclic ligands P (1) and MC (2). The complexes were isolated as the dilead macrocyclic tetrathiocyanate. Interest derives from the unusual binding mode of thiocyanate as a single atom 'N-only' bridge between the pair of lead ions bound by the macrocycle. An X-ray crystallographic structure determination, carried out by Dr. V.McKee, on the dilead MC complex demonstrates the existence of a single thiocyanate 'N-only' bridge between the lead ions. The N-only bridging mode of thiocyanate is retained in derivatives containing two or three triflate anions.

Transmetallation of the P complex, $Pb_2P(NCS)_4$ with transition metal triflates gave homobinuclear products with M = Cu(II), Co(II) and heterobinuclear Pb/M products with M = Mn(II), Fe(II), Ni(II), whereas transmetallation of the dilead MC complex afforded homobinuclear Cu(II) and Ni(II) complexes and heterobinuclear complexes with M = Mn(II) and Fe(II). Infrared spectra suggest that the 'N-only' bridging mode of thiocyanate exists between the metal ions in the heterobinuclear MnPbMC and FePbMC complexes and X-ray structural confirmation has been obtained for the manganese/lead MC complex. There was evidence of the existence of heterobinuclear FeCuP and FeCuMC complexes which were formed by metal exchange of the lead ion, in the respective FePb macrocyclic complex, for Cu(I).

The cryptand GT, (3) was formed by Schiff-base condensation of the tripod amine $N(CH_2CH_2NH_2)_3$ with glyoxal, using group (11) metal ions as template. A wide range of metal ion GT cryptates were obtained by transmetallation, including transition metal ion, lanthanide ion and

group(1) metal ion cryptates. An X-ray crystal structure of the cobalt(II) GT cryptate has been obtained. Generally the cryptates are mononuclear with respect to the metal ion, an exception being the binuclear copper(I) cryptate. Transmetallation with copper(II) produces either the mononuclear or the dinuclear cryptate depending on conditions employed. The binuclear copper(II) cryptate has a particularly unusual 7-line esr spectrum which suggests formation of a mixed valence Cu(II)/Cu(I) species. Cyclic voltammetry has shown strong stabilisation of the Cu(I) state, with $E_{1/2}$ for the reduction lying in the range found for blue copper proteins.

Synthecic of transition metal ion complexes by transmetallation of disilver or dilead 3Bp (4), or metal ion insertion into the 3Bp ligand was investigated. Dicobalt(II) and dicopper (I) cryptates of 3Bp were obtained. The corresponding reduced metal-free cryptand, R3Bp (5), gave an interesting series of binuclear complexes of Ni(II), Cu(I), Cu(II) and Co(II). The dicopper(II) and dicobalt(II) cryptates are of particular interest due to the presence of a hydroxo bridge between the metal ions. Attempted insertion of Mn(II) into R3Bp failed but gave the tetraprotonated R3Bp triflate whose structure was crystallographically determined.

Attempts to insert metal ions into cryptand 3Bm (6) failed. However insertion of Ni(II) gave ring opening and a pendant arm macrocyclic complex was obtained. The reduced metal-free ligand, R3Bm (7) produced a wider range of complexes, including the dinickel(II), dicopper(II) and dicobalt(II) cryptates.

Transition metal complexes throughout, have been characterised using infrared, electronic, and e.s.r. spectroscopy. Magnetic susceptibility measurements and n.m.r. were employed where appropriate. The work

described in Chapters 2, 3, 4 and 5 is preceeded by a review of the relevant literature, in Chapter 1.

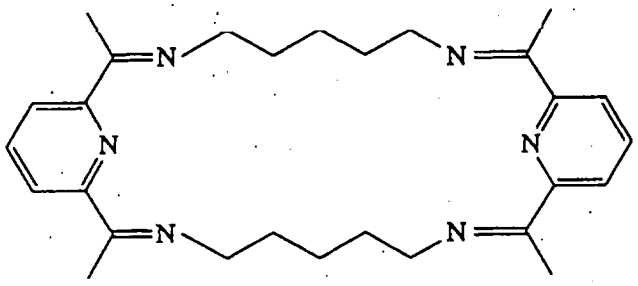

The macrocycle "P" (1)

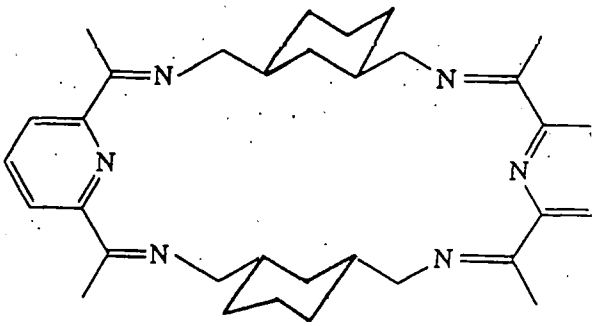

The macrocycle "MC" (2)

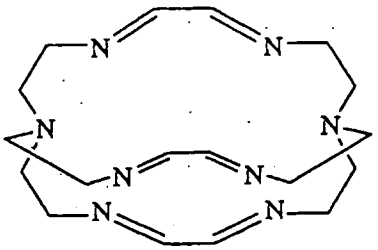

The cryptand "GT" (3)

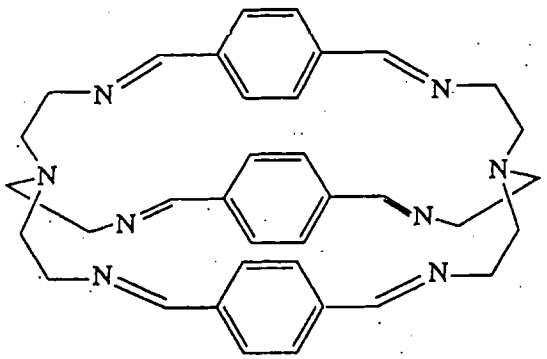

The cryptand "3Bp" (4)

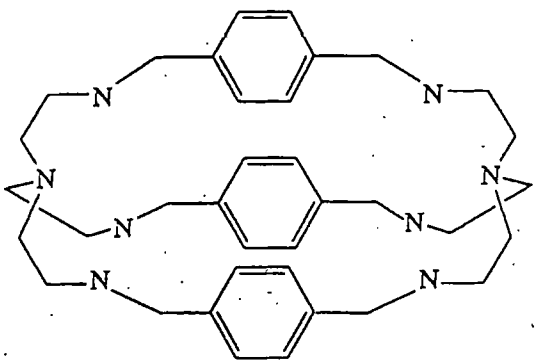

The cryptand "R3Bp" (5)

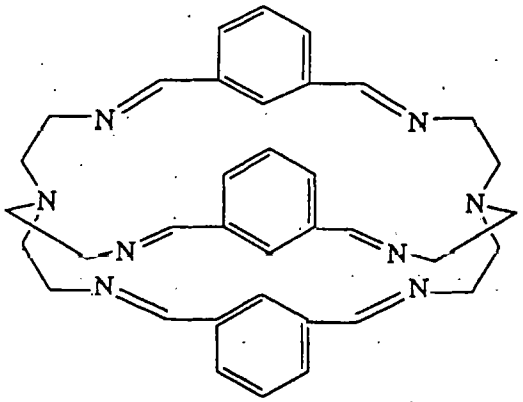

The cryptand "3Bm" (6)

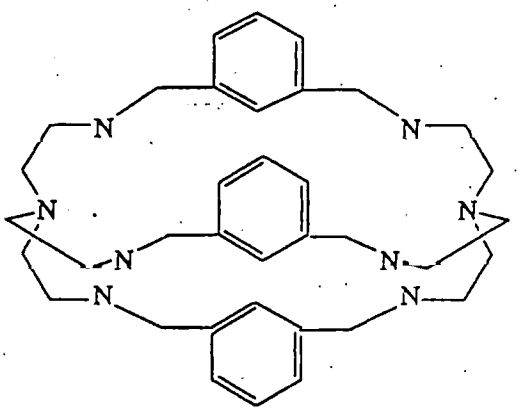

The cryptand "R3Bm" (7)

CHAPTER 1

INTRODUCTION

Over the last two decades there has been a growing awareness of the importance of metal ion complexes of macrocycles or cryptands as models or mimics of biological molecules such as enzymes. Recognition of possible commercial applications of macrocyclic and cryptate complexes as catalysts, or the application of the free ligands as metal sequestration agents for example has led to increasing interest in the area. In addition, various new potential uses in areas such as radionuclide transportation, luminescence labelling or magnetic resonance imaging have been the driving force behind some of the recent research in the field.

The aim of this review is an investigation of macrocycles and cryptands which are capable of binding one or more metal ions.

For the purposes of this review a macrocycle is defined as a cyclic compound which has nine or more members including three or more heteroatoms.[1] A cryptand is defined as a macrocyclic compound that contains at least one additional link. Commonly these are described as macrobicycles, macrotricycles and so on. A short section on anion binding within cryptands is also included.

Emphasis is placed on nitrogen donor ligands, on the preparative route to the metal complexes and on their physicochemical properties and structure. Throughout the discussion the complexes are numbered consecutively and if referred to by name, trivial names used by the original author are used. A brief history of the area is outlined, followed by sections on the synthesis of macrocycles, cryptands and their complexes. Binuclear transition metal complexes of Schiff-base macrocycles and cryptands and mono-metal ion cryptates are emphasised.

Background material considered fundamental to much of the work mentioned is included.

A BRIEF HISTORY

Coordination compounds containing macrocyclic ligands have been around since life began, and include complexes on which all life depends, chlorophyll and haem-protein provide pertinent examples. However, the study of macrocyclic complexes did not begin until around the beginning of this century. Porphyrins, corrins and phthalocyanines have been studied because of their resemblance to naturally occurring macrocyclic complexes such as chlorophyll or haem, or because of their potential as dyestuffs.

Only a few scattered reports of new synthetic macrocyclic ligands and their complexes appeared before 1960.[2-6] However, in the early 1960s various macrocyclic complexes were reported.

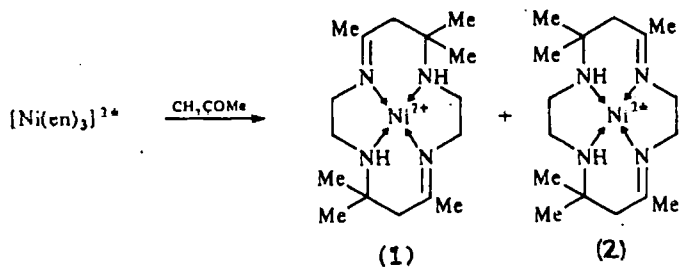

(1) (2)

Scheme 1

Curtis demonstrated the potential of the metal ion in formation of the isomeric macrocyclic products (1) and (2) , which were produced by reaction of tris-ethylene diamine nickel(II) perchlorate and acetone.[7] However the first deliberate synthesis of a metal ion complex of a new synthetic macrocyclic ligand (3) was reported by Thompson and Busch. [8]

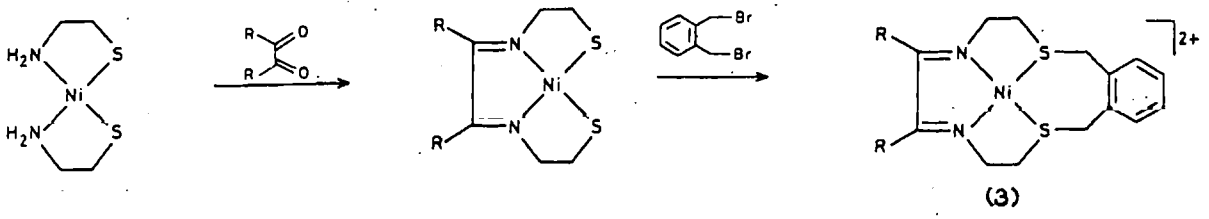

(3)

Scheme 2

The cyclic polyether or "crown" macrocycles (4) were introduced by Pederson in 1967.[9] These displayed moderate selectivity among group I and group II metal ions[10] and were capable of binding small non-metallic ions or molecules, however their ability to bind transition metal ions was limited.[11]

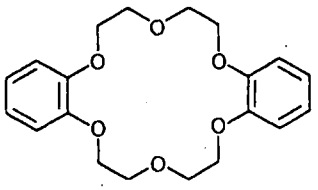

(4)

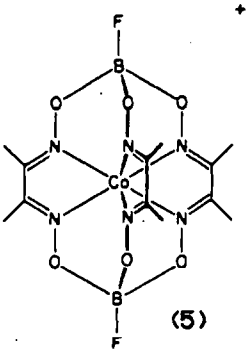

(5)

The extension from macrocycles to macrobicycles and into the 'third dimension' was initiated in 1968, with the reported synthesis of a clathrochelate (5) which contains α-diimine donor groups.[12] The term "clathrochelate" was introduced by Busch to mean an encapsulated metal ion complex.[13] In 1969 Lehn introduced the bicyclic polyether cryptands (6), containing tripod bridgehead nitrogen atoms that link polyether strands.[14]

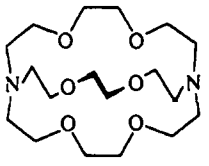

(6)

The cryptands were named by giving the number of oxygen atoms in each of the three strands linking the bridgehead nitrogen atoms, thus cryptand (6) was named 2.2.2.

Macrocyclic ligands have become increasingly topologically diverse and many subdivisions in the area now exist. Several classes of macrocycles are not reviewed here, these include polyphospha- and polyarsa-macrocycles, vaulted cyclidenes, cyclodextrins and porphyrins. Polyether macrocycles have been extensively reviewed elsewhere [15,16,17] and only some of the more relevant examples are included. Important contributions have been made by Stoddart's group. Space does not permit a description of this interesting work.

SYNTHESIS

The synthetic routes leading to macrocycles or cryptands fall into two main categories.

(1) Direct synthesis of the ligand by traditional organic methods.

(2) Template synthesis involving cyclisation in the presence of a metal ion - the *in situ* approach.

New macrocycles have also been obtained by modification of a previously synthesised parent macrocycle.

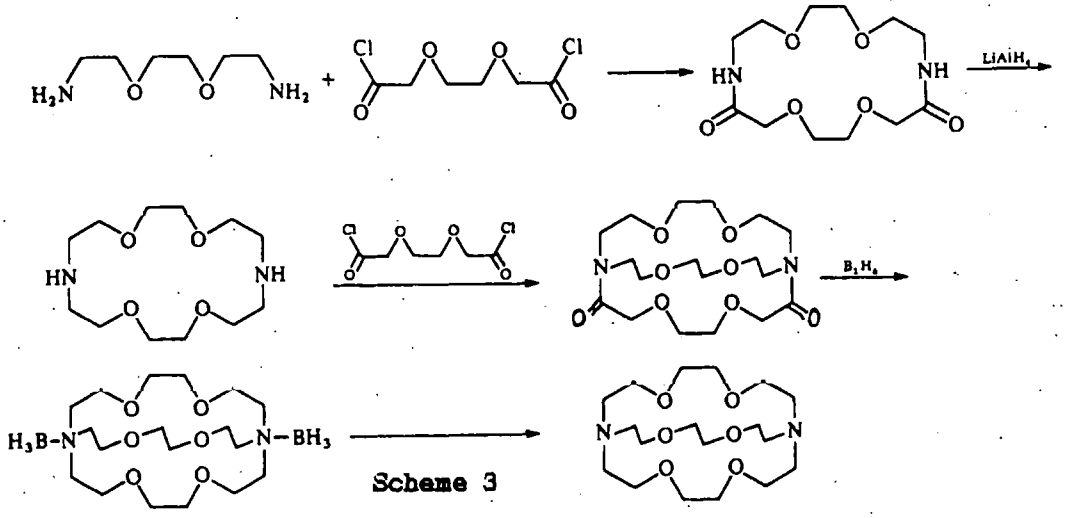

Scheme 3

Synthesis of macrocycles or cryptands by traditional organic methods often involves multistep syntheses such as that shown in scheme 3.[18] The yield of the desired product is sometimes low due to competing intermolecular polymerisation reactions. In order to circumvent this problem, steps involving ring closure are often carried out under conditions of high dilution thus encouraging intramolecular reaction which gives the macrocycle.[19-22] Examples of macrocycles and cryptands formed in this way are shown in figure 1.

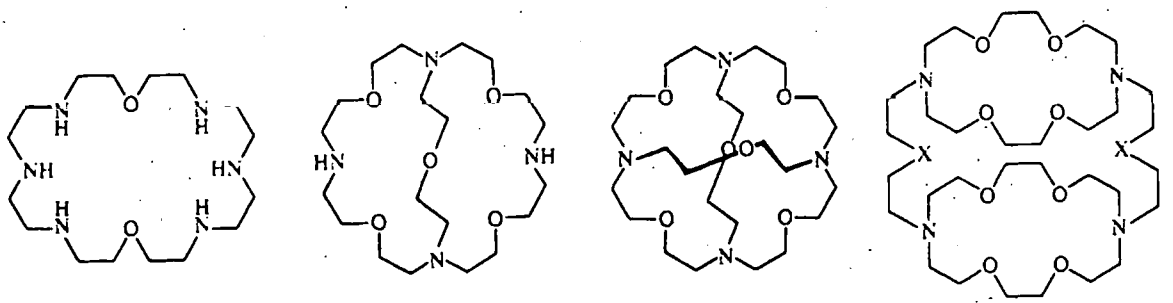

(7) (8) (9) (10)

Figure 1

However direct synthesis of a cryptand or macrocycle need not necessarily involve a multistep reaction employing conditions of high dilution.[23,24] Rigid groups may be incorporated into the reactants, both minimising unfavourable entropy effects on ring formation and fixing reactive sites in a favourable orientation for reaction.

The advantage of direct synthesis is the ease of purification and characterisation of the product. In addition, spectra of the ligand are available for comparison with those of the complex. Alternatively metal template syntheses offer high-yielding and selective routes to macrocyclic or macrobicyclic ligands and their complexes,[25,26] and can provide products that are not accessible by an alternative route. The *in situ* syntheses are commonly convenient one pot reactions resulting in formation

of a metal ion complex of the macrocycle or cryptand. The synthesis of macropolycyclic ligands requires consideration of synthetic strategies for the construction of the macrocyclic framework. The routes to macrobicyclic ligands have been categorised[27] and are represented schematically in figure 2.

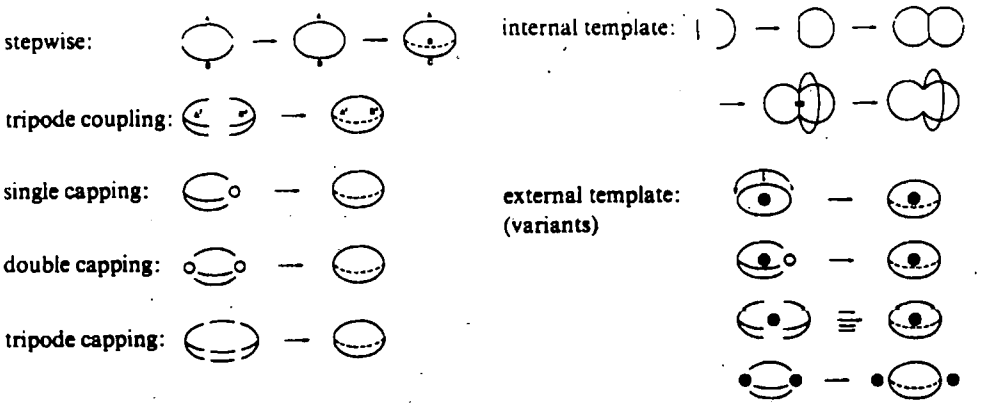

Figure 2 *Routes to macrobicyclic ligands*

(a) A stepwise approach can be employed, which involves synthesis of a macrocycle followed by bridging of the macrocycle. An example is shown in scheme 4.[29] The method includes two cyclisation steps effected under conditions of high dilution, each forming two bonds. The route provides access to cryptands containing three different strands between the bridgehead atoms.

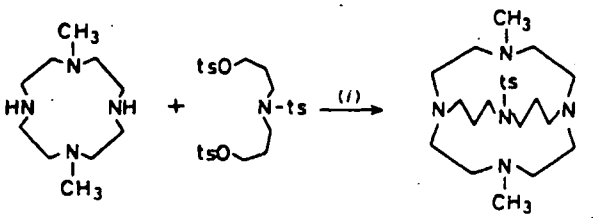

(11)

Scheme 4

(b) Tripode coupling involves C-N bond formation by coupling of a tripod containing three C-X groups with a tripod comprising three tosylamine groups (scheme 5).[28] This is a one pot procedure that requires formation

of three bonds. The use of two different tripodal subunits provides asymmetrical cryptands.

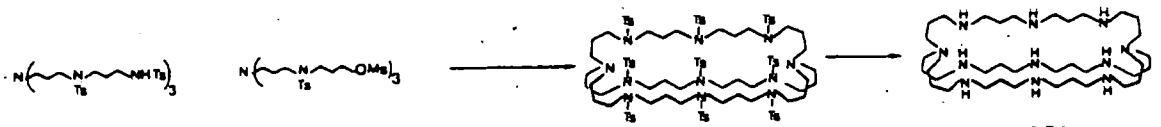

(12)

Scheme 5

(c) Single capping generally involves closure of a tripod ligand to give a cryptand. The ligand is often complexed with a suitable metal ion prior to capping as in the example shown in scheme 6.[30]

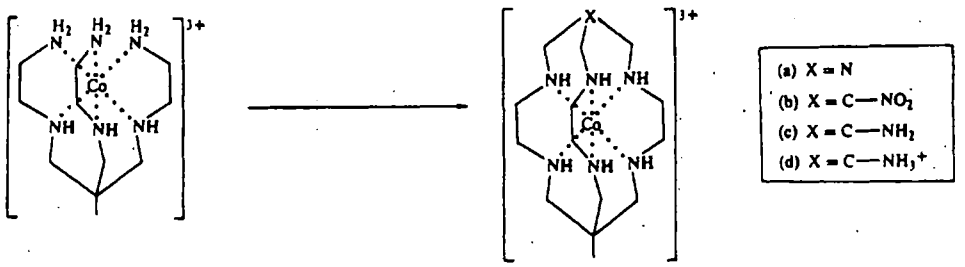

(13)

Scheme 6

(d) Double capping involves reaction of three difunctional bridging fragments with capping groups resulting in formation of a macrobicyclic ligand (scheme 7).[31]

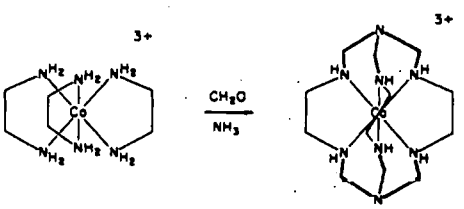

(14)

Scheme 7

(e) Tripode capping involves reaction of two tripod subunits with three bridging fragments to produce six new bonds. The method is used in formation of Schiff-base cryptands as shown in scheme 8.[24,28]

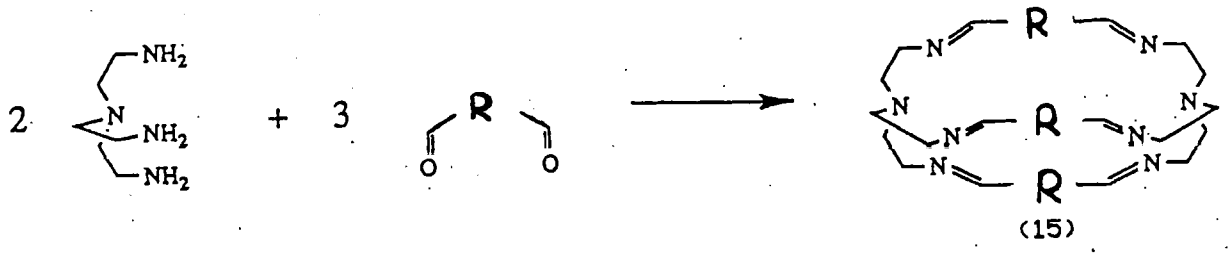

(15)

Scheme 8

Several classes of template reaction are commonly employed in the synthesis of macrocycles. One of the most common methods involves reaction of a dialdehyde or diketone with a diamine in the presence of a metal ion to give a Schiff-base macrocycle.[32] The synthesis of this class of Schiff-base macrocycles is considered in more depth later in this review. Schiff-base formation by reaction of a complexed multidentate amine with a dicarbonyl[32,33] or a ketone such as acetone[32,33] are illustrated in schemes 9 and 10.

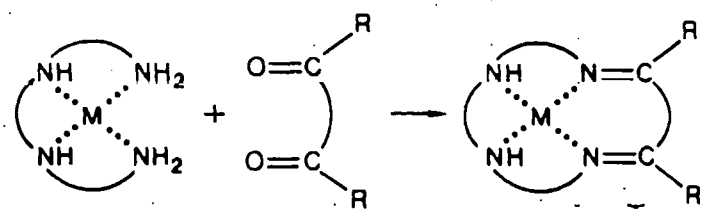

(16)

Scheme 9

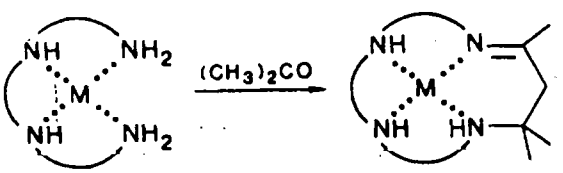

(17)

Scheme 10

Reaction of a complexed dicarbonyl with a simple diamine is frequently reported. The Jager-type macrocycles for example are produced by reaction between β-ketoiminato complexes with diamines as shown in scheme 11.[34,35]

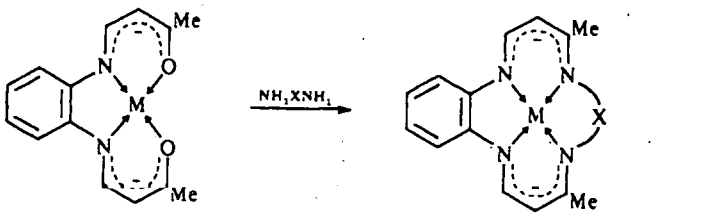

X = $(CH_2)_2$, $(CH_2)_3$, *o*-C_6H_4

(18)

Scheme 11

An alternative synthesis involving Schiff-base condensation is the self condensation of ortho-aminobenzaldehydes (scheme 12). The reaction provides access to complexes of the planar tetradentate macrocycle (19) and the tridentate macrocycle (20) on condensation in the presence of Ni(II) whereas the use of a Cu(II) template ion produces only the tetradentate macrocyclic complex.[35-37]

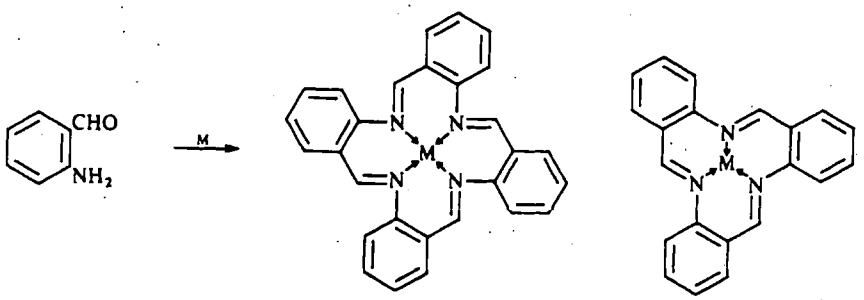

(19) (20)

Scheme 12

A related reaction between transition metal ion amine complexes , formaldehyde and ammonia or nitromethane in basic solution provides saturated tetraaza macrocycles[38], as illustrated in Scheme 13.

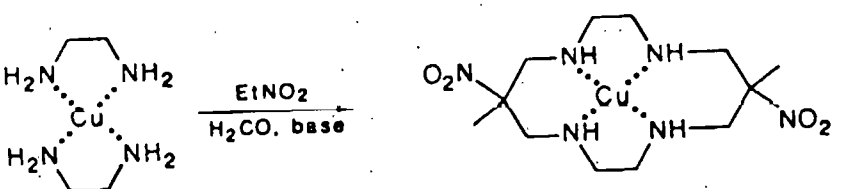

Scheme 13

(21)

Reaction between dithiolates and dibromoalkanes provide access to sulphur containing macrocycles[9]. A generalised reaction scheme is shown below.

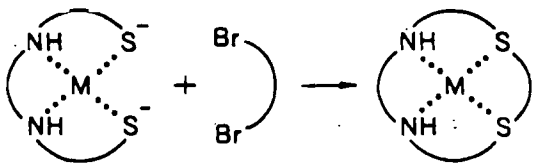

Scheme 14

Several polyether macrocycles, such as (4), have been produced in template reactions between diphenols and dichlorides.[14] The reaction yield is strongly dependent on the metal ion implying a template role for the cation. Less extensively studied reactions include capping of dimethylglyoxime complexes with boron compounds to form O-B-O linkages[21] and the reaction of a coordinated dihydrazine with formaldehyde which provides access to macrocycles containing N-N bonds.[22] Examples of such reactions are shown in Schemes 15 and 16.

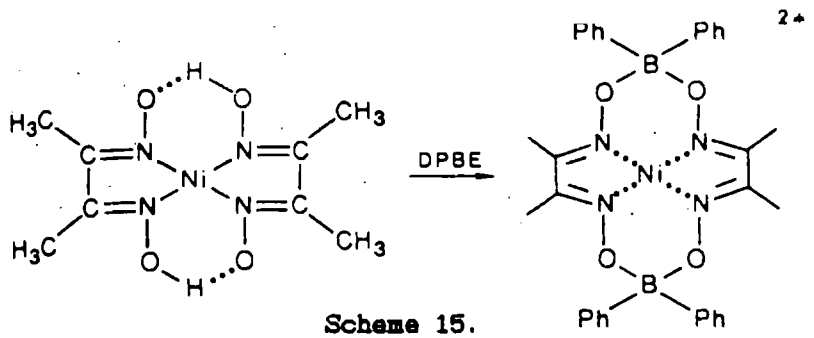

Scheme 15.

(22)

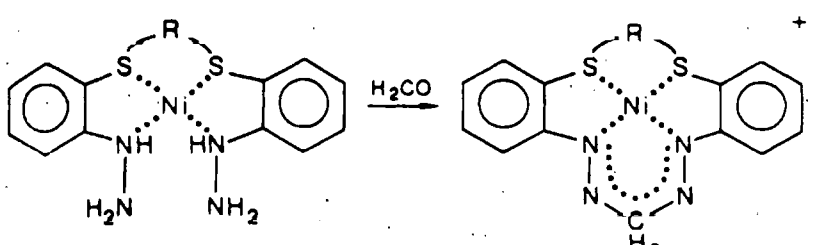

Scheme 16

(23)

Many of the synthetic methods used in the synthesis of macrocyclic complexes have also been employed in cryptate synthesis and are considered later in more detail.

THE MACROCYCLIC AND CRYPTATE EFFECT

It was realised from the early work on macrocyclic complexes that macrocyclic ligands confer unusual and potentially useful properties on their metal complexes. These include slow rates of dissociation [39], large stability constants compared to their open chain analogues[40] and high ligand field strengths.[41] The term 'macrocyclic effect' was introduced in recognition of these properties. An extension of the macrocyclic effect 'the cryptate effect' describes the analogous and often more pronounced stability enhancement observed in cryptates.[42,43] The term incorporates both thermodynamic and kinetic components.

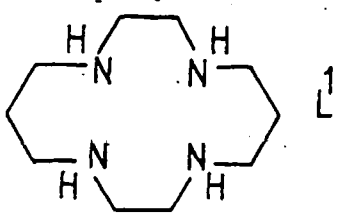

L^1

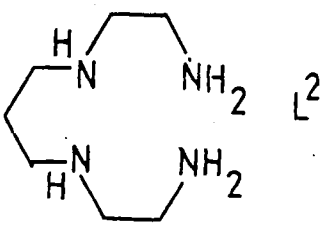

L^2

FORMATION: $Cu^{2+}(aq) + L \xrightarrow{k_f} Cu\,L^{2+}$

DISSOCIATION: $Cu\,L^{2+} + nH^{+} \xrightarrow{k_d} Cu^{2+}(aq) + LH_n^{n+}$

Ligand	k_f (M^{-1} s^{-1})	k_d (s^{-1})
L^1	5.8×10^{2}	3.6×10^{-7}
L^2	2.9×10^{4}	4.1

Figure 3 *Rates of formation and dissociation of CuL^1 and CuL^2*

The kinetic effects have been illustrated by Cabbiness and Margerum,[39] in a comparison of the rates of dissociation and formation of copper(II) complexes of a macrocyclic ligand L^1 and it's open-chain analogue L^2, shown in figure 3. Although the rate of formation of the acyclic complex is faster than that of the macrocyclic complex, the complex of the acyclic ligand dissociates *ca.* 10^7 times faster than the macrocyclic complex. The mechanism of dissociation can be envisaged as an unwrapping process whereby a terminal nitrogen donor is freed from the metal ion and replaced by a solvent molecule, followed by sequential replacement of the adjacent N donor of the chain. Such an unwrapping mechanism is not possible for the macrocyclic complex as the macrocycle does not contain a terminal N donor. Dissociation of the macrocycle is thought to require an initial folding of the macrocycle before breaking of the first coordinate bond.[40]

The enhanced thermodynamic stability of the macrocyclic complex is not entirely due to an increased chelate effect. Hinz and Margerum[44,45] carried out a thermodynamic study of the complexation of Ni(II) by macrocycle L^1 and acyclic ligand L^2 (Figure 4) and suggested that ΔH° for complexation of the macrocycle is more negative than that for the corresponding acyclic ligand because the acyclic ligand requires a greater degree of solvation in its uncomplexed state and the associated H_2O solvent molecules have to be displaced on complex formation. Paoletti *et al*[46-48] concluded that both the enthalpy and entropy terms were important in determining the thermodynamic stability of the complex. The entropy contribution is favourable since cyclic ligands do not lose configurational entropy on coordination to the same extent as do acyclic ligands. The enthalpy effect depends on ligand solvation, match between metal ion radius and macrocyclic cavity[45,48] and on the stereochemical preferences

of the metal ion. The enthalpy term may therefore be either favourable or unfavourable in comparison with the acyclic ligand.

TEMPLATE EFFECTS

Several types of template effect have been identified.[38]

(a) The coordination or kinetic template effect

- where a template effect arises from the stereochemistry imposed on some of the reactants by coordination to a metal ion.[28,49,50] This promotes a series of controlled steps and characteristically gives products not formed in the absence of the metal ion.[26,51-53]

(b) The thermodynamic template effect

- applies to reactions where the product is formed in the absence of metal ion but the metal ion improves the yield of product by removing it from the equilibrium.[54]

(c) The equilibrium template effect

- where both of the effects above act together. The distinctive feature here is the formation of different products in the absence of the metal ion.[38,52,53]

SCHIFF-BASE MACROCYCLES AND CRYPTANDS

The condensation of an amine and a carbonyl group to form the imine or Schiff-base function has been widely exploited in the synthesis of nitrogen donor macrocycles[25,50,55] and has recently been applied to cryptand synthesis.[24,28] The mechanism of Schiff-base formation is illustrated in figure 4. In the template process, the metal ion is coordinated by the oxygen atom of the carbonyl group, thus withdrawing electron density from the carbon of the carbonyl and activating the carbon

atom towards nucleophilic attack by the amine. The imine containing product is commonly isolated as a metal complex.

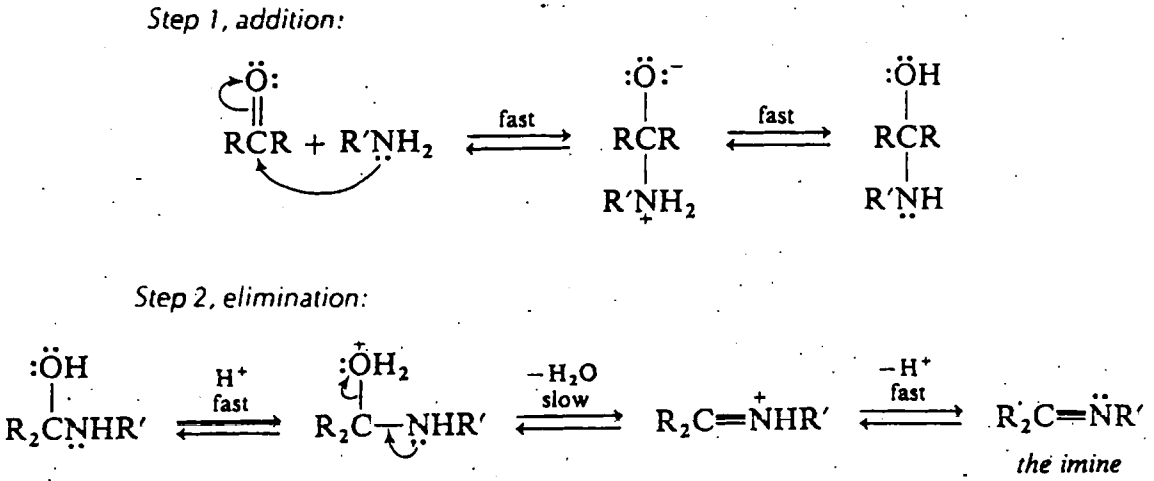

Figure 4 *The mechanism of Schiff-base formation*

The use of a template metal ion is widespread in the synthesis of Schiff-base macrocycles. The template ions most commonly employed are the stereochemically undemanding Group(II) metal cations, lead(II) or Ag(I) ions,[25,50] though the use of various other template ions has been reported, transition metal ions such as Cu(I) or Cu(II),[54] lanthanide ions[55] and actinide ions[55], for example. Recently, the actinide complex ion UO_2^{2+} has been used as a template in formation of Schiff-base macrocycles.[56] Lanthanide ion macrocyclic complexes and cryptates are considered in greater depth in a later section.

The dicarbonyl compounds employed in Schiff-base reactions frequently incorporate a heteroaromatic ring[25,50] such as pyridine, furan, thiophene, or pyrrole. Pyridine containing head units are particularly common, possibly because of the donating ability of the pyridine nitrogen

which may act as an anchor, assisting the coordination of the dicarbonyl reactant to the template ion.[53]

Schiff-base macrocycles are frequently classified according to the number of dicarbonyl and diamine reactant molecules that combine to produce the macrocycle. The macrocycles formed from reaction of one dicarbonyl unit with one diamine unit have been termed 1+1 macrocycles, whereas the 2+2 macrocycle incorporates two of each type of reactant.[26,50] Schiff-base cryptands have been formed in 2+3 reactions between two tripod amines and three dicarbonyl compounds. These are represented schematically in figure 5.

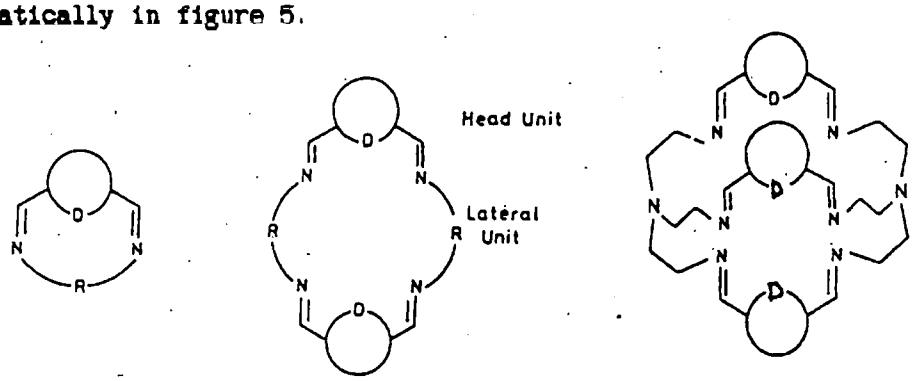

Figure 5 *Schematic representations of 1+1, 2+2 and 2+3 Schiff-base ligands*

The size of the template ion is of importance in directing the synthetic pathway in Schiff-base systems. The magnesium cation for example, is the only alkaline earth cation that generates the pentadentate 1+1 macrocycle shown in figure 6. However, magnesium is ineffective in forming the larger hexadentate macrocycle, though this is readily formed by template on the larger metal ions, calcium, strontium or barium.[57,58] If the template metal ion is too large for the 1+1 macrocyclic cavity, the 2+2 macrocycle may form. As shown in figure 6, use of the larger Pb^{2+} template ion generates the 2+2 macrocycle, and incorporates two lead template ions into the macrocyclic cavity.[59]

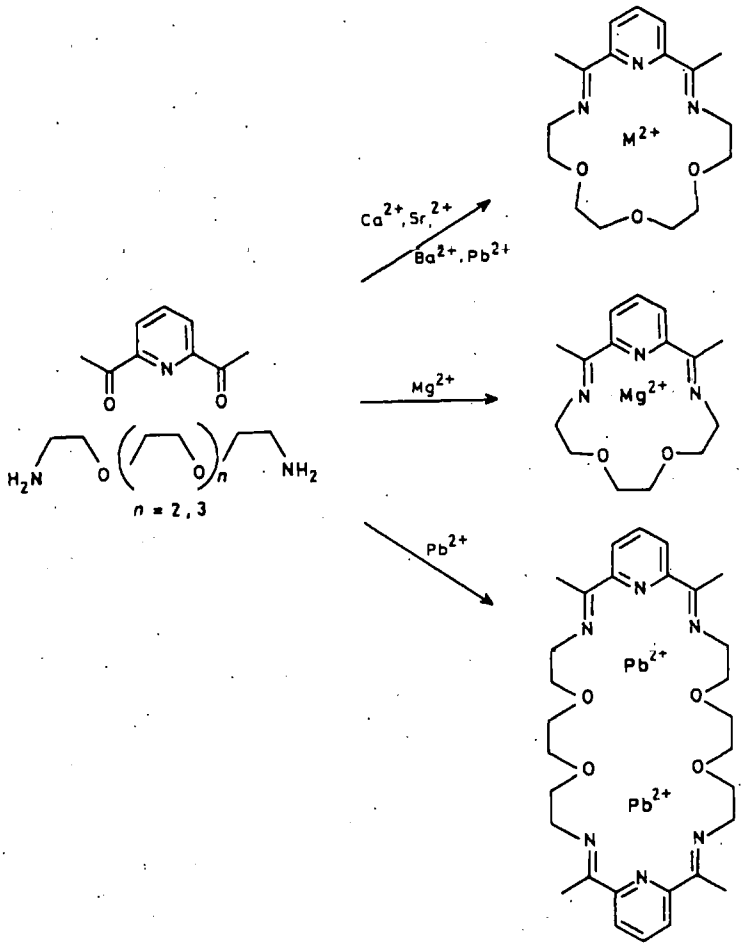

Figure 6 *Schiff-base macrocycle synthesis on non-transition metal template*

Similarly, binuclear complexes of macrocycle (24) are formed by use of Sr^{2+} (radius = 1.13Å) and Pb^{2+} (radius = 1.21Å) as template ions, but a mononuclear complex arises with the use of the barium ion as template (Ba^{2+} (radius = 1.35Å).[60]

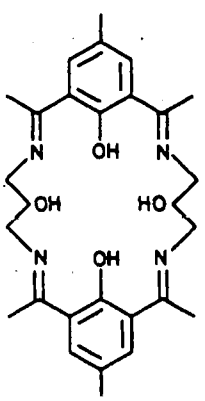

(24)

It appears that the macrocyclic cavity cannot accomodate two barium ions.

Mismatch between the cavity of the macrocycle and the ionic radius of the metal ion alters the geometry of the complex. A flexible macrocycle may fold around a small metal ion, whereas a metal which is too large for the cavity of the macrocycle can be accomodated outside the plane of the macrocycle. However this results in use of coordination sites on only one side of the ion and permits the formation of a 'sandwich' type structure, where another macrocycle coordinates to the other face of the ion. As an example, macrocycle (25) forms on alkaline earth metal template ions, Ca^{2+}, Sr^{2+} and Ba^{2+}. Calcium and strontium ions are each bound to one macrocycle however, the larger Ba^{2+} ion is coordinated to donors from two macrocycles, giving a twelve coordinate barium ion complex.[51] The geometry in this complex may be partly due to the preference of the barium ion for high coordination numbers.

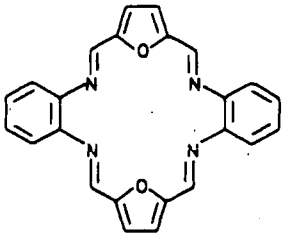

(25)

Another size-related effect is the metal induced ring contraction where a >NH or -OH functional group reacts with an imine of the macrocycle to produce a smaller macrocyclic ring. The example shown in figure 7 was reported by Fenton and coworkers.[51] The larger barium cation gives (a) as the product from the reaction of 2,6-diacetylpyridine and 1,3-diamino-2-hydroxypropane whereas the smaller lead(II) cation gives (b) as the product.

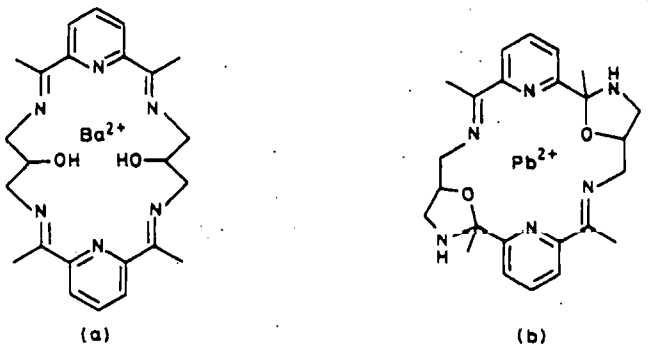

Figure 7 *Metal-induced ring contraction*

Similar ring contractions which result in formation of imidazolidine rings have been reported by Nelson and coworkers.[62,63] Presumably the mismatch of ionic radius with cavity size provides the thermodynamic driving force for the ring contraction.

The nature of the donor atoms also play a part in controlling the reaction pathway. This control is exercised through the strength of the interactions between metal ion and donor atoms. Although Pb(II) template ion leads to formation of the 2+2 macrocycle (L^6), shown in figure 8, when the diamine contains two ether oxygen donors, use of the corresponding tetraamine results in formation of the 1+1 macrocycle (L^2).[63] The lead ion is likely to form stronger and therefore shorter bonds with the N donors. As a result the terminal amino group can extend to a position where 1+1 ring closure can take place.

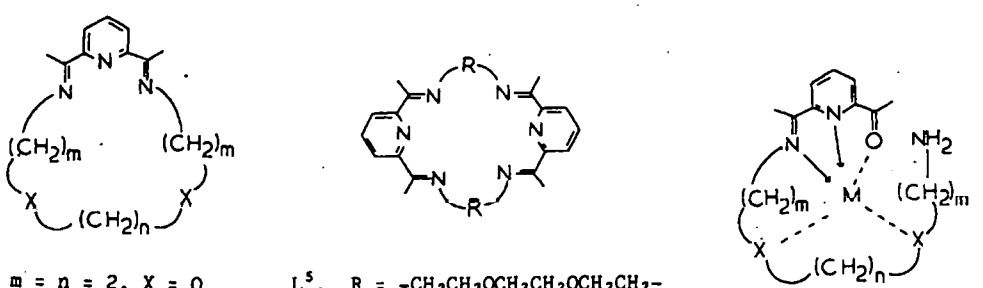

L^1, m = n = 2, X = O
L^2, m = n = 2, X = NH
L^3, m = 2, n = 3, X = NH
L^4, m = 3, n = 2, X = NH

L^5, R = $-CH_2CH_2OCH_2CH_2OCH_2CH_2-$

Figure 8

Sterochemical preference of the template ion also contributes towards the effectiveness of a synthetic pathway. Neither Cu(II) nor Ni(II) for example

act as templates for the pentadentate 1+1 macrocycles such as L^1 - L^4, yet they are commonly used in template synthesis of tetradentate N_4 macrocycles such as (26) which was templated on Ni(II).[50,55]

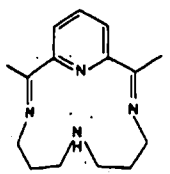

(26)

Presumably this is due to the preference of Cu(II) and Ni(II) cations for stereochemistries in which the bonding orbitals are in orthogonal arrangements as opposed to being pentagonally based.

Various 1+1 macrocycles have been reported, examples along with their reference are shown in figure 9.[56-70] Schiff-base 1+1 condensations lead to asymmetric macrocycles. The larger macrocycles which are capable of binding two metal ions can incorporate two different binding sites.[67]

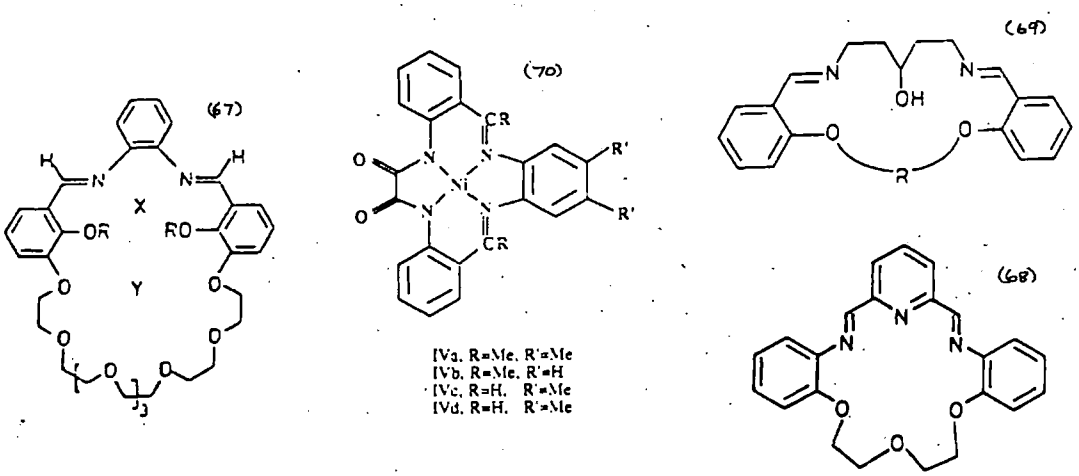

Figure 9 *Schiff-base 1+1 macrocycles*

Macrocycles derived from 2+2 condensation are generally symmetrical and incorporate equivalent binding sites, selected examples are shown in figure 10.[71-77]

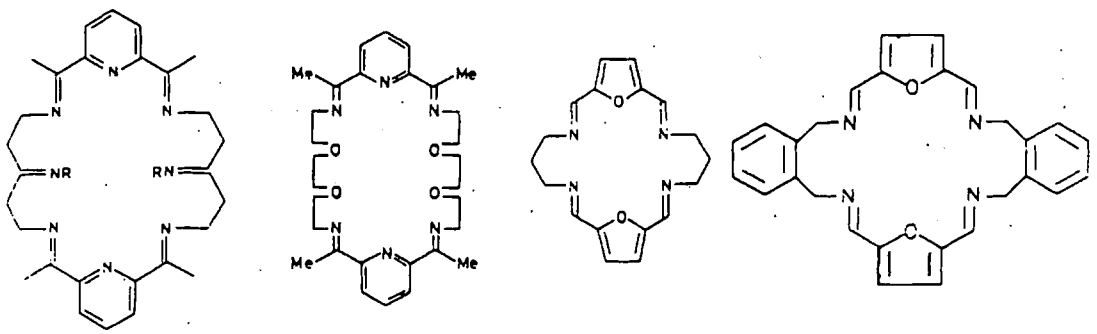

Figure 10 *Schiff-base 2+2 macrocycles*

However, asymmetric 2+2 macrocycles have been produced by stepwise processes. Macrocycles that incorporate different head units, or different lateral units have been described and several examples are shown below.

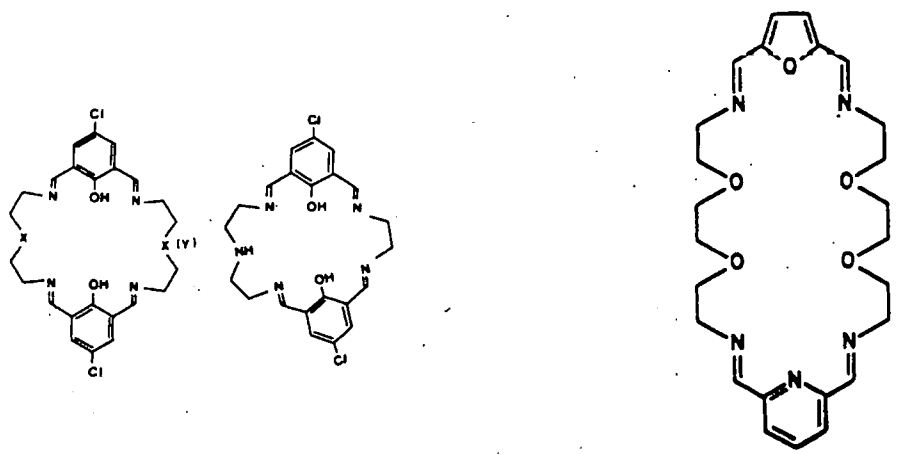

Figure 11 *Asymmetric 2+2 Schiff-base macrocycles*

Synthesis of the asymmetric macrocycle in which the lateral units differ, involved initial formation of an acyclic Schiff-base by reaction of a diamine with two dicarbonyl species. The intermediate dicarbonyl was

reacted with the different diamine either in the presence of a metal ion to give the macrocyclic complex , or without a template ion affording the metal-free macrocycle.[78] The macrocycle which incorporates different head units was obtained by reaction of a complex of the open-chain diamine intermediate with a different dicarbonyl.[79]

Lead(II) or silver(I) containing Schiff-base macrocycles or cryptands can be reductively demetallated to yield the corresponding metal-free amino derivative.[66] The reducing agents, sodium borohydride or lithium aluminium hydride are frequently used. Schiff-base macrocycles and cryptands prepared by non-template methods have also been reduced to the corresponding amino form.[28]

Although metal ion templates are generally used in Schiff-base syntheses, several Schiff-base macrocycles and cryptands have been obtained by non-template methods. Examples of such ligands are shown in figure 12.

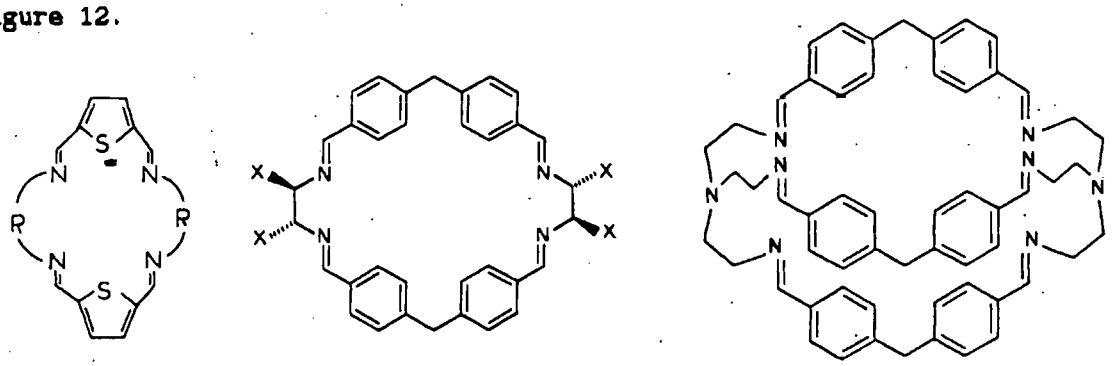

Figure 12 *Metal-free macrocycles and cryptands from Schiff-base reactions*

The ease of non-template synthesis of the thiophene containing macrocycle has been attributed to the predominant cis-cis conformation of the carbonyl groups in the precursor dialdehyde.[80,81]

The use of s- and p- block cations as template ions has led to a great variety of macrocyclic complexes, including many that are

inaccessible by template on transition metal ions. The kinetic lability of alkaline earth or main group templating agents has provided a synthetic pathway to otherwise inaccessible transition metal complexes.

TRANSMETALLATION

Transmetallation is a metal ion exchange process. Typically the template ion is replaced by a different ion through an exchange process in solution.[25] The precise mechanism of the exchange is unknown and may vary from system to system. The metal-free macrocycle may be temporarily liberated by the kinetically labile template ion, permitting capture of the free macrocycle by the incoming ion. Alternatively a concerted process may occur in which the incoming ion becomes partially bound to the macrocycle before the template ion is fully released. The template ion may be replaced by one, or more than one incoming ions, as shown by the example illustrated in figure 13.

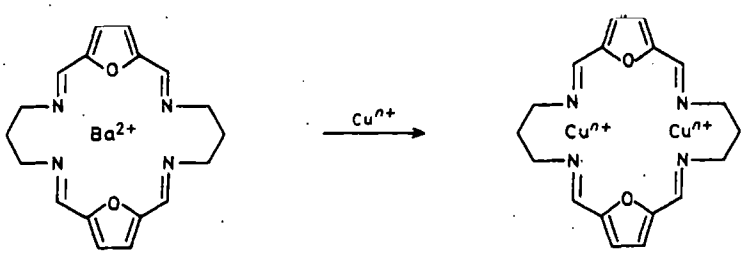

Figure 13 *Transmetallation reaction*

Generally the incoming ions have smaller ionic radius and/or form stronger bonds with the macrocyclic donor atoms. The incoming ions are commonly transition metal ions, though transmetallation with other metal ions such as the lanthanides[92] or vanadium[93] for example, have been successful.

Although metal exchange generally does not alter the framework of the macrocyclic ligand, there have been a few reports of modification of the

macrocyclic ligand on transmetallation. Ring contracted macrocycles such as those mentioned earlier have undergone ring expansion on transmetallation. Metal exchange of the barium ion in the ring contracted macrocycle (13) with two Cu^{2+} or two Ag^{+} ions yielded the binuclear complex of the expanded tetraimine macrocycle (figure 14).[84]

Figure 14 *Ring expansion on transmetallation*

A different type of modification occurred in the attempted transmetallation of the Ag^{+} complex of the quinquedentate macrocycle with Ni^{2+} (figure 15).[85] In this case, addition of methanol across one azomethine bond of the macrocycle resulted in formation of a macrocycle with sufficient flexibility to provide donors at positions approximating to five of the corners of an octahedron. The Ni^{2+} bound a sixth ligand to obtain approximate octahedral coordination geometry.

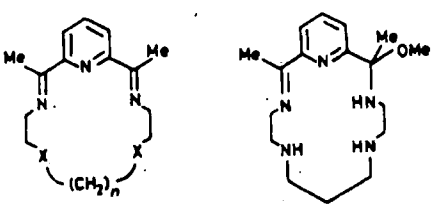

Figure 15

BINUCLEAR TRANSITION METAL COMPLEXES OF MACROCYCLES AND CRYPTANDS.

Many studies of complexes in which pairs of metal ions are secured by macrocyclic ligands have been reported and several reviews of the subject

have been published.[85,86] In binuclear complexes the distance between metal ions is dependent on ligand design; at short intercationic distance macrocyclic complexes facilitate study of properties dependent on metal-metal interactions such as magnetic coupling, electron transfer or modified redox properties. At larger separation, coordinatively unsaturated metal complexes can bind bridging substrates to form 'cascade' complexes[87] as represented in figure 16.

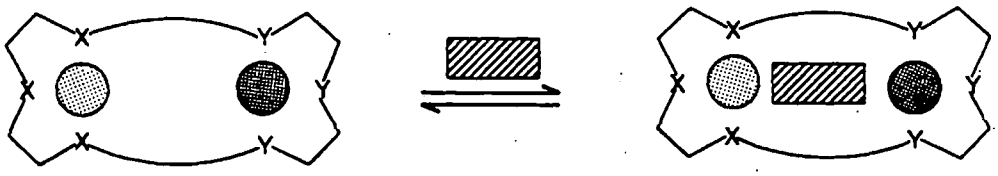

Figure 16 *Formation of a cascade complex*

The design of ligands capable of forming binuclear complexes requires a consideration of various structural features.[87]

- Nature of coordination sites (N, O, S, P) - the hard/soft nature of the binding sites as outlined by Pearson's hard/soft acid/base theory determine the selection of the cations. The binding sites determine the redox and substrate binding properties of the metal ion.

-The properties of the binding subunits, nature and geometry (chelating ,tripodal, cyclic), number and arrangement of coordination sites, conformational and stereochemical features.

- Macropolycyclic architecture, the framework linking the binding subunits, nature ,number and flexibility of the links, distance between the binding sites.

A variety of cyclic structures which are capable of binding pairs of metal ions have been reported. Four of the more common ligand frameworks and their binuclear complexes are represented schematically in figure 17.

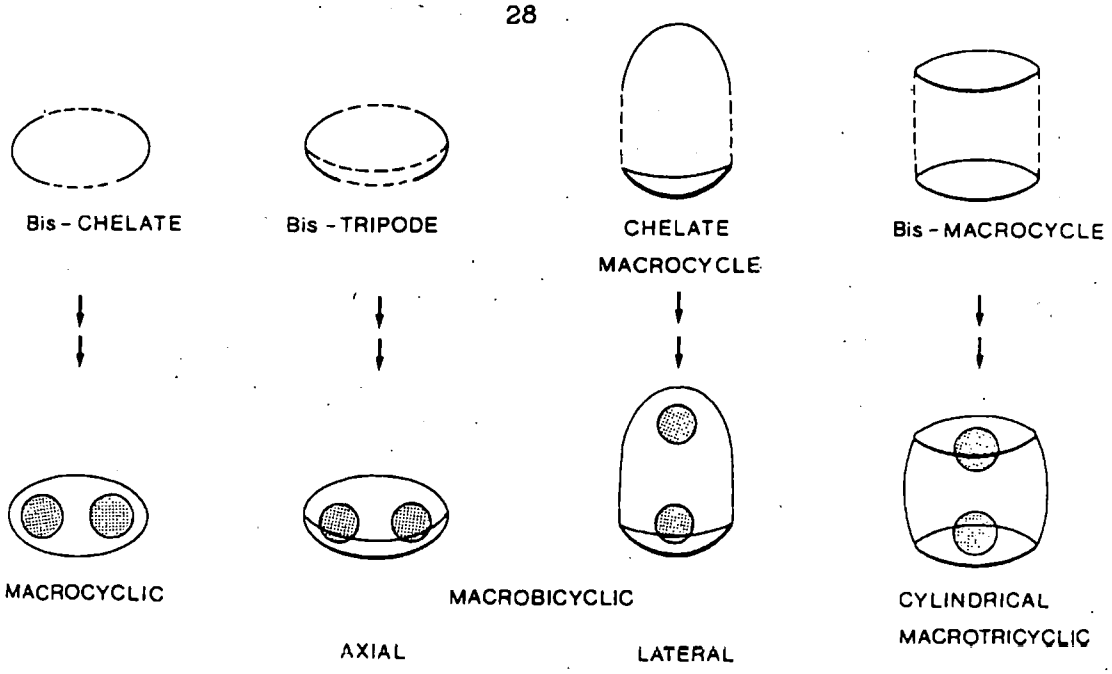

Figure 17 *Macropolycyclic ligands and their binuclear complexes*

Many binuclear transition metal macrocyclic complexes have been formed by transmetallation of a Schiff-base macrocyclic complex.[25,50] The transmetallation approach has proven particularly successful in the synthesis of binuclear copper(II) complexes of tetraimine Schiff-base macrocycles. Binuclear macrocyclic complexes are ideally suited to act as hosts for small bridging ligands such as OH^-, N_3^-, NCS^- or imidazolate. Much of this work involves dicopper complexes as these are of use as speculative models for the bimetallobiosites in copper proteins such as tyrosinase or haemocyanin. However many macrocyclic complexes of other transition metal ions which bind bridging ligands between the metal centres have been reported.[72,88-89]

Lehn and Martell have developed a series of macrocyclic and macrobicyclic ligands that form binuclear complexes which induce secondary binding of small bridging ligands.[87,90-100] Various ligands and their complexes are illustrated in figure 18. The macrocyclic ligand bisdien has a tendency to form mononuclear complexes[93,94], presumably due to its

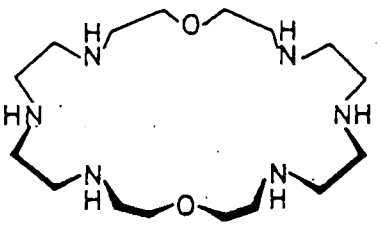

bisdien base

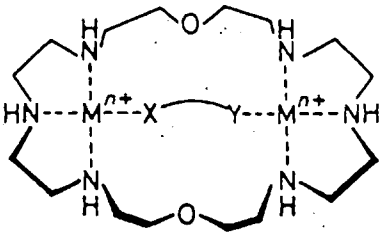

Binuclear bridged bisdien chelate
$M_2(X-Y)L^{2+}$ (X-Y = bidentate ligand)

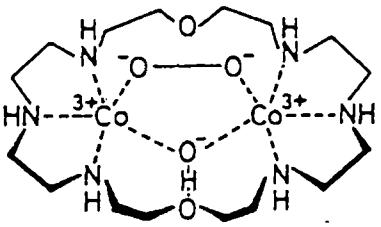

μ-Hydroxo-μ-peroxo-dicobalt bisdien chelate

$Co_2O_2(OH)_2L^{2+}$

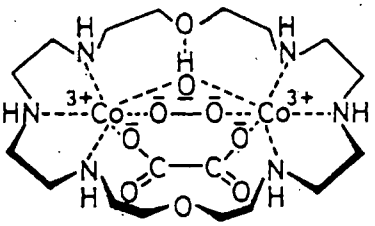

μ-Hydroxo-μ-oxalato-μ-peroxo-dicobalt bisdien chelate

$Co_2O_2(OH)_3L^{+}$

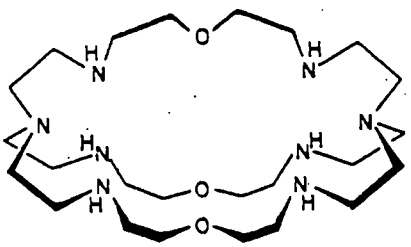

(O-BISTREN)

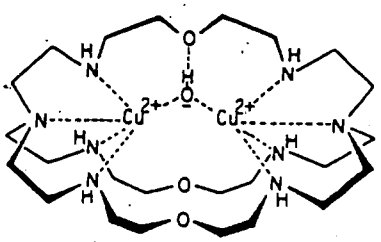

($[Cu_2(OH)L]^{3+}$) (L = O-BISTREN)

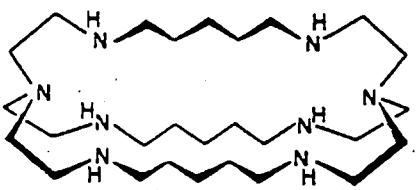

(C-BISTREN)

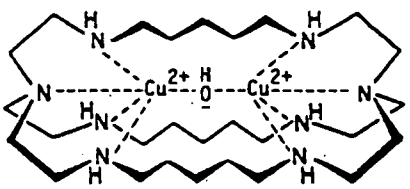

($[Cu_2(OH)L']^{3+}$) (L' = C-BISTREN)

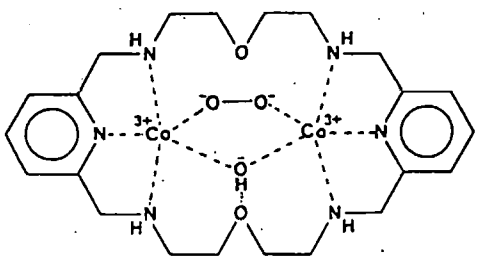

$Co_2LO_2(OH)^{3+}$

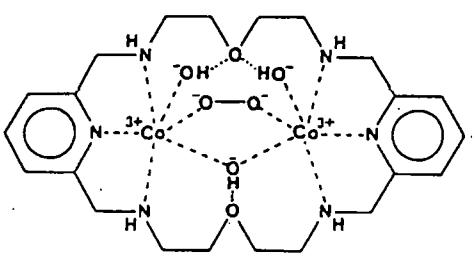

$Co_2LO_2(OH)_3^{+}$

Figure 18 *Lehn's macrocyclic ligands and their complexes.*

flexibility, however its ability to form binuclear complexes is greatly enhanced by the binding of bridging ligands between the metal centres.[94,95] The dicopper(II) complex induces binding of a bridging imidazole ligand, (27) which is represented below.[87,91]

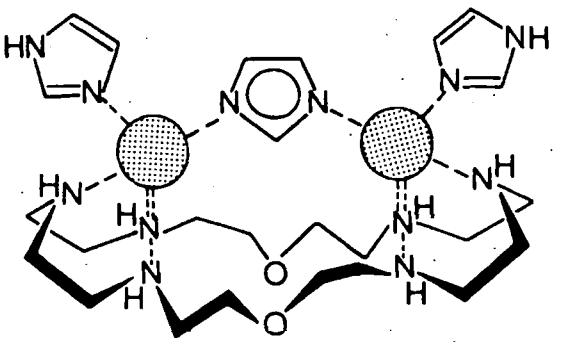

(27)

Magnetic exchange studies on complex (27) showed the existence of antiferromagnetic coupling with $J = -23\ cm^{-1}$, a value which is close to the value found for the tetra Cu(II) derivative of bovine superoxide dismutase.[91] The dicobalt(II) bisdien complex binds dioxygen to form the μ-peroxo-μ-hydroxo-dicobalt complex. This complex is particularly interesting as it binds a bridging oxalato group and a redox reaction between the two bridging ligands occurs. This results in oxidation of the oxalato group.[94]

Binding constants for chloride and hydroxide anion by dicopper(II) and monocopper(II) bistren have been determined by a potentiometric method.[96] Comparison with binding constants for O-bistren showed marked stabilisation of the hydroxo-bridged species within O-bistren, presumably as a result of hydrogen bonding of the hydroxo group to one or more of the ether oxygens of the O-bistren ligand.

Interesting binucleating Schiff-base macrocycles have recently been reported by Martell.[101] The binuclear copper (I) complex reacts with

dioxygen giving a dicopper(II) complex of the modified macrocycle containing a bridging phenolate oxygen donor and a hydroxo bridge as shown in figure 19.

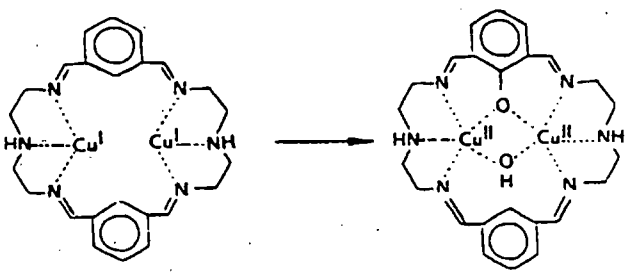

Figure 19

The cryptand shown in figure 20 provides an example of a 'chelate macrocycle' which binds a copper(II) ion in the macrocycle and another in the chelating bridge.[97] As a result of their different binding sites, the two copper ions have markedly different redox potentials. The copper(II) bound in the sulphur containing macrocycle is reduced at +550 mV whereas the second copper is reduced at much less positive potential +70 mV, suggesting relatively facile formation of a mixed valence cryptate.[97]

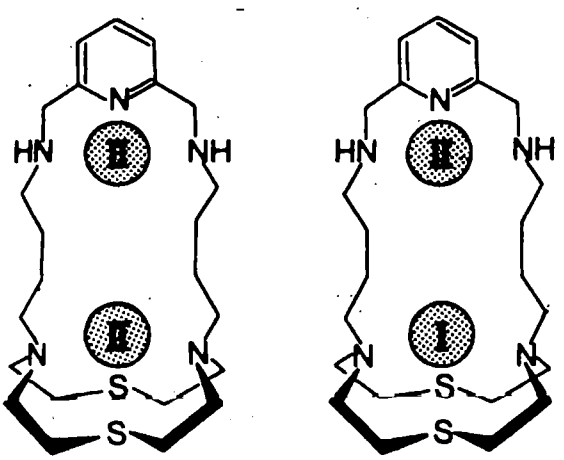

Figure 20

Dicopper (II) complexes of the 2+2 furan containing macrocycle (28) are readily reduced to dicopper(I) macrocyclic complexes on heating in acetonitrile.[102] However, in this case the ease of reduction of the Cu(II)

ion when bound in the macrocycle has been traced to geometrical factors.[102] The planar conformation of the macrocycle preferred by Cu(II) causes severe steric hindrance between the bridging groups and the uncoordinated furan oxygen atoms.

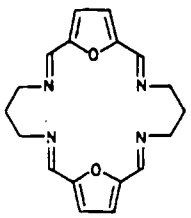

(28)

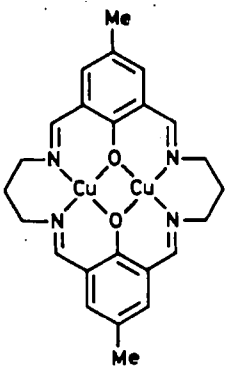

(29)

The steric hindrance is effectively removed if a tetrahedral geometry is attained. Tetrahedral coordination suits Cu(I) but is less acceptable to Cu(II) thus facile reduction is promoted.

Mixed valent dicopper complexes of macrocycles such as (29) have been obtained. The binuclear copper macrocycle was synthesised by Schiff-base condensation on copper (II). One electron electrochemical reduction gives the mixed valent Cu(II)/Cu(I) complex which exhibits photoassisted and thermal intramolecular electron transfer.[103] The complex exhibits a seven-line esr spectrum in solution, indicative of interaction of the odd electron with both metal centres. At lower temperature the odd electron becomes localised and a four-line esr spectrum results.

The effect of reduction of the imine functions of the Schiff-base macrocycle on the redox behaviour of the dicopper complex (29) has been investigated.[104] The stability of the dicopper(I) and the mixed valence Cu(II)/Cu(I) species were found to increase with increased ligand unsaturation. Dicopper (III) species and mixed valence Cu(II)/Cu(III) were

reported for the reduced derivatives. Electrochemical studies on dicopper complexes of similar macrocycles have been reported.[105] In all cases distinct one-electron transfer processes occurred, unlike the cooperative two-electron process found in Type 3 copper proteins.

Face to face linkage of two macrocycles by two bridges provides a varied range of cryptands,[106-109] examples are shown in figure 21.

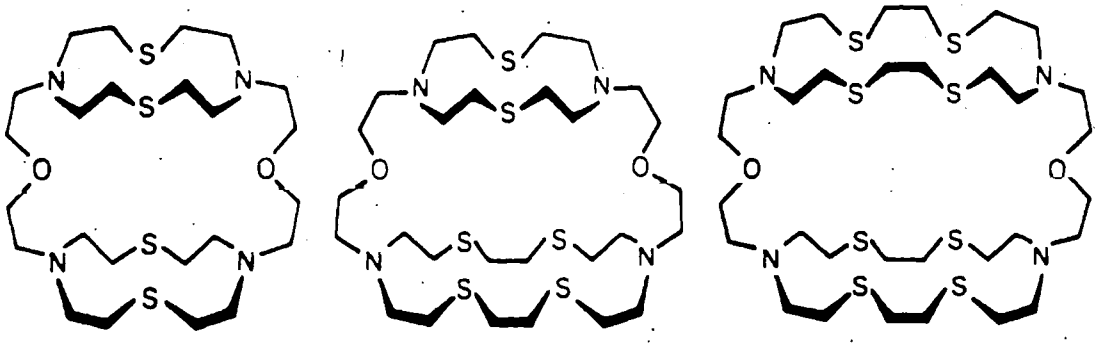

(30) (31) (32)

Figure 21

The dicopper(II) cryptate[110] of ligand (30) undergoes a reversible redox change at markedly positive potential (+ 455mV), a value similar to that found for blue copper proteins. An interesting mixed valence Cu(II)/Cu(I) cryptate is formed with the asymmetrical ligand (31) shown in figure 21. The Cu(I) and Cu(II) ions are probably located in the 18- and 12-membered rings respectively.[97]

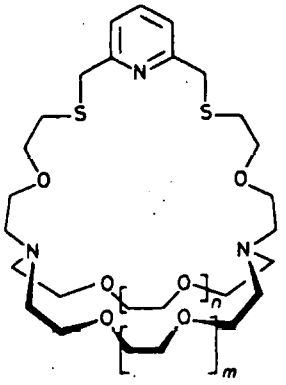

(33)

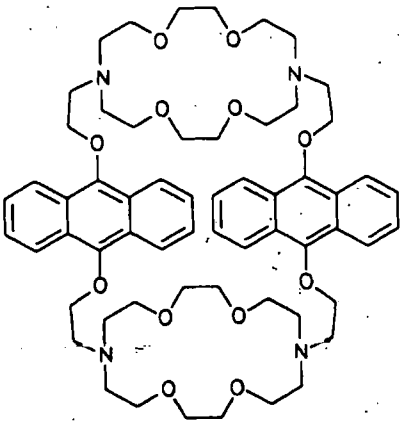

(34)

Heterobinuclear cryptates of cryptand (33) have been reported. The cryptand (33) binds Rh-CO at the pyridine binding site and binding of Cu(II) has been detected spectroscopically at the other binding site.[109] The orientation of the carbonyl is such that it points towards the metal bound by the macrocycle, and thus it may be activated towards nucleophilic reaction at the carbon centre.[109] A macrocyclic bis-anthracenyl cryptand (34) displays remarkable fluorescence properties which are modified by binding of rubidium ions. The X-ray crystal structure of the binuclear rubidium complex was reported.[110]

Many macrocycles that incorporate the phenol group or OH groups as part of the macrocyclic framework have been synthesised.[111-119] Examples are shown in figure 22. The deprotonated hydroxy or phenoxy (RO^-) groups are capable of acting as endogenous bridges between adjacent metal centres, thus the larger macrocycles of this type are suited to binding of clusters of metal ions.[113] A tetranuclear Mn(II) complex of macrocycle (35) results from 4+4 Schiff-base condensation using manganese(II) as the template ion.[116-117]

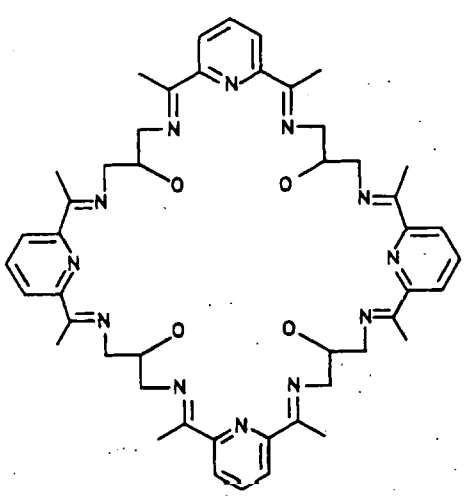

(35)

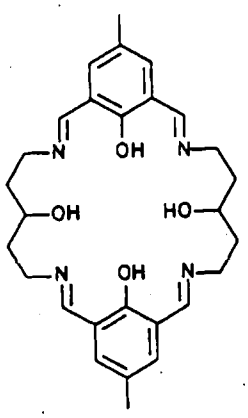

(36)

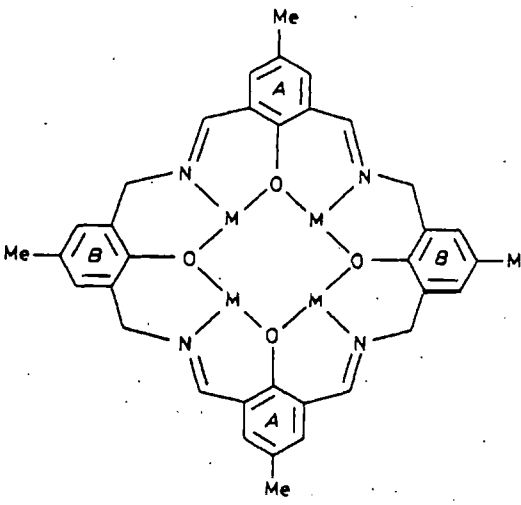

(37)

Figure 23

The manganese complex of (35) has potential as a structural model for the manganese bioproteins of photosystem II. The active site of the photosynthetic oxygen evolving complex is now generally believed to contain four Mn(II) ions bridged by oxygen donors.[120] Macrocycle (36) also binds a tetranuclear cluster of manganese ions.[115]

Macrocycle (37) binds a tetranuclear cluster of Ni(II) ions.[116] A 3+3 Schiff-base macrocycle which binds a hexanuclear cluster of copper ions was reported recently.[114] Two hydroxo groups occupy the central cavity and each bridge a pair of copper ions. Various other classes of macrocycle also bind metal ion clusters.[121,122] The trinucleating macrocycle (38) was reported by Lehn and coworkers[121] and is of interest in view of the recent structural determination of a trinuclear copper (II) site in ascorbate oxidase.[123] The macrocyclic iron-sulphur Fe_4S_4 clusters (39), which are reminiscent of ferredoxins, have been used in electrochemical reduction of CO_2 to give methanoate.[122]

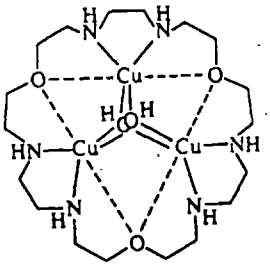

(38)

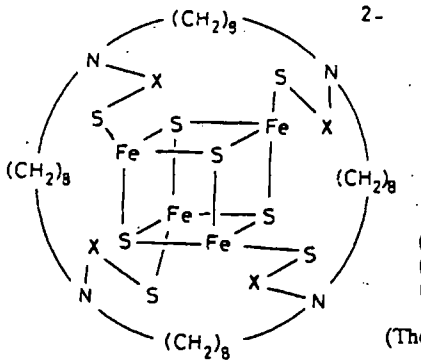

(1) X = $-COCMe_2-$
(2) X = $-COC_6H_4CH_2-$ (*p*)
(3) X = $-COC_6H_4-$ (*p*)

(The CO part of X is bonded to N)

(39)

Relatively few examples of heterobinuclear macrocyclic complexes have been reported. However heterobinuclear complexes have been obtained both with asymmetrical macrocycles which incorporate non-equivalent binding sites

and with symmetrical ligands which offer the same binding site to each metal ion. A series of Cu(II)/M(II) (M = Mn, Fe, Co, Ni and Zn) complexes of macrocycle (40) have been synthesised.[124] The reaction sequence shown in scheme 17 was used in the synthesis of the Cu/M complex (M = Mn, Fe, Zn) however the Ni(II)/Cu(II) complex was only available if Ni(II) was bound in the N2O4 site of the open chain intermediate, with subsequent addition of Cu(II) before the final ring closure.

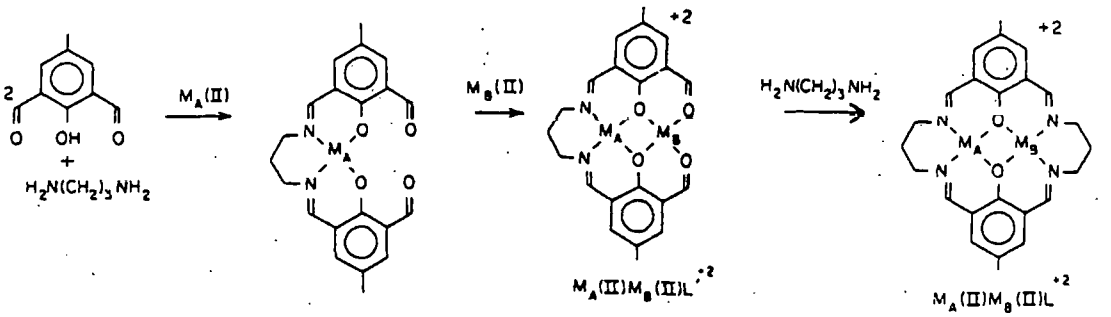

Scheme 17

(40)

The redox properties of the series, Cu(II)/Co(II) excepted, was investigated and the observed changes in the properties of the Cu(II) ion have been ascribed to some form of metal-metal communication between the Cu(II) and the other transition metal ion bound by the macrocycle.[125] The Ni(II)/Cu(II) complex of macrocycle (41) was formed by addition of one equivalent of nickel acetate to the acyclic ligand, followed by addition of diethylene triamine and another equivalent of copper acetate.[126,127] In addition a heterobinuclear complex containing uranyl(IV) was reported.[126]

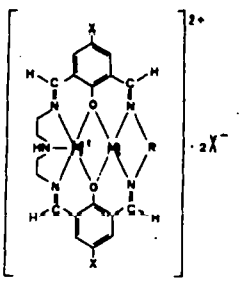

(41)

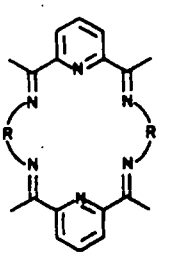

(42)

Heterobinuclear Pb(II)/M(II) macrocyclic complexes where M = Mn(II), Ni(II) and Fe(II) have been obtained by transmetallation of the dilead macrocyclic complex of macrocycle (42).[128] A Ni(II)/Cu(II) complex of macrocycle (43) has been reported.[129]

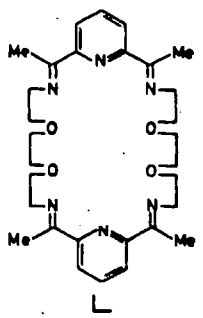

(43)

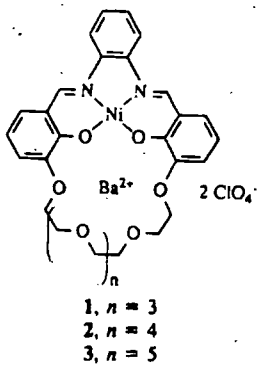

1, $n = 3$
2, $n = 4$
3, $n = 5$

(44)

The mononuclear copper(II) complex of the macrocycle was formed initially and reaction with Ni(II) acetate gave the heterobinuclear complex.[129]

A series of heterobinuclear complexes of 1+1 schiff-base macrocycles such as (44) have been obtained.[130,131] The barium complex obtained in the template process was reacted with Ni(II), Cu(II) or Zn(II) to give the heterobinuclear complex.

POLYAZAMACROCYCLES AND THEIR COMPLEXES

Metal complexes of polyazamacrocycles display unusual and potentially useful properties, such as high kinetic stability or stabilisation of unusual oxidation states of the metal, often high oxidation states are stabilised. As N-donor macrocycles, they are particularly suited to complexation of transition metal ions, whereas in their protonated form, they are capable of binding anions. Much of the recent work on the triaza and tetraazamacrocycles has involved modification of existing macrocycles

to produce pendant arm species. The pendant arms are generally functionalised so that they provide another donor for the metal ion, or provide means of linking the macrocycle to another molecule. Pendant arms incorporating primary amines, pyridine, imidazole, phenol, thiophene, and bipyridyl have been reported, among others.[132-137] Further variation results from the attachment of the arm to either nitrogen or carbon atoms of the macrocyclic framework. The number of pendant arms attached also varies, examples with between one and four arms have been reported. Some of the more recent examples are shown in figure 23.

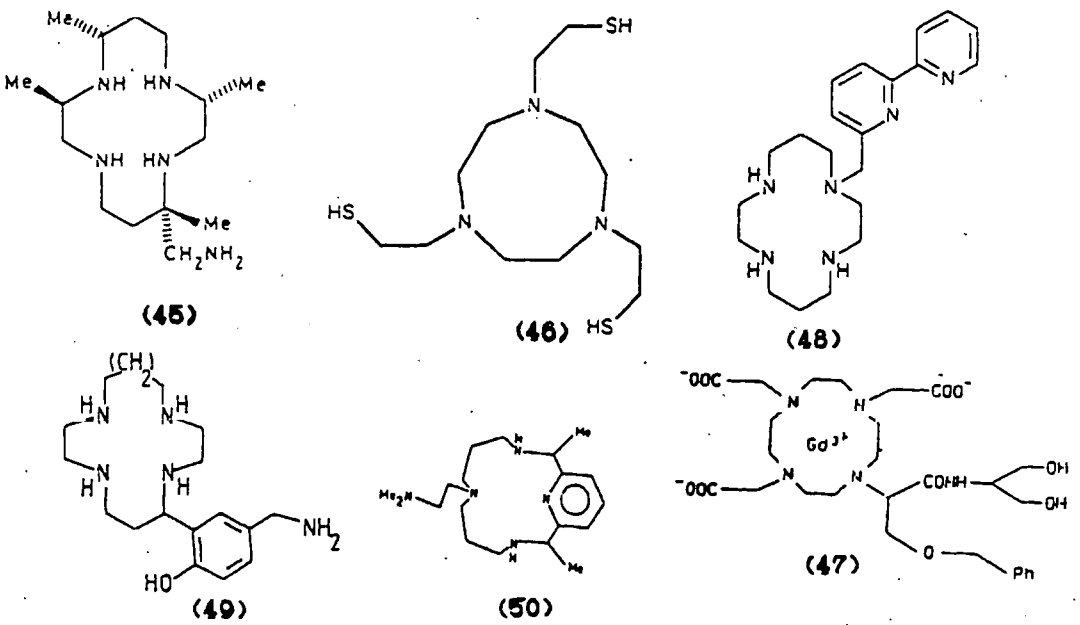

Figure 23 *Pendant arm macrocycles*

Triazamacrocycles coordinate the transition metal ion facially to form either 1:1 complexes where remaining coordination sites on the metal can be occupied by the pendant arm or other ligands, or form 1:2 complexes where a metal ion coordinates to two macrocycles forming a sandwich structure. By contrast the transition metal in tetraazamacrocycles generally lies in the plane of the ring (size permitting) and only 1:1

complexes are formed.[133-137] The introduction of pendant arms to a macrocycle was found to modify various properties of the macrocyclic complex. Both triaza and tetraazamacrocycles displayed increased stabilisation of the metal complex on addition of a chelating pendant arm. However N-functionalised species were more susceptible towards dissociation in acidic conditions.[138] In addition the kinetics of metal complexation were altered. The capture of a metal ion by a pendant arm was shown to aid in transfer of the metal ion into the macrocyclic cavity,[133] an ability of use in metal ion sequestration.[134]

As a result of the marked kinetic stability of pendant arm macrocycles, medical uses involving metal ion transport have been investigated. A functionalised pendant arm provides a site for attachment to monoclonal antibodies, permitting the transport of an imaging or cytotoxic radionuclide specifically to a tumour.[137,139-141] Use of 13 and 14 membered macrocycles (45) shown in figure 23, for example, provide stable ^{64}Cu or ^{67}Cu complexes of use in imaging or therapy.[137] Incorporation of ionisable groups into pendant arms provides access to neutral complexes of metal ions which have the higher lipophilicity required for use of radioactively labelled metal complexes in imaging organs such as the brain or heart. For example the hexacoordinating ligand (46) which has three ionisable groups provides a $N_3S_3^{3-}$ core for binding gallium III ion.[142]

An interesting gadolinium complex of a pendant arm macrocycle (47) has been prepared[143] for use as a paramagnetic contrast agent in magnetic resonance imaging.[144,145] The X-ray crystal structure of the complex has been determined.[143] Fabbrizzi[146] has reported an interesting Ni(II) complex of a functionalised cyclam which acts as an acid/base indicator

due to yellow/blue colour change on change of spin state of the Ni(II) ion. Coordination of the pendant arm to Ni(II) gives high spin Ni(II) which is blue in colour, on change of pH the pendant arm no longer coordinates the metal ion resulting in spin pairing of the Ni(II) electrons, a change accompanied by yellow colouration. Similar effects have been observed by Hay[147] and Kimura[134] using the Ni(II) complex of a pendant arm cyclam. Generally the pendant arm coordinates to the metal ion bound in the macrocycle to which it is attached. However in a few cases the pendant arm complexes other metal ions. For example a heterobinuclear complex for use as a photoredox catalysis system has been synthesised using a pendant arm cyclam.[148] The bipyridine-pendant cyclam macrocycle shown in figure 23 was used to form a complex with $Ru(bpy)_2Cl_2$, the heterobimetallic complex was formed by insertion of Ni (II) into the cyclam moiety.[137] Fabbrizzi has designed a mono N-functionalised cyclam which acts as a carrier capable of performing selective electron transport across a liquid membrane.[138] A series of 12-16 membered tetraazamacrocycles was investigated by Paoletti[133] and it was found that that the 14-membered ring coordinates most strongly with 3d metal cations.

Various bis-macrocycles have been reported and selected examples are shown in figure 24.

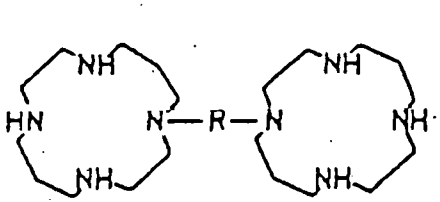

(51)

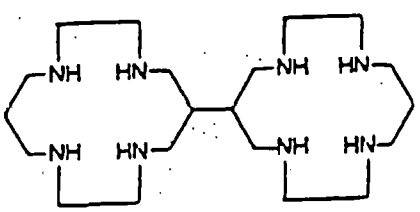

(52)

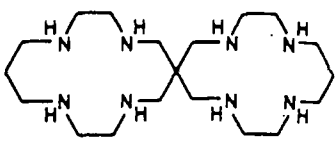

(53)

Figure 24 *Bis-macrocycles*

Macrocycles have been linked via N-N[149,150] or C-C bonds.[151-152] Cyclam macrocycles have also been joined at a single quaternary carbon atom forming C spiro bicyclams (53). Bis-macrocycles form binuclear complexes and display varying degrees of communication between the metal ions. Two consecutive one electron redox steps have been observed in homobinuclear bis-macrocyclic complexes. Redox change of one metal ion affects the redox change of the other metal ion implying communication between them.

Large polyazacycloalkanes such as (54) and (55), incorporating many nitrogen atoms are of interest as polytopic receptors for metal ions.

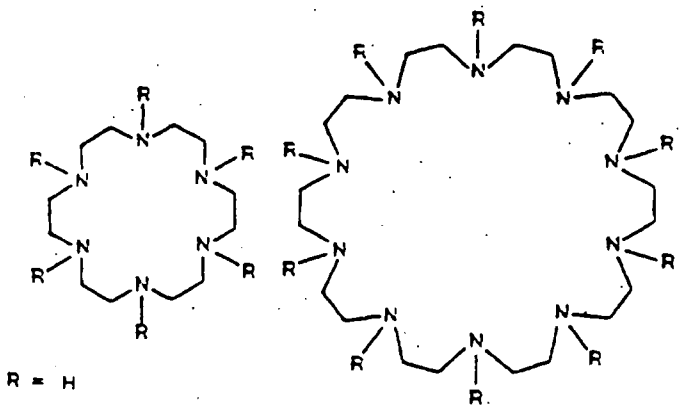

(54) (55)

The macrocycles containing from eight to twelve nitrogen atoms have been investigated by Paoletti.[154] Stable binuclear complexes were formed with N8-N10 rings, whereas trinuclear species were obtained with the larger polyaza rings.

Thio analogues of the polyazamacrocycles of varying ring sizes have been reported.[155,156] Sulphur donor macrocycles tend to favour the generation of low oxidation states due to the π-acidity of sulphur donors. Often high positive redox potentials for the Cu(II)/Cu(I) reduction are observed. Although the redox potential is often similar to that found in blue copper proteins, the applicability of copper complexes of S-donor

macrocycles as models can be hampered by oxidation of the sulphur donor sites of the macrocycle.[157] Various other types of macrocycle also incorporate sulphur donors, some examples are shown below. Metal complexes of some of these have been reported, for example binuclear rhodium or palladium complexes were obtained by metal insertion into the free macrocycle (57).[158]

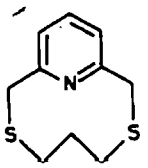

(56)

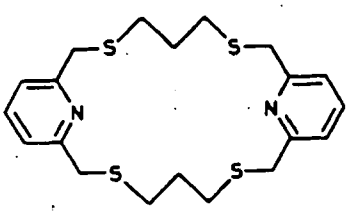

(57)

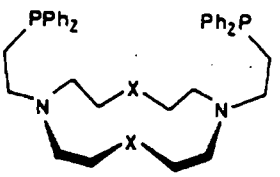

(58)

The phosphine functionalised pendant arm macrocycle (58) is capable of forming heterobimetallic complexes, binding a lewis acid metal centre in the macrocyclic ring and a redox active metal centre between the functionalised side arms.[159]

The catenate (59) described by Sauvage is a particularly interesting macrocyclic complex.[160,161]

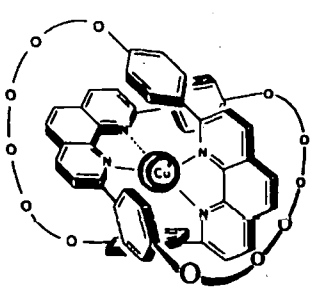

(59)

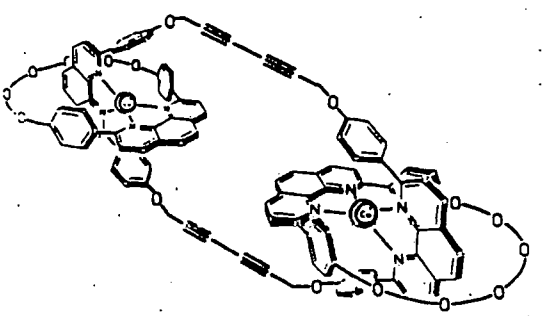

(60)

The catenate was produced by template synthesis on Cu(I) and only the N donors coordinate the 'soft' copper(I) ion. Catenates of metal ions Cu(II),

Ni(I), Li+, Ag(I), Zn(II), Cd(II) have been prepared by insertion of the metal ion into the free catenand. The catenand provides a distorted tetrahedral site for coordination of the metal ion. Low oxidation states of the metal are stabilised due to the π- acceptor ability of the phenanthroline groups. In addition, the poor ligand field of tetrahedral coordination destabilises higher oxidation states of the metal. Marked stabilisation of the lower oxidation state is particularly evident with the copper(II)/copper(I) redox couple. The tetrahedral coordination site suits copper (I) but destabilises copper(II). The combined effects of preferred geometry of the Cu(II) ion and the high π-acceptor ability of the ligand results in high positive potential for the reduction of Cu(II) to Cu(I). Catenates made up of three interlocked rings and providing two phen based binding sites (60), have been reported.[162]

Lindoy[163-165] has developed an interesting series of macrocyclic ligands with the aim of achieving metal ion discrimination (figure 25). Parameters of the macrocyclic ligand such as ring size, the nature of the donor atoms and the degree of substitution on the macrocycle were varied in a systematic way and a matrix relating macrocyclic structure and complex stability with a metal ion was prepared.

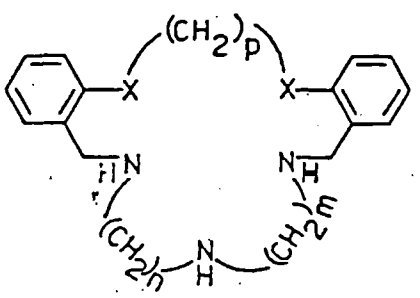

X	m	n	p
O	2	2	1
O	2	2	2
O	2	3	2
O	3	3	2
O	2	2	4
S	2	2	1
S	2	2	2
S	3	3	2

Figure 25 *Mixed donor macrocycles for metal ion discrimination*

The gradual variation in properties along a series of closely related ligands can trigger a sudden change in coordination geometry for complexes of adjacent ligands. This has been termed a 'dislocation'. The occurrence of dislocations along a ligand series for different ions and can form the basis for discrimination between these ions.

The affinity of a particular macrocycle for some metal ions can be 'detuned' by appending bulky substituent groups to the macrocycle. Steric interaction of the bulky subetituent can prevent the macrocycle providing an acceptable coordination geometry to a metal ion with specific coordination requirements. Macrocycles such as (61) have been synthesised for this purpose.

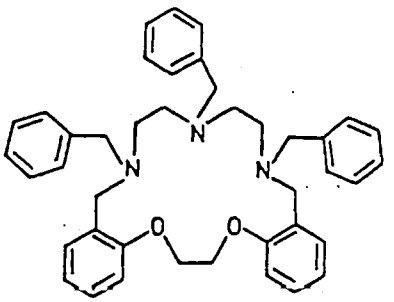

(61)

MONO-METAL ION CRYPTATES.

Various transition metal cryptates incorporating α-diimine binding groups have been synthesised by template methods. In all cases the transition metal ion is 6-coordinate and bound to three α-diimine groups. The synthesis of a cobalt(III) cryptate (5) from reaction of potassium tris-(dimethylglyoximato)cobaltate(III) and boron trifluoride etherate in ether was described by Boston and Rose.[12] The orange-red complex contains three dimethylglyoximate ions "capped" at both ends by BF groups. Iodide ion has been used to reduce the cobalt ion from 3+ to the 2+ oxidation state while leaving the cage ligand intact.[166] In the complex, the N6 coordination polyhedron has D_3 symmetry and is only slightly distorted from trigonal prismatic geometry.[167] Electrochemical studies of the cryptate have been carried out and Co(I) species were generated electrochemically.[168]

Synthesis of the analogous Fe(II) cryptate was reported. Both BF_3 and boric acid in n-butanol have been used to cap the cage ligand. Use of boric acid gives hydroxy or alkoxy substituents, which are derived from solvent, on the boron capping atoms.[169,170]

The cage-like nature of the product has been established by X-ray diffraction. The stereochemistry about iron (II) is intermediate between a trigonal prism and a trigonal antiprism, the twist angle being 16.5°. Attempts to oxidise the complex chemically to an iron (III) cryptate were not successful, and led either to decomposition products or no reaction. Oxidants used included Br_2, I_2, O_2, H_2O_2, Ce(IV) and Cu(II). Attempted synthesis of the analogous Ni(II) cryptate failed.

Holm and co-workers developed a more general synthetic procedure leading to a series of 6-coordinate divalent transition metal cryptates.[171,172]

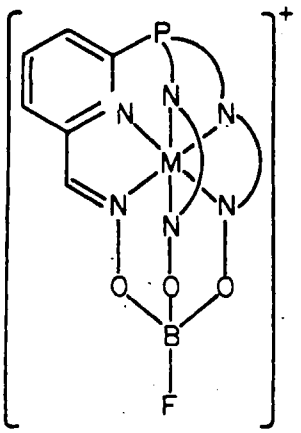

(62)

The approach used by Holm features the synthesis of a trigonally symmetric hexadentate ligand with a phosphorous bridgehead and three oxime parts. Following coordination to a metal ion Fe(II), Co(II), Ni(II) or Zn(II), a cryptate (62) is formed by treatment with BF_3 or BF_4^-. The cage ligand is designed to encapsulate and impose a trigonal prismatic or near trigonal prismatic geometry on the first row transition metal ions. However, two factors may prevent the attainment of trigonal prismatic coordination. The metal ion may have a configuration that favours an alternative stereochemistry or the metal ion may be larger or smaller than the cavity of the cryptand. The X-ray structure of the nickel cryptate has been reported[173] and shows the stereochemistry about the nickel ion to be almost trigonal prismatic (twist angle 1°35'). The Co(II) and Zn(II) cryptates[174] also have small twist angles whereas the low spin iron(II) complex has much larger twist angle.[175-176] An X-ray crystal structure shows the coordination sphere around the iron ion to be distorted by approximately 21.5° from trigonal prismatic geometry.[175]

Initially, it was suggested that the conformation adopted by the iron(II) complex was a compromise between trigonal prismatic geometry imposed by the ligand and the preference of the low spin iron ion for octahedral geometry due to the high crystal field stabilisation energy associated with a low spin d^6 ion. However, Churchill and Reis later concluded that ligand field stabilisation effects were more important in flexible ligand systems. The geometry of the metal coordination sphere in the series of rather rigid cage structures was consistent with being determined by relative sizes of metal ion and the cavity of the ligand. The iron(II) ion was said to be too small to fit the cavity without causing severe distortion towards octahedral geometry. The Ni(II) ion is close to ideal size but both Co(II) and Zn(II) are slightly too large and significant deviations from threefold symmetry are observed. The Ni(II) and Co(II) cryptates were reported to be high-spin, whereas the Fe(II) cryptate was essentially diamagnetic.

The non-occurrence of a Mn(II) derivative was said to be a size effect. Attempts to prepare the Cu(II) cryptate were also unsuccessful, presumably this is due to unfavourable spatial arrangement of reactive sites so that closure cannot be accomplished and/or unfavourable stability of the intermediate complex. A comparison of the properties of the cryptates and other complexes with trigonal prismatic or trigonal antiprismatic and intermediate stereochemistries has been made. Factors controlling the stereochemistry adopted have been discussed.[178]

Goedken and Peng have reported syntheeis of metal ion cryptates (63) in a metal ion directed condensation of butane-2,3-dihydrazone with formaldehyde.[180] Metal ions Fe(II), Co(II) and Ni(II) were successful as template species, however both Zn(II) and Mn(II) failed to give cyclisation

products under similar conditions. The low spin Fe(II) cryptate was found to be highly stable in acidic solution.

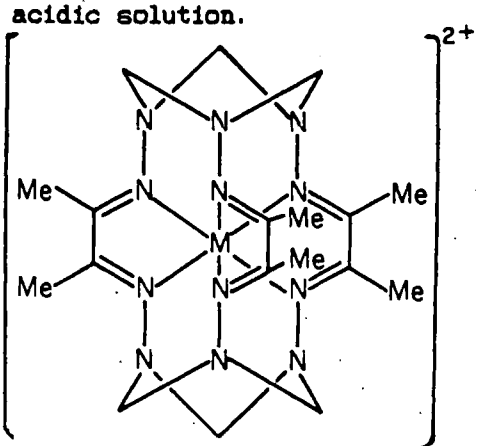

(63)

Elegant examples of the use of the template method can be found in the synthesis of macrobicyclic cobalt amine complexes by Sargeson and coworkers.[101] A wide variety of mononucleating cage ligands incorporating amino nitrogen donors have been reported.[21,102,103] Metal ion cryptates were synthesised by reaction of inert metal ion complexes such as $[Co(en)_3]^{3+}$ (en = ethylenediamine) with formaldehyde and ammonia in basic solution; a 95% yield of the cobalt(III) complex (64) was reported.

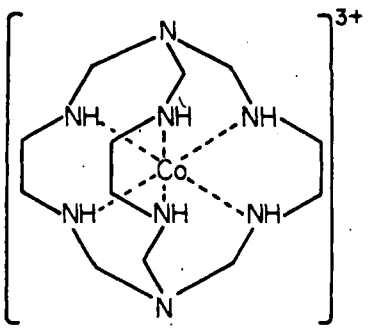

(64)

An X-ray crystal structure demonstrates the macrobicyclic nature of the product and shows that the cage contains six nitrogen donor atoms and two aza caps which are not bonded to the metal ion. The mechanism of the reaction is shown in scheme 18.

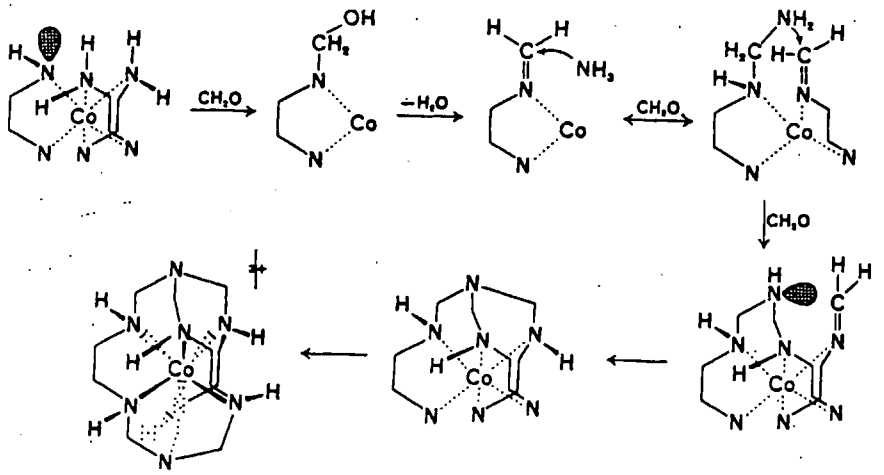

Scheme 18 *Proposed synthesis of [Co(III)Sepulchrate]$^{3+}$ ion*

Synthesis occurs with retention of chirality of the $[Co(en)_3]^{3+}$ ion. The electron self exchange rate for Co(III)/(II) sepulchrate was found to be 10^5 times higher than that for the parent $Co(en)_3$III/II couple.[194,195] The increase in the electron self exchange rate for cobalt within the cryptate has been explained on the basis that the cavity of the cage is slightly too large for Co(III) and a little too small for Co(II) and the transition state may be stabilised within the cryptand.

Template condensation reactions involving inert metal complexes of rhodium(III),[196] iridium(III)[196] and platinum(IV)[197,198] with formaldehyde and ammonia have been reported to give analogous cryptates. The yield of cryptate varied from around 40% for the iridium and platinum cryptates to 90-100% for the rhodium cryptate

In the platinum and rhodium cryptates, the cage ligand was found to stabilise unusual oxidation states of the metal. Platinum(III) transients have been detected by esr spectroscopy. The rare mononuclear Rh(II) ion is stabilised within the cage. Reductions of Rh(III) amine complexes are normally irreversible processes. The Rh(II) intermediates dimerise, disproportionate and/or undergo further reductions to square planar Rh(I) species.

Use of nitromethane in place of ammonia produces an analogous cage with carbon atom caps and nitro substituents.[189]

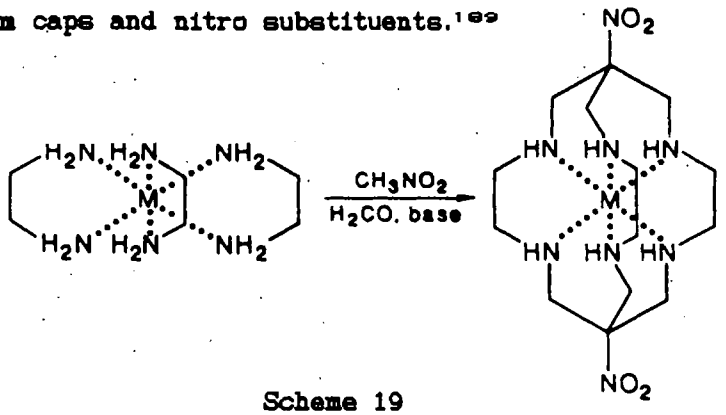

Scheme 19

The carbon capped derivative 'sarcophagine' (65) is more stable toward disruption of the cage than is the N-capped 'sepulchrate'cage (64).

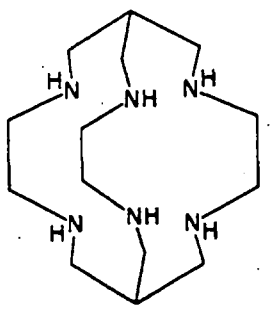

(65) *Sarcophagine*

Furthermore, functional groups with varied electron withdrawing or electron donating powers can be attached to the carbon cap.[190] Numerous substituents have been documented, including $-NH_2$, $-NH_3^+$, $-N(CH_3)_3^+$, $-NH_2NH_3^+$, -NHOH, -NO, $-NO_2$, OH, Cl, Br, I, COOH, COOR, $NHCOCH_3$, $-CONH_2$, CN, CH_2OH and $NHCOCH_3$. Cryptands with different substituents on either cap have been obtained. These substituents lead to wide variation in the redox potential of the encapsulated cobalt ion, a span of at least 0.6V has been reported.[190] The Co(III)/Co(II) redox couple for the cryptates was reversible however reduction to Co(I) or the metal was irreversible and caused cage rupture.[191]

The extent of variation of redox potential with substituent is surprising in view of the distance of the substituent from the metal ion and implies relatively close communication between the apical substituents and the metal centres. This communication is also reflected in the NMR chemical shifts of the apical C atoms and the large coupling constants with the encapsulated metal ion.[190,192] In addition, several of the apical substituents introduced provide means of coupling the cage to other molecules. As a result dimer cages such as (66) have been synthesised and the cage ligands have also been attached to polymers to provide chiral ion exchange columns.[190]

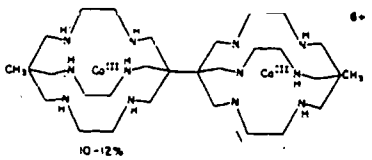

(66)

Asymmetrical cages have been obtained by stepwise capping processes as shown in scheme 20.

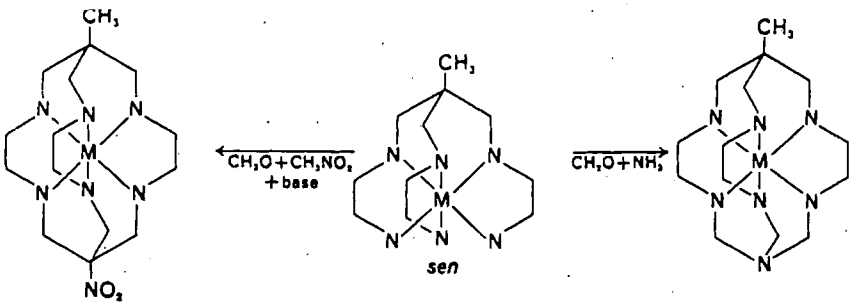

Scheme 20

The nitrogen donor sites of cryptands have been derivatised by treatment of Co(III) cage complexes with H_2O_2 in basic solution.[193] This results in oxidation of up to three coordinated N sites to hydroxylamine groups. Three complexes (figure 26) were isolated by ion exchange chromatography and the site of oxidation in one of the products was established by an X-

ray structure determination. Deprotonation of the hydroxyl substituents had substantial effect on the redox properties of the caged metal ion.

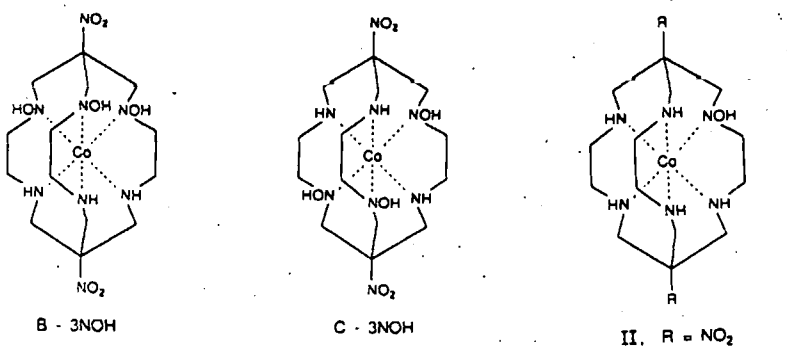

Figure 26

The synthetic method was extended to formation of cryptates with different cavity size in order to modulate redox potential of the metal ion and investigate the effect on rates of electron transfer reactions. The use of alternative chelating amines in inert metal-amine complexes has provided a range of cavity sizes.

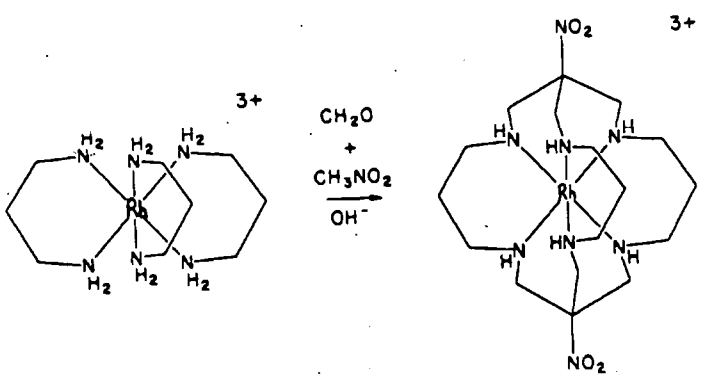

Scheme 21 (70)

The rhodium cryptate (70) obtained from reaction of tris(1,3-propane diamine)Rh(III) with formaldehyde and nitromethane has provided a cryptand with larger cavity which resulted in stabilisation of the rhodium(II) state by approximately 0.4V relative to that found for the rhodium complex of the equivalent 1,2-ethanediamine based cryptand.[69] The

more rigid cryptate (71) was synthesised by reaction of (R,R or S,S) Co(trans 1,2 cyclohexanediamine)$_3$ with formaldehyde and nitromethane.[179]

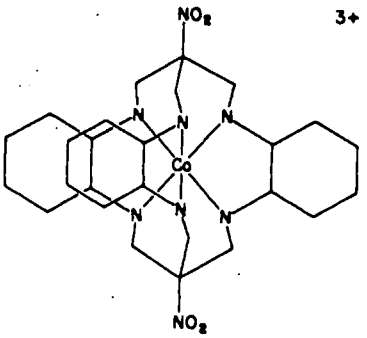

(71)

The cryptate (71) was found to be configurationally and conformationally rigid and substitutionally inert in both Co(II) and Co(III) oxidation states. As a result the cryptate was suitable for the investigation of Co(II)/Co(III) outer-sphere electron transfer processes. The Co(III) cryptate of (72) was synthesised recently by Hendry and coworkers.[195] As a result of the methyl substituents' preference for an equatorial position on the chelate rings, the cryptate has stabilised chelate ring conformations.

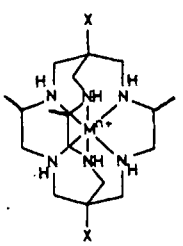

(72)

Tripod amine complexes of cobalt(III) have been used in cryptate synthesis. The Co(tach)$_2^{3+}$ ion, on reaction with formaldehyde and nitromethane under basic conditions, produces the cryptate shown in scheme 22.[196]

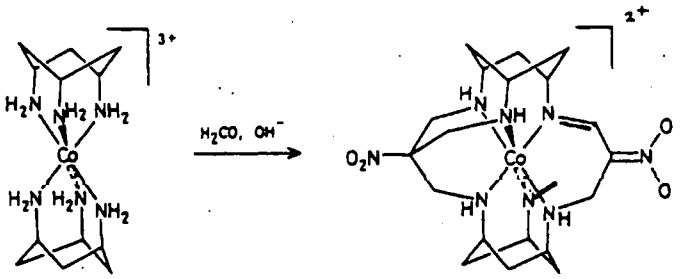

(73)

Scheme 22

In cryptate (73), a carbanion is stabilised by delocalisation and an amine site is methylated. The ligand is relatively rigid and has larger cavity than those produced from $Co(en)_3$, resulting in greater stabilisation of the Co(II) oxidation state relative to Co(III).[135]

The closely octahedral complex, Co(tame)3+ gives a mixture of products on reaction with formaldehyde and nitromethane in basic solution.[197] Four major products were isolated by ion exchange chromatography and are shown in figure 27.

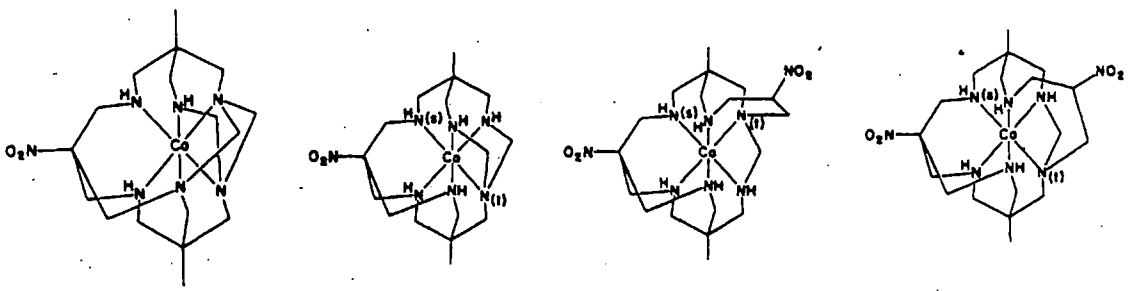

Figure 27

A crystal structure determination was carried out on a major product of the reaction which was obtained in 10% yield. The crystal structure shows a macrotetracyclic cryptate containing three fused four-membered rings, all of which are fused to the six-membered rings of the cap.The three fused four membered rings result in distortions of 16-21° from octahedral values

for five of the N-Co-N angles.[197] Another of the cryptates isolated is interesting as it has two highly strained 4-membered rings on one side and the nitromethane cap on the other side of the cryptate. As a result the N6 coordination sphere is severely distorted from octahedral geometry which is unusual in Co(III) amine chemistry. In addition, the cryptate shows the lowest reduction potential observed in Sargeson's Co(III) cryptates, presumably due to ring strain effects that would inhibit generation of the larger Co(II) ion.[198] The redox properties of the macrotricyclic hexaamine Co(III) complexes have been investigated.[199]

An alternative approach leading to asymmetric cryptates has been used by Sargeson and coworkers and is illustrated below. The synthetic method involves synthesis of a pendant arm macrocycle (78), followed by oxidation of a mixture of the macrocycle and Co(II) to give the Co(III) complex, and finally ring closure using formaldehyde and ammonia or nitromethane to give the corresponding macrotricyclic cage complex (79).[199]

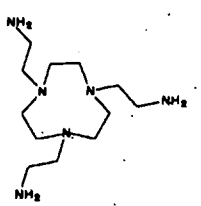

(taetacn)

(78)

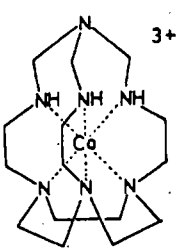

(79)

Cryptates containing both nitrogen and sulphur donor atoms have been synthesised by a similar approach as shown in scheme 23.

An X-ray crystal structure of the cryptate shows octahedrally coordinated Co(III).[200]

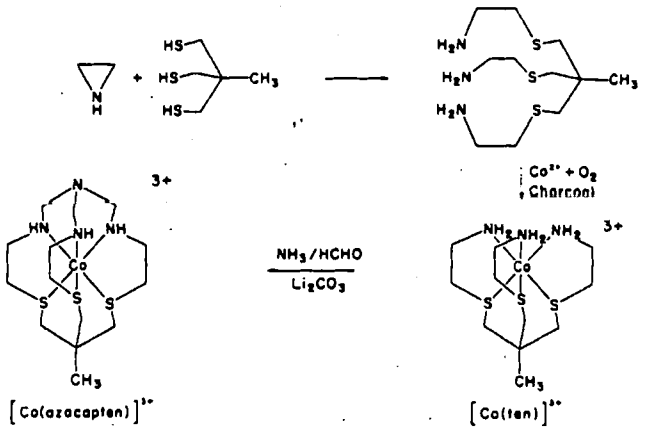

Scheme 23

A similar method has been applied to the synthesis of the pendant arm cryptates, (80) and (81) as shown in scheme 24.[201,202]

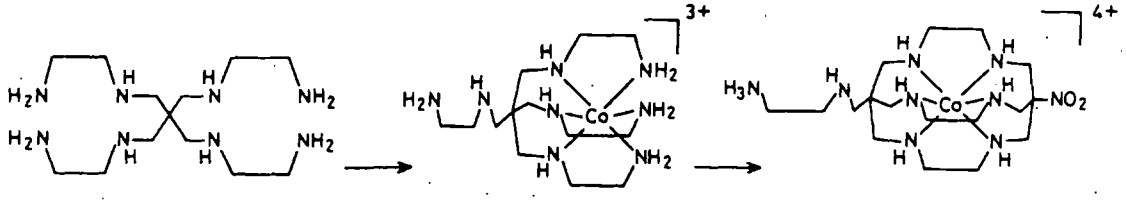

Scheme 24 (80)

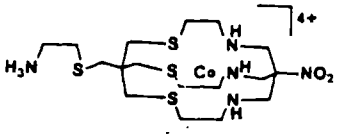

(81)

A cryptate (82) which has a smaller cavity has been obtained by a rearrangement of the parent crypate as shown below.

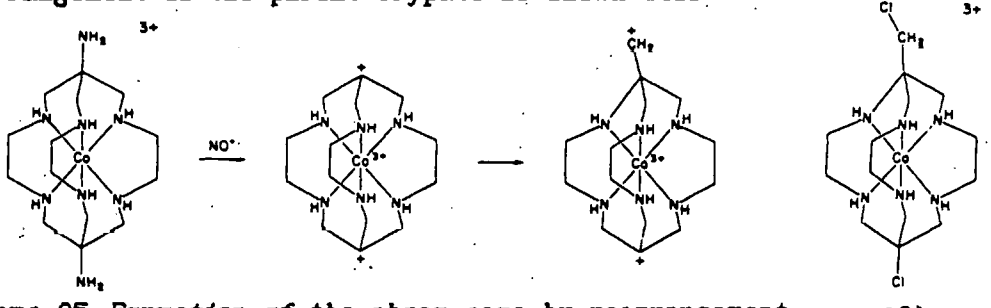

Scheme 25 *Formation of the absar cage by rearrangement* (82)

Recently Sargeson has reported the synthesis of a pyruvate imine Co(III) complex which has been used in cryptate synthesis. A variety of new cryptates were obtained as shown in scheme 26.[202]

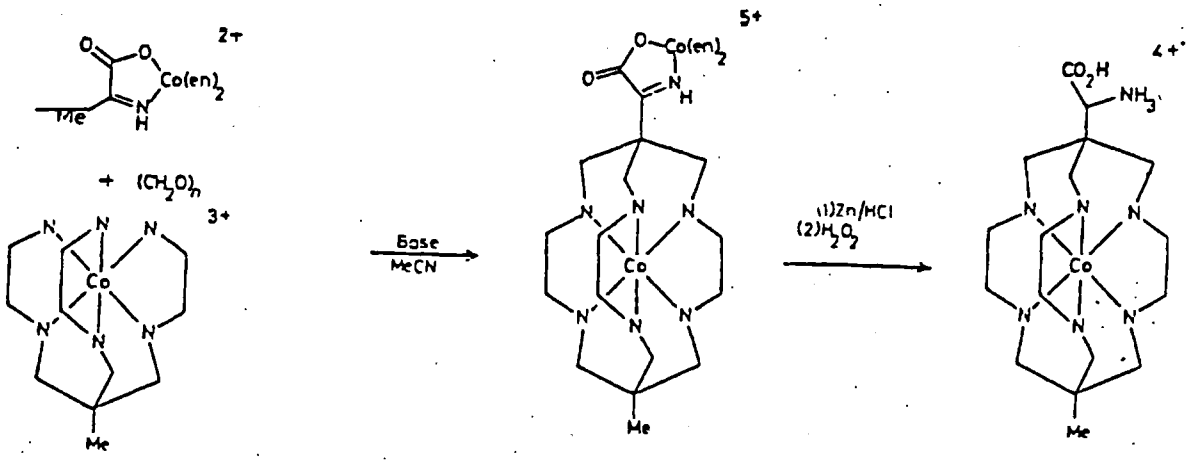

Scheme 26

A limitation of the synthetic strategy employed by Sargeson and coworkers is that inert metal-amine complexes are required for reaction. Attempts to carry out analogous syntheses with more labile trien complexes have given very poor yield of cryptate. A yield of less than 1% has been reported for Ni(II) sepulchrate formed by the template approach. The crystal structure of the complex has been determined, and shows the octahedrally coordinated Ni(II) ion.[204] Condensation about Cu(II) gave a range of macrocyclic products though the cryptate was not obtained. However, the metal-free sarcophagine cryptand has been obtained by treatment of the cobalt(II) cryptate with concentrated HCl or HBr at high temperature(130-150°C).[205]

Many of the cryptates, particularly the N capped cages do not withstand this metal ion removal process. However, recently removal of the Co(II) ion from cryptand (72) was achieved in concentrated NaCN solution.[195] The free macrobicyclic sarcophagine ligand (65) encapsulates a wide range of labile metal ions,[206] including Mg^{2+}, Ti(IV), V(IV),(III), Cr(III), Mn(III),(II), Fe(III),(II), Ni(III),(II), Cu(II), Zn(II), Cd(II),

Hg(II), Ag(II), Ga(III) and In(III). The redox span obtained for the metal ion couples of the sar complexes is approximately 2V , ranging from about +1V to -1V. Redox couples occur at intervals of 0.1V using the sar cage or di(NH_2) substituted sar cage, providing an impressive array of redox reagents.

Electron transfer reactions of encapsulated Ru, Mn, Fe, Ni sarcophagine cryptates have been investigated. Estimates of the self-exchange rate constants for the M(sar)2+/3+ redox couple have been interpreted in terms of known structural and kinetic data for the complexes. High rate constants were found where there was little reorganisation of the metal coordination sphere involved in the redox process.[207] The relatively low value for the rate constant for Mn cryptates reflects the large structural differences between the Mn(II) and Mn(III) complexes. The X-ray structure determinations of Mn(II)(sar) and Mn(III)(sar) reveal a trigonally twisted coordination around Mn(II) and a strongly Jahn-teller distorted coordination around Mn(III).[208]

Various practical applications have been investigated for Sargeson's cryptates. Cobalt (III) sepulchrate was reported to produce hydrogen from water after single electron reduction in an electrochemical process in which the cryptate acts as an electron relay.[209] Encapsulation of a copper radionuclide within the sarcophagine cage has provided a kinetically inert and aqueous soluble complex, this has been coupled to monoclonal antibodies for use in imaging or treatment of tumours.[210]

A considerable amount of work has been reported on the ruthenium sarcophagine cryptate.[211-213] The complex is of particular interest because of the potential of ruthenium complexes as photosensitisers in significant processes such as reduction of water or carbon dioxide and in

catalysis of oxidation processes. The ruthenium(II) cryptate was obtained by metal insertion into the free sarcophagine cage using the remarkably labile $Ru(DMF)_6(CF_3SO_3)_2$ complex.[211]

The pale yellow cryptate was extremely sensitive towards oxidants. Thermodynamic and kinetic parameters of ruthenium sar have been studied and the autooxidation of Ru(sar)2+, involving H atom transfer to O_2- has been investigated by elecrochemical and spectrophotometric techniques.[212] The sar ligand, when coordinated to Ru(III) (83), rapidly undergoes oxidative dehydrogenation to introduce an imine group into the cap of the ligand (84).[213] A stable ruthenium(II) hexaimine cryptate (85) has been obtained by successive two electron oxidations (85). Each imine group stabilises the Ru(II) state with respect to Ru(III) by approximately 0.15V.

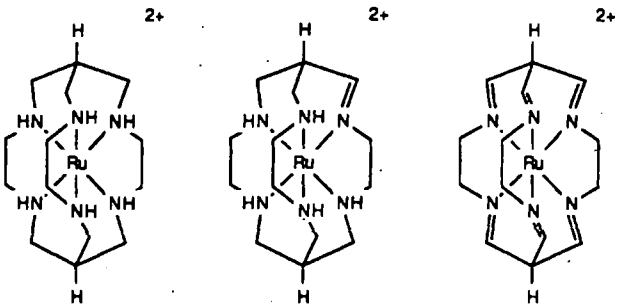

$Ru(sar)^{2+}$ $Ru(imsar)^{2+}$ $Ru(hexaimsar)^{2+}$

(83) (84) (85)

Although the photochemical properties of ruthenium complexes containing unsaturated nitrogen ligands have been extensively investigated, few ruthenium(II) cryptates incorporating unsaturated nitrogen donors have been reported. The polypyridine containing cryptate (86) shows extraordinary stability towards photodecomposition,[214] about 10^4 times higher than that of $Ru(bpy)_3^{2+}$. In addition encapsulation of the ruthenium ion enhances the excited state lifetime of the ruthenium ion.

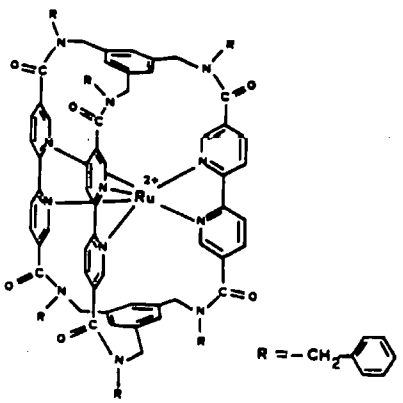

(86)

Various mono-metal ion cryptates have been obtained by organic synthesis of the cryptand followed by metal insertion. The small pentaza cryptand (87) has been used to form mononuclear cryptates of Cu(II), Ni(II), Co(II) and Zn(II). The X-ray crystal structure of the Cu(II) cryptate was determined and demonstrates that the Cu(II) ion is 5-coordinate and has distorted square pyramidal coordination within the cryptand. A similar thiaaza cryptand (88) was synthesised and its Cu(II) cryptate was described.[215] A marked inertness of the copper cryptates towards strong acids was noted.

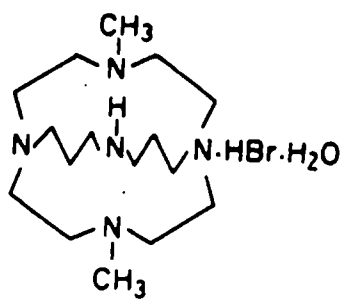

(87)

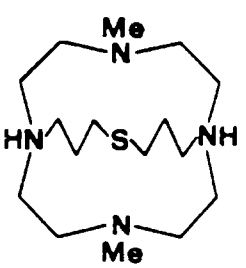

(88)

Several cage ligands have been designed to mimic the selectivity found in binding of Fe(III) by siderophores which mediate the uptake of Fe(III) by microorganisms. Ferric iron is bound by six catechol oxygen donors both in ferric enterobactin and in the synthetic analogues. The cryptand of complex (89) has been synthesised by two alternative routes, a template

method resulting in 90% yield and by high dilution techniques leading to 27% yield.[216-218]

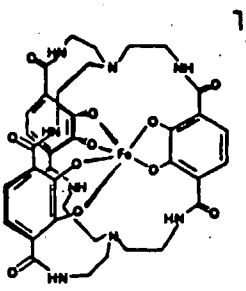

(89)

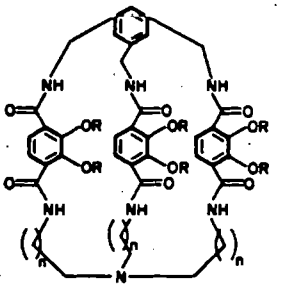

(90)

Vogtle and coworkers have reported the synthesis of a similar cryptand containing a larger bridgehead unit based on triphenylbenzene.[219,220] Asymmetrical ligands such as (90) have been obtained.[219]

A new synthetic cryptand siderophore (91), containing three endocyclic hydroxamate donor groups was recently reported by Martell.[221] The cage was prepared by tripodal coupling of a tris acid chloride with a tris O-benzylhydroxylamine. Complexes of Fe(III) and Ga(III) were prepared

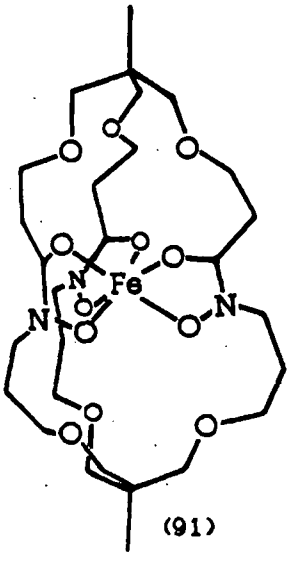

(91)

The selectivity of a series of cryptands (figure 28) for toxic metal ions has been investigated by Lehn and coworkers.[222] High selectivity for

complexation of toxic metal cations Cd^{2+}, Hg^{2+} and Pb^{2+} with respect to biologically important cations (Na^{+}, K^{+}, Mg^{2+}, Zn^{2+}) was achieved by manipulation of the structural parameters of cavity size and the nature of the binding sites.

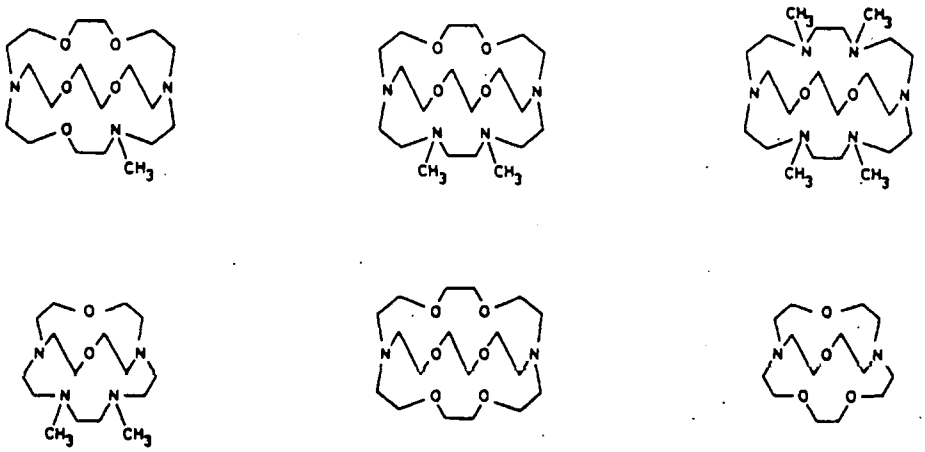

Figure 28

The N_4O_4 cryptand was found to have selectivity for cadmium, mercury and lead ions with respect to zinc(II) as high as 10^{6},10^{18} and 10^{9} respectively, which is of obvious interest in detoxification, either in the body or in environmental depollution.

Stability constants of the cryptands, shown above, have also been measured with alkali or alkaline earth metal and transition metal ions. The stabilities and selectivities for group 1 and group 2 cations decreased as the number of N donors in the cryptand increased. Remarkably strong complexation properties towards transition metal ions were observed in the N4O4- donor cryptand. The intramolecular cavity of N3O5, N4O4 and N6O2 is too large for the small cations Co^{2+},Ni^{2+},Zn^{2+} and the complexes formed are weak, however these cations are strongly complexed by the smaller N4O4 cryptand.

Several mononuclear cryptates of lanthanide ions have been reported. These are included in the following section.

MACROCYCLIC COMPLEXES AND CRYPTATES OF LANTHANIDE IONS.

In view of the similarities between lanthanide (III) ions and group (11) metal ions, such as their relatively 'hard' character and the often electrostatic nature of their bonding, it is not surprising that lanthanide ions are effective template species for Schiff-base macrocycles. The synthesis of Schiff-base macrocyclic complexes of lanthanide ions has recently been reviewed by Fenton and Vigato.[55] The synthesis of a Schiff-base macrocycle employing a lanthanide template ion was first reported in 1979. The reaction of 1,2 diaminoethane with 2,6 diacetylpyridine on La(III) or Ce(III) gave the 2+2 macrocycle (92) whereas the heavier lanthanides were found to be ineffective as templates for the 18 membered ring.[223,224]

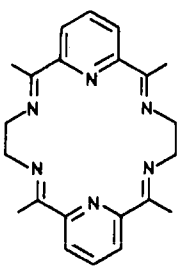

(92)

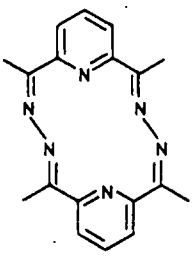

(93)

More recently though this work was reinvestigated and complexes of (92) with all of the lanthanides, except promethium which is radioactive, were obtained. It was found that the ease and yield of the synthesis depended on the counterion present, good oxygen donor anionic ligands such as acetate were found to favour the reaction to a greater extent than chloride or perchlorate.[225] Lanthanide complexes of (92) have also been obtained by transmetallation of the barium complex.[226] The lanthanide complexes of (92) were resistant to hydrolysis and ^1H NMR experiments indicated marked stability towards dissociation in D_2O unlike the

corresponding lanthanide complexes of cyclic polyethers. In addition, typical precipitating agents for Ln ions, such as fluoride or hydroxide ion do not remove the lanthanide ion from the complex. Recently a lanthanum Schiff-base macrocyclic complex of (92) was shown to be an effective catalyst for the hydrolysis of the phosphate ester 2,4-dinitrophenyl diethyl phosphate.[227] The complex has potential as a model system for metallo-phosphatase enzymes and as a catalyst for detoxification of anticholinesterase agents used in chemical warfare. The complex is kinetically stable to dissociation in water. The crystal structure has been reported.[227] Lanthanide (III) ions (Tb, Dy, Ho, Er, Tm, Yb, Lu) were effective in template synthesis of the 14- membered macrocycle (93)[55,228]. The complexes of the 14 membered macrocycle were susceptible to hydrolysis.

The large ionic radius of the lanthanides combined with the elecrostatic nature of their bonding with ligands lead to high coordination numbers in their complexes.[229] The X-ray structures of complexes of (92) show a steady decrease in coordination number from lanthanum to lutetium La=12, Ce=11, Nd=10, and Lu=9.[226,230,231] Similar trends have been noted in lanthanide complexes of cyclic polythers.[229,231] The lanthanide ions, except promethium, have been used as template ions in the synthesis of macrocycle (94).[232]

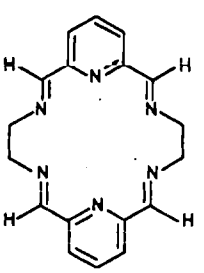

(94)

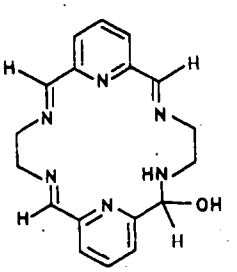

(95)

The lighter lanthanides La-Pr and Eu gave complexes of macrocycle (94) whereas the heavier lanthanides (Nd-Lu, except Eu and Pr) gave complexes in which a water molecule had added across an imine bond of the macrocycle affording a carbinolamine species (95). The resultant increase in flexibility of the macrocycle makes it capable of accomodating the smaller lanthanide ions. The X-ray crystal structure of the Pr complex of (96) was reported by Bombeiri.[232] The praesodymium ion was 11 coordinate, using the six macrocyclic donors, two bidentate nitrates and a methanol molecule.

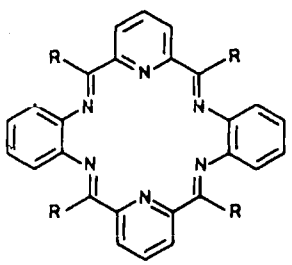

a; R = Me

(96)

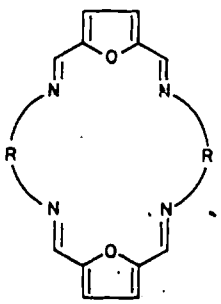

(97)

Schiff-base 2+2 macrocycles containing furan head units such as (97), have been obtained using Ln template ions.[235] The lanthanum complex has been transmetallated to give the dicopper (II) complex. Macrocyclic 2+2 complexes derived from phenols have been produced by template on lanthanides and ring contractions on use of smaller lanthanide template ions have been observed.[236]

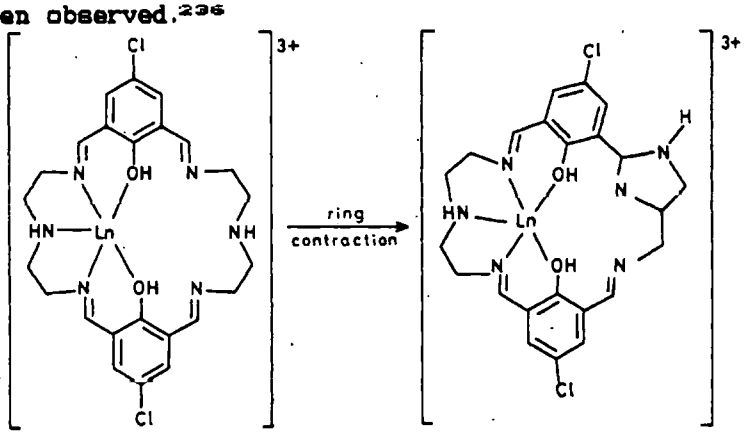

Figure 29 *Ring contraction of lanthanide complexes*

Homo and heterobinuclear lanthanide (III) complexes of macrocycle (98) were reported recently.[237]

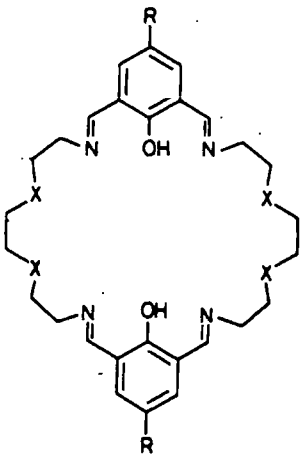

(98)

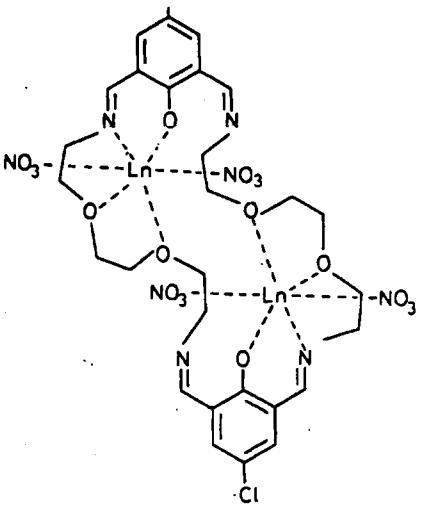

(99)

The heterobinuclear complexes (99) were obtained by an *in situ* prodedure involving synthesis of the macrocycle and successive addition of the lanthanide ions Ln and Ln' where (Ln,Ln' = La,Sm; La,Gd; La,Eu; Gd,Eu; Gd,Tb; Eu,Tb among others). Data presented supports the formation of heterobinuclear species but does not prove it unambiguously. Fast atom bombardment mass spectroscopy of the heterobinuclear complexes was not reported.

Pyridine containing 1+1 macrocycles such as (100), have been synthesised by template reactions on lanthanides. The diamino reactant generally contains several O or N donors in addition to the primary amino[238] groups providing high coordination number at the metal centre. The 1+1 complexes readily precipitate metal hydroxide on dissolution in water.

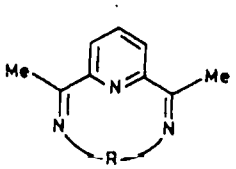

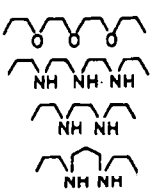

(100)

The first preparation of a lanthanide cryptate was reported in 1977 by Gansow and coworkers.[239] Cryptates of the tripositive ions lanthanum, praesodymium, europium, gadolinium and ytterbium were obtained by metal insertion into Lehn's polyether cryptands 2:2:1 and 2:2:2. The europium and gadolinium cryptates exhibited kinetic stability in water and were claimed to be the first truly substitutionally inert lanthanide complexes. As a result, the $Gd(2:2:1)_{2+}$ is of use as a T_1 shiftless relaxation reagent for NMR spectroscopy.[240] Electrochemical studies revealed that encapsulation of the europium ion had remarkable effect on the Eu(III)/Eu(II) redox couple. The $Eu(2:2:1)^{3+/2+}$ shows reversible electrochemistry, unlike the aqueous Eu(III)/(II) couple.[239] The 2+ oxidation state of europium was stabilised relative to the 3+ when encapsulated in the 2:2:1 cage. Since this initial paper, the study of the lanthanide cryptates of Lehn's polyether cryptates has been extended to include electrochemical studies of the europium 2:2:2 cryptate and ytterbium cryptates of both 2:2:2 and 2:2:1.[241,242,243]

The effects of varying the metal oxidation state on cryptate thermodynamics and kinetics have been investigated. The stability constants of lanthanide cryptates have been measured in various solvents using a variety of methods,[240,244,245] in aqueous solution using pH titration methods,[246] in dimethylsulphoxide using visible spectroscopic techniques,[247] in propylene carbonate by electrochemical methods.[248]

Electrochemical studies have also been used as a probe for the degree of shielding of the lanthanide ion from interaction with solvent in polyether cryptates.[249] The inclusive nature of the polyether cryptates of La^{250} Eu^{251}(b), Sm^{252} and Nd^{253} has been demonstrated by X-ray crystal structure determinations. The lanthanum ion was 12 coordinate, whereas

the others were ten coordinate complexes. All of the donor atoms in the cryptand were found to coordinate to the lanthanide ion and in addition nitrate or perchlorate anions were able to coordinate to the metal through the strands of the cryptand.

A ytterbium(III) cryptate of a small polyamine cage ligand (101) was obtained by template synthesis on ytterbium using the tripod amine $N(CH_2CH_2NH_2)_3$ and bis(dimethylamino)methane. The major products of the reaction were pendant arm macrocyclic complexes and the cryptate was a minor product isolated from the mother liquor.[254]

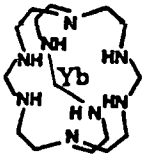

$(CF_3SO_3)_3{\cdot}CH_3CN$

(101)

Several cryptands that incorporate heterobiaryl groups have been synthesised recently by Lehn and coworkers. Generally the symmetrical cryptands were synthesised by template on Na+ or Li+ by reaction of the dibromo derivative of the biaryl with ammonia in the presence of base. Conditions of high dilution were not required, presumably due to the templating role of the cation and the rigidity of the bridges introduced. Asymmetric cryptands were obtained by a stepwise procedure involving reaction of a dibromo compound with a preformed macrocycle in the presence of Li+ and base. Transmetallation afforded the corresponding lanthanide cryptate. A wide variety of heterobiaryl groups have been incorporated into the ligands including 2,2-bipyridine,[258] bithiazole,[256] bisimidazole,[256] 1,10-phenanthroline,[255] bipyrimidine[256] and bipyrazolyl[257]. Some examples are illustrated in figure 30. Photoactive europium and terbium cryptates that display strong luminescence were

obtained and are of interest both as new luminescent materials and as labels for time-resolved photo-immunoassays. The heterobiaryl groups act as light absorbers and the energy of the singlet excited state S_1 is transferred in a radiationless process through the triplet state T_1 to the resonant level of the lanthanide ion. As the metal ion is protected by the cryptand from radiationless deactivation by solvent molecules it emits its characteristic visible light, red from europium and green from terbium.[260]

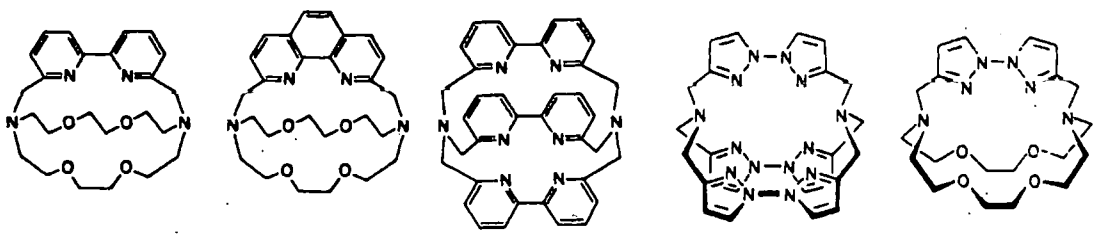

Figure 30

More recently, a europium cryptate containing heterocyclic N-oxide groups (102), was synthesised and was found to be particularly strongly luminescent.[261] However, cryptates incorporating the 3,3-biisoquinoline unit (103) gave only weakly luminescent cryptates as this aromatic group is itself strongly fluorescent and loses its excited-state energy by light emission.[261]

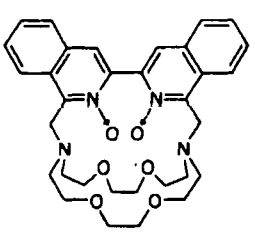

(102)

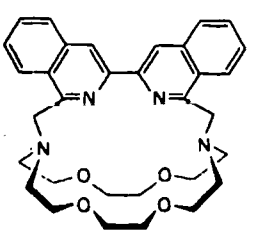

(103)

Although metal ion complexes of cryptand ligands have received most attention, interest in protonated cryptands as anion receptor molecules is growing.

ANION RECEPTOR MOLECULES

Protonated polyamines represent the most extensively studied coordinating ligands for binding inorganic as well as organic anions.[262-264] The area has been recently reviewed.[266] Protonated forms of bistren form stable inclusion complexes with anions.[266]

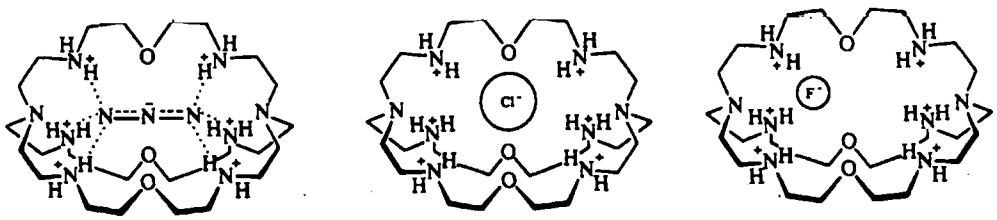

Figure 31 *Anion cryptates of Bistren*

Crystal structure determinations of the hexaprotonated ligand with F-,Cl-,Br- and N_3^- have been reported. Ligand distortions on binding small spherical anions in the ellipsoidal cavity are apparent. However the linear azide anion complements the cavity of the cryptand and is bound by two pyramidal arrays of three hydrogen bonds each interacting with a terminal N-atom of the anion, as represented in (54).[267] The formation constants of the complexes formed by hexaprotonated bistren with a range of anions (nitrate, carboxylate, ATP^{4-},ADP^{3-}, sulphate for example) have been determined. Strong complexations were found accompanied by marked electrostatic and structural effects on stability and selectivity. The binding of chloride ion by protonated polyamine macrocycles and cryptand has been investigated by ^{35}Cl-NMR spectroscopy.[268]

A new octaaza cryptand (104), which has a more spherical cavity than bistren has been synthesised by Lehn and coworkers. The hexaprotonated cryptand formed a fluoride cryptate and the X-ray crystal structure of this was determined. The crystal structure shows that the secondary nitrogen atoms are protonated and the fluoride anion is hexacoordinated to the six ammonium sites in a quasitrigonal-prismatic geometry.[269]

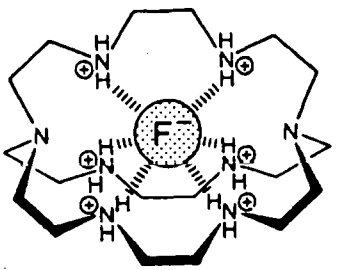

(104)

Crystal structure determinations of chloride and ammonium ion complexes of a spheroidal macrotricyclic ligand (105) have been reported.[270]

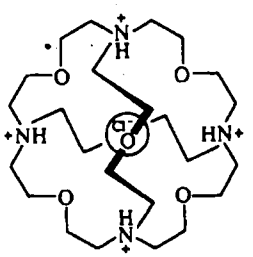

(105)

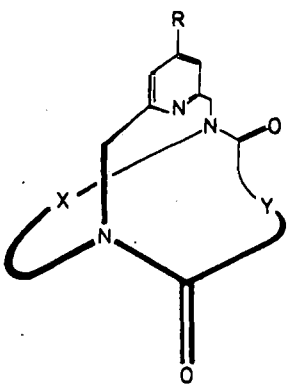

X	Y	R
$CH_2[CH_2OCH_2]_2CH_2$	$[CH_2]_{10}$	OMe
$CH_2[CH_2OCH_2]_3CH_2$	$[CH_2]_{10}$	OMe
$CH_2[CH_2OCH_2]_2CH_2$	$[CH_2]_{10}$	H
$CH_2[CH_2OCH_2]_2CH_2$	$[CH_2OCH_2]_3$	H
$CH_2[CH_2OCH_2]_3CH_2$	$[CH_2]_{10}$	H

(106)

A series of interesting cryptands (106) have been synthesised recently with the aim of increasing or altering the selectivities of standard reagents (acids and bases, reagents for oxidation or reduction) in organic chemistry. The use of concave pyridine ligands as protonating agents in a regio- and stereoselective protonation of nitronate anions is reported.[271]

CHAPTER 2

EXPERIMENTAL

Preparation of first transition series metal triflate salts.

Transition metal triflates, $M(CF_3SO_3)_2 : 6H_2O$, were prepared by reaction of transition metal carbonate with aqueous trifluoromethanesulphonic acid (triflic acid).

$$MCO_3 + 2CF_3SO_3H \rightarrow M(CF_3SO_3)_2 + CO_2 + H_2O$$

Iron(II) triflate was prepared, both by the above method and by reaction of iron powder with triflic acid.

$$Fe + 2CF_3SO_3H \rightarrow Fe(CF_3SO_3)_2 : 6H_2O + H_2$$

The following method was used to prepare Manganese, Nickel and Cobalt triflates.

Deionised water(5-10ml) was added to metal carbonate (0.05mol) Triflic acid 2M solution (0.1mol 50ml) was added dropwise with caution. The mixture was stirred at room temperature until fizzing had stopped and was filtered. The filtrate was reduced in volume by heating gently and the solid obtained was dried *in vacuo*. (Yield 60-85%)

Infrared spectrum :*inter alia* ν(O-H) 3504(br), $\nu(CF_3SO_3)$ 1246(s), 1189(s), 1035(s) and 642cm^{-1}.

Transition metal carbonates (M = Mn, Co) were prepared by anion exchange with sodium carbonate in water.

$$M(NO_3)_2 + Na_2(CO_3) \rightarrow MCO_3 \text{ (s)} + 2NaNO_3$$

Iron triflate $Fe(CF_3SO_3)_2 : 6H_2O$

This experiment was performed under nitrogen.

Triflic acid 2M (0.06mol 30ml) was deoxygenated and added in portions to $FeCO_3$ (0.06mol). The mixture was stirred for one hour at 50°C and was filtered to remove unreacted iron carbonate. The pale green filtrate was reduced in volume by bubbling nitrogen and heating. The solid obtained was dried with a nitrogen stream , dried *in vacuo* overnight and stored in a dessicator.(Yield 87%)

Iron triflate has also been prepared by reaction of triflic acid with iron powder. The reaction was carried out under nitrogen. Triflic acid 2M (20ml) was deoxygenated and added, with care, to a threefold excess of iron powder. The reaction mixture was stirred until fizzing had ceased, approximately one hour. The mixture was filtered to remove unreacted iron powder and the filtrate was brought to dryness by bubbling nitrogen. Pale green product solid resulted and was dried *in vacuo* overnight and stored in a dessicator. A yield of 88% was obtained.

$Cu(MeCN)_4CF_3SO_3$.

This experiment was performed under nitrogen and dry deoxygenated solvents were used throughout. Acetonitrile (30ml) was deoxygenated, cooled to room temperature and approximately 10ml of the deoxygenated solvent was added to Cu_2O (0.025mol). Concentrated triflic acid (0.06mol) was cautiously added to acetonitrile and the solution was added in portions to the copper oxide suspension. The reaction mixture was stirred at room temperature until the copper oxide had dissolved. The beige coloured solution was filtered and the filtrate was brought to dryness by bubbling nitrogen without heating. It is important to avoid heating the reaction

mixture, as heat caused disproportionation. The solid was dried *in vacuo* (yield 93%). The cream coloured product was stored under nitrogen.

$Cu(MeCN)_4CF_3SO_3$ was also prepared by an alternative method using deoxygenated 2M triflic acid, Cu_2O and a stoicheiometric amount of deoxygenated acetonitrile. Although more crystalline product results from this preparation, the product proved difficult to dry thoroughly and became blue on storage due to surface oxidation. It is necessary to avoid heating as heat caused disproportionation in this preparation.

$Cu(MeCN)_4ClO_4$

This complex was prepared by the method reported by Hemmerich and Sigwart.[272] The reaction was performed under nitrogen using dry deoxygenated solvents. Cu_2O (0.05mol) and acetonitrile (0.4mol 16ml) were refluxed in deoxygenated 2M $HClO_4$ until the copper oxide had dissolved, *ca* 2 hours. The white crystalline product formed on cooling and was filtered , washed with cold acetonitrile and dried under a stream of nitrogen. The complex was stored under nitrogen.

$Ba(CF_3SO_3)_2$

$Ba(CF_3SO_3)_2$ was prepared from barium carbonate and triflic acid by the method used for manganese ,nickel and cobalt triflates.

mer-[$RuCl_2(P(C_6H_5)_3)_3$]

This complex was prepared by the standard method.[272]

Triphenylphosphine (0.01mol 2.62g) was dissolved in 50ml of hot, dry deoxygenated methanol under nitrogen, giving a colourless solution. $RuCl_3:3H_2O$ (0.0025mol 0.65g) was added as a solid and the brown reaction mixture was refluxed with vigorous stirring for one hour. The product fell out of solution as a brown microcrystalline solid. Following cooling on ice, the product was filtered under nitrogen and washed with portions of dry deoxygenated methanol. After a final wash with dry ether the product was dried with a stream of nitrogen (91% yield).

TEMPLATE SYNTHESIS OF THE DILEAD COMPLEX OF MACROCYCLE P.

Template synthesis of the dilead complex of macrocycle P was previously reported by B.Murphy.[274]

The reactants 1,5-diaminopentane $NH_2(CH_2)_5NH_2$ and 2,6-diacetylpyridine (DAP) were obtained from Aldrich Chemical Company Ltd. and were used without further purification.

DAP Infrared spectrum *Inter alia*: 3070, 2970, 1705, 600cm^{-1}.

The macrocycle P

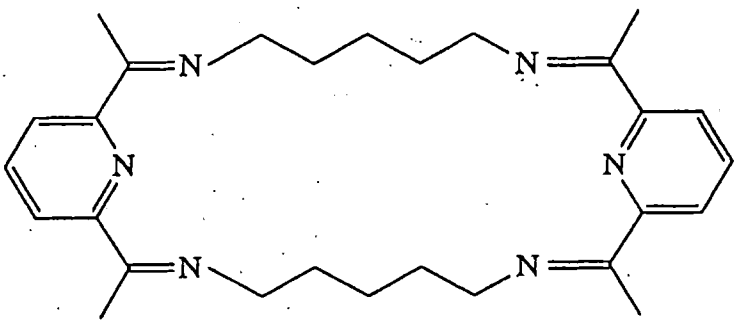

$[Pb_2P(NCS)_4]$ Template synthesis.

$Pb(NCS)_2$ (0.005mol) , diacetylpyridine (0.005 mol) and 1,5 diaminopentane (0.005mol) were stirred vigorously at 60°C in 600ml acetonitrile/ 200ml ethanol for 5 hours. The reaction mixture was filtered and the yellow filtrate was reduced in volume to *ca.* 600ml. Cooling and slow evaporation gave yellow crystalline product in 75% yield.

Analysis.

Calc:	C 34.8	H 3.5	N 12.7
Found:	C 34.7	H 3.7	N 12.4

$Pb_2P(CF_3SO_3)_4$: MeCN

$Pb_2P(NCS)_4$ (0.0005mol) was suspended in acetonitrile (150ml.) at 40°C. Addition of $AgCF_3SO_3$ (0.002mol) produced an immediate white precipitate. After stirring at 40-50°C for ½hr the AgNCS precipitate was removed by filtration. Excess $LiCF_3SO_3$ was added to the filtrate and this was reduced in volume to *ca.* 100ml Cooling and slow evaporation produced cream needle shaped crystals in 64% yield.

Analysis.

Calc:	C 27.04	H 2.74	N 6.49
Found:	C 27.21	H 2.83	N 6.43

Anion exchange did not occur when $LiCF_3SO_3$ was used in place of $AgCF_3SO_3$. The infrared spectrum of the complex showed νMeCN.

$[Pb_2P(NCS)](CF_3SO_3)_3$: $2H_2O$

$Pb_2P(CF_3SO_3)_4$ (0.0001mol) was suspended in acetonitrile (100ml) and warmed to 40-50°C. NaNCS (0.0001mol) was added and the reaction mixture was stirred at 45°C for 45 minutes. After filtration, the filtrate was reduced in volume. Ethanol (10ml) was added and cooling on ice produced cream semi-crystalline product (42%yield).

Analysis.

Calc:	C 27.18	H 2.99	N 6.93
Found:	C 27.66	H 3.05	N 6.69

This complex did not have infrared ν_{as}(NCS) absorption below 2000cm^{-1}

$[Pb_2P(NCS)](CF_3SO_3)_3$: EtOH

$Pb_2P(NCS)_4$ (0.0005mol) was suspended in acetonitrile (100ml) at 55°C. $AgCF_3SO_3$ (0.0015mol) was dissolved in acetonitrile (50ml) and added dropwise. After one hour at 55°C the reaction mixture was filtered and the filtrate was reduced in volume to *ca.* 20ml. Addition of ethanol, followed by cooling on ice gave cream coloured microcrystals (71% yield).

Analysis.

Calc:	C 28.67	H 3.11	N 6.88
Found:	C 28.36	H 3.02	N 6.57

This compound showed ν_{as}(NCS) absorption below 2000cm^{-1} in the infrared spectrum.

FAB Mass Spec.

m/e	Formula	% of base peak at 77.
666	$[PbP]^+$	(45)
724	$[PbP(NCS)]^+$	(25)
815	$[PbP(CF_3SO_3)]^+$	(50)
965	$[PbP(CF_3SO_3)_2+H]^+$	(5)
1079	$[Pb_2P(NCS)(CF_3SO_3)+2H]^+$	(5)
1139	$[Pb_2P(NCS)_2(CF_3SO_3)]^+$	(5)
1230	$[Pb_2P(NCS)(CF_3SO_3)_2]^+$	(15)

Throughout this chapter possible formulae of the fragment ions are suggested as above. The formulae have been calculated using the mass of the most abundant isotope of the atoms present. Where the mass calculated by this simple method does not exactly match the most intense peak of the cluster (the m/e value), the formula has been adjusted to match the m/e by suggesting protonation or deprotonation.

$[Pb_2P(NCS)_2](CF_3SO_3)_2$

$Pb_2P(CF_3SO_3)_4$ (0.0001 mol) was suspended in acetonitrile (75ml.) at 45°C. NaNCS (0.0003mol) was added and the reaction mixture was stirred at 50°C for 45 minutes. The solution was filtered and ethanol was added to the filtrate, which was then reduced in volume. Pale yellow microcrystalline solid resulted on cooling the solution on ice.

Analysis.

Calc:	C 29.86	H 2.97	N 8.70
Found:	C 29.45	H 3.00	N 8.93

This product has also been formed by the addition of two equivalents of $AgCF_3SO_3$ to the complex $Pb_2P(NCS)_4$.

FAB Mass Spec.

m/e	Formula	% base peak at 815.
664	$[PbP-2H]^+$	(70)
724	$[PbP(NCS)]^+$	(60)
815	$[PbP(CF_3SO_3)]^+$	(100)
1139	$[Pb_2P(NCS)_2(CF_3SO_3)]^+$	(40)
1230	$[Pb_2P(NCS)(CF_3SO_3)_2]^+$	(75)
1321	$[Pb_2P(CF_3SO_3)_3]^+$	(15)

TRANSMETALLATION OF $Pb_2P(NCS)_4$.

(a) Homobinuclear complexes of macrocycle P.

$[Cu_2P(NCS)_2](CF_3SO_3)_2 \cdot H_2O$

$Pb_2P(NCS)_4$ (0.0005mol) was suspended in 100ml ethanol at 55°C. $Cu(CF_3SO_3)_2$ was dissolved in ethanol (20ml) and added dropwise. The reaction mixture was stirred at 55°C for one hour and a blue-green solid was filtered off in 85% yield. Recrystallisation from an acetonitrile/ethanol solvent mixture gave microcrystalline product.

Analysis.

Calc:	C 37.75	H 3.96	N 11.01
Found:	C 37.62	H 4.26	N 11.33

$[Co_2P(NCS)_2 \cdot 2H_2O](CF_3SO_3)_2$

$Pb_2P(CF_3SO_3)_4$ (0.0005mol) was suspended in 100ml acetonitrile and warmed to 55°C. $Co(CF_3SO_3)_2$ was dissolved in ethanol (20ml.) and added dropwise. NaNCS (0.001mol) was added and the reaction mixture was stirred for 2-3 hours at 55°C. After filtration the filtrate was reduced in volume and cooling on ice produced black crystals in 33% yield.

Analysis.

Calc:	C 37.43	H 4.12	N 10.91
Found:	C 37.14	H 3.82	N 10.58

(b) Heterobinuclear complexes of macrocycle P.

$[PbMnP(NCS)_2](CF_3SO_3)_2 : 2H_2O$.

$Pb_2P(NCS)_4$ (0.0005mol) was suspended in acetonitrile (200ml) and warmed to 55°C. $Mn(CF_3SO_3)_2$ (0.002mol) was dissolved in ethanol (50ml) and added dropwise. The reaction mixture was stirred at 55°C for 3 hours. A precipitate of $Pb(NCS)_2$ was removed by filtration and the yellow filtrate was reduced to *ca.* 100ml. Slow evaporation gave yellow needle shaped crystals in 46% yield.

Analysis.

Calc:	C 32.82	H 3.62	N 9.57
Found:	C 32.74	H 3.32	N 9.38

FAB Mass Spec.

m/e	Formula	% of base peak at 986
512	$[MnP-H]^+$	(60)
664	$[MnP(CF_3SO_3)-2H]^+$	(30)
815	$[PbP(CF_3SO_3)]^+$	(45)
837	$[MnPbP(NCS)_2]^+$	(40)
927	$[MnPbP(NCS)(CF_3SO_3)-H]^+$	(35)
986	$[MnPbP(NCS)_2(CF_3SO_3)]^+$	(100)
1077	$[MnPbP(NCS)(CF_3SO_3)_2]^+$	(50)
1139	$[Pb_2P(NCS)_3]^+$	(5)
1230	$[Pb_2P(NCS)(CF_3SO_3)_2]^+$	(20)

$PbMnP(NCS)_3(O_2CCH_3)$: $3H_2O$.

$Pb_2P(NCS)_4$ (0.0005mol) was suspended in acetonitrile (100ml) and ethanol (100ml) solvent mixture and warmed to 55°C. $Mn(O_2CCH_3)_2{:}4H_2O$ (0.002mol) was added and after 3 hours at 55°C a small amount of brown powder was removed by filtration. The brown filtrate was reduced in volume and cooling on ice gave dark brown microcrystals in 45% yield. Esr spectral evidence suggests that this is a Mn(II) complex.

Analysis.

Calc:	C 39.32	H 4.70	N 12.50
Found:	C 39.59	H 4.41	N 12.06

FAB Mass Spec.

m/e	Formula	% of base peak at 895
460	$[P+2H]^+$	(70)
512	$[MnP-H]^+$	(40)
721	$[MnPbP]^+$	(20)
895	$[MnPbP(NCS)_3]^+$	(100)
949	$[MnPbP(NCS)_3(O_2CCH_3]^+$	(85)

$[PbNiP(NCS)_2](CF_3SO_3)_2$: $4H_2O$

$Pb_2P(NCS)_4$ (0.0005mol) was suspended in acetonitrile (200ml) at 55°C. A solution of $Ni(CF_3SO_3)_2$ (0.002mol) in ethanol (50ml) was added dropwise. After heating for 2 hours at 55°C , the reaction mixture was filtered to remove $Pb(NCS)_2$ and the green filtrate was reduced in volume to approximately 75ml. Cooling on ice produced green needle shaped crystals in 57 % yield.

Analysis.

Calc:	C 31.76	H 3.83	N 9.26
Found:	C 31.81	H 3.58	N 8.73

FAB Mass Spec.

m/e	Formula	% base peak at 989
516	$[NiP]^+$	(85)
840	$[NiPbP(NCS)_2-H]^+$	(40)
931	$[NiPbP(NCS)(CF_3SO_3)]^+$	(25)
989	$[NiPbP(NCS)_2(CF_3SO_3)]^+$	(100)
1080	$[NiPbP(CF_3SO_3)_2(NCS)]^+$	(10)

Species containing $[Pb_2P]$ were not present.

$[PbNiP(NCS)_4] : H_2O$

$MnPbP(NCS)_2(CF_3SO_3)_2$ (0.0003mol) was dissolved in acetonitrile with stirring at 50°C. $Ni(CF_3SO_3)_2$ (0.0003mol) was dissolved in acetonitrile and added dropwise. After heating for 2 hours at 50-55°C , the reaction mixture was filtered and excess NaNCS was added to the filtrate. Reduction in volume followed by cooling on ice produced green crystals in 63% yield.

Analysis.

Calc:	C 40.16	H 4.21	N 14.64
Found:	C 39.74	H 3.92	N 14.61

$[PbFeP(NCS)_2(H_2O)](CF_3SO_3)_2$

This reaction was performed under nitrogen and dry deoxygenated solvents were used throughout. $Pb_2P(NCS)_4$ (0.0005mol) and $Fe(CF_3SO_3)_2$ (0.002mol) were stirred together in acetonitrile (200ml). After heating for 2 hours

at 60°C the dark wine coloured suspension was filtered to remove $Pb(NCS)_2$. The filtrate was reduced in volume by bubbling nitrogen. Addition of ethanol produced blackcurrant coloured solid which was filtered off and dried with a stream of nitrogen.

Analysis:

Calc:	C 33.31	H 3.49	N 9.71
Found:	C 33.59	H 3.10	N 9.66

FAB Mass Spec.

m/e	Formula	% base peak at 987
513	$[FeP-H]^+$	(75)
663	$[FeP(CF_3SO_3)]^+$	(25)
837	$[FePbP(NCS)_2+H]^+$	(30)
928	$[FePbP(NCS)(CF_3SO_3)+H]^+$	(10)
987	$[FePbP(NCS)_2(CF_3SO_3)]^+$	(100)
1078	$[FePbP(NCS)(CF_3SO_3)_2]^+$	(15)
1136	$[FePbP(NCS)_2(CF_3SO_3)_2]^+$	(5)

Species containing $[Pb_2P]$ or $[Fe_2P]$ were not present.

ATTEMPTED PREPARATION OF HETEROBI-TRANSITION METAL COMPLEXES OF P

Attempts were made to substitute another transition metal ion for the lead ion in the heterobinuclear complexes of macrocycle P. The complexes $MnPbP(NCS)_2(CF_3SO_3)_2$, $NiPbP(NCS)_2(CF_3SO_3)_2$ and $FePbP(NCS)_2(CF_3SO_3)_2$ were used as starting materials.

Triflates of the transition metal ions Mn(II), Fe(II), Co(II), Ni(II), Cu(II) and Cu(I) were used in attempted transmetallation. In several experiments

$Cu(MeCN)_4(ClO_4)$ was used. The following experimental methods were employed.

Transmetallation attempts involving oxygen sensitive complexes, $FePbP(NCS)_2(CF_3SO_3)_2$, $Cu(MeCN)_4(CF_3SO_3)$, $Cu(MeCN)_4(ClO_4)$ or $Fe(CF_3SO_3)_2{:}6H_2O$ were carried out in dry deoxygenated solvents under nitrogen.

$MPbP(NCS)_2(CF_3SO_3)_2$ (0.0003mol) was dissolved in dry deoxygenated MeCN (200ml) with stirring at 55°C. The transition metal triflate (0.00029mol) was added as the solid. After heating for 3 hours at 55°C the reaction mixture was filtered and the filtrate was bubbled down in volume. The addition of ethanol gave products which were filtered and dried with a nitrogen stream.

In reactions that did not involve oxygen sensitive reactants, the following method was used.

To a stirring solution of $MPbP(NCS)_2(CF_3SO_3)_2$ (0.0003mol) in acetonitrile (200ml) at 55°C, a solution of transition metal triflate(0.00029mol) in acetonitrile was added dropwise. After heating for 3 hours at 55°C the reaction mixture was filtered and reduced in volume. Ethanol was added and products were filtered after cooling on ice.

The results of the experiments are presented in Table 1. Products have been identified, where possible, by CHN analysis, fast atom bombardment mass spectroscopy, magnetic measurements, esr and infrared spectroscopy.

TABLE 1 ATTEMPTED SYNTHESIS OF HETEROBINUCLEAR TRANSITION METAL COMPLEXES OF MACROCYCLE P

Incoming ion	STARTING MATERIAL - HETEROBINUCLEAR P COMPLEX		
	$MnPbP(NCS)_2(CF_3SO_3)_2$	$FePbP(NCS)_2(CF_3SO_3)_2$	$NiPbP(NCS)_2(CF_3SO_3)_2$
Cu(II)	Blue-green crystals $Cu_2P(NCS)_2(CF_3SO_3)_2:2H_2O$ Calc C 37.10 H 4.09 N 10.82 Found 36.92 3.50 11.30 μ = 2.06BM per Cu(II) yellow crystals $MnPbP(NCS)_4$	Brown oil No products isolated	Blue-green crystals $Cu_2P(NCS)_2(CF_3SO_3)_2$ infrared spectrum identical to previous sample
Cu(I)	Pale yellow powder, became green in air. Fab mass spec m/e 642(45%) $[Cu_2P(NCS)]+$ 700(40%) $[Cu_2P(NCS)_2]+$ 936(25%) $[CuPbP(NCS)(CF_3SO_3)]+$ 1144(30%) $[CuPbP(NCS)_2(CF_3SO_3)_2]+$ No evidence of Mn	Purple/black powder Fab 521(20%) $[CuP]+$ 586(10%) $[Cu_2P]+$ 693(20%) $[FeCuP(NCS)_2]+$ 784(25%) $[FeCuP(CF_3SO_3)]+$ 842(5%) $[FeCuP(NCS)_2(CF_3SO_3)]+$ no evidence of FePbP or CuPbP	Fawn powder i.r. shows MeCN, NCS and ClO_4 from $Cu(MeCN)_4(ClO_4)$, Fab m/e 939(100%) $[NiPbP(NCS)_2(ClO_4)]+$ 794(15%) $[NiCuP(NCS)_2(ClO_4)]+$
Ni(II)	Yellow-green powder m/e 839(30%) $[NiPbP(NCS)_2]+$ or $[Ni_2P(NCS)_2(CF_3SO_3)]+$ 988(30%) $[NiPbP(NCS)_2(CF_3SO_3)]+$ $[Ni_2P(NCS)_2(CF_3SO_3)_2]+$ probably NiPbP	Brown oil No products isolated	-
Co(II)	Brown oil No products isolated	Brown/black oil No products isolated	Brown needle crystals, CHN analysis fits CoNiP, Ni_2P, Co_2P, based on $CoNiP(NCS)_2(CF_3SO_3)_2:2H_2O$ Calc C 32.76 H 4.12 N 8.19 Fnd C 32.96 H 3.67 N 9.28 $\chi = 4.417\times10^{6}$ gives μ = 3.43BM per CoNiP complex; 2.43 for Ni_2P, 3.65 for PbNiP
Mn(II)	-	Not attempted	Starting material

TEMPLATE SYNTHESIS OF THE MACROCYCLE MC.

The reactants $C_6H_{10}(CH_2NH_2)_2$ [1,3-cyclohexanebis(methylamine)] and 2,6-Diacetylpyridine were obtained from Aldrich Chemical Company Ltd. and were used without further purification.

The macrocycle MC

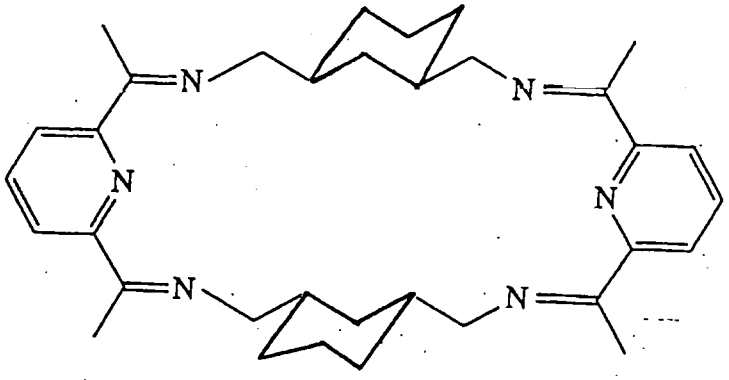

$[Pb_2MC(NCS)_4]$: EtOH

$Pb(NCS)_2$ (0.01mol), 2,6-diacetylpyridine (0.01mol) and 1,3-$C_6H_{10}(CH_2NH_2)_2$ (0.01mol) were stirred together vigorously in acetonitrile(600ml) and ethanol(200ml) at 60°C for 5 hours. The reaction mixture was filtered and the yellow filtrate was reduced in volume to about 600ml. Slow evaporation gave yellow crystals suitable for X-ray diffraction. Further crops of product were obtained (81% yield).

Analysis.

Calc:	C 39.01	H 4.26	N 11.37
Found;	C 39.09	H 4.17	N 11.84

Synthesis of the MC complex was successful in acetonitrile/methanol solvent mixture, however the yellow colour of the complex did not develop in acetonitrile alone.

FAB Mass Spec.

m/e	Formula	% of base peak at 804
537	$[MC-H]^+$	(65)
744	$[PbMC+2H]^+$	(60)
804	$[PbMC(NCS)]^+$	(100)
1068	$[Pb_2MC(NCS)_2+2H]^+$	(45)
1128	$[Pb_2MC(NCS)_3]^+$	(65)

ANION EXCHANGE REACTIONS OF $Pb_2MC(NCS)_4$

$[Pb_2MC](ClO_4)_4 : H_2O$

$Pb_2MC(NCS)_4$ (0.0005mol) and $AgClO_4$ (0.003mol) were stirred in acetonitrile (150ml) for ½ hour at 45°C. A fine precipitate of AgNCS was filtered off and the filtrate was reduced in volume to ca. 15ml. Addition of ethanol followed by cooling on ice produced cream coloured microcrystals.

Analysis.

Calc:	C 29.83	H 3.53	N 6.14
Found:	C 29.98	H 3.47	N 5.95

$[Pb_2MC(NCS)](CF_3SO_3)_3$

$Pb_2MC(NCS)_4$ (0.0005mol) was dissolved in 150ml acetonitrile at 50°C. $AgCF_3SO_3$ (0.0015mol) in acetonitrile solution was added dropwise. After about 45 minutes at 50°C the reaction mixture was filtered and reduced in volume to 40ml cooling and slow evaporation gave cream microcrystals.

Analysis.

Calc:	C 31.29	H 3.18	N 6.72
Found:	C 31.33	H 2.79	N 6.41

The complex $[Pb_2MC(NCS)](CF_3SO_3)_3$ has also been formed in an attempt to transmetallate $Pb_2MC(NCS)_4$ using $Ni(CF_3SO_3)_2$.

$[Pb_2MC(NCS)_2](CF_3SO_3)_2$: MeCN EtOH.

$Pb_2MC(NCS)_4$ (0.0005mol) was dissolved in 150ml acetonitrile at 50°C. $AgCF_3SO_3$ (0.001mol) was added and the reaction mixture was stirred at 50°C for ½ hour. After filtration, the filtrate was reduced in volume to 50ml. Ethanol was added and cooling on ice produced pale yellow microcrystalline product. The infrared spectrum of the complex showed νMeCN.

Analysis.

Calc:	C 34.68	H 3.81	N 8.67
Found:	C 35.10	H 4.07	N 8.91

Λ = 227 S cm^2 mol^{-1}

FAB Mass Spec.

m/e	Formula	% of base peak at 804
537	$[MC-H]^+$	(80)
744	$[PbMC+2H]^+$	(75)
804	$[PbMC(NCS)]^+$	(100)
895	$[PbMC(CF_3SO_3)]^+$	(45)
1068	$[Pb_2MC(NCS)_2+2H]^+$	(40)
1128	$[Pb_2MC(NCS)_3]^+$	(45)
1219	$[Pb_2MC(NCS)_2(CF_3SO_3)]^+$	(65)
1310	$[Pb_2MC(NCS)(CF_3SO_3)_2]^+$	(15)

$[Pb_2MC](CF_3SO_3)_4$: EtOH MeCN

$Pb_2MC(NCS)_4$ (0.0005mol) was dissolved in 150ml acetonitrile at 60°C. $AgCF_3SO_3$ (0.002mol) was dissolved in acetonitrile and added. The reaction mixture was stirred for two hours at 60°C and AgNCS was removed by filtration. The filtrate was reduced in volume to about 20ml and ethanol was added. Further reduction in volume and cooling on ice gave pale cream coloured crystals. The infrared spectrum of the complex showed ν(MeCN).

Analysis

Calc:	C 30.82	H 3.39	N 5.99
Found:	C 30.93	H 3.26	N 5.69

TRANSMETALLATION OF $Pb_2MC(NCS)_4$

(a)Homobinuclear complexes of MC.

$[Cu_2MC(NCS)_2](CF_3SO_3)_2$: $2H_2O$

$Pb_2MC(NCS)_4$ (0.0005mol) and $Cu(CF_3SO_3)_2$ (0.002mol) were stirred together in ethanol(150ml) at 40-45°C for one hour and stirred for another hour at room temperature. A green semicrystalline product was removed by filtration. Recrystallisation from acetonitrile/ethanol solvent mixture gave crystalline product in 67% yield.

Analysis.

Calc:	C 40.89	H 4.52	N 10.04
Found:	C 41.01	H 4.27	N 9.63

[$Ni_2MC(NCS)_2(NO_3)_2$]

$Pb_2MC(NCS)_4$ (0.0005mol) was dissolved in acetonitrile (100ml)/ethanol (100ml) solvent mixture with stirring at 55-60°C and $Ni(NO_3)_2{\cdot}6H_2O$ (0.002mol) was added as the solid. After heating for 4 hours at 55°C, cream coloured precipitate was filtered off and the green filtrate was reduced in volume. A sage green powder was obtained in 35% yield on cooling on ice.

Analysis.

Calc:	C 48.24	H 5.17	N 15.63
Found:	C 46.05	H 4.99	N 17.05

This product was not adequately soluble for recrystallisation. Despite repeated preparation, acceptable CHN analysis figures were not obtained.

FAB mass spec

m/e	Formula	% base peak at 841.
713	$[Ni_2MC(NCS)+H]^+$ or $[NiMC(NCS)_2+H]^+$	(50
775	$[Ni_2MC(NCS)(NO_3)+H]^+$	(90)
841	$[Ni_2MC(NO_3)_3+H]^+$	(100)

Species containing [NiPbMC] or [Pb_2MC] were absent from the Fab mass spectrum.

Microcrystalline sage green heterobinuclear $NiPbMC(NCS)_2(NO_3)_2$ product was obtained in 10% yield as a second crop from the reaction.

Use of a 1:1 stoicheiometric quantity of $Ni(NO_3)_2$ to Pb_2P complex did not stop formation of the dinickel MC complex. Attempts to transmetallate Pb_2MC using $Ni(CF_3SO_3)_2$ were unsuccessful. Attempted transmetallation with $NiCl_2$ gave a mixture of insoluble products

(b) Heterobinuclear complexes of MC.

$[PbMnMC(NCS)_2](NO_3)_2 \cdot 2H_2O$

$Pb_2MC(NCS)_4$ (0.0005mol) was suspended in 100ml ethanol/50ml acetonitrile solvent mixture and heated to about 55°C. $Mn(NO_3)_2 \cdot 4H_2O$ (0.002mol) was dissolved in acetonitrile 20ml and added to the reaction mixture. The reactants were stirred together for 3 hours at 60°C . A white precipitate was removed by filtration and the yellow filtrate was reduced in volume to *ca.* 75ml. On cooling on ice yellow crystals were obtained.

Analysis.

Calc:	C 40.14	H 4.68	N 13.00
Found:	C 40.59	H 4.30	N 12.62

FAB Mass Spec.

m/e	Formula	% of base peak at 979
916	$[MnPbMC(NCS)_2+H]^+$	(65)
979	$[MnPbMC(NCS)_2(NO_3)]^+$	(100)

This PbMnMC complex was unstable and was stored in a freezer. On storage at room temperature, the complex became brown and lost the N-only bridging thiocyanate ligand. Preparation of the complex in a solvent mixture containing a higher proportion of acetonitrile gave a product that became brown more quickly. Transmetallation of $Pb_2MC(NCS)_4$ using manganese triflate or perchlorate gave heterobinuclear product mixed with dilead anion exchange products.

[MnPbMC(NCS)$_4$]: H_2O

This complex was made by an analogous method to that outlined for [PbMnMC(NCS)$_2$](NO$_3$)$_2$: 2H_2O except that an excess of NaNCS was added to the filtrate before reduction in volume. Orange crystals suitable for X-ray diffraction were obtained on slow cooling.

Analysis

Calc:	C 43.42	H 4.60	N 13.32
Found:	C 43.09	H 4.32	N 13.15

PbMnMC(NCS)$_4$: MeOH H_2O.

$Pb_2MC(NCS)_4$ (0.0005mol) was dissolved in acetonitrile(100ml) and methanol(100ml) solvent mixture. Mn(O$_2$CCH$_3$)$_3$(0.002mol.) and one pellet of KOH was dissolved in methanol (50ml). The brown manganese acetate solution was added dropwise to the solution containing the macrocyclic complex. The reactants were refluxed together gently for 5 hours. A small amount of brown solid was filtered off and excess NaNCS was added to the filtrate. Concentration to approximately 30ml followed by cooling on ice produced brown microcrystalline solid in 54% yield. Esr spectral evidence suggests that this is a Mn(II) complex.

Analysis.

Calc:	C 43.28	H 4.75	N 12.94
Found:	C 43.42	H 4.60	N 13.32

$[PbFeMC(NCS)_2](CF_3SO_3)_2 \cdot 2H_2O$

$Pb_2MC(NCS)_4$ (0.0005mol) and $Fe(CF_3SO_3)_2$ (0.0005mol) were stirred together in dry deoxygenated acetonitrile under nitrogen at 55°C for two hours. The reaction mixture was filtered under nitrogen to remove grey $Pb(NCS)_2$ precipitate. The dark purple filtrate was reduced in volume, without heating, by passing a stream of nitrogen through it. Dry deoxygenated ethanol was added and the solution was concentrated further until a blackcurrant coloured solid appeared. Cooling on ice yielded further product which was filtered and dried under nitrogen.(Yield 40%)

Analysis.

Calc:	C 36.45	H 4.03	N 8.95
Found:	C 36.61	H 3.78	N 9.02

FAB Mass Spec.

m/e	Formula	% of base peak at 143
918	$[FePbMC(NCS)_2]^+$	(15)
976	$[FePbMC(NCS)_3]^+$	(15)
1008	$[FePbMC(NCS)(CF_3SO_3)+H]^+$	(10)
1067	$[FePbMC(NCS)_2(CF_3SO_3)]^+$	(60)
1158	$[FePbMC(NCS)(CF_3SO_3)_2]^+$	(10)

$NiPbMC(NCS)_2(NO_3)_2$

$PbNiMC(NCS)_2(NO_3)_2$ has been obtained as a minor product of the transmetallation of $Pb_2MC(NCS)_4$ using $Ni(NO_3)_2$.

Analysis.

Calc:	C 40.68	H 4.55	N 13.12
Found:	C 40.95	H 4.83	N 13.82

FeCuMC(NCS)$_2$(CF$_3$SO$_3$)$_2$

This reaction was performed under nitrogen using dry deoxygenated solvents throughout. FePbMC(NCS)$_2$(CF$_3$SO$_3$)$_2$(0.0003mol) was dissolved in dry deoxygenated acetonitrile and Cu(MeCN)$_4$(CF$_3$SO$_3$)(0.0003mol) was added as a solid. After 3 hours at 45°C, the reaction mixture was filtered and the filtrate was bubbled down in volume. Ethanol was added and on further reduction in volume, brown solid was filtered off and dried with a nitrogen stream. Fab mass spec showed that the brown powder contained a mixture of heterobinuclear [CuFeMC] macrocyclic complex and [Cu$_2$MC] species. It may be possible to isolate the [CuFeMC] complex using ion exchange chromatography. The mixture of products dissolve in acetonitrile. The esr spectrum of the product mixture suggests that Cu(II) is present.

FAB mass spec.

m/e	Formula	% base peak at 474
773	[FeCuMC(NCS)$_2$]$^+$	(50)
809	[FeCuMC(CF$_3$SO$_3$)]$^+$ or [CuPbMC]$^+$	(20)
952	[PbFeMC(CF$_3$SO$_3$)]$^+$	(15)
1108	[CuPbMC(CF$_3$SO$_3$)$_2$+H]$^+$ or [FeCuMC(CF$_3$SO$_3$)$_3$]$^+$	(25)

TEMPLATE SYNTHESIS OF COMPLEXES OF THE CRYPTAND GT.

The tripod amine tris(2-aminoethyl)amine (tren) was obtained from Aldrich Chemical Company. Ethanedial (glyoxal) was obtained from Fluka AG. Both compounds were used without further purification.

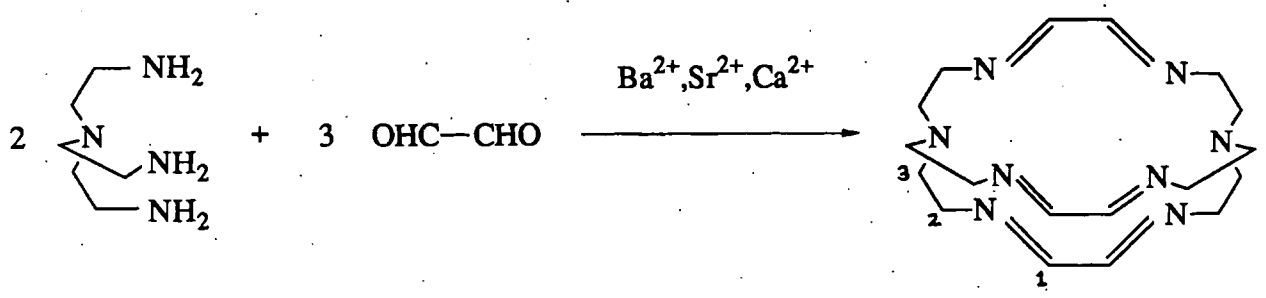

The cryptand GT

Proton NMR

Proton	Shift /ppm	Multiplicity	Integral
1	8.0	s	6
2	3.7	t	12
3	2.8	t	12

$BaGT(ClO_4)(BPh_4): 2H_2O$ (Template synthesis.)

Glyoxal (0.003mol), $Ba(ClO_4)_2$ (0.001mol) and $NaBPh_4$ (0.002mol) were refluxed together gently in methanol (200ml) for 15 minutes and cooled to 40-45°C. Tris(2-aminoethyl)amine, $N(CH_2CH_2NH_2)_3$, tren (0.002mol) in 50ml methanol was added dropwise and the reaction mixture was stirred at 45°C for 4 hours. Cream coloured solid was filtered off. Further crops of product were obtained on concentration of the filtrate (Yield 58%). The product was recrystallised from acetonitrile/ethanol solvent mixture.

Analysis

Calc:	C 53.07	H 5.73	N 11.79	Ba 14.4
Found:	C 58.95	H 5.90	N 11.95	Ba 10.4

Despite recrystallisation and analysis of various samples of $BaGT(ClO_4)(BPh_4)$, satisfactory CHN analysis was not obtained on this complex.

$SrGT(BPh_4)_2 : 2H_2O$ (Template synthesis)

Glyoxal (0.003 mol) and $Sr(ClO_4)_2$ (0.001mol) were refluxed gently in methanol (200 ml) for 15 minutes. Tren (0.002mol) in 50ml methanol was added dropwise and the reaction mixture was refluxed gently for 45 minutes. $NaBPh_4$ (0.002 mol) was added and the cream coloured precipitate was filtered off. Further product was obtained on concentration of the filtrate and later crops contained both perchlorate and tetraphenylborate counterion. The product was recrystallised from acetonitrile/ethanol solvent mixture in the presence of $NaBPh_4$. Concentration of the filtrate and cooling on ice gave cream microcrystalline product (yield 61%).

Analysis.

Calc:	C 70.74	H 6.66	N 10.00	Sr 7.8
Found:	C 69.84	H 6.65	N 10.54	Sr 7.7

FAB Mass Spec.

m/e	Formula	% of base peak at 359
359	$[GT+H]^+$	(100)
446	$[SrGT]^+$	(99)

$CaGT(BPh_4)_2 : 2H_2O$ (Template synthesis)

$Ca(NO_3)_2$ (0.001mol) and glyoxal (0.003mol) were refluxed together in methanol (200ml) for 10-15 minutes. $NaBPh_4$ (0.002 mol) was added as a solid. Tren (0.002mol) in 50ml methanol was added dropwise to the reaction

mixture with stirring at 50°C. After three hours at 50°C, cream coloured solid was filtered off in 66% yield.

Analysis.

Calc:	C 73.82	H 6.95	N 10.43	Ca 3.8
Found:	C 72.66	H 6.83	N 10.57	Ca 4.3

$MgGT(BPh_4)_2$: $2H_2O$ (Template synthesis)

$Mg(NO_3)_2$ (0.001mol), glyoxal(0.003mol) and $NaBPh_4$ (0.002mol) were refluxed together in methanol (200ml) for approximately 15 minutes. The solution was cooled to 45-50°C and tren (0.002mol) in 50ml methanol was added dropwise. The reaction mixture was stirred at 45°C for 3 hours. Yellow solid was filtered off. Attempts to recrystallise the product failed.

Analysis.

Calc:	C 74.98	H 7.06	N 10.60
Found:	C 68.56	H 7.01	N 16.60

Despite analysis of many different samples of $MgGT(BPh_4)_2$, acceptable CHN analysis was not obtained.

Fab mass spec.

m/e	Formula	% base peak at 359
359	$[GT+H]^+$	(100)
382	$[MgGT]^+$	(6)
700	$[MgGT(BPh_4)-H]^+$	(4)

$LaGT(BPh_4)_2(NO_3)$ (Template synthesis)

Glyoxal (0.003mol) was refluxed in ethanol (200ml) for 15 minutes. $La(NO_3)_3.6H_2O$ (0.002mol) was dissolved in ethanol(100ml.)and brought to gentle reflux. A solution of tren (0.002mol) in ethanol (300ml) and the glyoxal solution were added dropwise simultaneously to the stirring lanthanum nitrate solution. After 3 hours at gentle reflux the reaction mixture was filtered and excess $NaBPh_4$ was added to the filtrate. On reduction in volume, followed by cooling on ice, a mixture of pale yellow powder and yellow microcrystals was obtained.

Analysis.

Calc:	C 64.25	H 6.05	N 10.22
Found:	C 61.36	H 5.99	N 12.06

Despite recrystallisation, acceptable CHN analysis was not obtained.

FAB Mass Spec

m/e	Formula	% base peak at 169
496	$[LaGT-H]^+$	(4)
558	$[LaGT(NO_3)-H]^+$	(2)

All attempts to synthesise the GT cryptate without a template metal ion failed. Various metal ions have been tried as templates. Ag+ was not successful as a template ion and only oil was obtained. Use of praseodymium (III) nitrate as source of template ion gave yellow powder. The infrared spectrum of the yellow product was broad and showed νNH absorptions in addition to ν(C=N). Metal ions Co(II) and Fe(II) were used as possible template ions but only oil was obtained. Pb(II) appeared to act as a template in that $Pb(NCS)_2$ dissolved to give a yellow solution but products obtained did not give acceptable CHN analysis.

TRANSMETALLATION OF GT COMPLEXES.

Strontium or barium GT complexes have been used in transmetallation with transition metal ions. Product from the template process was used without prior recrystallisation.

(a)Transition metal cryptates of GT.

Mononuclear cryptates

[MnGT](BPh$_4$)$_2$: 2H$_2$O.

SrGT(BPh$_4$)$_2$ (0.0005mol) was suspended in acetonitrile (250ml) and warmed to 50°C. Mn(NO$_3$)$_2$:4H$_2$O (0.0015mol) was dissolved in MeCN (30ml.) and added dropwise. NaBPh$_4$ (0.001mol.) was added and the reaction mixture was stirred at 45-50°C for 3 hours. A fawn coloured solid was filtered off and the filtrate was reduced in volume to about 150ml. Ethanol was added and cooling on ice gave yellow microcrystals in 44% yield.

Analysis.

Calc:	C 72.87	H 6.85	N 10.30
Found:	C 73.21	H 6.49	N 10.08

FAB Mass Spec.

m/e		base peak
413	[MnGT]$^+$	(100)

Λ = 223 S cm^{2}mol^{-1}

MnGT(BPh$_4$)$_2$ has also been made by the following method.

SrGT(BPh$_4$)$_2$(0.0003mol.) , Mn(O$_2$CCH$_3$)$_3$(0.0006mol.) and NaBPh$_4$ 0.001 mol.) were stirred together in acetonitrile(200ml) for 2 hours at 50°C. The reaction mixture was filtered and the brown filtrate was reduced in volume

until yellow product began to crystallise. Cooling on ice gave yellow microcrystalline product.

[NiGT](BPh$_4$)$_2$: ½H$_2$O.

SrGT(BPh$_4$)$_2$ (0.0005mol.) was suspended in acetonitrile (200ml.) and warmed to 45°C. Ni(ClO$_4$)$_2$: 6H$_2$O was dissolved in acetonitrile and added dropwise. NaBPh$_4$ (0.001mol.) was added and the reaction mixture was stirred for 2 hours at 50°C. After filtration the yellow filtrate was reduced in volume until solid was starting to crystallise out (*ca.* 130ml.) Addition of ethanol and cooling gave orange microcrystals in 39% yield.

Analysis.

Calc:	C 74.46	H 6.72	N 10.53
Found:	C 74.37	H 7.13	N 10.73

Λ = 219 S cm^{2}mol^{-1}

[CoGT](BPh$_4$)$_2$: 3H$_2$O.

SrGT(BPh$_4$)$_2$ (0.0005mol.) was suspended in acetonitrile (250ml.) and warmed to 50°C. Co(ClO$_4$)$_2$:6H$_2$O(0.0015mol.) was dissolved in MeCN (30ml.) and added dropwise giving a rust-brown reaction mixture. NaBPh$_4$ (0.001mol.) was added and the reaction mixture was stirred at 45-50°C for 3 hours. Fawn coloured solid was filtered off and the filtrate was reduced in volume to *ca.* 150ml. Ethanol was added and cooling on ice gave rust coloured microcrystals in 49% yield.

Analysis.

Calc:	C 71.42	H 6.90	N 10.10	Co 5.3
Found:	C 71.60	H 6.63	N 9.92	Co 5.3

Λ = 236 S cm^{2}mol^{-1}

[CoGT]$(ClO_4)_2$: H_2O.

$Ba(ClO_4)_2$ (0.001mol.) and glyoxal (0,003mol.) were refluxed together in methanol (200ml.) for 15 minutes. The solution was cooled to 45°C and tren (0.002mol.) in 50ml methanol was added dropwise.The reaction mixture was stirred at 40-50°C for 3 hours. $Co(ClO_4)_2{:}6H_2O$ (0.001mol.) was added and the reactants were stirred together for 2 hours at 50-55°C. A small amount of fawn solid was filtered off and the rust-brown filtrate was reduced in volume until solid started to come out of solution. Cooling on ice gave a rust powder which was recrystallised from acetonitrile /ethanol solvent mixture. Slow evaporation gave rust hexagon-shaped crystals which were suitable for X-ray diffraction. (23% yield)

Analysis.

Calc:	C 34.08	H 5.08	N 17.66
Found:	C 34.29	H 4.94	N 16.73

Λ = 254 S cm^2mol^{-1}

The reaction was also successful when $Sr(ClO_4)_2$ was used in place of $Ba(ClO_4)_2$. Attempts to produce $NiGT(ClO_4)_2$ by this method gave crystalline product, but in 10% yield. Attempted preparation of $MnGT(CF_3SO_3)_2$ and $FeGT(CF_3SO_3)_2$ by template of GT on $Ba(CF_3SO_3)_2$, followed by addition of the transition metal triflate gave oily mixtures from which product could not be isolated.

[NiGT]$(ClO_4)_2$: H_2O

$SrGT(BPh_4)_2$(0.0005mol) and $AgClO_4$(0.001mol) were stirred together in acetonitrile for about 30 minutes. $AgBPh_4$ precipitate was filtered off and $Ni(ClO_4)_2:4H_2O$ (0.00075mol) was added to the filtrate. After 1-2 hours at *ca* 50°C the reation mixture was filtered, reduced in volume and cooled on ice. Orange microcrystalline product was obtained.

Analysis.

Calc:	C 34.09	H 5.09	N 17.67
Found:	C 34.64	H 5.30	N 16.72

$CoGT(ClO_4)_2$ has been obtained by an analogous method in 30% yield.

[ZnGT]$(ClO_4)_2$: EtOH H_2O

This complex was made by an analogous method to that outlined above. $Zn(ClO_4)_2$: $4H_2O$ was added in place of $Ni(ClO_4)_2$. Pale orange microcrystalline product resulted.

Analysis

Calc:	C 34.82	H 5.55	N 16.24
Found:	C 34.35	H 5.17	N 15.82

Attempted synthesis of $ZnGT(BPh_4)_2$ by the method described for $CoGT(BPh_4)_2$ gave orange product which contained both perchlorate and tetraphenylborate counterions, acceptable CHN analysis was not obtained.

$FeGT(ClO_4)_2$: $2H_2O$

This reaction was carried out under nitrogen and dry deoxygenated solvents were used throughout. $SrGT(BPh_4)_2$ and $AgClO_4$ were stirred together in acetonitrile. $AgBPh_4$ precipitate was filtered off and $Fe(ClO_4)_2$ was added as a solid. After 1-2 hours at 40°C the blackcurrant coloured solution was

bubbled down in volume without heating. Addition of ethanol and cooling on ice gave deep blackcurrant coloured product which was filtered and dried under nitrogen. Acceptable CHN analysis was not obtained.

CAUTION! this compound is potentially explosive. The frit used to collect the product should not be scraped to loosen the solid.

Analysis

Calc:	C 33.30	H 5.28	N 17.68
Found:	C 28.59	H 4.75	N 14.16

FeGT$(BPh_4)_2$: $2H_2O$

This experiment was performed under nitrogen and dry deoxygenated solvents were used. SrGT$(BPh_4)_2$ was dissolved in acetonitrile with stirring at 40-45°C. Fe$(CF_3SO_3)_2$: $6H_2O$ was added as a solid and a wine coloured reaction mixture resulted. $NaBPh_4$ (0.002mol) was added and the mixture was stirred at 45°C for 2 hours. The solution was filtered and the filtrate was reduced in volume by bubbling nitrogen. Dry deoxygenated ethanol was added and further concentration gave blackcurrant coloured solid which was filtered off and dried under nitrogen.

Analysis.

Calc:	C 72.80	H 6.85	N 10.29
Found:	C 72.34	H 6.72	N 10.36

CuGT$(ClO_4)_2$: $4H_2O$

SrGT$(BPh_4)_2$(0.0005mol) and $AgClO_4$)(0.001mol) were stirred together together in acetonitrile 200ml./ethanol 50ml. solvent mixture. $AgBPh_4$ was filtered off and $Cu(O_2CCH_3)_2$(0.0004mol) and $Cu(ClO_4)_2$:$6H_2O$ (0.0002mol) were added to the filtrate. After 3 hours at 40-45°C the solution was

filtered and the filtrate was reduced in volume. Cooling on ice gave bottle green hexagon-shaped microcrystals.

Analysis.

Calc:	C 31.20	H 5.53	N 16.17
Found:	C 31.32	H 4.77	N 15.89

FAB Mass Spec.

m/e	Formula	% of base peak at 421
421	$[CuGT]^+$	(100)
520	$[CuGT(ClO_4)]^+$	(40)
585	$[Cu_2GT(ClO_4)+2H]^+$	(10)

$CuGT(ClO_4)_2$ is soluble in water but the solution becomes yellow within an hour.

Binuclear cryptates.

$Cu_2GT(ClO_4)_4 : 2H_2O$

$SrGT(BPh_4)_2$ (0.0005mol) and $AgClO_4$ (0.001mol) were stirred together in 100ml MeCN/MeOH solvent mixture. $AgBPh_4$ precipitate was filtered off and $Cu(O_2CCH_3)_2$ (0.001mol) was added and the mixture was refluxed for 15 minutes. After filtration the green filtrate was reduced in volume to 30ml, green crystals were obtained on cooling.

Analysis.

Calc:	C 23.51	H 3.72	N 12.18
Found:	C 23.52	H 3.52	N 11.85

FAB Mass Spec.

m/e	Formula	% base peak at 136
585	$[Cu_2GT(ClO_4)+2H]^+$	(95)
484	$[Cu_2GT]^+$	(43)
421	$[CuGT]^+$	(40)

$Cu_2GT(BPh_4)_2$

$SrGT(BPh_4)_2$ (0.0004mol) was suspended in acetonitrile (200ml.) $Cu(ClO_4)_2$: $6H_2O$ (0.0004mol) and $Cu(O_2CCH_3)_2$ (0.0004mol.) were added and the mixture was stirred at room temperature for 3-4 hours. Green colour developed on adding Cu^{2+} and gradually yellow/brown colour appeared. After filtration the yellow /brown filtrate was reduced in volume and ethanol was added. Cooling on ice gave bronze coloured microcrystals.

Analysis.

Calc:	C 70.53	H 6.28	N 9.97
Found:	C 69.46	H 6.35	N 9.96

Attempts to obtain a dicopper(I) cryptate with perchlorate counterion by transmetallation of $SrGT(ClO_4)_2$ with $Cu(MeCN)_4(ClO_4)$ failed.

Transmetallation of $SrGT(BPh_4)_2$ using $Cu(MeCN)_4(CF_3SO_3)$ gave only impure and insoluble brown powder that did not analyse correctly. The percentages of carbon, hydrogen and nitrogen found suggested $Cu_2GT(BPh_4)_2$ rather than the monocopper $CuGT(BPh_4)$ cryptate. The product was too insoluble for recrystallisation and did not give a Fab mass spectrum (too insoluble in fab matrix).

Attempted preparation of $CuZnGT(ClO_4)_4$ and $CuNiGT(ClO_4)_4$ by reflux of the mononuclear $CuGT(ClO_4)_2$ with an equimolar equivalent of $M(ClO_4)_2$ failed. Fab mass spectroscopy of the products showed that only copper GT cryptate was present.

Anion exchange.

NiGT(NCS)$_2$:2H$_2$O

NiGT(BPh$_4$)$_2$ (0.0002mol) was suspended in acetonitrile. AgClO$_4$ (0.0002mol) was added as a solution in acetonitrile and the suspension was stirred at 45°C for ½ hour. The cream coloured precipitate was filtered off and excess NaNCS was added to the filtrate. The solution was filtered again to remove traces of AgNCS and reduced in volume. Cooling on ice gave orange microcrystals.

Analysis

Calc:	C 42.19	H 6.02	N 24.60
Found:	C 41.96	H 6.31	N 24.73

Attempts to obtain products with NO_3^- or $CF_3SO_3^-$ counterions by analogous methods gave oils.

(b) Lanthanide (III) ion cryptates of GT.

$LaGT(BPh_4)_2(NO_3)$: H_2O

$BaGT(BPh_4)(ClO_4)$ (0.0003mol) was suspended in acetonitrile (200ml.) and warmed to 45°C. $La(NO_3)_3$: $6H_2O$ was dissolved in MeCN (50ml.) and added dropwise. $NaBPh_4$ (0.001mol) was added and the reaction mixture was stirred at 45°C for 5 hours and stirred 18 hr at room temperature. The reaction mixture was filtered and the filtrate was reduced in volume to about 40ml. Addition of ethanol followed by cooling on ice gave pale yellow microcrystals in 31 % yield.

Analysis

Calc:	C 64.25	H 6.05	N 10.22
Found:	C 57.29	H 5.54	N 10.41

FAB Mass Spec.

m/e	Formula	% base peak at 723
496	$[LaGT-H]^+$	(25)
559	$[LaGT(NO_3)]^+$	(5)
876	$[LaGT(NO_3)(BPh_4)-2H]^+$	(10)

Synthesis of praesodymium, terbium and gadolinium cryptates was attempted by the following method.

$BaGT(BPh_4)(ClO_4)$ (0.0003mol) was suspended in acetonitrile and warmed to 40-45°C. $M(NO_3)_3$: $6H_2O$ was dissolved in MeCN (50ml) and added. A fine suspension formed gradually. $NaBPh_4$ (0.001mol) was added and the reaction mixture was stirred at 35-40°C for 5 hours. After filtration the pale yellow filtrate was reduced in volume to *ca.* 20ml and ethanol was added dropwise until cloudiness appeared. Cooling on ice gave pale yellow microcrystals in *ca.* 20% yield. Attempts to recrystallise the lanthanide

cryptates failed. Magnetic measurements confirmed the presence of the paramagnetic lanthanide ion in the following complexes.

Analysis.

$PrGT(BPh_4)(NO_3)_2 : 2H_2O$.

Calc:	C 51.58	H 5.56	N 14.32
Found:	C 52.08	H 5.30	N 13.18

$TbGT(BPh_4)_2(NO_3) : 2H_2O$

Calc:	C 63.22	H 5.94	N 10.05
Found:	C 62.16	H 4.83	N 10.10

$GdGT(BPh_4)_2(NO_3)$

Calc:	C 65.18	H 5.80	N 10.36
Found:	C 71.25	H 7.01	N 10.00

FAB Mass Spec.

m/e		% base peak at 337
359	$[GT+H]^+$	(50)
515	$[GdGT-H]^+$	(45)
835	$[GdGT(BPh_4)]^+$	(8)

$EuGT(BPh_4)_3 : 4H_2O$.

$BaGT(BPh_4)(ClO_4)$ (0.0003mol) was suspended in acetonitrile (100ml.) and warmed to 35°C. $EuCl_3:6H_2O$ (0.00035mol) was dissolved in ethanol (50ml.) and added. $NaBPh_4$ (0.0015mol) was added and the reaction mixture was stirred at 35-40°C for 5 hours and stirred overnight at room temperature. After filtration the pale yellow filtrate was reduced in volume to

approximately 30ml. Addition of ethanol and cooling gave pale yellow microcrystals in 21 % yield.

Analysis.

Calc:	C 70.90	H 6.41	N 7.28
Found:	C 70.13	H 6.94	N 7.65

FAB Mass Spec.

m/e	% base peak at 308
510 [EuGT-H]$^+$	(40)

Preparation of $EuGT(BPh_4)_3$ has also been carried out in dry solvents under nitrogen in the presence of dimethoxypropane. This improved the yield of EuGT complex to 27%.

$CeGT(BPh_4)_2(NO_3)$: H_2O

$BaGT(BPh_4)(ClO_4)$ (0.00015mol) was suspended in MeCN (200ml) at 40°C. $Ce(NO_3)_3$: $6H_2O$ was dissolved in MeCN and added. After 3 hours at 40-45°C, the reaction mixture was filtered and the filtrate was reduced in volume to 50ml. Cooling on ice produced rust coloured crystals which were separated from accompanying beige powder (34% yield).

Analysis

Calc:	C 65.13	H 5.96	N 10.40
Found:	C 66.40	H 6.08	N 10.74

The cerium cryptate did not recrystallise successfully.

FAB Mass Spec.

m/e	Formula	% base peak at 136
497	[CeGT-H]$^+$	(30)
561	[CeGT(NO_3)+H]$^+$	(10)

Transmetallation using Ru(II), Pb(II) or Group 1 ions

The following experiment was performed under nitrogen using dry deoxygenated solvents.

Attempted preparation of RuGT$(BPh_4)_2$

$SrGT(BPh_4)_2$ (0.0003mol) was suspended in acetonitrile and brought to reflux. $Ru(Cl)_2(P(C_6H_5)_3)_3$ was added as a solid and the reaction mixture was refluxed for 2-3 hours. The orange reaction mixture was filtered and reduced in volume to *ca.* 15ml. Cooling on ice gave orange microcrystals.

Analysis

Calc:	C 72.19	H 6.43	N 10.21
Found:	C 71.00	H 6.51	N 9.67

Fab mass spectroscopy did not show peaks attributable to RuGT, SrGT or GT, although the infrared spectrum showed that the GT cryptand was present in the complex.

NaGT$(BPh_4)\cdot 2H_2O$

$BaGT(BPh_4)(ClO_4)$ (0.0003mol) was suspended in MeCN (200ml.) and heated to 50-55°C. Na_2SO_4 (0.0009mol) was dissolved in a minimum of hot water and added dropwise. After 2-3 hours at 50°C $BaSO_4$ precipitate was filtered off. Ethanol was added to the pale yellow filtrate and this was reduced to 10ml. Cooling on ice gave pale yellow microcrystals in 14% yield.

Analysis

Calc:	C 68.91	H 7.43	N 15.31
Found:	C 68.20	H 7.55	N 14.36

FAB Mass Spec.

m/e	Formula	% base peak 167
359	$[GT+H]^+$	(25)
381	$[NaGT]^+$	(15)

The fab mass spectrum of NaGT(BPh_4) showed no evidence of [BaGT]$^+$ at m/e 496.

KGT(BPh_4)

Attempted exchange of barium ion for K^+ by an analogous method, using K_2SO_4 gave pale yellow crystals surrounded by oil.

Fab Mass Spec

m/e 397 [KGT]$^+$ (80)

The fab mass spectrum showed no evidence of [BaGT]$^+$ or [GT]$^+$ at m/e 358.

PbGT(BPh_4)$_2$: $3H_2O$.

BaGT(BPh_4)$_2$ (0.0003mol) was suspended in methanol/acetonitrile solvent mixture (100ml/50ml) at 50°C. $Pb(NO_3)_2$(0.0006mol) was ground finely, dissolved in hot methanol and added dropwise. After four hours at 55°C the barium nitrate precipitate was filtered off and excess $NaBPh_4$ was added to the filtrate. Concentration and cooling on ice gave pale yellow microcrystals.

Analysis

Calc:	C 63.00	H 6.08	N 8.90
Found:	C 63.35	H 5.71	N 8.06

FAB Mass Spec.

m/e	Formula	% base peak at 399
566	[PbGT]$^+$	(35)
884	[PbGT(BPh_4)-H]$^+$	(8)

ATTEMPTED PREPARATION OF REDUCED METAL-FREE GT LIGAND

$Pb(NCS)_2$(0.002mol) and glyoxal(0.006mol) were refluxed together in methanol(150ml.) for 15 minutes. Tren(0.004mol) in 100ml of methanol was added dropwise with stirring. The lead thiocyanate dissolved and yellow colour developed. After 3 hours at 50-55°C, an excess of $NaBH_4$ was added in portions. After each addition, an instant black lead precipitate formed which dissolved within minutes to give yellow solution again. After 2-3 hours at 55°C, $NaBH_4$ was added in portions and lead was filtered off under suction. The cream coloured filtrate was brought to dryness, NaOH, 8 pellets in *ca.* 15ml deionised H_2O was added. The solution was extracted with six portions of chloroform. The extracts were combined, washed with deionised water and dried with Na_2SO_4. After filtration the filtrate was brought to dryness, the oil obtained was redissolved in methanol, filtered and rotary evaporated to dryness. The product was dried *in vacuo* overnight and remained a pale yellow oil.

Mass spec.

m/e	Formula	%height of base peak.
370	$[RGT]^+$ (GT + 12 H)	1.61
369	$[GT + 11\ H]^+$	0.91
368	$[GT + 10\ H]^+$	1.54
367	$[GT + 9\ H]^+$	0.70
366	$[GT + 8\ H]^+$	0.91
365	$[GT + 7\ H]^+$	0.49
364	$[GT + 6\ H]^+$	0.63
358	$[GT]^+$	0.91

Fully reduced GT, partially reduced GT and unreduced GT ligand gave 7.7% of the height of the base peak in total.

$BaGT(BPh_4)(ClO_4)$ (0.002mol) and $Pb(NO_3)_2$(0.003mol) were stirred together in methanol for 3 hours at 55°C. $Ba(NO_3)_2$ was not filtered off as $PbGT(BPh_4)_2$ was only slightly soluble in methanol. $NaBH_4$ was added giving lead precipitate which dissolved again. The reaction mixture was refluxed gently for 4 hours. Cream coloured solid, containing $MGT(BPh_4)_2$ and $Ba(NO_3)_2$, was filtered off. Work up of the filtrate as outlined above gave an oil.

Mass spec.

m/e	Formula	% height of base peak
370	$[RGT]^+$	0.63

Reduction of manganese (II) GT cryptate was attempted. It was hoped that reduced manganese would not be solubilised by the cryptand.

$MnGT(BPh_4)_2$(0.0015mol) and $NaBH_4$(excess) were refluxed together in ethanol(400ml) for 4-5 hours. Fawn coloured solid was filtered off and the cream coloured filtrate was brought to dryness and worked up in the usual way.

Mass spec.

m/e	Formula	% height of base peak
370	$[RGT]^+$	1.1

The following attempt avoided the presence of tetraphenylborate counterion.

GT was templated on $Ba(ClO_4)_2$ in methanol as previously described. $Mn(NO_3)_2$ was added giving a yellow solution. After 2 hours at 50°C excess $NaBH_4$ was added. The reaction mixture was stirred for 3 days. Fawn precipitate was filtered off and the filtrate was worked up as outlined

earlier. Mass spectroscopy showed no evidence of RGT, GT or semireduced GT cryptand.

Attempts to obtain a silver cryptate for use in the reduction were unsuccessful. Both template attempts on silver (I) and transmetallation with silver(I) failed.

It is possible that reduced GT is unstable in the conditions of the mass spectrometer, this may account for the low peak percentage in mass spec. However there are additional problems in that the reduced cryptand appears to complex lead. The complex does not go into the chloroform layer and is lost in the work up procedure.

COMPLEXES OF THE CRYPTAND 3Bp.

Terephthaldicarboxaldehyde C_6H_4-1,4-$(CHO)_2$ (terephthalaldehyde) was obtained from Aldrich Chemical Company Ltd. and was used without further purification. Template synthesis of the 3Bp cryptand was reported previously.[275] The complexes $Pb_2$3Bp$(SCN)_4$ and $Ag_2$3Bp$(CF_3SO_3)_4$ were obtained.

The cryptand 3Bp

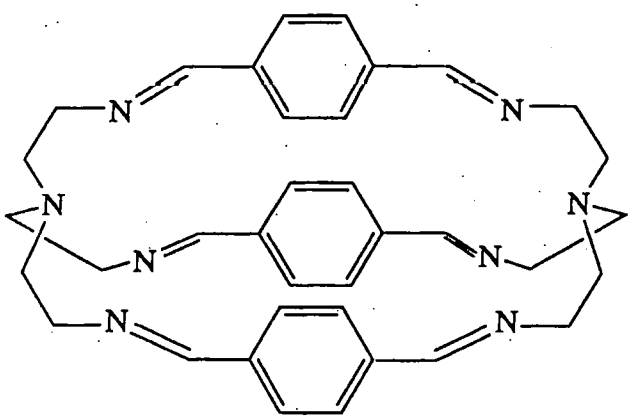

$Ag_2$3Bp$(ClO_4)_2$:4H_2O

Tren (0.002mol) was dissolved in methanol (100ml) and terephthalaldehyde (0.003mol) was dissolved in methanol (100ml). The two solutions were added simultaneously and dropwise to a solution of $AgNO_3$ (0.002mol) in methanol (200ml) stirring at 35°C. The reactants were stirred together for 3 hours at 35°C. After filtration excess $NaClO_4$ was added and the filtrate was reduced in volume. Slow evaporation gave yellow-brown cube shaped microcrystals in 73% yield.

Analysis.

Calc:	C 40.28	H 4.69	N 10.44
Found:	C 40.47	H 4.32	N 10.40

$Ag_2$3Bp$(BPh_4)_2$ and $Ag_2$3Bp$(CF_3SO_3)_2$ were prepared by analogous methods, with addition of $NaBPh_4$ and $LiCF_3SO_3$ respectively.

$Ag_2$3Bp$(BPh_4)_2$:H_2O.

Analysis

Calc:	C 69.15	H 5.80	N 7.68
Found:	C 69.52	H 5.17	N 7.33

$Ag_2$3Bp$(CF_3SO_3)_2$

Analysis

Calc:	C 41.47	H 3.95	N 10.52
Found:	C 41.35	H 3.96	N 10.18

$Pb_2$3Bp$(NCS)_4$

This complex was made by modification of the method reported by D.Marrs.[27a] $Pb(SCN)_2$(0.004mol) and terephthalaldehyde (1,4-$C_6H_4(CHO)_2$)(0.006mol) were stirred together vigorously in absolute alcohol (300ml) at 60°C. Tren(0.004mol, 60ml.) in 100ml. absolute alcohol was added dropwise. The reaction mixture was stirred at 60°C for 4 hours. Pale yellow coloured semicrystalline solid was filtered off. Further crops of crystalline product were obtained on concentration of the filtrate and cooling on ice.

Satisfactory CHN analysis was not obtained for this starting material thus the formula of the complex is uncertain. The infrared spectrum of the product shows that the 3Bp cryptand is present.

TRANSMETALLATION OF 3Bp COMPLEXES.

$Co_2$3Bp(SCN)$_4$

$Pb_2$3Bp(SCN)$_4$(0.0003mol) was suspended in acetonitrile (200ml) with stirring at 50-55°C. Co(NCS)$_2$(0.00065mol) was dissolved in ethanol (50ml) and added dropwise, giving a turquoise coloured reaction mixture. After one hour, a turquoise powder was filtered off. The product did not give satisfactory CHN analysis and was not adequately soluble for recrystallisation.

Analysis

Calc:	C 49.00	H 4.32	N 17.14
Found:	C 39.18	H 3.38	N 14.40

FAB Mass Spec

m/e	Formula	% of base peak
587	$[3Bp+H]^+$	(100)
703	$[Co3Bp(NCS)]^+$ or $[Co_2 3Bp-H]^+$	(50)
759	$[Co_2 3Bp(NCS)-3H]^+$ or $[Co3Bp(NCS)_2-2H]^+$	(55)

Many attempts were made to transmetallate dilead or disilver 3Bp complexes, most resulted in anion exchange or ring opening. Conditions employed in the various attempts and the results are summarised in table 2.

SYNTHESIS OF THE METAL-FREE CRYPTAND 3Bp.

3Bp: $6H_2O$

Synthesis of this cryptand was reported previously by D.Marrs[27a]

Terephthalaldehyde (0.003mol) was warmed to 50°C in methanol (100ml). A solution of tren (0.002mol) in methanol (50ml) was added dropwise. The

reaction mixture was stirred at 50°C for 2-3 hours. The yellow solution was filtered and reduced in volume to *ca.* 50ml. Acetonitrile was added and slow evaporation gave pale yellow crystals in 58% yield.

Analysis

Calc:	C 62.1	H 7.8	N 16.1
Found:	C 61.7	H 7.9	N 16.5

Infrared spectrum : 3650-3000 ν(O-H), 2841 ν(C-H), 1643 ν(C=N), 1450, 1437, 1375, 1338, 1077, 1033, 907, 823, 742, 722 and 514cm^{-1},

COMPLEX FORMATION USING THE METAL-FREE CRYPTAND 3Bp

$Cu_2$3Bp$(CF_3SO_3)_2$

3Bp (0.0002mol) was dissolved in ethanol (100ml), $Cu(CF_3SO_3)_2$ (0.0004mol) was dissolved in acetonitrile (100ml) and added. The green solution was stirred for 3 hours at 40-45°C, filtered and reduced in volume. Orange crystals were obtained on slow evaporation.

Analysis.

Calc:	C 45.10	H 4.18	N 11.07
Found:	C 45.09	H 4.19	N 10.70

Λ = 247 S cm^{2}mol^{-1}

$Cu_2$3Bp$(CF_3SO_3)_2$ has also been obtained by metal insertion into 3Bp using $Cu(MeCN)_4CF_3SO_3$.

Attempts to precipitate a Cu(II) complex by mixing a solution of 3Bp in dichloromethane/ethanol solvent mixture with a solution of $Cu(CF_3SO_3)_2$ in ethanol, gave pale green precipitate. The infrared spectrum of the green product showed a carbonyl frequency suggesting ring opening.

$Cu_2$3Bp(SCN)$_2$: ½MeCN

3Bp (0.0002mol) and $Cu(CF_3SO_3)_2$ (0.0004mol) were stirred together in acetonitrile /ethanol solvent mixture at 40°C. NaNCS (0.0006mol) was dissolved in acetonitrile (100ml) and added dropwise. Orange-red colour developed and product crystallised out of solution. Mustard coloured microcrystals were isolated by filtration. The infrared spectrum showed ν(MeCN).

Analysis

Calc:	C 54.99	H 5.10	N 16.88
Found:	C 55.07	H 5.17	N 17.29

$Co_2$3Bp(NCS)$_4$:3H_2O

3Bp(0.0002mol) was dissolved in ethanol(75ml). $Co(CF_3SO_3)_2$ (0.0001mol) in acetonitrile was added, giving a pale brown colour. A solution of $Co(NCS)_2$(0.0001mol) in acetonitrile(100ml) was added dropwise with stirring giving a green-blue solution. After 4 hours at room temperature the solution was filtered and reduced in volume. Cooling on ice gave turquoise powder which was recrystallised from dma/MeoH/Et_2O in low yield.

Analysis.

Calc:	C 48.48	H 4.88	N 16.96
Found:	C 49.28	H 5.19	N 16.28

Anion exchange was attempted to try to obtain a more soluble dicobalt 3Bp complex. $Co_2$3Bp(NCS)$_4$ when stirred with $AgClO_4$ or $AgCF_3SO_3$ in acetonitrile gave rust coloured solution after filtration. Complexes with perchlorate or triflate counterions could not be isolated. Addition of sodium cyanate to the filtrate gave a blue-green solution, only green oil resulted.

[3Bp+2H+](CF$_3$SO$_3$)$_2$

Attempted insertion of Fe(II) into 3Bp using Fe(CF$_3$SO$_3$)$_2$ gave the doubly protonated ligand.

Analysis

Calc:	C 48.50	H 5.35	N 11.90	Fe 0.0
Found:	C 48.73	H 4.56	N 12.36	Fe 0.2

The attempted preparation of metal ion complexes of 3Bp are summarised in table 3.

SYNTHESIS OF THE REDUCED CRYPTAND R3Bp

The reduced 3Bp cryptand was produced by modification of the method reported previously.[275]

The cryptand R3Bp

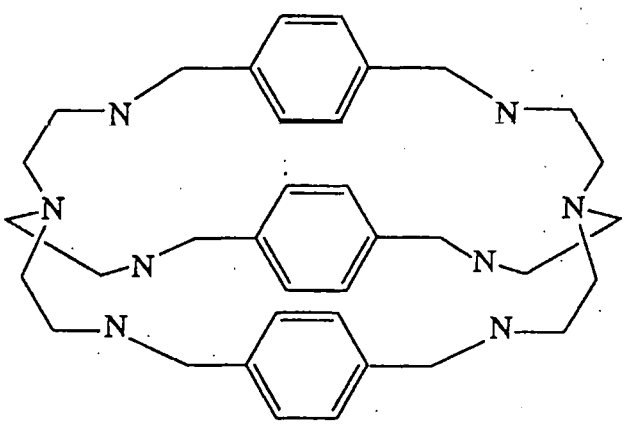

Pb$_2$3Bp(SCN)$_4$(0.001mol) was suspended in ethanol(200ml.) and brought to gentle reflux. A large excess of NaBH$_4$ was added in portions which produced fizzing and a black precipitate of lead. The black suspension was refluxed for 5 hours and the black precipitate was filtered off. The cream coloured filtrate was taken to dryness and the resulting solid was dissolved in NaOH solution (10 NaOH pellets in 15ml. deionised water). The resultant R3Bp solution was extracted with six portions of chloroform and

the extracts were combined, washed with deionised water and dried with Na_2SO_4. After filtration the filtrate was brought to dryness. The solid obtained was redissolved in methanol, filtered and rotary evaporated to dryness. The solid was dried *in vacuo* overnight and to give a cream powdery solid in 69% yield.

Mass Spec.

m/e 598 $[R3Bp]^+$ base peak 100%

Peaks due to partially reduced ligand were absent from the mass spectrum.

Infrared spectrum : 3273, 3231, 3041, 2797, 1623, 1513, 1458, 1362, 1326,1295, 1127, 1054, 1017, 799,772cm^{-1} *inter alia.*

COMPLEX FORMATION USING THE REDUCED CRYPTAND R3Bp

Cu_2R3BpμOH$(ClO_4)_3$: MeCN: $3H_2O$.

R3Bp (0.0001mol) was dissolved in ethanol(50ml) and $Cu(ClO_4)_2{\cdot}6H_2O$ (0.0003mol) was dissolved in acetonitrile (100ml) and added giving a green solution. The reaction mixture was stirred at 50°C for 2 hours, filtered and reduced in volume to *ca.* 100ml. Slow evaporation gave green microcrystals in 81 % yield.

Analysis.

Calc:	C 40.16	H 5.41	N 11.09
Found:	C 39.64	H 5.15	N 11.49

Λ = 311 S cm^2mol^{-1}

Co_2R3BpμOH$(CF_3SO_3)_3$

R3Bp(0.0001mol) and $Co(CF_3SO_3)_2$(0.0003mol) were stirred together in acetonitrile/ethanol solvent mixture for 2 hours at 45°C. Slow evaporation of the filtrate gave pale green microcrystalline product.

Analysis.

Calc:	C 39.67	H 4.69	N 9.49
Found:	C 39.63	H 4.66	N 9.14

FAB Mass Spec.

m/e	Formula	% base peak at 151
657	$[CoR3Bp]^+$	(40)
867	$[Co_2R3Bp(CF_3SO_3)+2H]^+$	(20)
1178	$[Co_2R3Bp(CF_3SO_3)_3OH-2H]^+$	(90)

Addition of a few drops of water to the preparation outlined above gave a darker green solution and improved the yield of the dicobalt R3Bp μOH complex. Apple-green microcrystals were obtained.

Co_2R3BpμOH$(ClO_4)_3$: $2H_2O$.

R3Bp(0.0001mol) and $Co(ClO_4)_2$:$6H_2O$(0.0003mol) were stirred together in MeCN/EtOH solvent mixture for 2 hours at 50°C. The green solution was filtered and reduced in volume, cooling on ice gave green microcrystals in 89% yield.

Analysis

Calc:	C 40.48	H 5.57	N 10.49
Found:	C 40.44	H 5.22	N 10.90

Co_2R3Bp(NCS)$_4$:2H_2O

R3Bp(0.0001mol) was dissolved in methanol and a solution of Co(NCS)$_2$, in methanol, was added. The green precipitate was filtered off and recrystallised from acetonitrile/ethanol solvent mixture. Petrol blue microcrystals were obtained. Acceptable CHN analysis was not obtained.

Analysis

Calc:	C 48.77	H 5.93	N 17.06
Found:	C 42.98	H 5.16	N 16.51

Cu_2R3Bp(CF_3SO_3)$_2$: H_2O

R3Bp(0.0002mol) was dissolved in dry deoxgenated ethanol under nitrogen. Cu(MeCN)$_4$(CF_3SO_3)(0.0005mol) was added as a solid and gave an instant cream precipitate. On addition of dry deoxygenated MeCN, the precipitate dissolved. The solution was stirred at 45°C for 2 hours, reduced in volume and cream coloured microcrystalline solid was filtered off and dried with a nitrogen stream. The complex became slightly green on storage

Analysis

Calc:	C 43.80	H 5.42	N 10.75	Cu 12.20
Found:	C 42.08	H 4.99	N 10.12	Cu 12.26

Λ = 241 S cm^{2}mol^{-1}

FAB Mass Spec.

m/e	Formula	% base peak at 107
599	[R3Bp+H]$^+$	(10)
659	[CuR3Bp-2H]$^+$	(55)
721	[Cu_2R3Bp-3H]$^+$	(15)
873	[Cu_2R3Bp(CF_3SO_3)]$^+$	(90)

Ni_2R3Bp$(NO_3)_4$: $4H_2O$.

R3Bp(0.00015mol) and $Ni(NO_3)_2{:}6H_2O$(0.0006mol) were refluxed together in EtOH/MeCN solvent mixture for 4 hours. The solution was filtered and allowed to evaporate down slowly. Turquoise microcrystals resulted.

Analysis

Calc:	C 41.72	H 6.02	N 16.22
Found:	C 41.68	H 5.45	N 16 38

[R3Bp+4H$^+$]$(CF_3SO_3)_4$

R3Bp(0.0001mol) and $Mn(CF_3SO_3)_2$(0.0003mol) were stirred together in MeCN/EtOH solvent mixture for 2 hours at 50°C. The reaction mixture changed from yellow to brown. After filtration the brown filtrate was left to evaporate down slowly. Dark brown powder (inorganic) was filtered off and the filtrate gave colourless crystals on slow evaporation.

Analysis

Calc:	C 39.47	H 4.97	N 9.21
Found:	C 39.69	H 5.32	N 9.15

Attempted insertion of Fe(II) into R3Bp using $Fe(CF_3SO_3)_2$ gave protonated ligand complex [R3Bp+4H$^+$]$(CF_3SO_3)_4$.

Fab mass spec showed peaks due to protonated R3Bp and there was no evidence of the iron R3Bp complex.

SYNTHESIS OF THE METAL-FREE CRYPTAND 3Bm.

Synthesis of the 3Bm cryptand was reported previously.[275]

The cryptand 3Bm

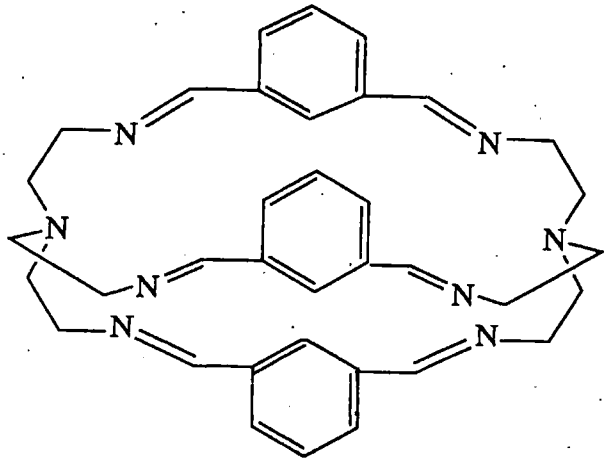

Isophthalaldehyde (0.006mol) was brought to gentle reflux in methanol (300ml) and tren (0.004mol) was added dropwise in concentrated form. The reaction mixture was refluxed gently for 2 hours and the yellow solution was then filtered and reduced in volume by rotary evaporation. Several crops of crystalline product were filtered off (Yield 91%).

Analysis

Calc:	C 73.7	H 7.2	N 19.1
Found:	C 73.9	H 7.3	N 19.2

Infrared spectrum : 3281, 3042, 2900-2800, 1643, 1432,1354, 1336,1290, 1065, 1034,926, 799, 693cm^{-1} *inter alia*

$Ni_2L(NO_3)_4$: $2H_2O$: EtOH

Ligand 3Bm was dissolved in ethanol(150ml) with stirring at 50°C. $Ni(NO_3)_2{:}6H_2O$ (0.0002mol) was dissolved in acetonitrile (150ml) and added dropwise. The reaction mixture became dark green initially and gradually changed to blue. After 2 hours at 50°C , the reaction mixture was filtered

and reduced in volume to *ca.* 50ml. Purple microcrystals were obtained on slow evaporation.

Analysis.

Calc:	C 37.36	H 5.15	N 18.67
Found:	C 37.29	H 4.90	N 17.83

FAB Mass Spec

m/e	Formula	% base peak at 266
790	$[Ni_2L(NO_3)_3]^+$	(70)
845	$[Ni_2L(NO_3)_2]^+$	(5)
908	$[Ni_2L'(NO_3)_3]^+$	(15)

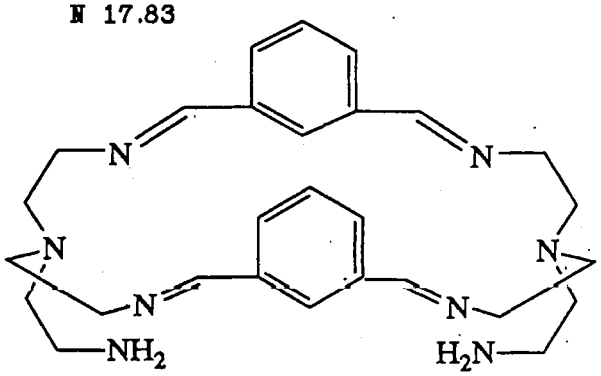

"L"

SYNTHESIS OF THE REDUCED CRYPTAND R3Bm

The cryptand 3Bm was reduced by modification of the method reported by D. Marrs.[278]

The cryptand R3Bm

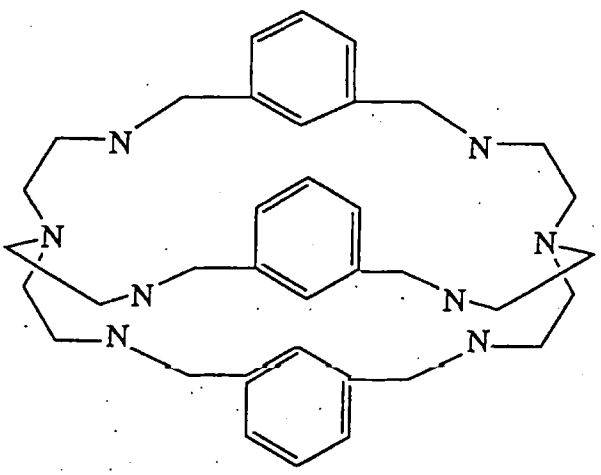

3Bm was brought to reflux in ethanol and a large excess of $NaBH_4$ was added in portions. The reaction mixture was refluxed strongly for 6 hours and stirred for 48 hr at room temperature. After filtration, the filtrate was taken to dryness. The product was worked up as described in the

reduction of $Pb_2$3Bp(NCS)$_4$. The 3Bm ligand was more difficult to reduce thoroughly.

Mass Spec.

m/e	Formula	% base peak
598	[R3Bm]$^+$	100

COMPLEX FORMATION USING THE REDUCED CRYPTAND 3Bm

Co_2R3Bm(ClO$_4$)$_4$: EtOH

R3Bm(0.0002mol)was dissolved in ethanol(100ml) and a solution of Co(ClO$_4$)$_2$: 6H_2O(0.0006mol.) in acetonitrile(100ml.) was added. dropwise giving a green solution. After 1 hour at 50°C , the reaction mixture was filtered and the filtrate was reduced in volume. Cooling on ice gave green microcrystals.

Analysis

Calc:	C 39.33	H 5.21	N 9.65
Found:	C 39.32	H 5.48	N 9.35

FAB Mass Spec

m/e	Formula	% base peak at 875
656	[CoR3Bm]$^+$	(35)
710	[Co_2R3Bm-4H]$^+$	(35)
813	[CoR3Bm(ClO$_4$)]$^+$	(75)
1003	[Co_2R3Bm(ClO$_4$)$_3$-7H]$^+$	(95)

Ni_2R3Bm$(NO_3)_4$: $4H_2O$

R3Bm(0.0002mol) and $Ni(NO_3)_2{:}6H_2O$(0.0005mol) were stirred together in acetonitrile/ethanol solvent mixture at 50°C for 2 hours.The blue-green solution was filtered and reduced in volume to 100ml. Slow evaporation gave turquoise microcrystals.

Analysis

Calc:	C 41.72	H 6.03	N 16.50
Found:	C 42.18	H 6.23	N 15.85

FAB Mass Spec.

m/e	Formula	% base peak at 290
654	$[NiR3Bm]^+$	(25)
775	$[Ni_2R3Bm(NO_3)]^+$	(50)
838	$[Ni_2R3Bm(NO_3)_2]^+$	(40)
901	$[Ni_2R3Bm(NO_3)_3]^+$	(60)

Cu_2R3Bm$(ClO_4)_4$: $2H_2O$

This complex was made by an analogous method. Green microcrystals were obtained on slow evaporation.

Analysis

Calc:	C 37.28	H 5.04	N 9.66
Found:	C 37.47	H 5.52	N 9.50

Attempts to produce a copper(I) cryptate by metal insertion into R3Bm using $Cu(MeCN)_4(CF_3SO_3)$ gave dicopper(II) cryptate despite nitrogen protection. Only impure product was obtained from the reaction. Reaction of R3Bm and $Mn(NO_3)_2$ gave $[R3Bm+2H^+](NO_3)_2$.

Attempted insertion of Fe(II) into R3Bm failed. Only orange gel resulted.

TABLE 2 - ATTEMPTED TRANSMETALLATION OF 3Bp COMPLEXES

$Pb_2$3Bp$(NCS)_4$ - starting material.

METAL	CONDITIONS	SOLVENT	RESULT
$Co(NO_3)_2$	3hr 60°C	MeCN	$Pb_2$3Bp$(NO_3)_4$
$Co(NO_3)_2$	5hr reflux	MeCN	ring opened, C=O present in i.r.
$Mn(NO_3)_2$	2hr 60°C	MeCN/EtOH	brown inorganic powder + $Pb_2$3Bp$(NO_3)_4$ crystals
$Ni(NO_3)_2$	3hr 60°C	"	pale green powder, weak C=O 1695
$Ni(NO_3)_2$	5hr reflux	"	lilac powder, strong C=O.
$NiCl_2$	3hr 55-60°C	"	green oil
$MnCl_2$	3hr 55-60°C	"	Brown powder and $Pb_2$3Bp$(NCS)_4$

$Ag_2$3Bp$(BPh_4)_2$ - starting material.

METAL	CONDITIONS	SOLVENT	RESULT
$Co(NO_3)_2$	3hr reflux	MeCN	pale coloured solution, some ring opening
$Co(NCS)_2$	2hr 60°C		crude blue precipitate insoluble, ir no C=O

$Ag_2$3Bp$(CF_3SO_3)_2$ - starting material.

METAL	CONDITIONS	SOLVENT	RESULT
$Mn(CF_3SO_3)_2$	2hr 60°C	MeCN	starting material
$Ni(NO_3)_2$	5hr reflux	MeCN/EtOH	oil
$Ni(CF_3SO_3)_2$	3hr 55-60°C	"	starting material

TABLE 3 - ATTEMPTED METAL INSERTION INTO 3Bp

Free 3Bp starting material

METAL	CONDITIONS	SOLVENT	RESULT
$Co(NO_3)_2$	3hr 60°C	MeCN/EtOH	rust coloured solution gave brown oil only
$Co(CF_3SO_3)_2$	3hr 60°C	"	rust coloured solution gave brown oil
$Co(CF_3SO_3$ NaN_3 present	3hr 40°C	"	gave brown oil
$Co(NCS)_2$	1hr 50°C	"	green precipitate
$Ni(NO_3)_2$	5hr 60°C	"	pale coloured solution complex not formed
$NiCl_2$	6hr reflux	"	complex not formed
$Fe(CF_3SO_3)_2$	2hr 55°C	dry deoxy MeCN/EtOH	protonated 3Bp-CF_3SO_3) % Fe test -no Fe present
$Mn(NO_3)_2$	3hr 50°C	MeCN/EtOH	brown solution gave cream crystals, protonated 3Bp nitrate fab mass spec -no Mn present

ATTEMPTED CRYPTATE SYNTHESIS USING GLUTARALDEHYDE, TREN AND TEMPLATE ION

Glutaraldehyde($OHC(CH_2)_3CHO$) was extracted with chloroform from a 50% solution in water. The solution in chloroform was dried, filtered and reduced in volume to yield a yellow oil.
Infrared spectrum, 2960(s), 2900(s), 1720(s) *inter alia*. Glutaraldehyde oil polymerises to give a hard plastic-like material within a month.
The experimental method used in the following attempts involved reflux of glutaraldehyde(0.003mol) with template species(0.002mol) in (200ml) solvent for 10-15 minutes. A solution containing tren(0.002mol) was added dropwise with stirring.

TABLE 4

TEMPLATE SPECIES	CONDITIONS	SOLVENT	RESULT (infrared frequency/cm^{-1})
$Ba(ClO_4)_2$	45°C 2hr	MeOH	Flocculent solid formed beige colour, MeCN insol. i.r. spectrum broad, -polymer.
$Ba(ClO_4)_2$	45°C 2hr	MeCN/EtOH	Fawn powder, MeCN sol. i.r. strong NH_2, no C=N Ba-tren complex
$Ba(NO_3)_2$	40°C 3hr	MeCN/MeOH	didnt solubilise $Ba(NO_3)_2$ -polymer.
$Ba(ClO_4)_2$	reflux 2hr	MeOH	Addition of $NaBPh_4$ did not give precipitate
$Ba(ClO_4)_2$	40-45°C 3hr $NaBPh_4$ present	MeCN/MeOH	Flocculent solid formed i.r. broad -polymer later crop Ba-tren complex
$AgNO_3$	30°C 3hr	MeOH	Silver precipitate formed black oil and a few colourless crystals were obtained, i.r. C=N, C=O, NH_2
$AgClO_4$	50°C 4hr dark reaction	MeOH	mustard coloured solid i.r. some NH_2, possible C=N 1600, 1659 Fab m/e 700 Ag_2cage 5%
$Pb(NCS)_2$	50°C 1hr RT 3hr	MeOH	$Pb(NCS)_2$ dissolved, gave yellow solution, BPh_4- gave cream precipitate. i.r. C=N 1615, 1635 some NH_2, but hopeful.
$Pb(NCS)_2$	reflux 3hr	MeOH	i.r. broad over C=N, no NH_2 polymer, crop 2 Pb-tren complex
$Sr(NO3)_2$	40-45°C	MeOH	$Sr(NO_3)_2$ dissolved. Cream crystals, i.r. sharp strong NH_2, sharp C=O, sharp 1601 peak.
$Sr(ClO_4)_2$	40-50°C 3hr $NaBPh_4$ present	EtOH	Cream solid, Sr-tren complex. crop 2 pale yellow crystalline, pendant arm macrocycle? i.r. NH_2, C=N 1625, BPh_4

ATTEMPTED CRYPTATE SYNTHESIS USING PYRUVIC ALDEHYDE, TREN AND TEMPLATE

Pyruvic aldehyde(CH_3COCHO) was extracted from aqueous solution. CH_3COCHO(0.003mol) and template species(0.001mol) were refluxed together in solvent for 15-20 minutes. A solution of tren(0.002mol) was added dropwise with stirring.

TABLE 5

TEMPLATE	CONDITIONS	SOLVENT	RESULT
$Sr(ClO_4)_2$	45-50°C 3hr $NaBPh_4$ present	MeOH	Orange colour developed gave ginger solid, soluble in MeCN, i.r. C=N 1610, 1650, NH_2, ClO_4 BPh_4 present
$Sr(ClO_4)_2$	45°C 6hr	MeOH	fawn powder, i.r. broad no C=N present
$Sr(ClO_4)_2$	reflux 3hr	MeOH	$NaBPh_4$ added no precipitate. fawn powder, i.r. broad
$Ca(NO_3)_2$	45-50°C 5hr $NaBPh_4$ present	MeOH	gave beige solid at reduced volume, recryst MeCN/EtOH, i.r. possible C=N 1632. Fab - no cage/macrocycle
$Ba(ClO_4)_2$	50°C 1hr overnight stir	MeOH	Crop 2 yellow crystalline i.r. NH_2 sharp C=N 1615, 1655, BPh_4 strong. -pendant arm macrocycle?

ATTEMPTED CRYPTATE SYNTHESIS USING 2,3-BUTANEDIONE, TREN AND TEMPLATE $CH_3COCOCH_3$(0.003mol) and template species(0.001mol) were heated in solvent(250ml). A solution of tren(0.002mol) was added dropwise with stirring.

TABLE 6

TEMPLATE	CONDITIONS	SOLVENT	RESULT
$Sr(ClO_4)_2$	50°C 5hr overnight stir $NaBPh_4$ present	MeOH	ginger solid, i.r. slight NH_2, broad 1700-1300 recryst from MeCN still broad over C=N region.
$Ba(ClO_4)_2$	40-50°C 5hr overnight stir $NaBPh_4$ present	MeOH	ginger solid, broad i.r. spectrum
$Pb(NCS)_2$	Reflux	MeCN/EtOH	$Pb(NCS)_2$ dissolved yellow solution, became brown, gave brown oil.

CHAPTER 3

INTRODUCTION

The discussion of the binuclear complexes of macrocycles P and MC is preceded by a brief review of the role and characteristics of the copper ion in relevant metalloproteins. A short section on bonding modes of the thiocyanate ligand is included, as the thiocyanate ligand is present in many of the metal ion complexes of P and MC.

The activity of many metalloproteins is associated with the binding of pairs of metal ions within a protein molecule. Consequently, there is considerable interest in the synthesis of model systems; binucleating ligands which are capable of binding metal ions. Table 7 summarises some of the pairs of metal ions bound in the active sites of enzymes and indicates their biological function.

TABLE 7

BINUCLEAR SITE	ENZYME	FUNCTION
Cu Cu	Haemocyanin	reversible O_2 carrier
Cu Cu	Tyrosinase	monooxygenase
Cu Cu	Laccase	oxidase
Cu Cu	Ceruloplasmin	oxidase
Cu Cu	Ascorbate oxidase	oxidase
Cu Fe	Cytochrome-c-oxidase	electron transport
Cu Zn	Superoxide dismutase	O_2^- disproportionation.
Fe Fe	Haemerythrin	reversible O_2 carrier
Fe Fe	Rubredoxin	O_2 transfer in photosynthesis

It is apparent that the copper ion is involved in a wide range of biological processes. Copper(II) sites in proteins can be classified into three types based on their spectral properties.[276,277]

TYPE 1 COPPER

These intensely blue copper proteins are characterised[276-279] by a visible absorption band close to 600nm with a high extinction coefficient, typically around $3000M^{-1}cm^{-1}$. In addition type 1 copper proteins have an esr spectrum with unusually small hyperfine coupling constant, and high positive redox potential indicating appreciable stability of the copper(I) state (e.g plastocyanin).

TYPE 2 COPPER

This type of copper has less intense electronic spectral absorptions than type 1 copper proteins. Copper proteins of this type exhibit normal Cu(II) esr spectra. Type 2 copper is often found in association with type 3 copper.

TYPE 3 COPPER

Type 3 copper(II) exhibits an intense 330nm absorption with extinction coefficient in the range $3000-5000M^{-1}cm^{-1}$. This type is also characterised by the presence of two copper ions in close proximity. The copper(II) is esr inactive as a result of strong antiferromagnetic coupling interactions between the copper ions. The site can act as a two electron donor/acceptor centre, and is essential to the reduction of dioxygen.

In addition to the three types outlined above, there are non-blue copper proteins. Although these exhibit similar properties to those of type 2 copper proteins, they differ significantly with respect to prosthetic groups, quaternary structure and reactivity.[276] (e.g. haemocyanin)

HAEMOCYANIN

The oxygen-carrying non-heme proteins have very high molecular weights and are found in various molluscs and arthropods. Deoxyhaemocyanin

contains copper(I) and is capable of binding one mol of dioxygen per pair of copper ions. An early crystal structure of the copper(I) dinuclear active site of *Panulirus interruptus* haemocyanin indicated coordination of copper by three histidine ligands, a Cu-Cu separation of 3.7Å was reported.[200] A more recent crystal structure of the deoxy form of *Panulirus interruptus* haemocyanin at 3.2Å resolution[201] showed that each copper is coordinated by two tightly bound histidine and one distant histidine residue. The two distant histidine ligands are located in apical positions and are on opposite sides with respect to the approximate plane defined by the four more tightly bound histidine ligands and the two copper ions. The copper to copper distance is between 3.5 and 3.6Å in four of the subunits, but this distance deviates considerably in two other subunits. A view of the binuclear copper site of haemocyanin is shown in figure 1. The copper coordinating histidine residues are shown in thick lines and the copper ions are shown by crosses.

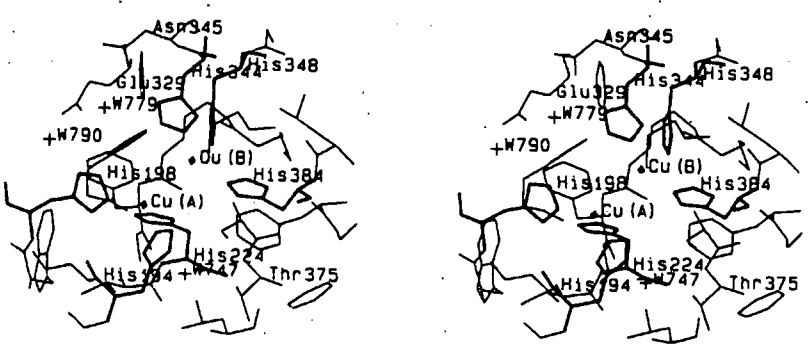

Figure 1 *The dinuclear copper site of Panulirus Interruptus haemocyanin*

Resonance raman studies have shown that haemocyanins bind oxygen between the copper(II) ions as μ-1,2-peroxide and the oxidation state of the copper ions change from (I) to (II).[202] Oxidation results in a change in both coordination sphere and geometry to give two tetragonally

coordinated copper(II) ions in an environment of 6 histidine ligands.[203] The dinuclear Cu(II) site remains esr silent after oxygenation as a result of strong antiferromagnetic coupling between the Cu(II) ions. As a result of this property haemocyanins are classed as type 3 copper proteins. It has been suggested that a μ-OH ligand exists in copper(II) forms of haemocyanin[204-206] and in related dinuclear copper proteins[207], though this is not certain.

Haemocyanin shows cooperativity in binding O_2 which is probably triggered by the structural changes involved in the change in oxidation state that results from dioxygen binding.[208] A structure intermediate to that preferred by Cu(I) and that preferred by Cu(II) may exist in one or both of the oxy and deoxy forms.[208] High co-operativity of carbon monoxide binding at high oxygen activity has been reported.

TYROSINASE

Tyrosinase catalyses both the 2-electron oxidation of o-diphenols to o-quinones and the monooxygenation of phenols to o-diphenols. The binuclear type 3 copper active site found in tyrosinase[209] is similar to the active site of haemocyanin.

THE BLUE COPPER OXIDASES.

The blue copper oxidases , laccase, ceruloplasmin and ascorbate oxidase contain copper(II) of each of the major types listed. Laccase is the simplest of the blue oxidases and contains a type 1, a type 2 and a type 3 copper(II) site. The type 2 and 3 sites are in close proximity and a strong dependence of the geometric and electronic structure of the type 2 copper(II) ion on the oxidation state of the type 3 copper centre was noted. Studies of the binding of small anions to laccase suggest that a trinuclear copper active site comprising type 2 and 3 copper ions may be

active in the irreversible binding and multielectron reduction of dioxygen to water.[289] It was suggested that the trinuclear copper cluster assists in oxygen reduction by providing rapid three-electron transfer leading to irreversible cleavage of the O-O bond.

The structure and nature of the copper active sites in ceruloplasmin are not fully established. The enzyme is thought to contain seven copper ions, two type 1, one type 2 and two pairs of type 3 copper sites.[290]

Ascorbate oxidase contains a trinuclear active site in which type 2 and 3 copper ions may work together to achieve the reduction of dioxygen.[291] It was for this work that, among other contributors, Huber was awarded the 1988 Nobel Prize for Chemistry. The trinuclear site is shown in figure 2 and contains a pair of type 3 copper ions each with three histidyl ligands. The remaining ion is a type 2 copper(II) which has two histidyl ligands.[291]

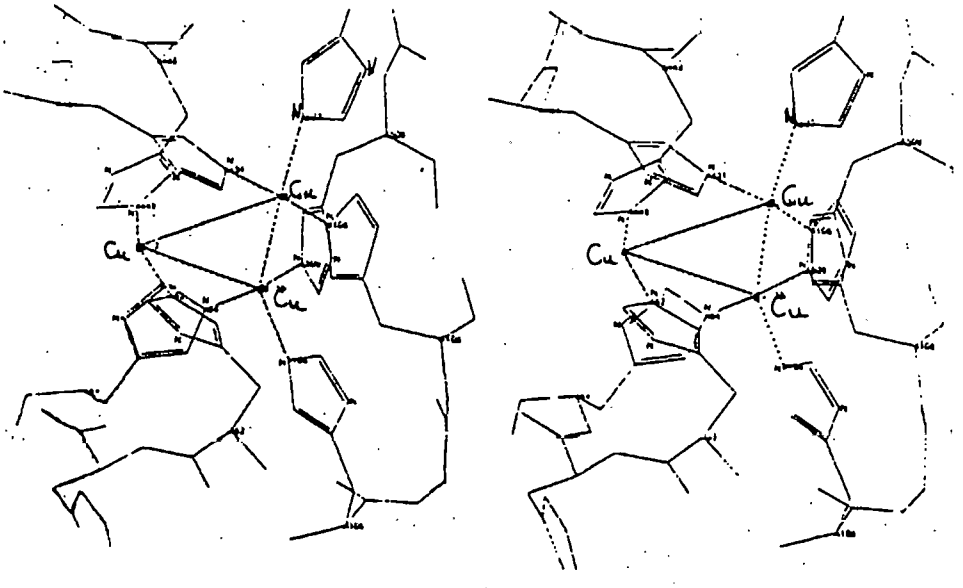

Figure 2 *The trinuclear active site of ascorbate oxidase*

Dioxygen is known to bind at the tricopper cluster. The proximity of the three copper ions in the active site may facilitate cooperative donation

of three electrons enabling cleavage of the O-O bond. In addition to the trinuclear site, ascorbate oxidase contains a site where a copper ion is bound in a strongly distorted tetrahedral geometry (approaching trigonal pyramidal geometry) by two histidine ligands, a cysteine and a methionine ligand.

CYTOCHROME-C-OXIDASE

Cytochrome-c-oxidase is a heteronuclear Cu/Fe containing metalloprotein. The enzyme is the terminal member of the electron transport chain in mitochondria and couples the respiration process to oxidation by molecular oxygen.[276] The enzyme functions by accepting electrons from ferrocytochrome c and then donating them to dioxygen. Although the enzyme is difficult to study because it is anchored to the mitochondrial membrane, it is known that four metal centres, two copper and two iron ions are present. The magnetic properties of the components of cytochrome-c-oxidase suggest that one heme centre and one copper centre are antiferromagnetically coupled. Only one copper centre has been detected by esr spectroscopy and the other is undetectable by both esr and electronic spectroscopy. The fully oxidised cytochrome-c-oxidase is believed to contain high spin iron. The temperature dependence of the paramagnetic susceptibility of the oxidised form was studied in the temperature range 200-7K and 4.2-1.5K. The results are consistent with a model in which two isolated S = ½ centres and a spin-coupled S = 2 centre are present, corresponding to low-spin Fe(III)(d^5)Cu(II)(d^9) and high-spin Fe(III)/Cu(II) respectively. A model in which the iron and copper centres are linked by an imidazolate bridge has been proposed for the antiferromagnetically coupled Fe/Cu centre.[276]

SUPEROXIDE DISMUTASE

Bovine superoxide dismutase is a heterobinuclear Cu/Zn metalloprotein which catalyses dismutation of superoxide anion to dioxygen and hydrogen peroxide.

$$2O_2^{\cdot-} + 2H^+ \rightarrow H_2O_2 + O_2$$

An X-ray structure of the metalloprotein at 3Å has been reported. The metalloprotein contains a copper(II) ion which is coordinated by four histidine ligands and a water molecule in a slightly distorted square pyramidal geometry.[291] The coordination about the zinc ion is pseudotetrahedral.

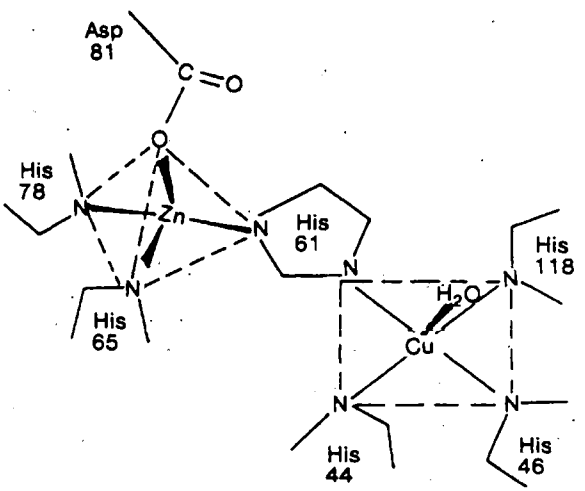

Figure 3 *Schematic drawing of active site of bovine superoxide dismutase*

Superoxide dismutase has been structurally characterised only in the Cu(II) oxidation state.[292] The electronic spectrum of the enzyme shows an absorption at 680nm which has an extinction coefficient of $300M^{-1}cm^{-1}$ as is typical of a type 2 copper(II) ion.

PLASTOCYANIN

Although plastocyanin does not contain a binuclear active site, it is included here due to it's relevance to some of the work described later

in this thesis. The structure of oxidised poplar plastocyanin has been determined at 2.7Å resolution. In the blue copper protein plastocyanin,[202,203] the copper(II) ion is bound in an unusual distorted tetrahedral coordination geometry provided by two unsaturated N-donors from two histidine ligands, and two sulphur donors one from a cysteine and the other from a methionine ligand. The interaction between copper and methionine is weak at 2.9Å.

The donor groups provide a compromise between the preference of Cu(I) for soft donors and the preference of Cu(II) for harder donors. The coordination sphere around the copper ion is intermediate between the square planar and tetrahedral geometries favoured by Cu(II) and Cu(I) respectivly, which further suggests enhancement of electron transfer. Nuclear magnetic resonance studies reveal that the active site is relatively inaccessible to solvent molecules.[204]

THIOCYANATE : AN AMBIDENTATE LIGAND

X-ray structural studies of crystalline KSCN derivatives[295] indicate that the free thiocyanate ion is linear and exists as a hybrid of $^{-}S-C\equiv N$ and $S=C=N^{-}$ canonical forms. The stabilisation of one canonical form relative to another depends on the chemical environment, thus formally, charge may be located at either end of the ion resulting in ambidentate character.[296] The thiocyanate anion displays various bonding modes, which are illustrated in figure 4.

(a) N-terminal M—NCS

(b) S-terminal M—SCN

(c) 3-atom bridges M—NCS / SCN—M

(d) 3-atom bridges M(SCN)(SCN)M

(e) N-only M(NCS)M

(f) S-only M(SCN)M

Figure 4 *Bonding modes of the thiocyanate ligand*

The terminal nitrogen or sulphur bonding modes are common and the choice of nitrogen or sulphur donor is normally dependent on the hardness (N-bonding) or softness (S-bonding) of the metal ion. In addition to electronic factors, steric factors are often involved. In a crowded complex steric interactions may cause coordination of the NCS through nitrogen. The M-N-CS arrangement has a bond angle of about 170° which is almost linear whereas the alternative M-S-CN bonding has a bond angle which is close to 100°.[297]

The three-atom bridging mode of thiocyanate is often found in binuclear metal complexes and in heterobinuclear systems the soft S-donor tends to bind to the softer metal ion. By contrast, coordination in a

single atom bridging mode is relatively rare. Relatively few examples of the S-only bridging mode of thiocyanate have been described. In 1977 Kivekas *et al* described a complex containing both a 1,1-μ-S bonded thiocyanate and a terminal thiocyanate.[297] A structurally determined example of an S-only bridge between copper(I) ions bound within a macrocycle was reported by Nelson[298] and coworkers (figure 5).

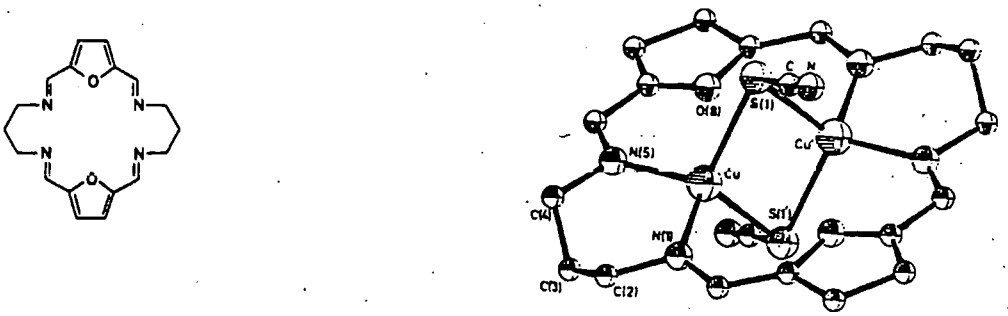

Figure 5

The S-only bridging thiocyanate occurs at internuclear separation of 2.87Å. The mode of coordination of the thiocyanate ligand is presumably determined both by the soft nature of Cu(I) and the cavity space available between the metal ions bound by the macrocycle. More recently another example of a 1,1-μ-S bonded thiocyanate has been reported in a dilead complex.[299]

The N-only bridging bonding mode of thiocyanate was first reported by Cotton[300] in 1979 in an X-ray structural determination of a dirhenium complex anion $[Re_2(NCS)_{10}]^{2-}$ and subsequently in 1982 by Reedijk[301] in a dicadmium complex. However the first example of N-only bridging within a macrocyclic complex was reported by Nelson[302,303] the following year. Shortly afterwards Lindoy reported the N-only bridge in a macrocyclic Ni(II) dimer.[304]

Observation of thiocyanate in a bridging mode is indicative of the separation of two metal centres. At internuclear separation greater than

6Å bridging configurations are impossible and terminal -NCS or -SCN depending on the hard/soft nature of the metal ion is observed. The formation of two long bridges between metal ions is often found. The arrangement shown in figure 4(c) typically occurs at internuclear distances in the range 5.3-5.8Å.[205,206] Alternatively, two long bridges can be be accomodated in the manner shown in figure 4(d) where both S-donors bond to the same metal ion. This arrangement is common in heterobinuclear systems where difference in the hard/soft nature of the two metal ions determine the orientation of the thiocyanate 3-atom bridge. The internuclear distance required for accomodation of the two bridging units is reduced[206] in this arrangement.

There are fewer examples of structurally determined N-only bridging thiocyanate. An example of bridging between lead ions via the N-atom only of the thiocyanate occurs in the macrocycle L^1 shown in figure 6.[128] The internuclear separation of the lead ions was 4.34Å.

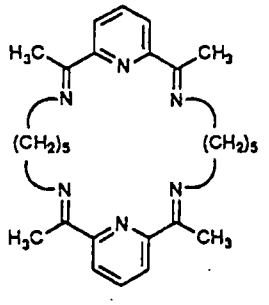

L^1

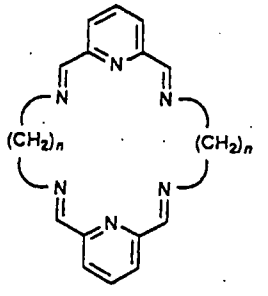

L^2 n=4, L^3 n=3

Figure 6 *Macrocycles that bind the N-N(CS)-N assembly*

Recently, N-only bridged binuclear complexes of all five members of the first transition series from Mn(II) to Cu(II) were reported.[206,207] The presence of the N-only bridging thiocyanate was detected by infrared spectroscopy of binuclear tetrakis- or bis-(thiocyanato) complexes of Mn(II), Fe(II), Co(II), Ni(II) with macrocycle L^2 (figure 6), and in

binuclear Co(II) and Ni(II) complexes of macrocycle L^3.The dicopper(II) N-only bridged assembly was observed with the macrocycle shown in figure 5. Two N-only bridging thiocyanates have been found between Ni(II) ions, in a structurally characterised complex. The internuclear separation of the Ni(II) ions was 3.28Å. Various reports of N-only bridging thiocyanate have appeared in recent years.[208-211]

The infrared spectroscopy of coordinated thiocyanate was reviewed in 1971.[212] Despite the small number of structurally defined examples of N-only bridging, a simple physico-structural correlation based on infrared data has emerged. There are three normal vibrations of thiocyanate, ν(CN), ν(CS) and ν(NCS). The ν(CN) vibration is most studied as it is normally a strong vibration that occurs around 2050cm^{-1} which is a region that is normally free of ligand vibrations. By contrast the lower energy ν(NCS) and ν(CS) vibrations appear at around 470 and 700-800cm^{-1} respectively regions where there is often interference from ligand vibrations.

The ν(CN) frequency ranges of the various bonding modes of thiocyanate, with the first row transition metals, along with that of the free ion are summarised in figure 7.

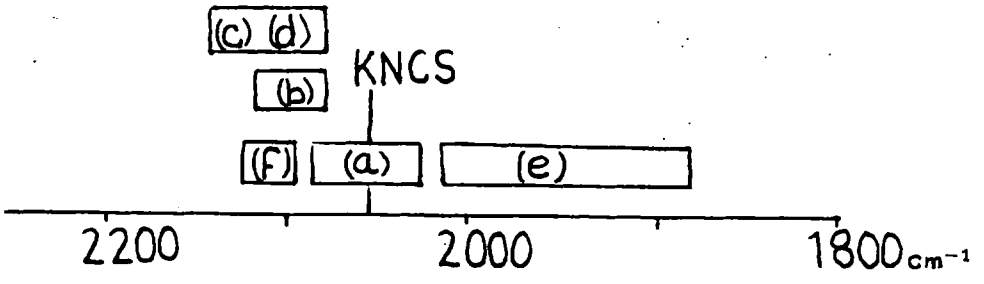

Figure 7 *Infrared spectral ν(CN) and their structural assignments*

Examination of figure 7 shows that there is overlap of the absorptions of the various types of coordination involving sulphur. Absorption due to

terminal nitrogen bonded thiocyanate occurs at lower frequency between 2030-2080cm^{-1}. However the most striking feature is that N-only bridging thiocyanates exhibit ν(CN) absorption at frequencies below 2030cm^{-1} and usually below 2000cm^{-1}. The lowest recorded frequency for the N-only bonded thiocyanate is 1885cm^{-1}.[212]

The bonding of the higher alkaline earth metal ions to the thiocyanate anion is relatively ionic in character and thus higher values for ν(C≡N) are observed in both N- and S- terminal bonding. For example, the Ca^{2+} complex of benzo-15-crown-5, $CaL(NCS)_2{:}H_2O$ has absorption bands at 2100 and 2075cm^{-1} for the N -bonded anions.[57] The free ion value occurs at *ca.* 2100cm^{-1}. X-ray crystallographic data show that different Ca-N-CS angles for the two thiocyanates result in the non-equivalence that causes the splitting of the infrared spectral frequency.

In some cases the use of C-S stretching frequencies can aid in further assignment of the thiocyanate bonding mode. N-bonded terminal thiocyanates have C-S stretching in the range 780-860cm^{-1}, whereas S-terminal thiocyanate absorbs in the range 690-720cm^{-1}. The N-C-S bending mode occurs in the range 465-480cm^{-1} for N-terminal thiocyanate or between 410 and 470cm^{-1} for S bonded terminal thiocyanate. In view of the occurrence of N-S linkage switches in metal isothiocyanate complexes caution is advisable in applying these assignment criteria.

COMPLEXES OF THE MACROCYCLIC LIGANDS P AND MC

Macrocycles P and MC were prepared by template methods in the presence of $Pb(NCS)_2$, as described in the experimental section. Template synthesis of the P macrocyclic complex, $Pb_2P(NCS)_4$ (1), was reported previously[274] and the structure of the complex was determined by X-ray crystallography.

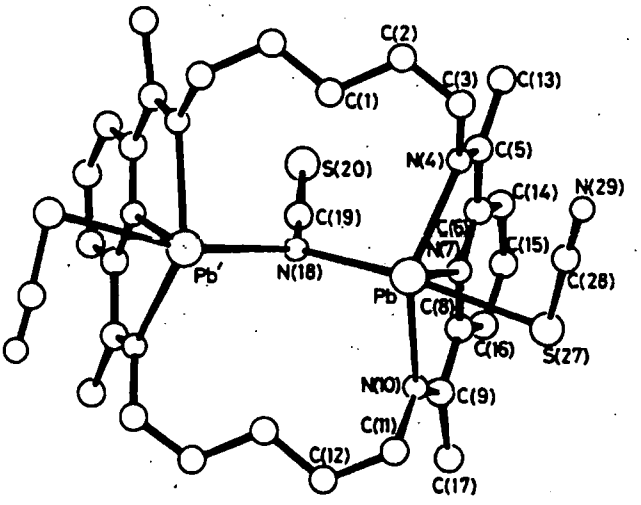

Figure 8 *The X-ray crystal structure of* $Pb_2P(NCS)_4$

The X-ray stucture demonstrated that 2+2 Schiff-base condensation had taken place to form the dilead macrocyclic complex and that the unusual N-only bridging mode of thiocyanate is found between the metal ions. A weakly bonded and very disordered thiocyanate was located between the two lead ions. Each lead ion was also bonded to an S-terminal thiocyanate.

The series of complexes of macrocycle P has been extended to include triflate derivatives. Triflate anion ($CF_3SO_3^-$) was used as an alternative to the potentially hazardous perchlorate anion, which was used in the original work reported by B.Murphy.[128] The macrocyclic ligand offers three equatorial donors to each metal ion, leaving the metal ions coordinatively unsaturated and capable of binding small bridging ligands. Triflate anion has relatively little tendency to act as a ligand[214] and

improves the solubility of the complex in polar solvents. Vacant coordination sites on the metal ion are available to anions, such as thiocyanate which coordinates more strongly. The thiocyanate anion, (NCS^-) coordinates the metal ion and has various bonding modes, which have been outlined in the introduction to this chapter.

Infrared spectral data for the various dilead P complexes is listed in Table 8. The presence of ν(C=N) and the absence of (C=O) and (NH_2) frequencies in the infrared spectra imply that the macrocyclic ligand remains intact throughout the various transformations.

TABLE 8 PHYSICAL DATA FOR THE DILEAD COMPLEXES OF MACROCYCLE P
Infrared spectral data /cm^{-1}.

COMPLEX	COLOUR	ν(C=N)	ν(pyr)	ν(NCS)	$\nu(CF_3SO_3)$	ν(OH)
1 $[Pb_2P(NCS)_4]$	yellow	1642	1582	2090(s) 2046(s) 2025(s) 1970(s)	-	-
2 $Pb_2P(NCS)_2(CF_3SO_3)_2$	primrose yellow	1644	1586	2097(s) 1964(s)	1278(s) 1238(s) 1027(s) 637(m)	-
3 $Pb_2P(NCS)(CF_3SO_3)_3$:EtOH	cream	1645	1586	1943(s)	1273(s) 1240(s) 1027(s) 638(m)	3430
4 $Pb_2P(NCS)(CF_3SO_3)_3$:$2H_2O$	cream	1647	1587	2097(s)	1273(s) 1239(s) 1027(s) 638(m)	3435
5 $Pb_2P(CF_3SO_3)_4$:MeCN	white	1649	1590	-	1272(s) 1240(s) 1219(s) 1012(s) 637(m)	-

Complex 5 shows ν(MeCN) at 2322cm^{-1}

The pseudo-asymmetric ν(NCS) region of the spectra is of interest and is illustrated in figure 9. The complex $[Pb_2P(NCS)_4]$ (1) shows four bands in the ν(C≡N) region. The strong absorptions at 1970 and 2090cm^{-1} are assigned to a single atom N-only bridging thiocyanate and a weakly bonded thiocyanate respectively. The absorptions at 2046 and 2025cm^{-1} are attributed to two S-terminal thiocyanates in slightly different environments, one bound to each lead ion. The slightly different environments may arise from the twisting of the structure that is apparent in the X-ray structure (figure 8).

Anion exchange provides a series of complexes in which the number of thiocyanate anions vary. Replacement of thiocyanate anion in the tetrathiocyanate complex with triflate anion was achieved by use of silver triflate. It proved necessary to use the silver salt as this gave a silver thiocyanate precipitate which was easily filtered off. Attempted anion exchange by use of lithium triflate gave only starting material. The tetrathiocyanate P complex was less soluble than the triflate derivatives and crystallised out of solution in preference to triflate containing products.

On proceeding to the bis- and mono-thiocyanato complexes, a progressive removal of the various bonding modes of thiocyanate is observed as illustrated in figure 9. Infrared spectral data shows which bonding mode is replaced. In complex (2), $[Pb_2P(NCS)_2](CF_3SO_3)_2$ only the thiocyanates giving rise to the absorptions at 1964 and 2097cm^{-1} remain. The lower frequency absorption is due to the N-only bridging thiocyanate and the absorption at 2097cm^{-1} is assigned to the weakly coordinated disordered NCS that lies between the lead ions. The residual 2+ charge is

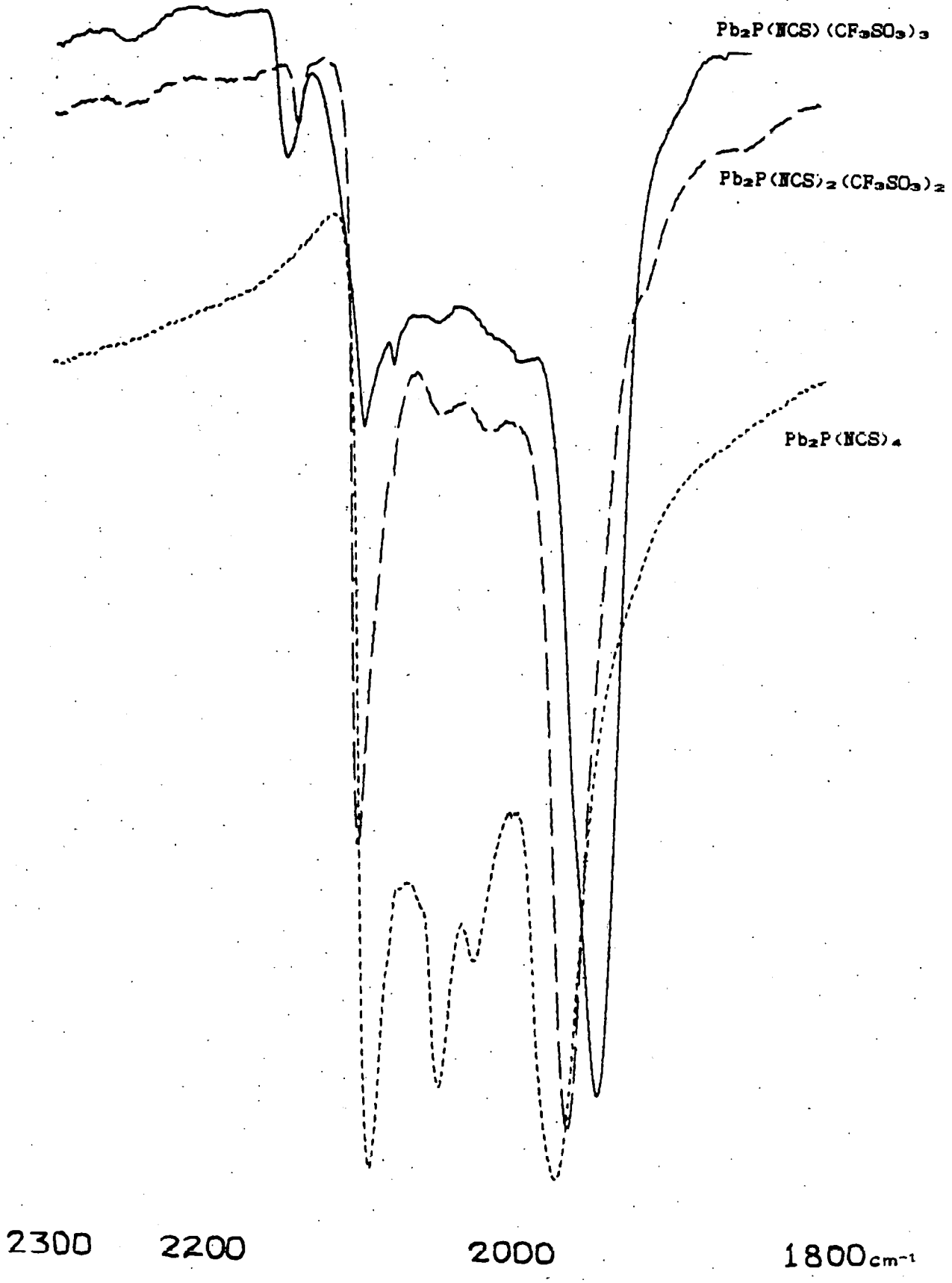

Figure 9 *The ν_{as}(NCS) stretching region of dilead P thiocyanates*

balanced by two triflate anions. On replacement of another thiocyanate by triflate, only the N-only bridging thiocyanate remains.

Progressive lowering of the frequency of absorption of the thiocyanate N-only bridge is observed in the series of complexes, 1970cm^{-1} in the tetrathiocyanate (1), 1964cm^{-1} in the dithiocyanate (2) and 1943cm^{-1} in the monothiocyanate (3). This indicates a progressive weakening of the C≡N bond in the thiocyanate ligand which may indicate stronger coordination of the N atom to the two lead ions.

Fast atom bombardment mass spectroscopy has been done on complexes (2) and (3). The fab mass spectrum of the monothiocyanate complex (3) gave seven peaks attributable to mono or dilead P containing fragments, which are listed in the experimental section. The peak corresponding to $[Pb_2P(NCS)(CF_3SO_3)_2]^+$ was the most intense of the dilead P fragment ions. However a low intensity peak (5%) at m/e 1139 corresponding to $[Pb_2P(CF_3SO_3)(NCS)_2]^+$ was observed. It is possible that the dithiocyanate forms during fab mass spectroscopy or there may be some contamination of the monothiocyanate complex with the dithiocyanate complex. However, if the latter is the case, the CHN analysis did not suggest the presence of impurity and the infrared spectrum did not show a strong absorption due to another bonding mode of thiocyanate. The intensity of the peak in the mass spectrum need not necessarily reflect the percentage of the parent species in the material, as peak intensity is also dependent on the stability of the fragment ion.

The fab mass spectrum of the dithiocyanate (2) shows the fragment ion $[PbP(CF_3SO_3)]^+$ as the base peak. The peak due to the dithiocyanate $[Pb_2P(NCS)_2(CF_3SO_3)]^+$ was of moderate intensity, however a relatively low intensity peak due to $[Pb_2P(CF_3SO_3)_3]^+$ was observed. Analysis of the

percentage of carbon, hydrogen and nitrogen in the complex did not suggest impurity.

Although the N only bridge is retained throughout all of the thiocyanate derivatives, this configuration is not introduced first when a triflate anion in the tetratriflate P dilead complex (5) is exchanged for a thiocyanate anion. The infrared spectrum of $Pb_2P(NCS)(CF_3SO_3)_3$ (4) exhibits ν(C≡N) of thiocyanate at 2097cm^{-1}, this frequency suggests that the weakly bonded thiocyanate was introduced. It is possible that formation of this bonding mode of thiocyanate is kinetically favoured.

The infrared spectrum of the tetratriflate (5) shows an increase in the number of absorptions due to the triflate group on comparison of the infrared spectrum of the complex with that of the triflate salt. Coordination of metal ions by triflate has been reported and induces only slight anion structural changes.[315] Ionic triflate has strong asymmetric stretch of (SO_3) at *ca.* 1278cm^{-1} and ν_{as} (SO_3) in bound triflate has been reported to occur at 1248cm^{-1}. Therefore it is possible that triflate coordinates the lead ion in the absence of adequate numbers of more strongly coordinating ligands.

It is likely that the lead ion in complex (5) is coordinated by acetonitrile. A ν(MeCN) absorption at 2322cm^{-1} was observed in the infrared spectrum of this complex. There appears to be a trend in the νC=N frequencies in the series towards higher frequency imine absorption in the derivatives that have fewer thiocyanate ligands. The tetrathiocyanate ν(C=N) occurs at 1642cm^{-1}, ν(C=N) for the monothiocyanate occurs at 1645cm^{-1} and ν(C=N) for the tetratriflate occurs at 1649cm^{-1} in the infrared spectrum.

HOMOBINUCLEAR TRANSITION METAL COMPLEXES OF MACROCYCLE P

Transmetallation of $Pb_2P(NCS)_4$ using copper(II) triflate as described in the experimental section gave the complex, $[Cu_2P(NCS)_2](CF_3SO_3)_2{\cdot}H_2O$. Attempted preparation of the analogous dicobalt complex by a similar method gave mixtures of relatively insoluble products. The difficulty was solved by limiting the amount of thiocyanate present in the reaction mixture. This was achieved by use of dilead P tetratriflate (5) as starting material, addition of cobalt triflate and two equivalents of sodium thiocyanate gave crystalline dicobalt complex (7), $[Co_2P(NCS)_2(H_2O)_2](CF_3SO_3)_2$ as the product. Physical data for the homobinuclear complexes of macrocycle P is shown in Tables 9 and 10.

TABLE 9 PHYSICAL DATA FOR THE HOMOBINUCLEAR COMPLEXES OF MACROCYCLE P. Infrared spectral data /cm^{-1}.

COMPLEX	ν(C=N)	ν(pyr)	ν(NCS)	ν(CF_3SO_3)	ν(OH)
6 $[Cu_2P(NCS)_2](CF_3SO_3)_2{\cdot}H_2O$	1627(m)	1589	2116(s)	1280(s) 1256(s) 1224(s) 1162(m) 1029(s) 638(s)	3420
7 $[Co_2P(NCS)_2(H_2O)2](CF_3SO_3)_2$	1634(w,br)	1586	2133 2109	1286(s) 1241(s) 1221(s) 1160(m) 1029(s) 636(s)	3430

TABLE 10 Magnetic, electronic spectral and conductivity data

COMPLEX	COLOUR	μ eff / BM[a] 293K	93K	Λ	ELECTRONIC SPECTRAL DATA ν max	ε
6 $[Cu_2P(NCS)_2](CF_3SO_3)_2 \cdot H_2O$	blue-green	1.85	1.81	218	26,700sh 15,000	 316
7 $[Co_2P(NCS)_2(H_2O)_2](CF_3SO_3)_2$	black-brown	3.5	2.1		23,200sh 19,000 15,300	 2300 305

(a) moment per transition metal ion. ε in mol^{-1} l cm^{-1}
Λ in S cm^2 mol^{-1}

The infrared spectra of the dicopper (6) and dicobalt (7) complexes show significant differences. The dicopper complex (6) displays a medium intensity, sharp and unsplit ν(C=N) absorption at 1627cm^{-1}, which is a frequency typical of the imine group when coordinated to a transition metal ion. Although the dicobalt P complex (7) shows an absorption at similar frequency to the ν(C=N) absorption of the dicopper complex, a markedly different intensity of the ν(C=N) absorption is observed. The ν(C=N) absorption is weak, broad and jagged in appearance and is likely to include a contribution from δ(OH). The infrared spectrum of the dicobalt P complex(7) is shown in figure 10.

Similar low intensity absorptions of the coordinated imine have been noted in complexes where the metal ion was in spin equilibrium.[316-317] The ν(C=N) absorption is often absent or strongly reduced in intensity in trimethine complexes of low spin Co(II) or Fe(II). The intermediate intensity band observed for complex (7) suggests operation of a $^4T_{1g} \rightarrow {}^2E_g$ spin equilibrium, with appreciable occupation of both states at room

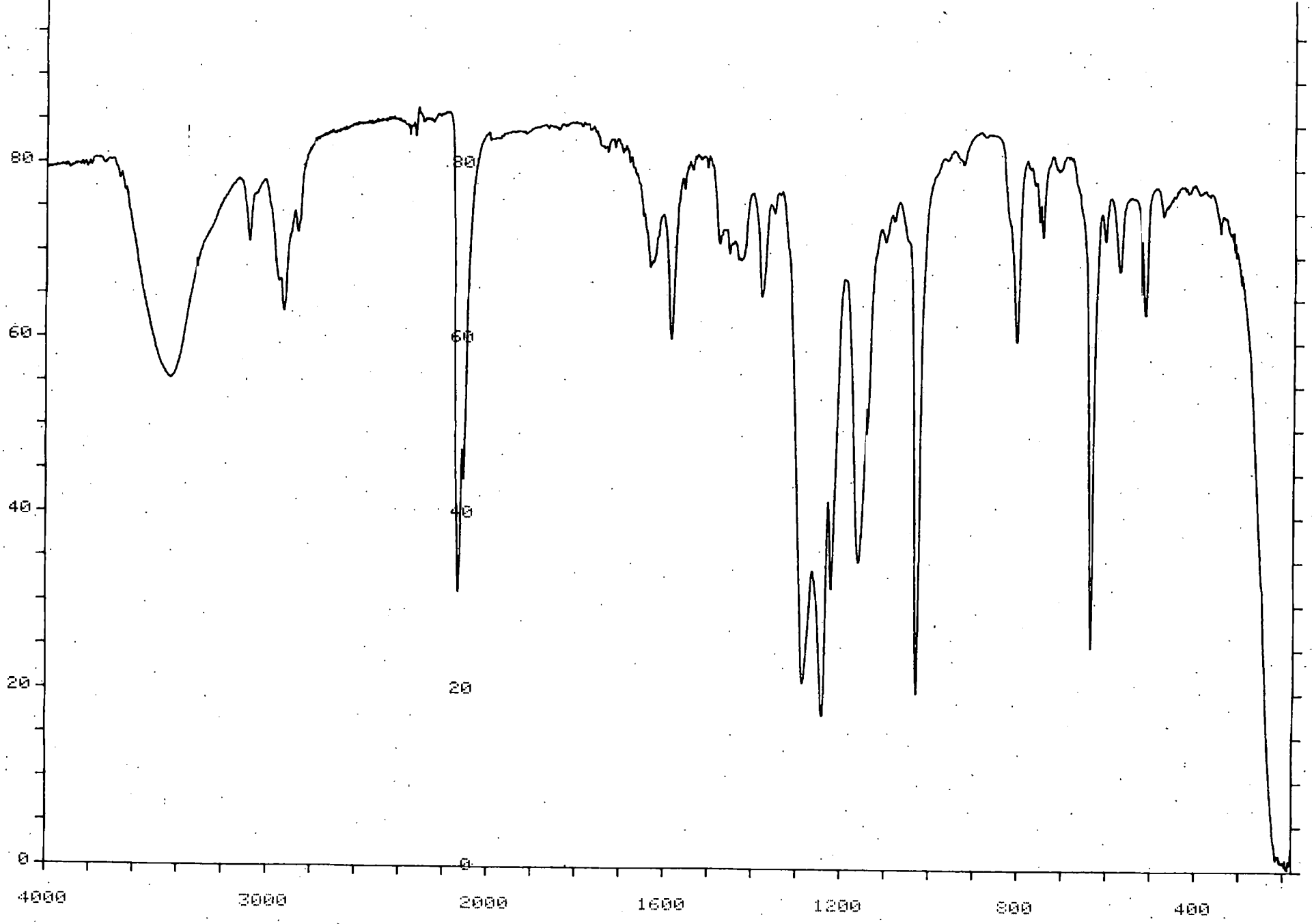

Figure 10 ***The infrared spectrum of*** $Co_2P(NCS)_2(H_2O)_2(CF_3SO_3$

temperature. The black-brown colour of complex (7) is not found for high spin Co(II) complexes and suggests the presence of the low spin isomer.

The appearance of the esr spectrum of (7) as a frozen glass in MeCN (figure 11) is another indication of the accessibility of the low spin state of the complex.

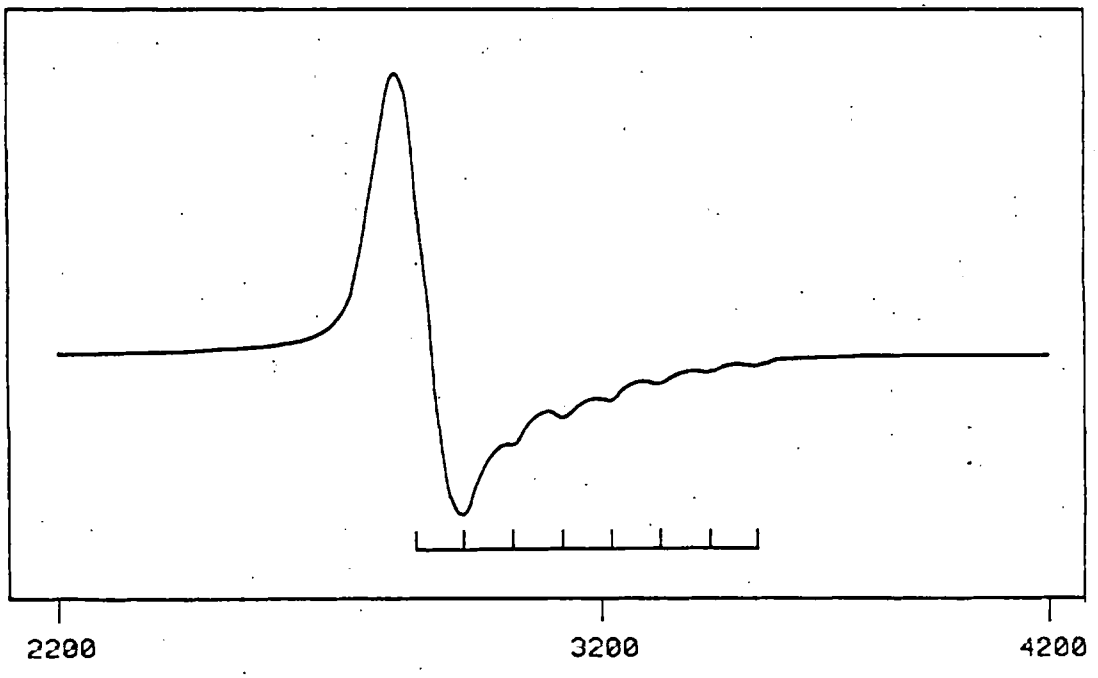

Figure 11 *The e.s.r. spectrum of* $[Co_2P(NCS)_2(H_2O)_2](CF_3SO_3)_2$ *as MeCN glass at 173K.*

The dicobalt complex has the simple esr spectrum expected for spin-paired cobalt(II) instead of the broad zero-field split spectrum characteristic of high-spin Co(II). There was no indication of splitting of the eight hyperfine components into fifteen, with reduction of the hyperfine splitting to 40-50G as might be expected if the two cobalt ions were strongly interacting via the thiocyanate bridges. The spectrum (figure 11) shows a $g \simeq 2$ signal with eight broad components in the parallel band appearing to high field of $g_\perp$ indicating an axially extended Jahn-Teller distorted tetragonal geometry for the cobalt(II) ion.

Variable temperature magnetic susceptibility measurements over the temperature range 293-93K support this interpretation. The room temperature moment of 3.5 BM per cobalt(II) ion is intermediate between that expected for the high-spin $^4T_{2g}$ and low-spin ^2E_g ground states and a further reduction in moment with temperature demonstrates the existence of a thermally controlled $^4T_{2g} \rightarrow {}^2E_g$ spin equilibrium. The dicobalt complex displays two ν(NCS) absorptions in the range typical of the long -NCS- bridging mode of thiocyanate. These are presumably disposed in centrosymmetric axial/equatorial fashion as illustrated in figure 12.

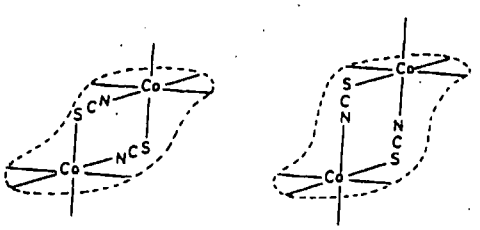

Figure 12 *Suggested arrangement of thiocyanate ligands in dicobalt P*

A solvent H_2O molecule completes each donor set, leading to 6-coordination of each cobalt (II) ion.

The dicopper complex (6) shows only one thiocyanate frequency, at 2116cm^{-1} in the thiocyanate ν(C≡N) region of the infrared spectrum. The absorption is strong and slightly broadened when compared to either of the thiocyanate ν(C≡N) absorptions observed for the dicobalt complex (7). The analytical data for the dicopper complex (6), when considered in conjunction with the infrared spectrum, suggests two thiocyanates in approximately equivalent environments. The macrocyclic ligand supplies three donors to each copper ion and the two bridging -NCS- groups supply two donors to each Cu(II), as shown schematically in figure 13.

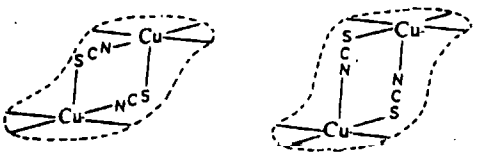

Figure 13 *Suggested coordination of Cu(II) in* $[Cu_2P(NCS)_2]^{2+}$

Thus donors filling five positions of a square pyramid provide a geometry that is acceptable to the Cu(II) ions. The residual 2+ charge is balanced by the triflate counterions.

The electronic spectrum of the dicopper complex is not particularly helpful in assigning a coordination geometry to the metal ions. One unsplit d-d absorption is observed, which is at least consistent with square based geometry. The DMF frozen glass esr spectrum of the dicopper (II) complex is shown in figure 14. The g = 2 spectrum shows $g_{11} > g_{\perp}$ (g_{11} = 2.24 and $g_{\perp}$ = 2.05) which suggests axially extended D_{4h} and eliminates the possibility of trigonal bipyramidal geometry. The small hyperfine splitting (A_{11} = 75G) together with the observation of 6 lines of the correct intensity ratio for a seven-line pattern on the low field wing of $g_{\perp}$ suggests weak interaction between the copper(II) ions. The observation of the 'forbidden' $\Delta M = 2$ signal at 10^3 times the sensitivity used to record the main band signal, provides further evidence that the two copper(II) ions bound in macrocycle P are weakly antiferromagnetically coupled. The half-band signal shows 6 of the 7 lines expected and has hyperfine splitting of ≈ 80G. However the variable temperature magnetic susceptibility data over the temperature range 293-93K suggest only weak antiferromagnetic interactions (Table 10).

The magnetic and esr data for complexes (6) and (7) indicate that the long -NCS- bridge is not a good transmitter of magnetic exchange interactions. Indication of only weak interactions were observed in the

esr and magnetic data for the dicopper complex. The temperature dependance of μ was not pronounced and only slight lowering of μ was observed with decreasing temperature. The presence of appreciable zero-field splitting in the esr spectrum further suggests that interaction is weak. The conclusion that the thiocyanate ligand is a poor transmitter of magnetic interactions is similar to that found in related studies of the thiocyanate ligand as a mediator of magnetic interactions.[129,306]

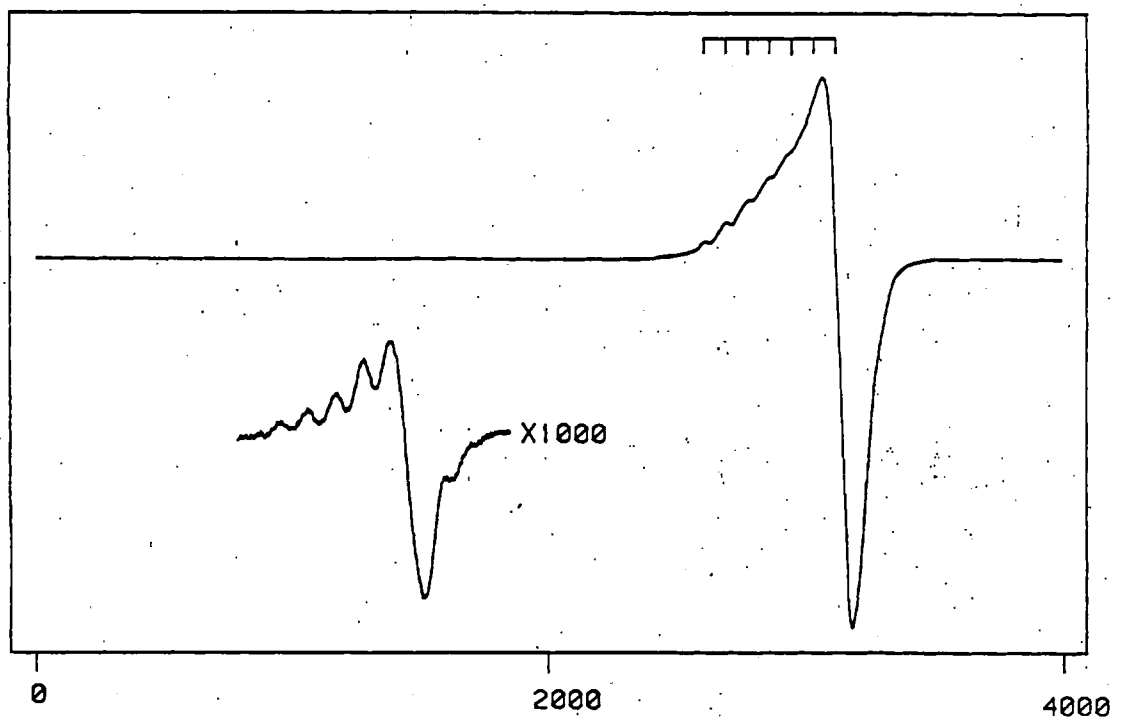

Figure 14 *The DMF frozen glass e.s.r. spectrum of* $[Cu_2P(NCS)_2]^{2+}$

THE HETEROBINUCLEAR COMPLEXES OF P

Transmetallation of $Pb_2P(NCS)_4$ with $M(CF_3SO_3)_2$ as described in the experimental section produced a series of heterobinuclear complexes that contain one Pb^{2+} ion and one transition metal ion M(II), where M = Mn, Fe, Ni. The complexes analysed as the heterobinuclear bis-thiocyanato-ditriflates $[PbMP(NCS)_2](CF_3SO_3)_2{\cdot}xH_2O$. Fast atom bombardment mass spectral data for the complexes is listed in the experimental section and confirms their heterobinuclear nature. Good agreement is obtained between the observed and calculated isotopic cluster pattern as shown in figure 15.

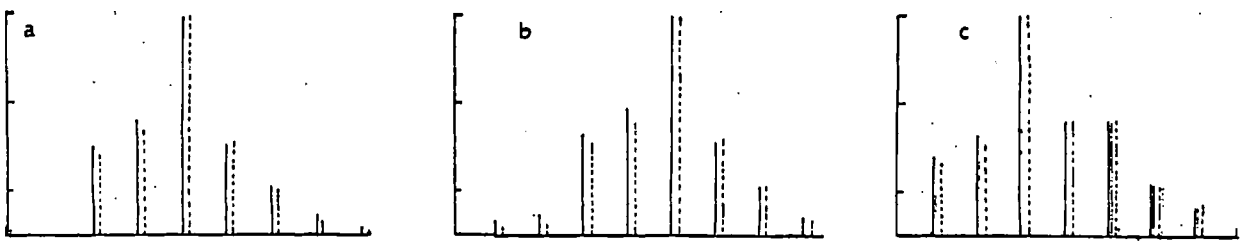

Figure 15 *Observed and calculated isotopic cluster patterns for heterobinuclear PbM P complexes, a) M = Ni, b) M = Fe, c) M = Mn.*

The fab mass spectra of the iron-lead (9) and nickel-lead (10) complexes show no evidence of the presence of either ditransition metal P or dilead P complexes. The base peak for these is due to $[PbMP(NCS)_2(CF_3SO_3)]^+$ species and clusters due to other $[PbMP]^+$ containing fragments appear in the spectra. The fab mass spectrum of the

manganese complex (8) shows no evidence of the presence of the dimanganese P complex. The base peak is due to $[MnPbP(NCS)_2(CF_3SO_3)]^+$ and various other clusters due to MnPbP containing fragments are evident. However there are also peaks at m/e 1230 and 1139 which are due to the dilead fragment ions $[Pb_2P(NCS)_2(CF_3SO_3)]^+$ and $[Pb_2P(NCS)_3]^+$ respectively. This suggests contamination of the heterobinuclear product with product resulting from anion exchange alone and possibly with starting material. Initially, difficulties were encountered in obtaining the pure heterobinuclear MnPb complex, as became evident from CHN analysis. The magnetic measurements obtained were low for a high spin manganese complex. It was this product which was sent for fab mass spectroscopy. Subsequently, it was found that increased reaction temperature and isolation by slow evaporation gave pure heterobinuclear product and acceptable CHN analysis was obtained for complex (8).

The physical data obtained for the heterobinuclear complexes is summarised in tables 11 and 12.

PHYSICAL DATA FOR THE HETEROBINUCLEAR COMPLEXES OF MACROCYCLE P

TABLE 11 Infrared spectral data /cm^{-1}.

COMPLEX	ν(C=N)	ν(NCS)	ν(CF_3SO_3)	ν(OH)
8 [MnPbP(NCS)$_2$](CF_3SO_3)$_2$:2H_2O	1646 1633	2101 2080	1249 1030 637	3430
9 [FePbP(NCS)$_2$(H_2O)](CF_3SO_3)$_2$	1646 1630	2104 2078	1248 1032 636	
10 [NiPbP(NCS)$_2$(H_2O)$_2$](CF_3SO_3)$_2$:2H_2O	1640sh 1635	2103 2124	1248 1030 638	3435
11 [NiPbP(NCS)$_4$]:H_2O	1645sh 1634	2112 2082 2058 2023	-	3449
12 MnPb(NCS)$_3$(O_2CCH_3):3H_2O	1640 1634	2070 2033	-	3434

Complex 12 shows acetate absorptions at 1581(s,br) and 1417(s,br) cm^{-1}
Triflate has a rich spectrum, only the strongest peaks attributable to triflate are tabulated. There is uncertainty regarding coordination of water or triflate in these complexes.

The presence of ν(C=N) and absence of amine or carbonyl frequencies in the infrared spectra confirm that the macrocyclic ligand remains intact on transmetallation. The ν(C=N) absorption is split into two equal intensity peaks in the MnPbP and FePbP complexes (8) and (9). The peak at 1646cm^{-1} is typical of imine groups that are coordinated to a lead ion whereas the peak at lower frequency *ca.* 1630cm^{-1} did not appear in the spectrum of the dilead starting material (see Table 1). This peak is assigned to the imine groups that are coordinated to the transition metal ion.

PHYSICAL DATA FOR THE HETEROBINUCLEAR COMPLEXES OF MACROCYCLE P.

TABLE 12 Magnetic, electronic spectral and conductivity data.

COMPLEX	COLOUR	μ eff 293K	BM[a] 93K	Λ	ELECTRONIC SPECTRAL DATA ν max	ε
8 $MnPbP(NCS)_2(CF_3SO_3)_2{:}2H_2O$	yellow	5.51	5.40	232		
9 $FePbP(NCS)_2(CF_3SO_3)_2{:}2H_2O$	purple	4.98	4.57	249	19,900 16,500sh	3200
10 $NiPbP(NCS)_2(CF_3SO_3)_2{:}4H_2O$	green	3.17	2.94	insol	25,000 mull 17,200 10,300	

(a) moment per transition metal ion. ε in mol^{-1} l cm^{-1}
Λ in S cm^2 mol^{-1}

The magnetic susceptibility data obtained for the complexes support the heterobinuclear formulation. The magnetic moments found per transition metal ion for the complexes fall in the ranges expected for high spin Mn(II), Ni(II) and Fe(II) complexes (Table 12).

Analysis of the FePbP complex (9) combined with the presence of a weak OH absorption in the mull infrared spectrum suggests that one water of crystallisation is present. This water molecule may coordinate the iron ion of the complex. In the previously reported work on heterobinuclear P perchlorate salts,[12a] a thermally controlled quintet-singlet spin equilibrium was observed in the the Fe/Pb complex which led to intermediate values of magnetic moment over the temperature range 293-93K. However in complex (9) it appears that change of solvation or counterion has altered the relative stability of quintet and singlet states to the extent that the first signs of reduced magnetic moment only begin to appear at 93K. Presumably replacement of coordinated MeCN, in

the perchlorate salt, with coordinated water or triflate oxygen in the triflate salt is the major factor affecting the temperature at which the $^5T \rightarrow {}^1A_g$ transition of coordinated Fe(II) occurs. The electronic spectrum gives some indication of the accessibility of the low spin state, in that a pair of intense metal to ligand charge transfer bands at around 20,000cm^{-1} are observed, as are normally observed in low spin Fe(II) trimethine complexes.[218] The presence of the 1630cm^{-1} ν(C=N) peak in the iron complex (9) fits well with the high spin nature of iron in this complex as shown by the magnetic measurement. In a low spin iron complex the ν(C=N) of the coordinated imine is often not visible in the infrared spectrum due to reduction in intensity or shifting of position, or both.[219] The conductivity measurement for the iron-lead complex falls in the range expected for a 2 : 1 electrolyte in acetonitrile. This suggests that the thiocyanates remain coordinated in solution whereas the triflates are ionic.

The NiPb complexes (10) and (11) do not show such clear splitting of the C=N frequency and have a strong peak at *ca.* 1635cm^{-1} and just a shoulder for the imine groups coordinated to the lead ion. Complex (10) shows a strong broad absorption at 3300 -3500cm^{-1} in both the mull and the KBr disc infrared spectra. This supports the presence of $4H_2O$ as suggested by the CHN analytical figures.

The infrared spectrum of the dark brown MnPbP complex (12) shows strong absorptions due to the acetate counterion. A strong absorption at *ca.* 1580cm^{-1} is assigned to ν_{as}(COO) and an absorption at 1417cm^{-1} is assigned to the ν_s(COO) asymmetric and symmetric stretching modes respectively.[220] Thiocyanate present in the complex gives strong absorptions at 2070 and 2030cm^{-1}. The fab mass spectrum of complex

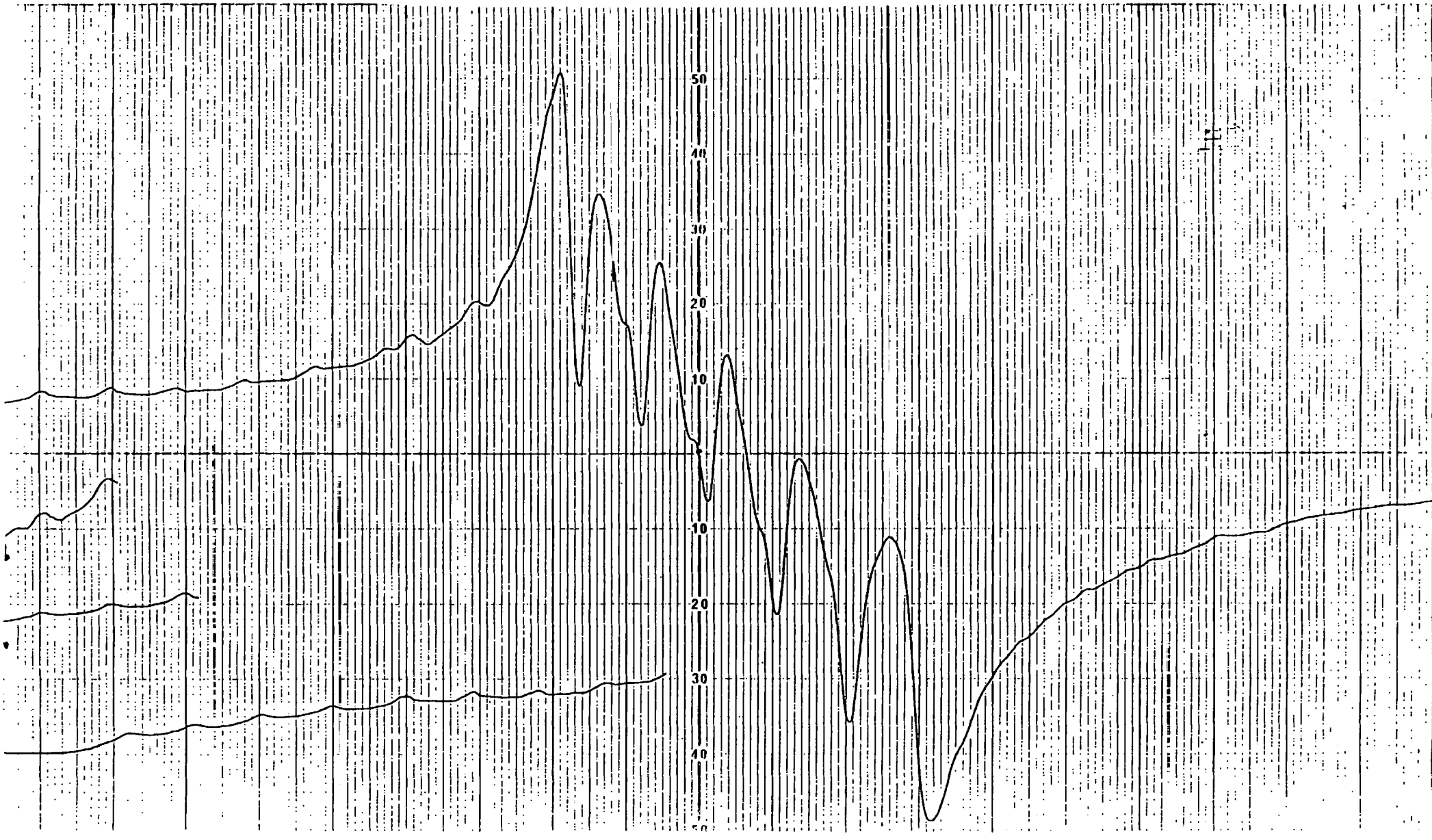

Figure 16 *The dmf glass esr spectrum of* $MnPbP(NCS)_3(O_2CCH_3):3H_2O$

(12) showed m/e 895 as the base peak. This peak is presumably attributable to the $[MnPbP(NCS)_3]^+$ fragment ion. A strong cluster around m/e 949 may be attributed to $[MnPbP(NCS)_3(O_2CCH_3)]^+$ (85%). E.s.r suggests that the manganese ion in (12) is Mn(II) as opposed to Mn(III) which is esr silent. A 6-line Mn(II) esr signal was observed in the dmf glass spectrum, which is shown in figure 16. Forbidden lines due to quadrupole interactions give weak signals between the allowed hyperfine lines. As expected, the hyperfine was absent in the esr spectrum of the solid and a broad g ≈ 2 signal was observed. The fine structure observed on the low field wing of the dmf glass spectrum is unusual and will be investigated further. It is possible that the complex could contain manganese clusters in which the manganese ions are linked by acetate.

The dithiocyanato- heterobinuclear complexes show two ν_{CN}(NCS) thiocyanate absorptions in the infrared spectrum. The absorptions fall in the range typical of 1,3-μ-NCS bridging. The X-ray crystal structure of $PbMnP(NCS)_4$ was solved previously and shows that two long bridging thiocyanates can be accomodated between lead and the manganese ion within the cavity of the P macrocycle (figure 17).

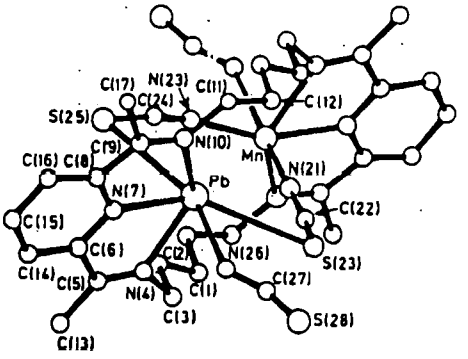

Figure 17 *The X-ray crystal structure of* $PbMnP(NCS)_4$

The bridging thiocyanates and the three macrocyclic donors make up five of the donors to manganese in the complex. The MnPb P complex (8) gives a magnetic moment in the range expected for an isolated high-spin Mn(II) ion. Absorptions due to d-d transitions are not observed in the electronic spectrum of the manganese complex, which is as expected as a result of the selection rules $\Delta S = 0$ and $\Delta L = \pm 1$. The esr spectrum of (8) displays a strong isotropic signal at $g \simeq 2$ which is split into six lines by hyperfine coupling of 94G. Forbidden lines due to quadrupole interactions appear weakly between the allowed hyperfine lines which are normally observed in Mn(II) esr spectra. The MnPb complex (8) analyses as the dihydrate and the mull spectrum indicates the presence of H_2O, though the water absorption is relatively less intense than in the mull spectrum of the NiPb complex (10).

Six coordination is confirmed for Ni(II) in complex (10) by electronic spectral measurements and magnetic susceptibility measurements. Absorption bands due to the three transitions expected for Ni(II) in octahedral symmetry are observed in the electronic spectrum. The highest energy transition appears as a shoulder at 25,000cm^{-1} on the intense charge transfer absorption above 24,000cm^{-1}. This shoulder is due to the $^3A_{2g} \rightarrow {}^3T_{1g}$ (P) transition. Absorption bands at 17,200 and 10,300cm^{-1} are attributed to $^3A_{2g} \rightarrow {}^3T_{1g}$(F) and $^3A_{2g} \rightarrow {}^3T_{2g}$ transitions respectively. The extinction coefficient of the lowest energy transition is typical of 6-coordinate Ni(II) and is much too low for tetrahedrally coordinated Ni(II). The room temperature magnetic moment (3.17 BM) is close to the spin-only value for octahedral Ni(II) ion and shows no hint of the orbital contribution expected in T_d symmetry.

It is not clear why heterobimetallic complexes form on transmetallation of $Pb_2P(NCS)_4$ with metal ions, Mn(II), Fe(II), and Ni(II). The formation of heterobinuclear complexes on transmetallation with these ions may occur as a result of lower solubility of the heterobinuclear complex causing this to crystallise out of solution in preference to homobinuclear transition metal complexes. Alternatively, it is possible that the macrocycle is only capable of providing a suitable site geometry to one of these transition series ions, while the less demanding lead ion can tolerate the irregular coordination geometry offered by the second binding site. Another possibility is that formation of heterobinuclear products with Mn(II), Fe(II) and Ni(II) may be a size effect. The P macrocyclic cavity is capable of accomodating the non-centrosymmetric bridge between Pb and Mn(II) but may not be able to accomodate the longer centrosymmetric bridge that may be more suitable for homobinuclear transition metal complexes. The centrosymmetric bridge requires 5.3-5.8Å between the the metal centres whereas the Pb-Mn distance in the non-centrosymmetrically bridged complex was 4.85Å.

The isolation of the heterobinuclear lead/transition metal P complexes offers the possibility of replacing the lead ion in heterobinuclear complexes of P with another transition metal ion to form heterobi-transition metal complexes. The various attempts to substitute the lead ion in heterobinuclear complexes of P for a transition metal ion are summarised in Table 1 in the experimental chapter. This is preliminary work which has indicated potentially productive systems.

The Cu(I) ion was considered to be a suitable metal ion for the transmetallation. Due to the d^{10} electronic configuration of Cu(I), the ion does not have marked stereochemical preferences, and therefore may be

suited to binding at the possibly irregular site occupied by the lead ion. In addition, the Fe/Cu heterobinuclear complex was the most sought after combination of transition metal ions, due to the potential of such a complex as a model for the Fe/Cu containing enzyme cytochrome-c-oxidase (see introduction to chapter 3).

Transmetallation of Fe/PbP with Cu(I) as described in the experimental chapter afforded a deep purple/black powder. Conveniently, the masses of Fe and Cu are sufficiently different for fab mass spectroscopy to be of use in determining the products present. The product consisted of a mixture of the heterobinuclear Fe/Cu P complex and a dicopper P complex. The fab spectrum exhibits peaks due to several Fe/CuP containing fragment ions. The clusters around m/e 693 (20%), 784 (25%) and 842 (15%) correspond to $[FeCuP(NCS)_2]^+$, $[FeCuP(NCS)(CF_3SO_3)]^+$ and $[FeCuP(NCS)_2(CF_3SO_3)]^+$ respectively. Clusters due to dicopper containing fragments were also present, m/e 586 (10%) which corresponds to $[Cu_2P + 2H]^+$. Fab mass spectroscopy is not particularly helpful in determining the oxidation state of Cu in the product as redox changes can occur in the fast atom bombardment process. There was no evidence of either FePbP or CuPbP containing fragments in the fab spectrum.

The esr spectrum of the product was recorded as a dmf glass and is shown in figure 18. The dmf was deoxygenated before use. The spectrum shows a strong copper(II) signal indicating that oxidation to Cu(II) had occurred. The presence of six hyperfine lines on the low field wing of $g_\perp$ suggests that there is some interaction between the metal ions of the complex. The observation of a forbidden half-band $\Delta M = 2$ signal provides further evidence of coupling. The small hyperfine splitting (75G) is typical of interacting dicopper(II) complexes. The esr spectrum is likely

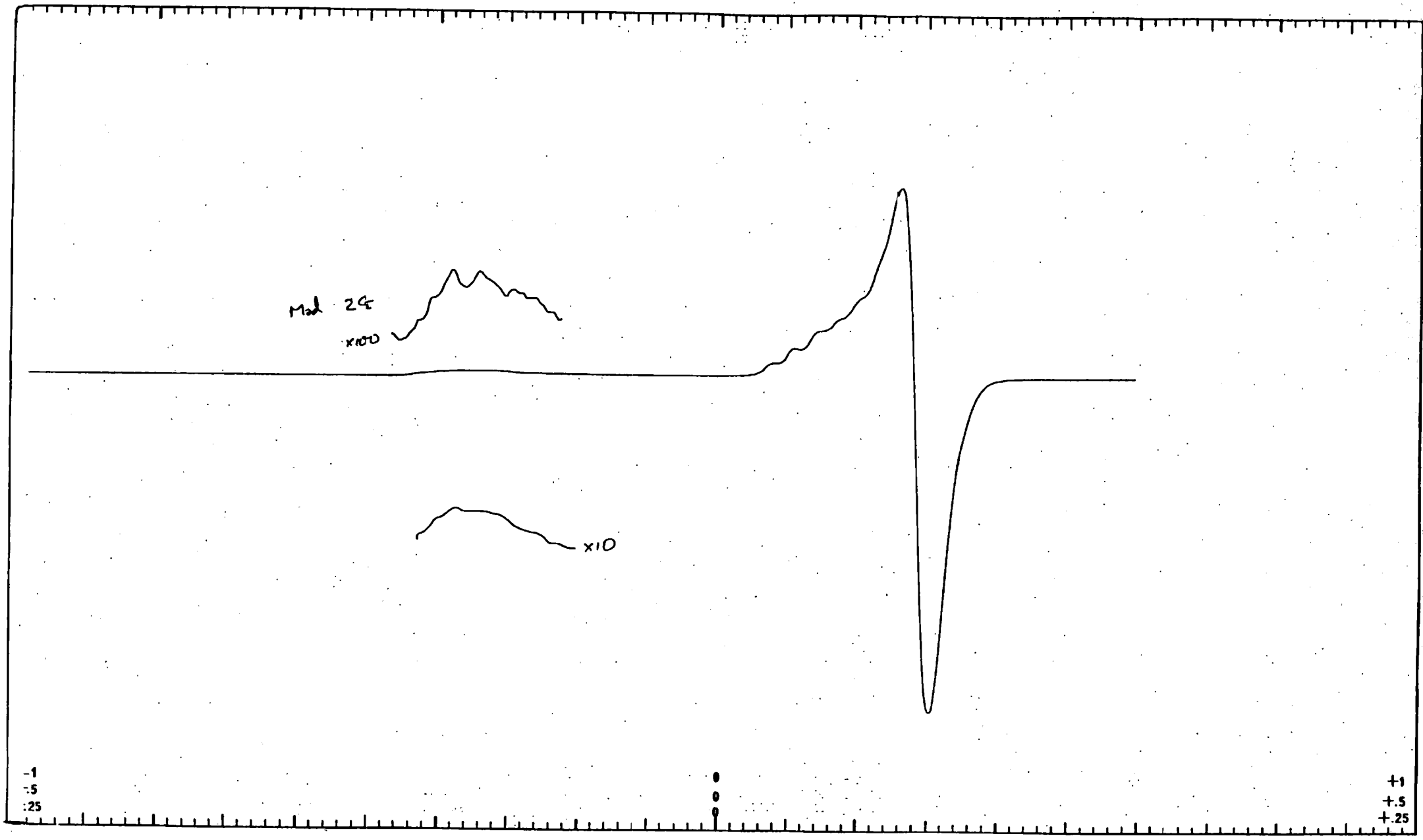

Figure 18 *The dmf glass esr spectrum of the product of [FeCuP]$^{n+}$ attempted synthesis*

to be mainly due to the dicopper(II)P complex that gave fragment ions in the fab spectrum of the product. The relative intensities of the hyperfine lines do not match those expected for the seven line pattern of interacting dicopper(II), and may indicate the presence of some non-interacting Cu(II) complex.

The product from the attempted FeCuP synthesis was darker in colour than the FePbP parent complex. The dark colour may be due to metal-ligand charge transfer absorptions involving the iron ion and may indicate accessibility of the low spin state of the iron ion. Recrystallisation of the mixture under nitrogen did not adequately separate the products and requires a relatively large amount of material. Separation of the products by ion exchange chromatography may be more successful.

Transmetallation of the NiPbP complex (10) using cobalt (II) triflate gave brown crystalline product. The fab mass spectrum showed a cluster at m/e 516 (75%) which is attributed to $[NiP]^+$. The isotopic pattern for this cluster closely matched that observed for $[NiP]^+$ in the fab spectrum of complex (10). A cluster at m/e 691 (10%) could be due to either $[CoNiP(NCS)_2]^+$ or $[Ni_2P(NCS)_2+H]^+$. As Co and Ni have similar mass these alternatives are distinguishable only by 4% ^{62}Ni peaks present in high abundance fragments. It is unlikely that this cluster is due to dinickel P as previous fab spectra of the NiPbP heterobinuclear complex did not show any trace of dinickel P complex. A cluster observed at m/e 840 (30%) may be due either to $CoNiP(NCS)_2(CF_3SO_3)$ or $NiPbP(NCS)_2$. However NiPbP seems more probable as a cluster observed at m/e 840 in the fab spectrum of the starting complex showed a similar isotopic cluster pattern. Clusters at m/e 931 and 989 were also observed in both fab spectra and are presumably due to $[NiPbP(NCS)(CF_3SO_3)]^+$ and

$[NiPbP(NCS)_2(CF_3SO_3)]^+$. The relative intensities of the peaks at 840, 931 and 989 are similar in both spectra. The cluster at 989 (100%) could possibly be due to $NiCoP(NCS)_2(CF_3SO_3)_2]^+$, generally in the fab spectra of the P complexes loss of a triflate anion from the complex gives a fragment ion that corresponds to the base peak. The isotopic cluster pattern for the base peak matches both formulations fairly well and does not provide firm evidence. The brown colour of the complex does not disprove the NiPbP possibility as samples of brown $NiPbP(NCS)_2(CF_3SO_3)_2$: MeCN have been obtained. It appears that coordination of MeCN can lead to brown colouration of the NiPbP complex.

Magnetic susceptibility measurements gave χ_ω = 4.417 10^{-6} cgsu which on the basis of the formulation MM'P$(NCS)_2(CF_3SO_3)_2$ led to μ = 3.43BM per complex for CoNiP, μ = 2.43 per Ni for Ni_2P and μ = 3.65 per Ni for NiPb. The ranges of magnetic moments usually observed for these ions are as follows, Ni(II) O_h 2.8-3.3, Co(II) hs 4.5-5.2, ls 1.8BM. Calculation of χ for the NiCoP alternative using the Ni(II) and Co(II) ranges above, can give a value that is close to the observed value. The NiPbP and Ni_2P alternatives do not fit the expected values.

Transmetallation of NiPbP (10) using $Cu(MeCN)_4(ClO_4)$ gave mainly anion exchange products. The fab mass spectrum of the product showed m/e 939 $[PbNiP(NCS)_2(ClO_4)]^+$ as the base peak. A weak cluster was observed around m/e 794 this may indicate the presence of the fragment ion $[NiCuP(NCS)_2(ClO_4)]^+$.

Attempted exchange of the lead ion in Mn/PbP complex (8) for Cu(I) gave pale yellow product which showed a tendency to become green in air suggesting the presence of Cu(I) in the product and its subsequent oxidation to Cu(II). However, fab mass spectroscopy indicated that both

the Mn(II) and Pb(II) ions of the P starting material were substituted by copper ion. Intense clusters due to dicopper P containing fragment ions were observed. The fab mass spectrum of the product shows peaks due to $[Cu_2P(NCS)]^+$ m/e 642 (100%), $[Cu_2P(NCS)_2]^+$ m/e 700 (80%), $[Cu_2P(NCS)(CF_3SO_3)]^+$ m/e 793 (70%) and $[Cu_2P(NCS)_2(CF_3SO_3)]^+$ m/e 894 (65%). The presence of less intense clusters at 8-9 m/e (10-15 %) lower than the dicopper peaks may indicate the presence of some of the heterobinuclear MnCuP complex.

Attempted exchange of the lead ion in MnPbP for Ni(II) was unsuccessful. The fab mass spectrum shows peaks at m/e 838 and 988. These are likely to correspond to $[NiPbP(NCS)_2-H]^+$ and $[NiPbP(NCS)_2(CF_3SO_3)-H]^+$ fragment ions.

Attempts to exchange the lead ion in heterobinuclear MnPb and NiPb complexes of P for a copper(II) ion resulted in formation of the dicopper complex $Cu_2P(NCS)_2(CF_3SO_3)_2$. The product was characterised by infrared spectroscopy, CHN analysis and magnetic measurements. The product had the same blue-green colour as the dicopper complex of P (6) which was obtained previously. The infrared spectra of the two were identical and magnetic measurements gave results that were close to those expected for Cu(II) (2.06BM / Cu(II) and unlike the value for μ expected for Ni(II) or Mn(II) complexes. The formation of dicopper(II) complex as the product of these reactions, necessitates both the replacement of the lead ion and the transition metal ion of the starting material. Thus both the transition metal ion and the lead ion bound in heterobinuclear complexes of P must be reasonably labile.

DILEAD COMPLEXES OF MACROCYCLE MC

The MC macrocyclic complex has the 5-carbon link between coordination sites elaborated by incorporating a 1,3 cyclohexyl unit. The major reason for investigating the 1,3 cyclohexyl containing macrocycle was the possibility that the cyclohexyl ring would offer increased steric protection to the binuclear bridged assembly. The increased hydrocarbon content of the macrocycle leads to superior solubility of the MC complex in polar organic solvents, relative to the analogous P complex. Template synthesis of the MC macrocyclic complex proceeded in a similar fashion to synthesis of the P complex. In both, the insoluble $Pb(NCS)_2$ template species dissolved to give a yellow coloured solution and product was isolated as yellow crystals. The similarity between the infrared spectrum of the MC complex and that of the P complex suggested that 2+2 Schiff-base condensation had occurred. The presence of ν(C=N) at *ca.* 1640cm^{-1} and the absence of amine absorptions in the region 3200-3400cm^{-1} or carbonyl frequencies around 1700cm^{-1} in the infrared spectrum implied that Schiff-base condensation was complete. In addition the presence of four strong thiocyanate absorptions, including a frequency due to a bridging mode, suggested that two template ions were bound in the macrocycle. Such factors, combined with the crystalline nature of the product and it's solubility in acetonitrile suggested macrocyclic rather than polymeric product. Subsequent CHN analysis and FAB mass spectroscopy showed that the 2+2 macrocycle had formed and that two lead ions were bound by the macrocycle. The various Pb(II) complexes of MC together with selected infrared spectral data are listed in Table 13.

PHYSICAL DATA FOR THE DILEAD COMPLEXES OF MACROCYCLE MC.

TABLE 13 Infrared spectral data /cm^{-1}.

COMPLEX	COLOUR	ν(C=N)	ν(NCS)	$\nu(CF_3SO_3)$	ν(OH)
13 $Pb_2MC(NCS)_4$:EtOH	yellow	1640	2091(s) 2048(s) 2007(s) 1969(s)	-	3430
14 $Pb_2MC(NCS)_2(CF_3SO_3)_2$:EtOH MeCN	primrose yellow	1644	2077(s) 1988(s)	1278(s) 1238(s) 1027(s) 637(m)	3420
15 $Pb_2MC(NCS)(CF_3SO_3)_3$	cream	1645	1955(s)	1273(s) 1238(s) 1027(s) 638(m)	-
16 $Pb_2MC(CF_3SO_3)_4$:EtOH MeCN	white	1646	-	1272(s) 1219(s) 1012(s) 637(m)	3420
17 $Pb_2MC(ClO_4)_4$:H_2O	cream	1647	-	-	3420

All of the complexes showed ν(pyridine) at *ca.*1587cm^{-1}.
Complexes 14 and 16 showed νMeCN at *ca.* 2280cm^{-1}

The presence of a ν(C=N) absorption and absence of amine or carbonyl frequencies indicates that the macrocyclic ligand remains intact throughout the various transformations. The tetrathiocyanate (13) shows four bands in the pseudo-asymmetric ν(NCS) region. The strong absorption at 1969cm^{-1} is assigned to the single atom N-only bridging mode of thiocyanate. The two absorptions at 2048 and 2007cm^{-1} are attributed to two S-terminal thiocyanates in different environments. Subsequent X-ray crystallographic evidence confirming the presence of the N-only bridge was supplied by Dr.V.McKee of the University of Canterbury, New Zealand.

THE X-RAY STRUCTURE OF $Pb_2MC(NCS)_4$

The X-ray crystal structure of $Pb_2MC(NCS)_4$ is shown in figure 19. The structure confirms that 2+2 Schiff-base condensation has taken place to give the dilead macrocyclic complex. The cyclohexyl rings adopt chair conformations and are folded away from the coordination site. Therefore the cyclohexyl rings do not provide additional steric protection to the coordination site. Each lead ion is bonded to two imine N donors and to a N of the pyridine head unit. In addition, each lead ion is coordinated by an S-terminal thiocyanate. The S-terminal coordination mode is expected for the relatively 'soft' lead ion on the basis of Pearson's hard/soft acid/base theory. This $Pb_2MC(NCS)_2$ fragment fits C_2 symmetry. There is also one thiocyanate which is bridged through the N atom only to both lead ions. The nitrogen atom of this thiocyanate lies on the two-fold axis, though the carbon and sulphur atoms are disordered to either side of the axis. Both orientations are shown in the crystal structure. Each pyridine 2,6-diimine subunit of the macrocycle is planar and is folded up like butterfly wings on either side of the N-only bridging thiocyanate. The fourth thiocyanate was severely disordered and is best considered only weakly coordinated. This thiocyanate is located somewhere between the lead ions on the exposed lower face of the macrocyclic complex. It is assumed that the fourth NCS does not form part of the coordination sphere. As a result each lead ion is assumed to be 5-coordinate. The geometry of the lead ion in the coordination sphere is a distorted trigonal bipyramid. The three macrocyclic donors fill the equatorial sites, though there is distortion as a result of steric constraints. The terminal -SCN and the N-only bridge fill the axial positions. The Pb-Pb

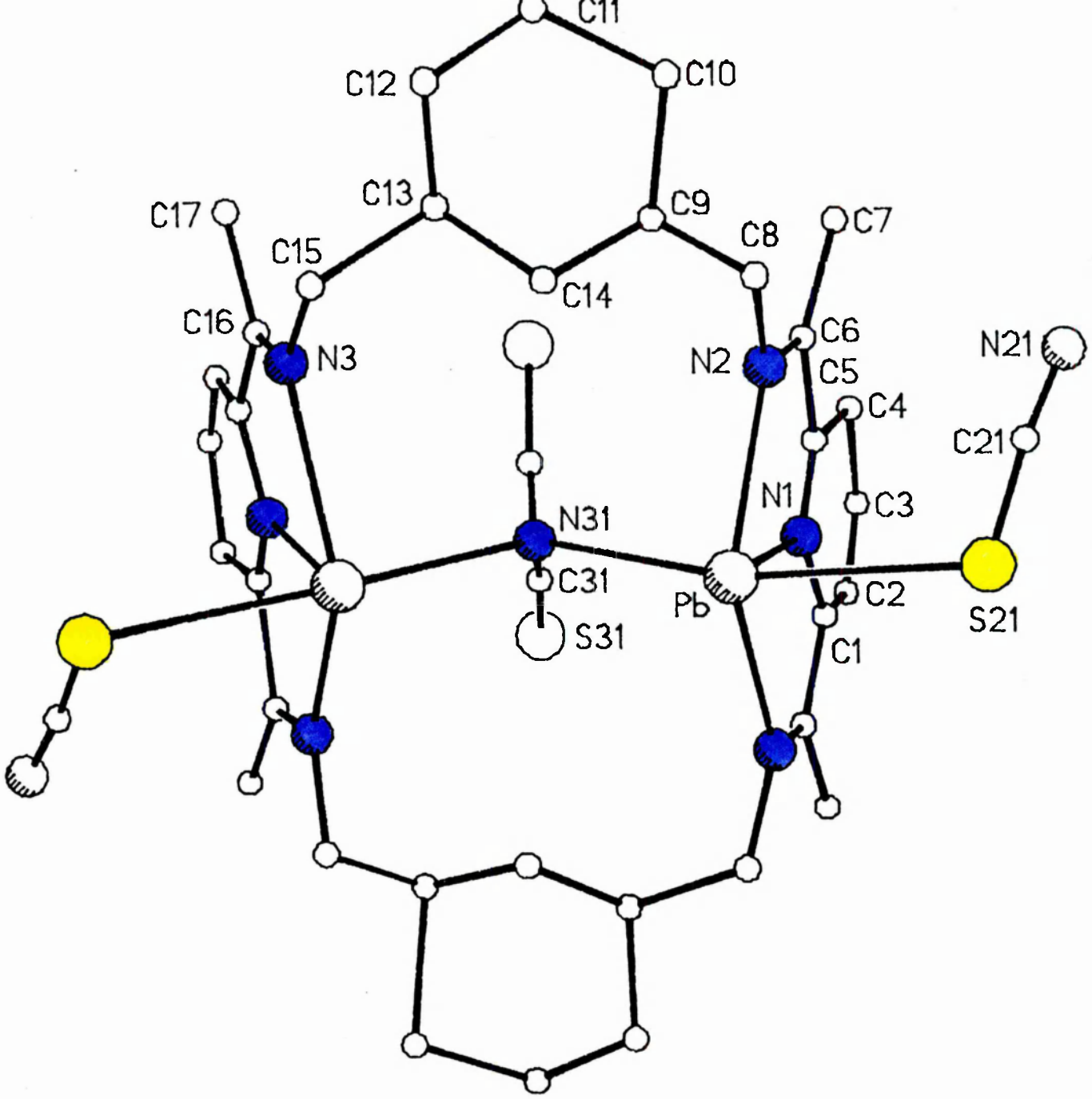

Figure 19 *The X-ray structure of* $Pb_2NC(NCS)_4$

distance was found to be 4.44Å which is remarkably similar to the Pb-Pb distance of 4.34Å in the analogous P complex.

Thus the N-only bridging mode of thiocyanate, which was suggested by the infrared spectrum of the dilead MC complex, was confirmed by X-ray structural analysis. The complex adds to the number of structurally defined compounds containing the unusual N-only bridging thiocyanate. The results strengthen the correlation between structure and infrared spectral frequency (< 2000cm^{-1}) for this bonding mode.

TABLE 14 Selected X-ray crystallographic data

BOND	BOND DISTANCE/Å	BOND	BOND ANGLE
Pb-N1	2.44	N1-Pb-N2	64°
Pb-N2	2.48	N1-Pb-S21	83°
Pb-S21	2.9	N2-Pb-S21	81°
Pb-N31	2.7	N1-Pb-N31	76°
Pb-N3	2.5	N2-Pb-N31	82°
		S21-Pb-N31	158°
		N1-Pb-N3	64°
		N2-Pb-N3	128°
		S21-Pb-N3	89°
		N31-Pb-N3	88°

Pb....Pb = 4.44Å

The pseudo-asymmetric ν(NCS) region of the spectra of dilead MC complexes are shown in figure 20. The tetrathiocyanate (13) shows four bands, the N-only bridging NCS at 1969cm^{-1} and two S-terminal thiocyanates in different environments at 2048 and 2007cm^{-1}. The weakly coordinated thiocyanate which was not precisely located in the crystal structure determination gives the absorption at 2091cm^{-1}. This frequency is somewhat higher than the free ion value. Treatment of the tetrathiocyanate MC complex (13) with $AgCF_3SO_3$ results in replacement of thiocyanate by triflate anion. The replacement can be carried out sequentially, substituting triflate for 2, 3, or 4 of the thiocyanate groups. A similar trend to that observed in the P series unfolds. In the complex $Pb_2MC(NCS)_2(CF_3SO_3)_2$ the two terminal thiocyanates have been replaced leaving the N-only bridging thiocyanate and an NCS that gives a 2077cm^{-1} absorption. Replacement of another thiocyanate leaves only the N-bonded thiocyanate.

In both the dilead P and dilead MC series replacement of NCS with triflate results in a gradual lessening of yellow colour as the number of thiocyanate groups decrease. This suggests that the strong yellow colour of the tetrathiocyanates is due to charge transfer processes involving the thiocyanate group. Removal of the coordinated thiocyanates create vacant coordination sites on the metal ion.

The tetraperchlorate (17) was obtained by treatment of complex (13) with silver perchlorate. The infrared spectrum of the tetraperchlorate MC complex (17) is informative. Splitting of the ν_3 perchlorate mode suggests that perchlorate is coordinated to the metal ion. The tetraperchlorate MC complex shows ν_3 perchlorate absorptions at 1101, 1012 and whereas the ν_4 absorption at 622cm^{-1} is unsplit. The

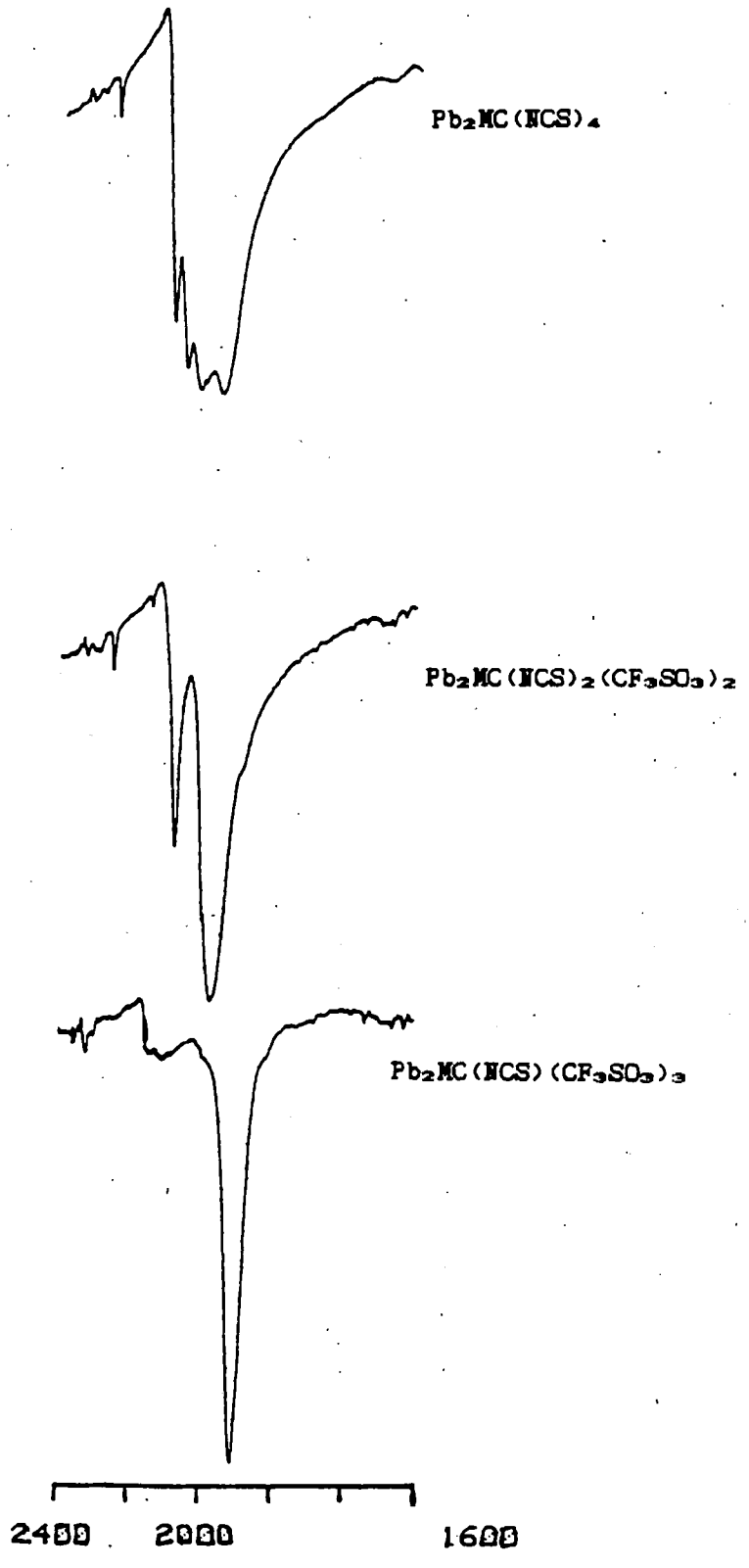

Figure 20 *The ν_{as}(NCS) stretching region of dilead MC thiocyanates*

splitting of the v_3 absorption suggests some reduction in symmetry of the perchlorate.

THE HOMOBINUCLEAR COMPLEXES OF MC

Transmetallation of $Pb_2MC(NCS)_4$ with Cu(II) or Ni(II) as described in chapter 2 resulted in formation of the dicopper and dinickel MC complexes (18) and (19) respectively. Physical data for the homobinuclear complexes is listed in Tables 15 and 16.

PHYSICAL DATA FOR THE HOMOBINUCLEAR COMPLEXES OF MACROCYCLE MC

TABLE 15 Infrared spectral data /cm^{-1}.

COMPLEX	ν(C=N)	ν(NCS)	$\nu(CF_3SO_3)$	$\nu(NO_3)$	ν(OH)
18 $Cu_2PbMC(NCS)_2(CF_3SO_3)_2{\cdot}2H_2O$	1627(m)	2111(s)	1276(s) 1255(s) 1157(s) 1030(s) 638(s)	-	3420
19 $Ni_2MC(NCS)_2(NO_3)_2$	1629(m)	2143(s) 2079(s)	-	1383(s) 1325(m) 1292(s) 805(w) 810(w)	-

The infrared spectra show a medium intensity unsplit ν(C=N) absorption and amine and carbonyl frequencies are absent indicating that the macrocyclic ligand remains intact in the transition metal complexes. The dicopper complex (18) shows a strong absorption at 2111cm^{-1} which is probably due to the long -NCS- bridging mode of thiocyanate. Consideration of the infrared spectral information along with the CHN analytical data suggests that the complex contains two thiocyanates in approximately equivalent environments.

The frozen glass esr spectrum of the dicopper complex (18) suggests that there is weak interaction between the copper centres, presumably via bridging thiocyanate. Although the frozen glass esr spectrum is not well resolved, five lines can be discerned on the side of the $g_{\perp}$ signal. Examination of the 1500-1600G region of the spectrum at high sensitivity reveals the forbidden 'half-band' $\Delta M = 2$ signal, which appears approximately 10^{-3} times the intensity of the $g = 2$ signal. The half-band signal is split by hyperfine coupling and five lines of the correct intensity ratio for a seven line pattern are observed, suggesting weak interaction between the copper(II) centres. Variable temperature magnetic susceptibility measurements also indicate weak interaction between the metal centres (table 15). A reduction in magnetic moment from 2.03BM at 300K to 1.66BM at 80K was observed.

TABLE 16 Magnetic, electronic spectral and conductivity data.

COMPLEX	COLOUR	μ eff(a) 300K	μ eff(a) 80K	Λ	ELECTRONIC SPECTRAL DATA ν	ε
18 $Cu_2MC(NCS)_2(CF_3SO_3)_2{\cdot}2H_2O$	green	2.03	1.66	238	14,600	185
19 $Ni_2MC(NCS)_2(NO_3)_2$	sage green	3.06	2.70	insol	28,000 22,200(sh) 16,900 10,270	mull

(a) moment per transition metal ion in BM.
Λ in S cm^2 mol^{-1}
ν in cm^{-1}, ε in l $mol^{-1}cm^{-1}$,

The electronic spectrum of the dicopper complex (18) shows a single unsplit d-d transition at 14,600cm^{-1}, ϵ = 185 l mol^{-1}cm^{-1}, which does not reveal much information on coordination geometry of the complex. However the presence of this absorption is consistent with tetragonal geometry.
The conductivity measurement for the complex in acetonitrile falls in the range expected for a 2:1 electrolyte. This suggests that the thiocyanate anions remain coordinated in acetonitrile solution and that the triflate anions are ionic.
The dinickel complex (19) was synthesised as described in the experimental section. It was found that use of nickel nitrate as source of Ni(II) ion facilitated removal of lead ion from the dilead MC complex as $Pb(NO_3)_2$ precipitate. The precipitate formed relatively quickly and was removed by filtration before the macrocyclic products were obtained. By contrast, transmetallation attempts using nickel triflate, nickel perchlorate or nickel chloride presented problems. Either only anion exchange took place or a mixture of insoluble sage-green products contaminated with lead thiocyanate was obtained.

The electronic spectrum of the dinickel complex (19) suggests octahedral coordination of the Ni(II) ions. The absorptions at 10,270cm^{-1} and 16,900cm^{-1} are attributable, respectively, to the $^3A_{2g} \rightarrow {}^3T_{2g}$ and $^3A_{2g} \rightarrow {}^3T_{1g}(F)$ transitions expected in octahedral symmetry. The highest energy band expected $^3A_{2g} \rightarrow {}^3T_{1g}(P)$ appears as a shoulder at 22,200cm^{-1} on the side of the intense charge transfer absorption. Due to the insolubility of the complex, only the mull spectrum is available and thus extinction coefficients were not obtained.

The suggested octahedral geometry may be obtained by coordination of the Ni(II) ion by three macrocyclic donors, the two bridging

thiocyanates and a nitrate. Coordination of nitrate is suggested by strong splitting of the nitrate absorption in the infrared spectrum.[220] Nitrate absorption bands occur at 1383, 1325, 1292, 805 and 810cm^{-1}. The magnetic susceptibility measurements for the dinickel MC complex fall in the range expected for high-spin 6-coordinate Ni(II), and confirm 6-coordination of the metal ion. A reduction in moment per Ni(II) ion from 3.0 to 2.7BM over the temperature range 300-80K was observed.

All attempts to produce a cobalt MC macrocyclic complex failed. Only dilead macrocyclic products incorporating the $Co(NCS)_4$ complex anion were obtained on attempted transmetallation using cobalt(II) thiocyanate or Co(II) nitrate. Strong reflux of the tetratriflate (16) complex with cobalt(II) triflate in acetonitrile gave only ring-opened species, as shown by the presence of amine and carbonyl frequencies in the infrared spectrum of the product.

THE HETEROBINUCLEAR COMPLEXES OF MC

Transmetallation of $Pb_2MC(NCS)_4$ (13) with transition metal ions Fe(II) and Mn(II), as described in the experimental section, produced heterobinuclear complexes that contain one lead ion and one transition metal ion. Fast atom bombardment mass spectroscopy verifies the heterobinuclear nature of the Mn/Pb and Fe/Pb macrocyclic complexes (21) and (23). The fab mass spectrum of the iron/lead macrocyclic complex showed a strong peak due to $[FePbMC(NCS)_2(CF_3SO_3)]+$ and various other peaks due to iron/lead fragment ions. These are listed in the experimental section. Peaks due to either Pb_2MC or Fe_2MC species did not appear in the spectrum. The fab mass spectrum of the heterobinuclear manganese/lead complex (21) showed $MnPbMC(NCS)_2(NO_3)+$ as the base peak

and peaks due to dimanganese or dilead species were not observed. The complexes analysed as the heterobinuclear MC bisthiocyanato- complexes, $FePbMC(NCS)_2(CF_3SO_3)_2$ and $MnPbMC(NCS)_2(NO_3)_2$.

Nitrate was used as the counterion in transmetallation with Mn(II) as it proved impossible to obtain pure heterobinuclear products on use of $Mn(CF_3SO_3)_2$ or $Mn(ClO_4)_2$. Metal exchange attempts using manganese triflate gave mixtures of heterobinuclear MC and dilead MC anion exchange products. Use of $Mn(NO_3)_2$ in transmetallation resulted in relatively rapid and complete formation of lead nitrate precipitate which was filtered off before reduction in volume to yield the heterobinuclear product. By contrast, the lead thiocyanate formed in the transmetallation of dilead MC with manganese triflate, formed more slowly and contaminated the macrocyclic products. Presumably the greater insolubility of lead nitrate in acetonitrile assists in driving the metal exchange forward.

The transmetallation of dilead MC with $Fe(CF_3SO_3)_2$ proceeded without difficulty, lead thiocyanate formed quickly and and was removed by filtration before the heterobinuclear product was obtained. It appears to be more difficult to exchange the lead ion for manganese(II) than for iron(II). (This may be a size effect, due to manganese(II) being larger than iron(II), it may be more difficult to accomodate Mn and bridging thiocyanates in the macrocyclic cavity. Infrared spectral data for the heterobinuclear complexes of the MC macrocycle is shown in Table 17.

PHYSICAL DATA FOR THE HETEROBINUCLEAR COMPLEXES OF MACROCYCLE MC

TABLE 17 Infrared spectral data /cm^{-1}.

COMPLEX	ν(C=N)	ν(NCS)	ν(CF_3SO_3)	ν(NO_3)	ν(OH)
20 MnPbMC(NCS)$_4$:H_2O	1643(m)	2056(s)	-		-
	1632(m)	2005(s)			
		1999(s)			
		1977(s)			
21 MnPbMC(NCS)$_2$(NO_3)$_2$:2H_2O	1647(m)	2054(s)	-	1424(m,br)	
	1635(m)	1975(s)		1383(s)	
				1285(m)	
				821(m)	
22 MnPbMC(NCS)$_4$:MeOH H_2O	1647(m)	2067(s)	-		
	1634(m)	2005(s)			
		1980(s)			
23 FePbMC(NCS)$_2$(CF_3SO_3)$_2$:2H_2O	1651(m)	2061(s)	1296(s)		-
	1627(m)	1961(s)	1258(s)		
			1237(s)		
			1169(s)		
			1026(s)		
			636(s)		
24 NiPbMC(NCS)$_2$(NO_3)$_2$	1628(m)	2137(s)	-	1425(br)	
		2079(s)		1382(s)	
				1285(m)	
				820(m)	

The presence of ν(C=N) and the absence of frequencies attributable to amine or carbonyl groups in the infrared spectra of the heterobinuclear complexes implies that the macrocyclic ligand remains intact on transmetallation. The imine absorption is split into two equal intensity peaks in the MnPbMC and FePbMC complexes (21) and (23). The ν(C=N) absorption at *ca.* 1630cm^{-1} is typical of an imine that is coordinated to a transition metal ion and the peak at *ca.* 1648cm^{-1} is at similar frequency to the ν(C=N) of the dilead starting material, and can be attributed the imines coordinated to the lead ion.

The presence of the imine absorption when coordinated to Fe(II) in the iron complex suggests that the Fe(II) ion is high spin as was confirmed by magnetic measurements in the temperature range 300-80K (table 18). There was no indication of a high-spin low-spin crossover in this temperature range. The ν(CN) of thiocyanate in the infrared spectra of MnPbMC and FePbMC bis-thiocyanato- complexes each display two strong absorptions. The infrared spectrum of MnPbMC, complex (21) shows an absorption at 1975cm^{-1} which is attributed to the N-only bridging mode of thiocyanate. Likewise the infrared spectrum of the FePbMC complex (23) (figure 21) shows an absorption which suggests the presence of an N-only bridge, at 1961cm^{-1}. The infrared spectrum of the complexes also show an absorption at *ca.* 2055cm^{-1} which may be due to a long bridging or terminal thiocyanate. The presence of a terminal thiocyanate is considered more probable as to date there are no reports of a structurally determined example of a complex that has both a N-only bridging thiocyanate and a long -NCS- bridge between the same two metal ions. This combination may not be feasible.

TABLE 18 Magnetic, electronic spectral and conductivity data.

COMPLEX	COLOUR	μ eff(a) 300K	90K	Λ	ELECTRONIC SPECTRAL DATA ν	ϵ
21 MnPbMC$(NCS)_2(NO_3)_2{:}2H_2O$	yellow	-		221		
23 FePbMC$(NCS)_2(CF_3SO_3)_2{:}2H_2O$	purple	4.98	4.48	-	19950 16300sh	3300
24 NiPbMC$(NCS)_2(NO_3)_2$	green	- 3.2	2.8	insol	25500 17100 10300	

(a) moment per transition metal ion in BM, Λ in S cm^2 mol^{-1}

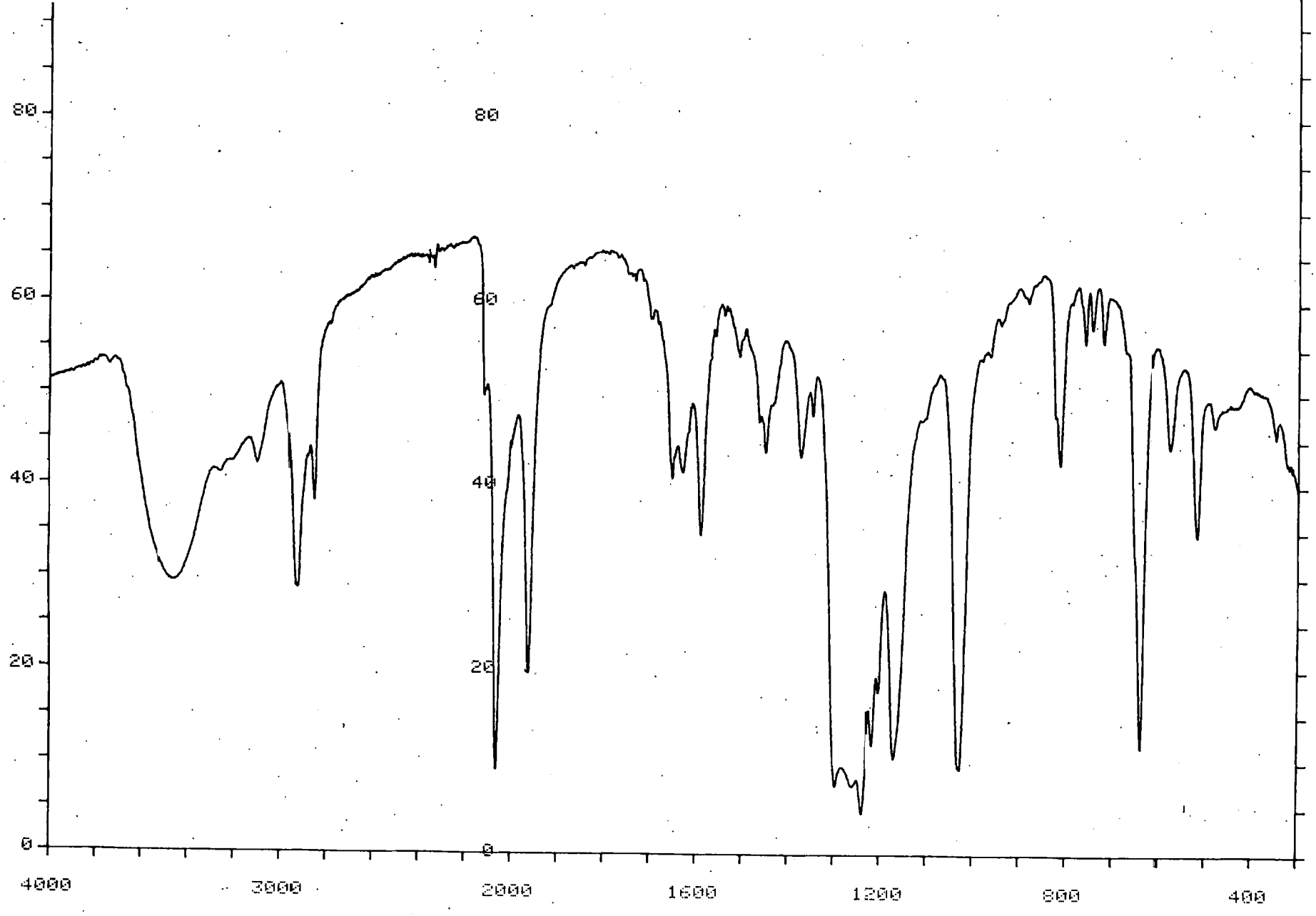

Figure 21 *The infrared spectrum of* $FePb_2NC(NCS)_2(H_2O)_2(CF_3SO_3)_2$

The esr spectrum of the MnPbNC complex (21) as a dma glass showed a strong g = 2 signal which is split into six lines by hyperfine coupling. Forbidden lines due to quadrupole interactions appear weakly between the hyperfine lines. The MnPbNC complex (21) proved to be unstable. In solution at room temperature the complex becomes brown within days. The solid sample also becomes brown if not stored at low temperature. The infrared spectrum of the resultant brown solid shows that the N-only bridging thiocyanate is lost. Although crystals of the MnPbNC complex (21) which were suitable for X-ray diffraction were obtained, these disintegrated while the data was being collected.

Preparation of the MnPbNC tetrathiocyanate complex (20)was attempted in the hope that crystals suitable for X-ray diffraction would result. The infrared spectrum of the orange tetrathiocyanate MnPbNC complex (20) displays four ν(CN) thiocyanate frequencies. The strong absorption at 1977cm^{-1} is attributed to an N-only bridging thiocyanate. The absorptions at 1999 and 2005cm^{-1} were thought unlikely to be bridging although they fall in the range associated with the N-only bridge. The remaining thiocyanate gives an absorption at 2056cm^{-1}, similar to that found in the dithiocyanato MnPb complex (21). The X-ray crystal structure of the complex has been determined by Dr. John Malone. The crystal was protected from the atmosphere while the data was collected.

THE STRUCTURE OF MnPbMC(NCS)$_4$

The X-ray crystal structure of MnPbMC(NCS)$_4$ is shown in figure 22 and selected X-ray crystallographic data is shown in table 19. The lead and the manganese ions are bound to a trimethine site at either end of the macrocycle. The manganese ion is coordinated by two terminal thiocyanates which are bound via the nitrogen atom. Coordination of the thiocyanate ligand through nitrogen is expected for the manganese ion on the basis of Pearson's hard/soft acid/base theory. A thiocyanate anion bridges the metal ions through the nitrogen atom only.

The manganese ion is six co-ordinate and has an irregular geometry, being bonded to the three macrocyclic N-donors which are coplanar (Mn-N3, Mn-N4, Mn-N5) and an N-terminal thiocyanate, the nitrogen of which is close to this plane. The remaining N-terminal thiocyanate and the N-only bridge occupy approximate axial positions. The coordination around manganese is represented below.

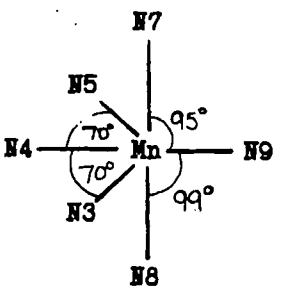

Figure 23 *The coordination around manganese*

The lead ion in the complex is five coordinate and has an irregular coordination geometry. Irregular coordination sites have been reported in many lead ion macrocyclic complexes.[126,68] The lead ion is quite adaptable and tolerates a range of coordination geometries.

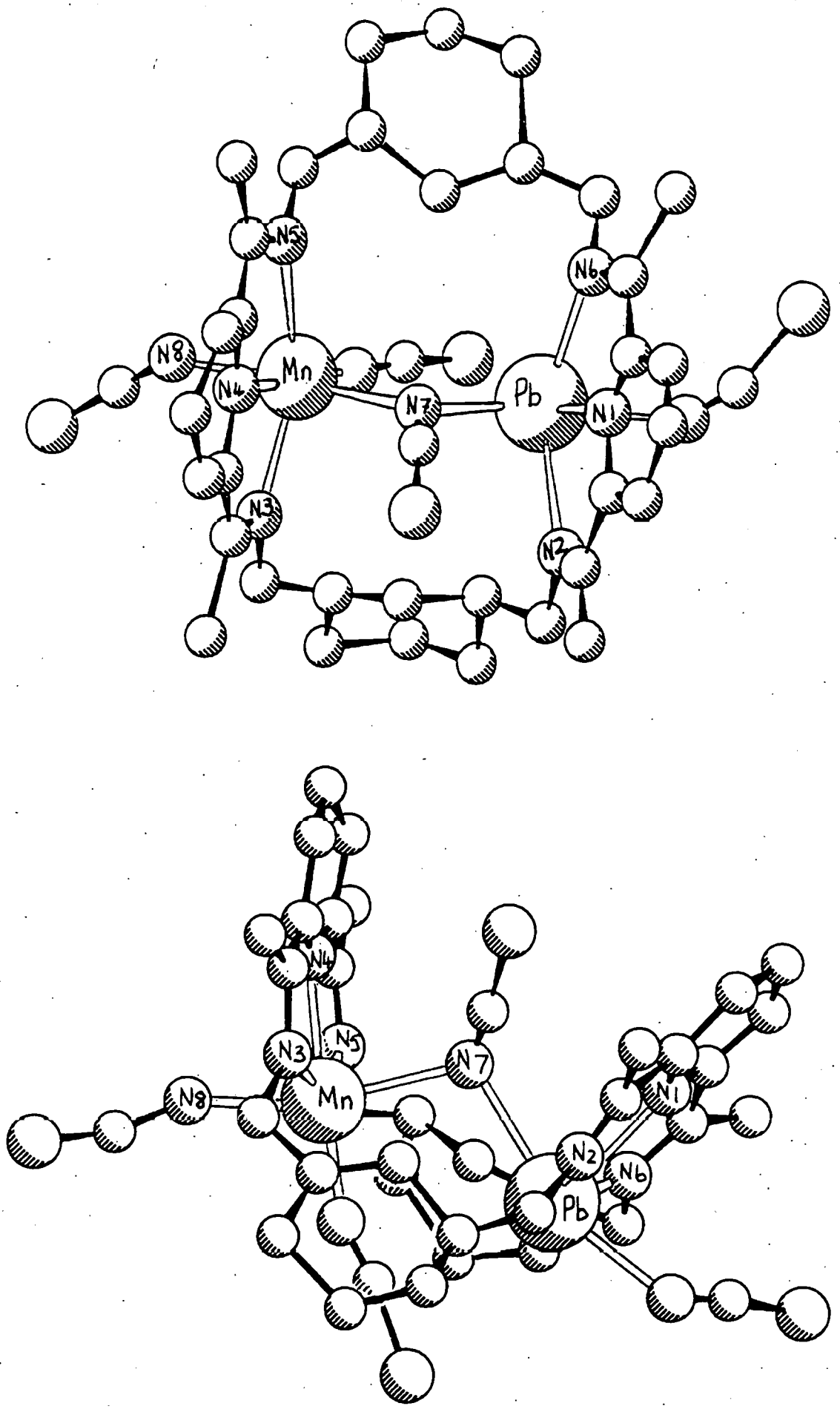

Figure 22 *The X-ray structure of* $MnPb_2MC(NCS)_4$

TABLE 19 Selected X-ray crystallographic data

BOND	BOND DISTANCE	BOND	BOND ANGLE
Pb-N1	2.60Å	N1-Pb-N2	68°
Pb-N2	2.54Å	N1-Pb-N6	64°
Pb-N6	2.47Å	N1-Pb-N7	78°
Pb-N7	2.62Å	N1-Pb-N10	82°
Pb-N10	2.55Å	N2-Pb-N6	131°
		N2-Pb-N7	84°
		N2-Pb-N10	83°
		N6-Pb-N7	94°
		N6-Pb-N10	83°
		N7-Pb-N10	159°
Mn-N3	2.34Å	N3-Mn-N4	70°
Mn-N4	2.34Å	N3-Mn-N5	140°
Mn-N5	2.42Å	N3-Mn-N7	87°
Mn-N7	2.53Å	N3-Mn-N8	86°
Mn-N8	2.25Å	N3-Mn-N9	109°
Mn-N9	2.00Å	N4-Mn-N5	70°
		N4-Mn-N7	81°
		N4-Mn-N8	85°
		N4-Mn-N9	176°
		N4-Mn-N8	92°
Pb...Mn	4.16Å	N5-Mn-N8	86°
		N5-Mn-N9	111°
		N7-Mn-N8	167°
		N7-Mn-N9	95°
		N8-Mn-N9	99°

The coordination of the lead ion by N-terminal thiocyanate contrasts with the structure of $Pb_2MC(NCS)_4$ (Figure 19), in which the lead ion is coordinated to an S-terminal thiocyanate. Coordination of lead by N-terminal thiocyanate is quite unusual. Generally lead is coordinated through the S atom of the thiocyanate ligand, in agreement with Pearson's hard/soft acid/base theory. It is possible that in the PbMnMC complex coordination of lead by S of the thiocyanate may result in steric interaction between the thiocyanate ligand and the macrocycle. Interaction may involve the macrocycle that binds the Pb-NCS subunit or the neighbouring macrocyclic complex in the crystal lattice. The M-N-CS arrangement has a bond angle of approximately 170° which is close to

linear whereas the alternative M-S-CN arrangement has a bond angle which is close to 100°. Steric interactions have previously been suggested to be responsible for coordination of thiocyanate through nitrogen to a 'soft' metal ion in sterically crowded complexes.

The X-ray structural determination provides the first example of an N-only bridging thiocyanate in a heterobinuclear complex. The structure confirms the inference, from the infrared spectrum of the complex, that the N-only bridging thiocyanate is present. In addition the structure lends further support to the correlation between 'low' infrared absorption frequency and the N-only bonding mode of thiocyanate.

Normally the N-only bridging mode of thiocyanate when found in a dilead parent complex would not exist after transmetallation with a transition metal ion. The change in size of the metal ion often results in an internuclear separation that is no longer suitable for binding a single atom bridge. The relatively large size of the manganese(II) ion, compared to that of the other transition metal ions, is likely to provide the smallest internuclear separation in the complex and is more likely to permit binding of the single atom bridge between the metal ions. However, comparison of the internuclear separation found in the parent Pb_2MC complex (13) with that found in the MnPbMC complex (20) shows that the internuclear separation is smaller in the MnPbMC case. The manganese-lead internuclear distance is 4.16Å which contrasts with the internuclear separation of 4.44Å found for the dilead parent MC complex.

The MnPbMC structure (figure 22) contrasts with the structure of $MnPbP(NCS)_4$ (figure 16) which shows two long -NCS- bridges between the manganese and lead ions. The lead and manganese ions of the P structure have a separation of 4.85Å. Each metal is six coordinate and is bonded to

three nitrogens of the macrocycle, a nitrogen atom of a terminal NCS group and two atoms of the bridging thiocyanate group. The lead ion is bonded to the sulphur atoms of the bridging thiocyanates and the manganese is bonded to the nitrogens of the bridging thiocyanates.

The brown manganese complex MnPbMC(NCS)$_4$:MeOH H_2O (22) as the solid gave a broad esr signal indicating that the manganese ion is Mn(II). A six-line hyperfine splitting was observed in the spectrum of the complex as a dmf glass. The electronic spectrum of complex (22)shows that the tail of the intense charge transfer absorption extends across the visible region, accounting for the brown colour of the complex. As expected, d-d bands were not observed.

The heterobinuclear NiPb complex (24) was obtained as a small second crop from the reaction that formed the dinickel MC complex (19). The infrared spectrum of the heterobinuclear PbNiMC complex showed thiocyanate absorptions at 2137 and 2079cm^{-1} which fall in the range for long bridging thiocyanate. Absorptions due to nitrate counterion were typical of uncoordinated nitrate. Bands at 1382, 815 and 721cm^{-1} were observed due to the three infrared active modes of ionic D_{3h} NO_3^-. The electronic spectral data for the complex suggests six coordination of the Ni(II) ion as the three bands expected for Ni(II) in octahedral symmetry were observed. The infrared spectrum did not show an absorption due to acetonitrile therefore it is probable that the sixth coordination position on the nickel (II) ion is occupied by a water molecule.

The formation of the heterobinuclear Fe/Cu complex with macrocycle P suggested that the Fe/Cu complex of macrocycle MC may be obtainable. This was the only preparation of a heterobinuclear transition metal complex of the MC macrocycle which was attempted. The reaction between FePbMC

complex (23) and $Cu(MeCN)_4(CF_3SO_3)$ as described in the experimental section gave a mixture of products. Fab mass spectroscopy indicated that the mixture included the heterobinuclear Fe/Cu MC complex, FePbMC starting material and possibly PbCuMC complex. The fab mass spectrum of the product showed a cluster at m/e 773 (50%) which is attributable to $[FeCuMC(NCS)_2]^+$. The cluster around m/e 809 (20%)may be due either to $[FeCuMC(CF_3SO_3)]^+$ or to $[CuPbMC]^+$, likewise the cluster at 1108 (25%) may be due to $[FeCuMC(CF_3SO_3)_3]^+$ or to $[PbCuMC(CF_3SO_3)_2+H]^+$. The cluster around m/e 952 (15%) can be assigned to $[FePbMC(CF_3SO_3)]^+$.

Esr showed that the product contains Cu(II). The dmf glass spectrum showed a non-interacting Cu(II) signal, with hyperfine splitting of 150G. The dmf glass esr spectrum of the product is shown in figure 24. The product mixture was soluble in acetonitrile and separation by ion exchange chromatography may be possible.

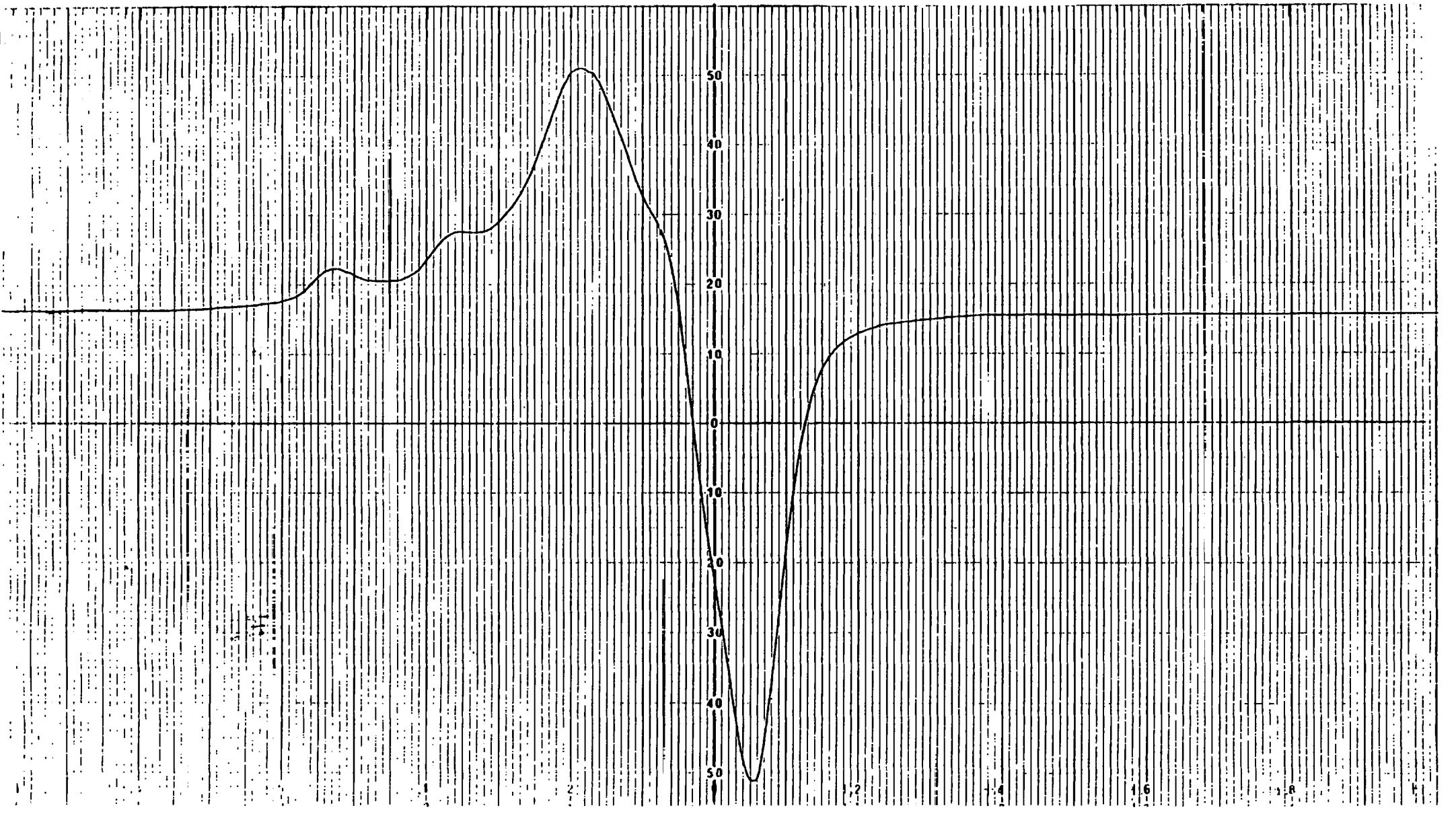

Figure 24 *The dmf glass esr spectrum of the product of* $[FeCuNC]^{4+}$ *synthesis*

CHAPTER 4

INTRODUCTION

Transition metal complexes of ligands containing the α-diimine group (-N=C-C=N-) have been studied extensively for the past thirty-five years. The distinctive nature of the α-diimine group was first recognised by Krumholz in 1953.[321] By comparison of complexes of phenanthroline and bipyridyl with those of simpler α diimine ligands he concluded that it was only of secondary importance whether or not the α diimine group belonged to a conjugated heterocyclic system.

The α-diimine group has excellent chelating ability and complexes of α-diimines with metals from each group of the periodic table are known.[322,323] The chemical and physical properties of α-dimine complexes have been reviewed.[324-326] One of the most striking properties of these ligands is their ability to stabilise metals in low oxidation states.[327,328] The infrared spectra of transition metal complexes of α-diimines show significant shifts of ν(C=N) to lower frequencies on coordination as a result of the ligands ability to act as electron acceptors.[329-331] The electronic spectral bands which are responsible for the intense colours of the transition metal complexes of α-diimine ligands have been assigned to metal to ligand (d - π*) charge transfer bands.[170] The delocalised character of the chelate rings can be represented as a resonating system as confirmed by nmr studies on diamagnetic tris α-diimine Fe(II) complexes.[332] and esr spectra of tris bipy complexes of ^{47}V and ^{53}Cr.[333] Low oxidation states of the metal are stabilised by a resonance system in which there is some charge transfer of the metal t_{2g} electrons into the pπ* orbitals of the chelate ring.[334,335] Although the metal is formally in a low oxidation state, some of it's electron density is delocalised over the chelate rings. The strength of this interaction is

shown by the high ligand field strengths of α-diimines, lying between ethylenediamine and cyanide in the spectrochemical series.[226]

The relative magnitudes of of the infrared spectral ν(C=N) shifts on coordination, Fe(II) >> Co(II) ≈ Ni(II) has been interpreted as indicating greater π-cloud delocalisation for the iron complex.[229] This is reflected in the relatively large number of spin-paired iron(II) complexes of α-diimine ligands.

GROUP II METAL ION CRYPTATES

Schiff-base [2+3] condensation of the tripod amine tren with glyoxal on Group II metal ion template produces the metal ion cryptate of the hexaimino cryptand GT as shown in figure 25.

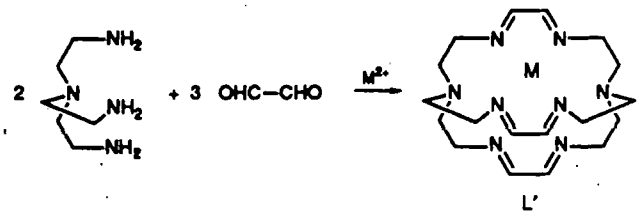

Figure 25.

Metal ions Ba^{2+}, Sr^{2+}, Ca^{2+} and Mg^{2+} were effective as template species. Physical data for the complexes is shown in table 20. The infrared spectra of the cryptates show a medium intensity ν(C=N) absorption at *ca.* 1610cm^{-1} and frequencies attributable to unreacted carbonyl or amine were absent from the spectra. This indicated that Schiff-base condensation was complete and had formed the cryptate rather than a pendant arm macrocyclic complex. A medium intensity, sharp absorption is observed at *ca.* 1650cm^{-1}. The origin of this band is uncertain, however this may be a combination tone arising from coupling of the ν(C=N) stretching vibration

with other ring deformations. The infrared spectra also display strong absorptions due to the tetraphenylborate counterion, suggesting that the metal complex has formed, as opposed to the metal-free Schiff-base cryptand. The presence of a quite sharp absorption at *ca.* 3510cm^{-1} in the ν(OH) region of the infrared spectra suggests the presence of non hydrogen bonded water (or alcohol), which may be coordinated to the metal ion. The infrared spectrum of SrGT(BPh$_4$)$_2$:2H$_2$O is shown in figure 26.

PHYSICAL DATA FOR TEMPLATED GT COMPLEXES

TABLE 20 Infrared spectral data / cm^{-1}

COMPLEX	COLOUR	vC=N	vBPh$_4$	vClO$_4$	vOH
25 BaGT(BPh$_4$)(ClO$_4$):2H$_2$O	cream	1609(m)	1577(m) 1476(m) 1425(m) 734(s) 706(s)	1120(s) 1072(s) 1032(s) 623(s) 611(s)	3517(sh)
26 SrGT(BPh$_4$)$_2$:2H$_2$O	cream	1610(s)	1575(m) 1476(m) 1425(m) 734(s) 707(s)	-	3503(sh)
27 CaGT(BPh$_4$)$_2$:2H$_2$O	cream	1610(s)	1575(m) 1476(m) 1424(m) 734(s) 704(s)	-	3513(sh)
28 MgGT(BPh$_4$)$_2$:2H$_2$O	yellow	1634(m)	1577(m) 1477(m) 1425(m) 734(s) 705(s)	-	3327(br)
29 LaGT(BPh$_4$)(NO$_3$)$_2$:2H$_2$O	yellow	1608(s)	1576(s) 1478(m) 1425(m) 734(s) 705(s)	-	3430(br)

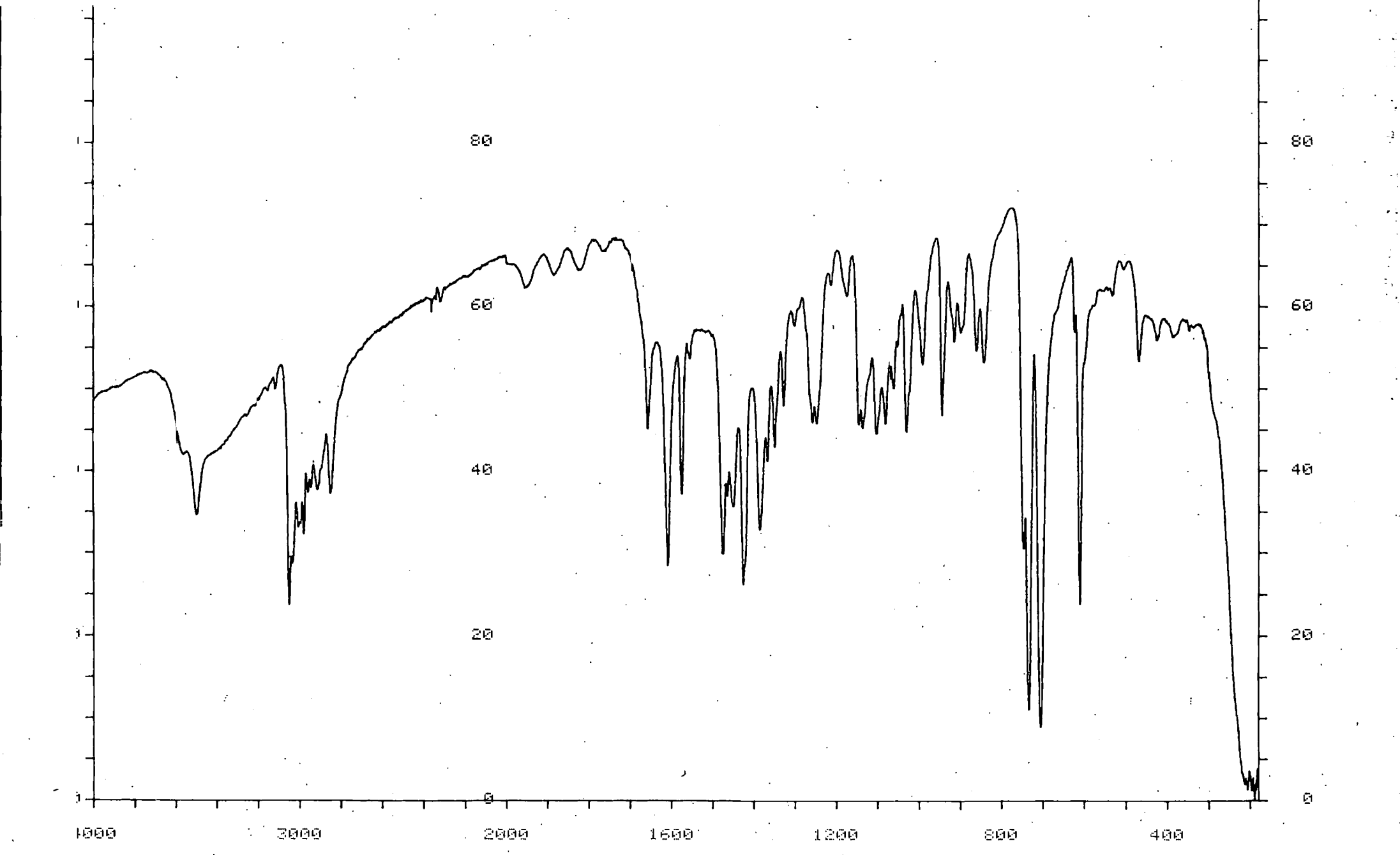

Figure 26 *The infrared spectrum of* $SrGT(BPh_4)_2:2H_2O$

The infrared spectra of the metal ion GT cryptates show an unexplained absorption at *ca.* 1650cm^{-1} which is possibly a combination tone. Skeletal absorptions of the GT cryptate occur at *ca.* 1450,1385 and 740cm^{-1} in the infrared spectra of all of the cryptates. A C-H stretch of GT occurs at *ca.* 2848cm-1 in the spectra.

It proved necessary to use tetraphenylborate as the counterion in order to isolate the cryptate from the reaction mixture. In addition, the insolubility of the cryptate as a tetraphenylborate may cause a shift in the equilibrium towards the cryptate product. However the use of BPh_4^- as counterion has led to problems in obtaining satisfactory CHN analysis. Presumably, as a result of the high molecular weight of the counterion and the large numbers of C and H present, presence of even small amounts of perchlorate counterion impurity, or a small amount of metal ion tetraphenylborate mixed with the cryptate make large differences to the analysis figures. Nevertheless, reasonable CHN analysis has been obtained for the calcium and strontium cryptates.

The barium cryptate retains perchlorate anion, even after recrystallisation in the presence of excess tetraphenylborate. This may be a result of the preference of the barium ion for a high coordination number due to it's large ionic radius combined with the ionic nature of the bonding in the group 2 metal ion cryptates. Trends in the coordination number of group 2 metal ions have been reported and tend to increase in coordination number down the group.[337] The perchlorate anion appears to supplement the donors provided to barium by the cage ligand. The infrared spectrum of the barium complex (25) shows splitting of the ν_3 absorption of perchlorate into four bands, 1135, 1120, 1072 and 1032cm^{-1} the ν_4 absorption is split into two bands at 611 and 623cm^{-1}. The presence of

four ν_3 absorptions may indicate that both $BaGT(BPh_4)(ClO_4)$ and $BaGT(ClO_4)_2$ are present. If the anions present in alkaline earth metal complexes are disposed in different environments or display different bonding modes complex infrared spectra can result.[57] In the absence of x-ray crystallographic evidence, assignment of anion disposition must remain tentative. Acceptable CHN analysis was not obtained for the barium complex. Although the precise formula of the BaGT complex is uncertain, the complex has proved a useful starting material for further reactions.

The GT cryptand appears to show some selectivity for Group II metal ions. Strontium and calcium cryptates appear to be relatively stable, these are easily recrystallised from acetonitrile and the solutions can be heated at gentle reflux without damage to the complex. The barium cryptate can be recrystallised, though the complex is not stable on strong heating. The magnesium complex is the least stable and does not recrystallise successfully even at room temperature, attempted recrystallisation attempts gave oils. Fast atom bombardment mass spectroscopy of the magnesium templated product showed the protonated GT ligand at m/e 359 as the base peak. A very weak peak due to $[MgGT]^+$ (6%) was observed. As a result of the uncertainty of the formula of this complex, further physical data was not collected for the complex. By contrast the fab spectrum of the SrGT cryptate showed a strong cluster at m/e 446 (99%) which is attributable to $[SrGT]^+$ and reflects the stability of this cryptate in the conditions of the mass spectrometer. The base peak was due to the protonated GT ligand at m/e 359.

Presumably the stability sequence observed in the series of group(II) metal ion cryptates is due to size effects. A relationship between the stability of alkaline-earth metal macrocyclic complex and the closeness of

fit between the cation and the macrocyclic cavity has been established.[57] The prefered cation is generally the one that fits the cavity most closely. The match of ionic radius of the metal ion to the cavity size of the GT cryptand determine the strength of the electrostatic interactions between the metal ion and the cryptand. The barium ion appears to be slightly too large for the cavity of the GT cryptand whereas the magnesium ion seems to be too small for the cryptand cavity. Both the strontium and the calcium ion appear to fit the cavity relatively well.

The complexes were sufficiently soluble in CD_3CN for ^1H n.m.r. spectra to be measured. Spectra of the calcium, strontium and barium cryptates were similar and the ^1H nmr spectrum of $CaGT(BPh_4)_2$ is shown in figure 27. The ^1H nmr spectra consisted of three resonances with relative intensities 1 : 2 : 2 at approximately 8.0$_{(s)}$, 3.7$_{(t)}$ and 2.8$_{(t)}$ p.p.m. downfield from $SiMe_4$. These are assigned to the imine H at 8.0 , the CH_2 adjacent to the imine group at 3.7 and the neighbouring CH_2 group at 2.8 p.p.m. Strong signals due to the tetraphenylborate counterion were observed at (7.3$_m$, 7.0$_t$ and 6.8$_t$). The protons of the methylene groups were coupled to each other. Additional slight splitting of the three cryptand resonances was observed. The imine resonance was split into three closely spaced peaks with J = 1.2 Hz (0.004ppm) The methylene triplet around 3.7 was also split further, each peak of the triplet was split into two with J = 1.2 Hz (0.004ppm.) There appears to be some coupling between the imine proton and the protons of the nearest methylene group. The resonance around 2.8 ppm. also showed slight splitting of the peaks, though this was not so well defined. The appearance of just three sets of resonances in the nmr spectra suggest that the cation is bound within the molecular cavity. In addition the simplicity of the spectra may be taken as evidence

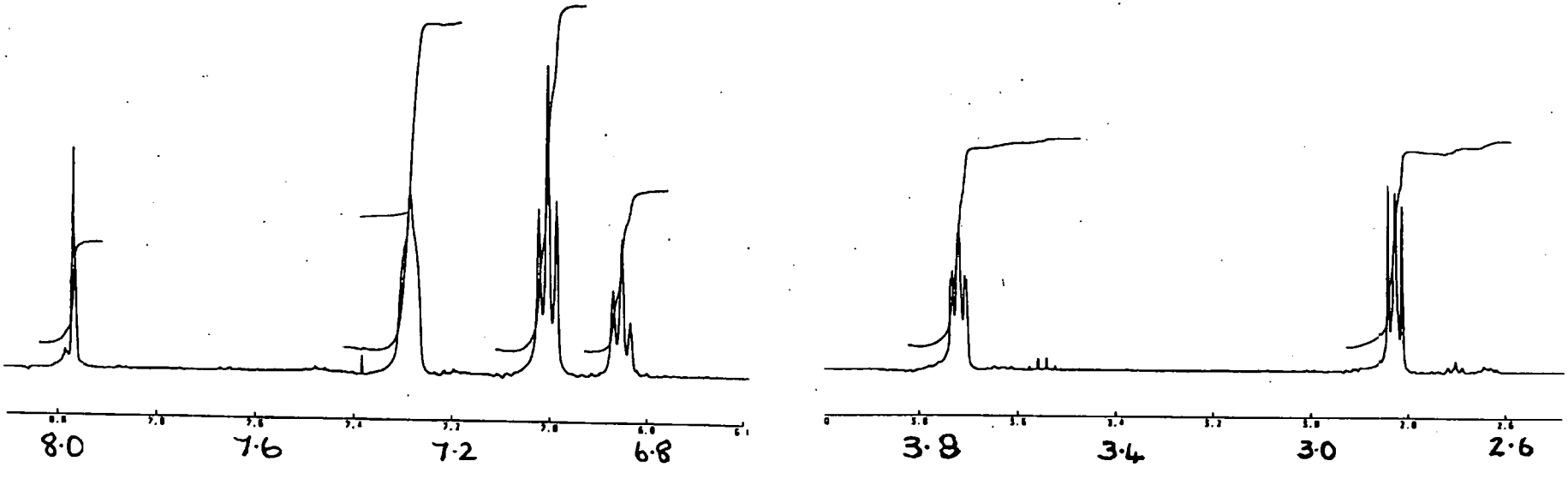

Figure 27 *The n.m.r. spectrum of* $CaGT(BPh_4)_2{:}2H_2O$

against any significant dissociation of the complexes in CD_3CN solution into the free metal ion and the cryptand.

The electronic spectra of the calcium and strontium complexes showed little dependence on the nature of the Group (II) cation. The spectra both showed a strong band at ca. 35,500cm^{-1} ($\epsilon \simeq 1800$). A shoulder on the low energy side of the main band was assigned to a $\pi - \pi^*$ transition of the complexed cryptand. The insensitivity of the energy of the transition is in keeping with a predominantly coulombic (ion - dipole) metal - cryptand interaction.

Attempted synthesis of the GT cryptand without use of a template metal ion failed. In the absence of metal ions only viscous oils were recovered, which from their nature are probably polymeric. Various solvents and reaction conditions were employed using relatively dilute solutions and controlled addition of the reactants, yet only oil resulted. The effect of the template ion in the cryptate synthesis may arise from an ability to hold the dicarbonyl glyoxal in a cis conformation suitable for reaction to form the cryptate. The free glyoxal is likely to be predominantly in the trans conformation and reaction of the trans form with the amine is likely to form polymer.

Several lanthanide ions were tested as template ions for the GT synthesis. Of the ions La^{3+} and Pr^{3+} , the lanthanum ion proved the better template species. The infrared spectrum of the lanthanum templated product showed the presence of the characteristic GT peaks and peaks attributable to amine or carbonyl groups were absent from the spectrum. The fast atom bombardment mass spectrum contained clusters at m/e 496 (4%) and 558 (2%) due to $[LaGT]^+$ and $[LaGT(NO_3]^+$ respectively.

MONONUCLEAR TRANSITION METAL ION GT COMPLEXES.

A series of mononuclear transition metal cryptates was obtained by transmetallation of the barium or strontium GT template complexes as described in the experimental section. Product from the template reaction was used without further purification for the synthesis of transition metal GT tetraphenylborates.

The perchlorate salts of the crypates were prepared for two reasons. Firstly, the crystals of the cobalt cryptate as a tetraphenylborate showed extensive disorder and the X-ray structure was impossible to solve. Secondly the tetraphenylborate counterion is electrochemically active in a region that could possibly overlap with the 2+/3+ redox couple of the cryptate, thus an alternative counterion was required for electrochemical studies. The transition metal GT perchlorates were accessible by two routes. In one route the SrGT tetraphenylborate was isolated and treated with $AgClO_4$ to remove the tetraphenylborate counterion prior to reaction of $SrGT(ClO_4)_2$ with transition metal perchlorate. Alternatively an *in situ* method was used which involved template synthesis of Sr or Ba GT perchlorate which was not isolated followed by addition of the transition metal perchlorate to the template solution. This reaction was carried out in methanol. Transition metal cryptate obtained by the latter method required recrystallisation from acetonitrile/ethanol solvent mixture and the overall yields were generally lower.

Infrared spectral data for the mononuclear transition metal cryptates is listed in tables 21 and 22.

PHYSICAL DATA FOR MONONUCLEAR TRANSITION METAL GT COMPLEXES

TABLE 21 Infrared spectral data /cm^{-1}

COMPLEX	COLOUR	vC=N	$vBPh_4$	vOH
30 $MnGT(BPh_4)_2:2H_2O$	yellow	1605(m)	1577(m) 1476(m) 1423(m) 733(s) 706(s)	3439(br)
31 $CoGT(BPh_4)_2:3H_2O$	rust	1591(m)	1576(m) 1476(m) 1421(m) 734(s) 706(s)	3434(br)
32 $NiGT(BPh_4)_2:\frac{1}{2}H_2O$	orange	1594(m)	1575(m) 1476(m) 1421(m) 733(s) 706(s)	3434(w,br)
33 $FeGT(BPh_4)_2:2H_2O$	deep-purple	absent	1575(m) 1476(m) 1421(m) 734(s) 707(s)	3465(br)

With the exception of the Fe(II) GT cryptates, the infrared spectra of the metal ion GT cryptates show an unexplained absorption at *ca.* 1650cm^{-1}. The absorption is not sensitive in position and is believed to be a combination tone. Skeletal absorptions of the GT cryptate occur at *ca.* 1450,1385 and 740cm^{-1} in the infrared spectra of all of the cryptates. A C-H stretch of GT occurs at *ca.* 2848cm-1 in the spectra.

TABLE 22 Infrared spectral data /cm^{-1}

COMPLEX	COLOUR	νC=N	νClO_4	νNCS	νOH
34 $ZnGT(ClO_4)_2:2H_2O$	orange	1620(m)	1171(s) 1100(m) 999(m) 622(s)	-	3509(br)
35 $CoGT(ClO_4)_2:2H_2O$	rust	1609(m)	1090(s) 622(m)	-	3436(br)
36 $NiGT(ClO_4)_2:EtOH\ H_2O$	orange	1608(m)	1086(s) 622(m)	-	3434(w,br)
37 $NiGT(NCS)_2:2H_2O$	orange	1601(m)	-	2091 2075	3455(w,br)
38 $FeGT(ClO_4)_2:2H_2O$	deep-purple	absent	1100(s) 622(m)	-	3465(br)

In the infrared spectra of the complexes skeletal GT absorptions occur at *ca.* 1450,1388 and 740cm^{-1}. The Fe(II) cryptate does not show the combination tone absorption at *ca.* 1650cm^{-1} which is present in the spectra of the other metal ion cryptates.

The infrared spectra of the complexes, show a sharp ν(C=N) absorption at *ca.* 1595cm^{-1}. The absence of amine or carbonyl frequencies indicates that the cryptand remains intact throughout the series of cryptates. The slight shift of the ν(C=N) from *ca.* 1610cm^{-1} in the group (II) metal ion cryptate to *ca.* 1600cm^{-1} reflects the change in the nature of the metal ion-ligand bonding in the transition metal cryptates.

The exceptions are the Fe(II)GT cryptates (33) and (38), the infrared spectra of the iron complexes do not exhibit a ν(C=N) absorption in the region 1590 - 1660cm^{-1}, although the other characteristic peaks of the GT complex such as ν(C-H) of GT at 2846cm^{-1} and skeletal vibrations of the cryptand at 1443, 1387 and 740cm^{-1} are present. The absence of the νC=N

absorption in the expected region of the FeGT infrared spectrum may be due to a reduction in intensity or a coordination shift of the absorption. Such changes are indicative of strong coupling of the Fe(N=C-C=N) chelate ring vibrations or metal dπ to ligand pπ* back coordination.[329,330] Related studies have noted that the ν(C=N) stretch in the tris(α-diimine) complexes is absent or very weak for low-spin Fe(II) but relatively intense for Co(II), Ni(II) and Cu(II).[329,330] The medium intensity peak at *ca.* 1650cm^{-1}, which is present in the infrared spectrum of the other cryptates, is absent in the spectra of the iron cryptates.

The absence of the ν(C=N) absorption in the spectra of the iron cryptates suggested that the iron(II) ion is low spin. The low spin nature of the iron ion was confirmed by magnetic susceptibility measurements (table 23). The magnetic moment obtained for FeGT tetraphenylborate (33) clearly rules out a high-spin ground state; the small paramagnetism observed at 293K could be attributed either to the presence of paramagnetic impurity or to the presence of a small quantity of the high-spin form at this temperature. Recrystallisation of the iron cryptate gave lower magnetic moments as purer samples were obtained, suggesting that at least some of the observed paramagnetism was due to paramagnetic impurity. Spin-pairing in the iron GT cryptates may arise from a combination of the strong ligand-field of the GT cryptand, a particularly good fit of the Fe(II) ion for the GT cavity and a coordination geometry around the Fe(II) ion which is not far from octahedral.

Table 23 Magnetic, electronic spectral and conductivity data

COMPLEX	μeff 293K	μeff 93K	Λ	ELECTRONIC SPECTRA ν max	ε
30 $MnGT(BPh_4)_2:2H_2O$	5.99	5.98	223	29400	930
31 $CoGT(BPh_4)_2:3H_2O$	4.30	4.20	236	26200	1900
				11430	19
32 $NiGT(BPh_4)_2:\frac{1}{2}H_2O$	3.04	3.01	219	33200	1600
				12500	18
33 $FeGT(BPh_4)_2:2H_2O$	0.95	0.40	-	23100	2300
				17400	5600
35 $CoGT(ClO_4)_2$	4.43	3.95	254	26430	1600
				11100	5
38 $FeGT(ClO_4)_2$	dia	dia	-	23100	1500
				17460	3800
39 $CuGT(ClO_4)_2:4H_2O$	1.86	1.61	-	35600	2700
				24300	2150
				15500	120

μ in BM, Λ in S cm^2 mol^{-1}
ν max in cm^{-1}
ε in l mol^{-1} cm^{-1}

The electronic spectra of the FeGT complexes (33) and (38) show a pair of intense absorptions close to 20,000 and 17,000cm^{-1}. Since a pair of intense bands found in the electronic spectrum of $[Fe(bipy)_3]^{2+}$ were assigned to M → π* transitions,[217] it is assumed that the pair of absorptions observed in the FeGT spectra are due to M → π* charge transfer transitions. The presence of one or more intense bands in the visible region of the spectrum is characteristic of iron(II)-tris (α-diimine) complexes.[217,221,222] The splitting into two charge transfer absorptions has been attributed to separation of the T_{2g} level into e and

b_2 levels as the symmetry diminishes from octahedral.[329] The spectrum did not show any evidence of d-d transitions. In comparison with the α-diimine complexes $[Fe(bipy)_3]^{2+}$ and $[Fe(phen)_3]^{2+}$,[321] $\bar{\nu}$max for the FeGT complexes occurs at lower energy. For example for $[Fe(bipy)_3]^{2+}$ $\bar{\nu}$max = 19,100cm^{-1}, $[Fe(phen)_3]^{2+}$ νmax = 19,600cm^{-1}. The extinction coefficients of ν max for FeGT are somewhat greater than those for the bipy and phen complexes of Fe(II).

The CoGT perchlorate (35) shows remarkable stability in water. Complexes of Schiff-base macrocycles and cryptands are often susceptible to hydrolysis, yet water proved to be one of the best solvents for recrystallisation of CoGT perchlorate. The CoGT cryptate appears to be kinetically inert with respect to removal of the Co(II) ion. Treatment of an aqueous solution of the cobalt (II) cryptate (35) with an excess of NaCN in aqueous solution failed to generate a $Co(CN)_2$ precipitate over a period of several weeks. During this time there was no reduction in the orange/rust (CoGT) colour of the solution.

The Co, Fe and Ni GT perchlorates (35),(38), and (32) show the strong ν_3 and ν_4 absorptions typical of uncoordinated perchlorate at *ca.* 1100cm^{-1} and 620cm^{-1} respectively. The infrared spectrum of $CoGT(ClO_4)_2$ is shown in figure 28. The electronic spectrum of both the tetraphenylborate and the perchlorate salt of CoGT is dominated by the broad and intense charge transfer absorption which extends into the visible region of the spectrum. Nevertheless a low intensity band around 11,000cm^{-1} is observed and is attributed to the lowest energy transition $^4T_{1g}(F) \rightarrow {}^4T_{2g}$ allowed in approximate octahedral symmetry for cobalt(II). Similarly the electronic spectrum of the NiGT complex (32) shows a broad and intense charge transfer absorption and only the lowest energy band expected for Ni(II) in

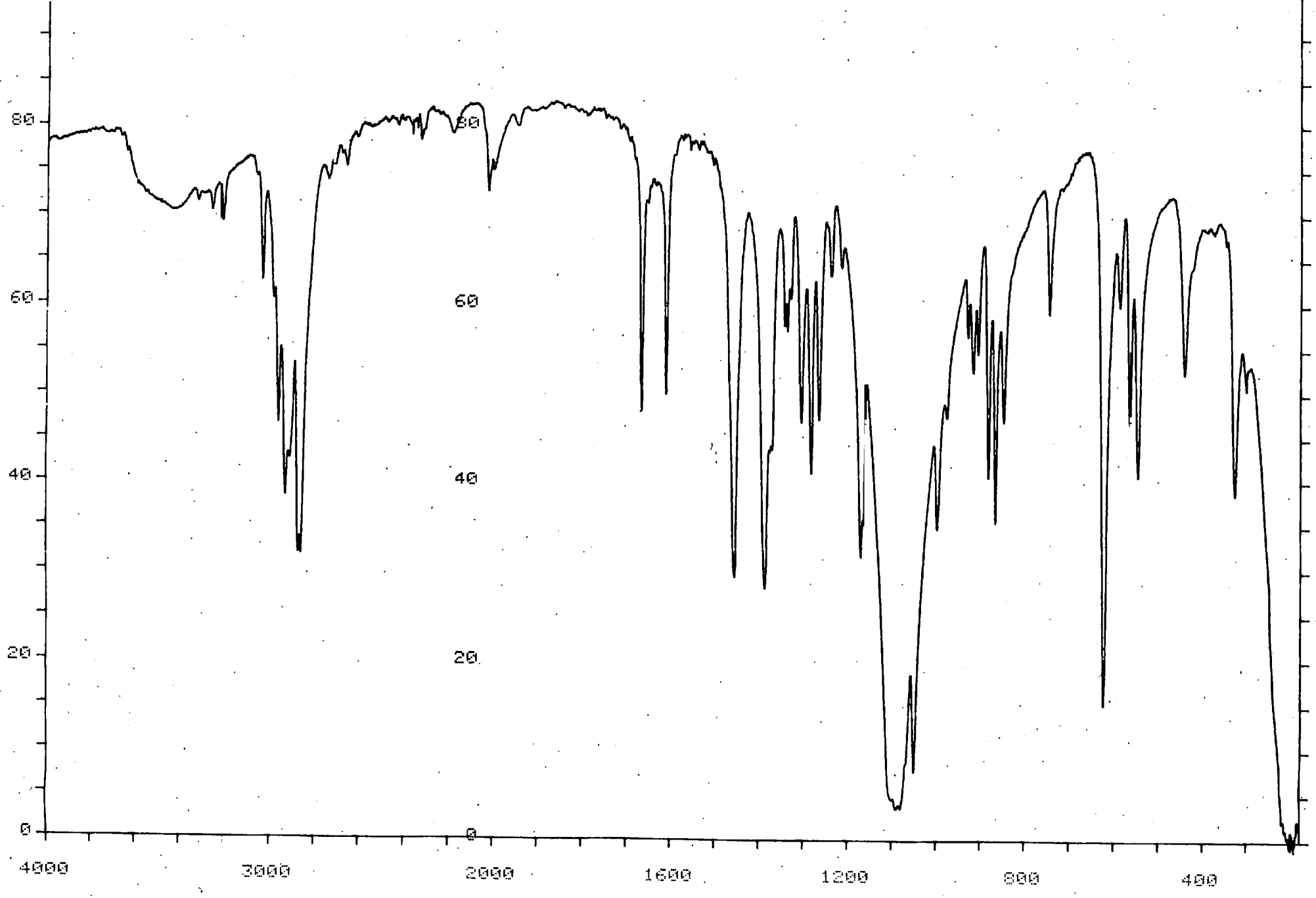

Figure 28 *The infrared spectrum of CoGT(ClO_4)*

approximate octahedral symmetry ($^3A_{2g} \rightarrow {}^3T_{1g}(F)$) is observed. Presumably the higher energy transitions expected are masked by the much stronger charge transfer absorption, which accounts for the intense orange colour of the complex.

The manganese GT cryptate (30) showed $[MnGT]^+$ at m/e 413 as the base peak in the fab mass spectrum. Peaks attributable to SrGT starting material were not present. The electronic spectrum of the MnGT complex showed a strong charge transfer absorption at 29,400cm^{-1} (ϵ = 930 dm^3mol^{-1}), as expected d-d bands were not observed. The formation of the Mn(II)GT cryptate on use of a Mn(III) salt as the source of manganese ion demonstrates the ability of the GT cryptand to stabilise the lower oxidation state. The tetraphenylborate counterion which was present during the reaction is likely to act as a mild reducing agent in the Mn(III)/Mn(II) reduction.

Despite the low ionic mobility of the tetraphenylborate counterion, the conductivity measurements for the Mn(II), Co(II) and Ni(II) cryptate tetraphenylborates fall in the range expected for 2 : 1 electrolytes. The perchlorate derivatives were also 2 : 1 electrolytes which is consistent with ionic ClO_4^- in solution.

The mononuclear cryptates show little dependence of magnetic moment on temperature, as expected. The manganese cryptate has a magnetic moment in the range expected for a high spin d^5 ion. Both the Ni(II) and Co(II) cryptates are high-spin. The relatively low magnetic moment measured for high-spin six co-ordinate cobalt(II) in the GT cryptate presumably results from the reduction in orbital contribution on deviation from regular octahedral geometry. Subsequent X-ray crystallographic confirmation was supplied by Dr. Vickie Mc Kee of the University of Canterbury, New Zealand.

THE CRYSTAL STRUCTURE OF $CoGT(ClO_4)_2$

The structure of the cation is shown in figure 29. The intimate twinning of the crystals prevented accurate determinations of bond lengths and angles, however the main features of the structure are clear. The cobalt ion is coordinated to the six imino donors of the cryptand and has D_3 symmetry. Only two of the six imino donors are crystallographically independent. The cobalt ion and the two bridgehead N atoms, which are not coordinated, lie on a crystallographic 3-fold axis. The Co-N (imine) distances of *ca.* 2.16Å are very similar to those in the analogous $[Co(sep)]^{2+}$ cryptate.[31] The X-ray structures of $[Co(sep)]^{2+}$ and $[Co(sep)]^{3+}$ are shown in figure 30.

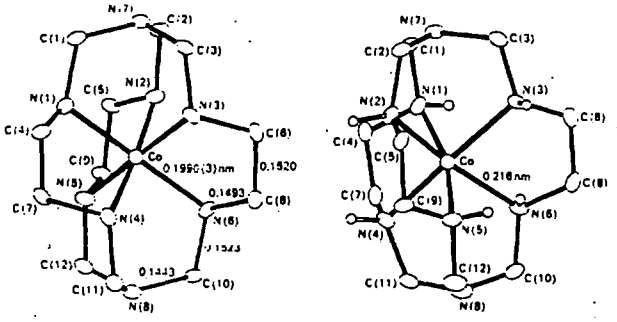

Figure 30 *The X-ray structures of $[Co(sep)]^{2+}$ and $[Co(sep)]^{3+}$*

In the X-ray structure of $[CoGT]^{2+}$, the amino N bridgehead atoms lie ≈ 3 Å from the metal ion within near-planar arrangement of adjacent methylene carbons, suggesting near sp^2 hybridization of tertiary amine nitrogens, as observed in $[Ni(sep)]^{2+}$.[204] The methylene caps of $[CoGT]^{2+}$ are staggered with a twist angle (ø) of 55°. The disorder observed mainly affects the diimino links and therefore only tentative conclusions are possible. The α-diimine links appear to be oblique rather than parallel. The perchlorate anions lie with one Cl-O bond along a threefold-axis and do not coordinate to the metal ion.

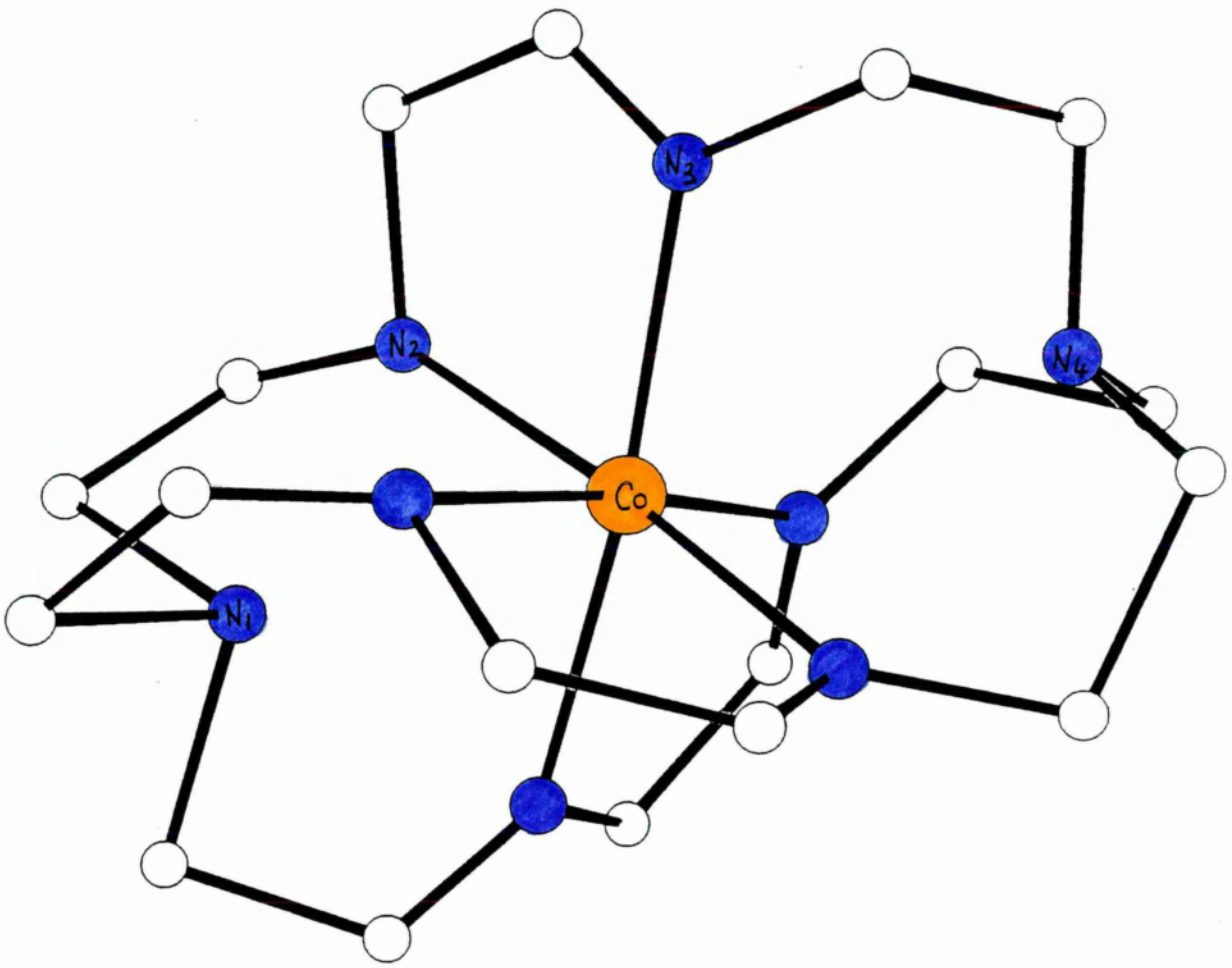

Figure 29 *The X-ray crystal structure of* $CoGT(ClO_4)_2$

Isomorphous powder patterns for $NiGT(BPh_4)_2$ (32) and $CoGT(BPh_4)_2$ (31) were obtained, however FeGT (33) and MnGT (30) are not isostructural with the nickel or cobalt cryptates or with each other. The degree of distortion from octahedral geometry may reflect the varying influence of LFSE effects in favouring trigonal anti-prismatic over the less strained trigonal prismatic geometry in the order Fe(II) low spin > Co(II) > Mn(II) high spin. Wentworth *et al.*[340] suggested that the tendency toward an octahedral rather than a trigonal prismatic geometry should decrease in the order d^6 low-spin > d^8 > d^7 > d^5 high-spin. However, the ionic radii of the metal ions also vary in the same order for Fe, Co and Ni (Fe(II) 0.83, Co(II) 0.82, Ni(II) 0.68, Mn(II) 0.91A). It is therefore difficult to separate LFSE effects from size effects. Since the Fe(II) cryptates are in the ^1A_g low spin state at ambient temperature, it is probable that distortion from octahedral geometry is not large for the Fe(II) cryptates.

COPPER GT CRYPTATES.

The CHN analysis figures for the monocopper GT cryptate suggest the presence of four waters of crystallisation. The mull infrared spectrum shows a broad and strong OH absorption. The δ(OH) bending vibration occurs at similar frequency to the ν(C=N) absorption and has the effect of broadening and intensifying the absorption in this region of the infrared spectrum. Fast atom bombardment mass spectroscopy showed a cluster at m/e 421 as the base peak. Presumably this is attributable to the $[CuGT]^+$ ion. A cluster around m/e 520 corresponds to $[CuGT(ClO_4]^+$ (40% of base peak), however a weak cluster at m/e 585 (10% of base peak) is probably due to the dicopper GT ion $[Cu_2GT(ClO_4]^+$. It is probable that there is some contamination of the monocopper GT cryptate with dicopper GT

cryptate. The presence of a small amount of the dicopper cryptate was confirmed by electronic spectroscopy. In addition to the CuGT absorption, a weak absorption which has been assigned to intervalence transfer in dicopper GT was observed. An intense band at this position is observed in the electronic spectrum of the dicopper cryptate.

TABLE 24 Infrared spectral data for copper GT cryptates /cm^{-1}

COMPLEX	COLOUR	νC=N	νBPh_4	νClO_4	νOH
39 $CuGT(ClO_4)_2:4H_2O$	green	1595(m)	-	1093(s) 622(m)	3439(br)
40 $Cu_2GT(ClO_4)_4:2H_2O$	green	1598(m)	-	1090(s) 623(m)	3427(br)
41 $Cu_2GT(BPh_4)_2$	bronze	1597(w)	1575(m) 1474(m) 1422(m) 734(s) 705(s)	-	3418(br)

The electronic spectrum of the monocopper GT cryptate (39) shows a single d-d band at 15,500cm^{-1} (ϵ = 120 l mol^{-1} cm^{-1}) and stronger charge transfer transitions at 24,300 (ϵ = 2150 l mol^{-1} cm^{-1} and 35,600 (ϵ = 2700 l mol^{-1} cm^{-1}). After approximately ½ hour in solution in acetonitrile, the colour of the copper GT solution had changed from green to yellow. The electronic spectrum of the yellow solution showed a reduction in intensity of the d-d band and a shift in position of the vmax for this absorption to *ca.* 15,400cm^{-1}. The reduction in intensity of the d-d band may indicate reduction of Cu(II) to Cu(I). The mononuclear copper(II) cryptate exhibits a four line esr spectrum which is consistent with interaction of the odd

electron with just one copper centre (I = 3/2). The spectrum is shown in figure 31 and is the normal axial-type four line spectrum. The spectrum shows g_{11} (≈ 2.28) > $g_{\perp}$ (≈ 2.07) and A_{11} 143 G, which indicates an extended tetragonal geometry for the Cu(II) coordination site.

DINUCLEAR COPPER GT CRYPTATES.

Initial attempts to obtain a copper(I) cryptate by transmetallation of $SrGT(BPh_4)_2$ using a copper(I) salt did not produce pure products. As a result of the low solubility of the copper(I) cryptate tetraphenylborate products precipitated too quickly and were too insoluble for recrystallisation. The products from these attempts did not give a fab mass spectrum, presumably as a result of the insolubility of the complex. Although acceptable CHN analysis was not obtained for the product, the elemental analysis (CHN) suggested that the product was a dicopper GT tetraphenylborate rather than a monocopper GT tetraphenylborate.

However, the formation of the dicopper(I) cryptate by transmetallation of $SrGT(BPh_4)_2$ using a copper (II) salt, as described in the experimental chapter, gave crystalline product which analysed as the dicopper(I) complex $Cu_2GT(BPh_4)_2$ (41). The tetraphenylborate counterion which was present during the reaction is known to be a mild reducing agent. The reduction of a copper (II) complex of a N_2S_2 Schiff-base ligand to the corresponding copper(I) complex by one equivalent of $NaBPh_4$ has been reported.[34] In addition a dicopper(I) complex of an N_6O_4 Schiff-base macrocycle has been prepared by BPh_4^- reduction.[102]

The formation of a dicopper(I) cryptate from Cu(II) starting material reflects the ease of reduction of copper (II) to copper (I) within the GT cryptand. The reaction mixture initially has the deep green colour

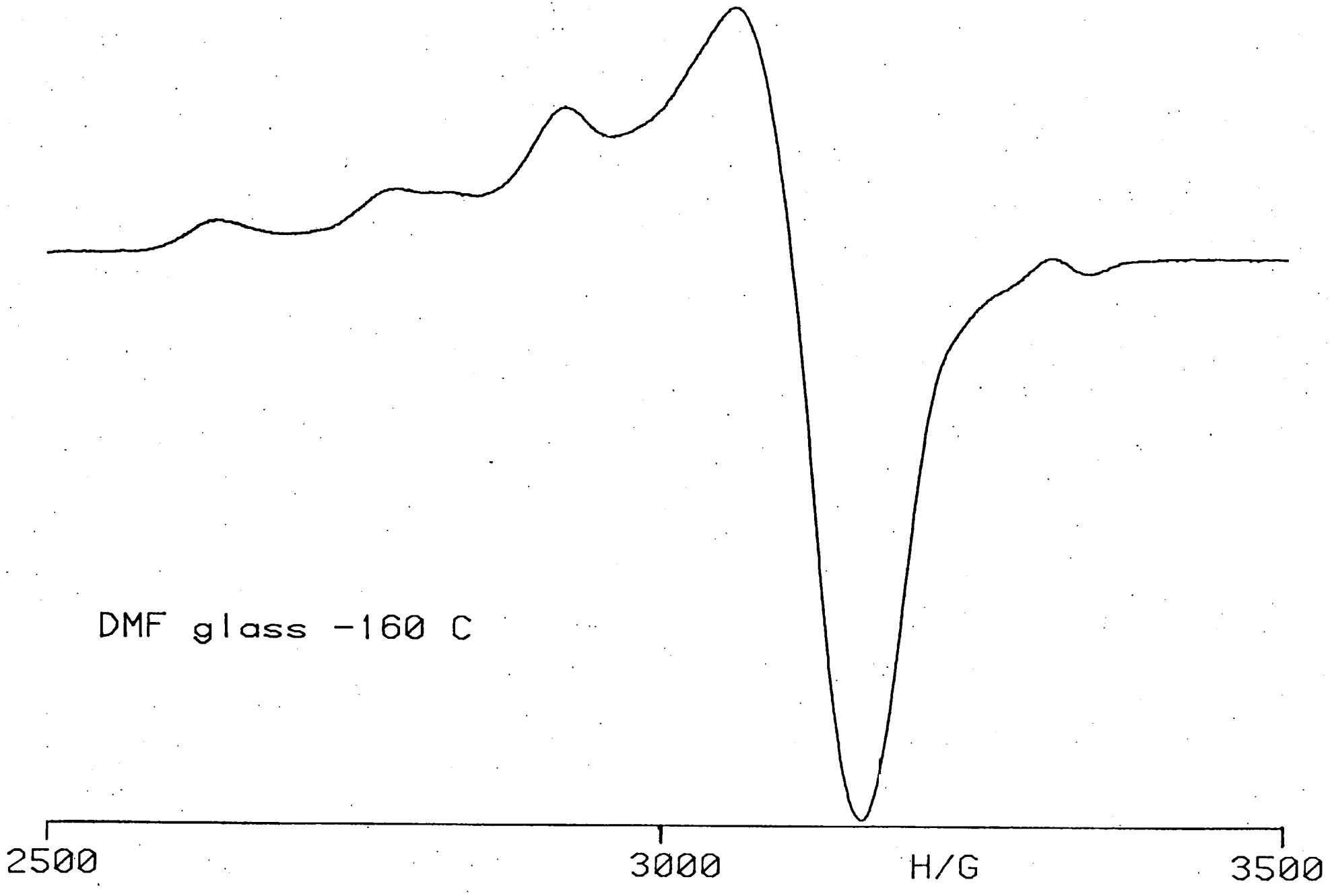

Figure 31 *The dmf glass esr spectrum of* $CuGT(ClO_4)_2{:}4H_2O$

associated with the copper(II) cryptate, and only gradually becomes yellow-brown on slow formation of the copper(I) cryptate tetraphenylborate. Attempted preparation of $Cu_2GT(ClO_4)_2$ via transmetallation of $SrGT(ClO_4)_2$ with the copper(I) complex $Cu(MeCN)_4(ClO_4)$ was not successful. The liking of Cu(I) for a tetrahedral binding site which can be found in each tren based subunit of the GT cryptand may favour access to the Cu(I) state. It is known that distortion of a Cu(II) binding site from tetragonal to pseudo-tetrahedral thermodynamically favours access to the copper(I) oxidation state. The solid state electronic spectrum of the dicopper (I) GT cryptate shows an intense broad absorption in the region 25,000 - 19,000cm^{-1} which is probably attributable to Cu(I) → imine charge transfer transitions.

The dinuclear copper cryptate $Cu_2GT(ClO_4)_4{:}2H_2O$ (40) was produced by reflux of $SrGT(ClO_4)_2$ with an excess of Cu(II) salt in acetonitrile as described in the experimental section. Elemental analysis (CHN) suggests the formulation $Cu_2GT(ClO_4)_4{:}2H_2O$ and the mull infrared spectrum indicates the presence of hydrogen bonded OH. The fab mass spectrum shows a strong cluster around m/e 585 which is attributable to $[Cu_2GT(ClO_4)]^+$ (95% height of the base peak). A cluster at m/e 484 (40% height of base peak) corresponds to $[Cu_2GT]^+$. The presence of a cluster at m/e 421 (40% height of base peak) is presumably due to $[CuGT]^+$, the monocopper fragment ion probably forms from the dicopper GT parent species and does not necessarily imply contamination of the dicopper cryptate with the monocopper cryptate.

The dmf glass e.s.r. spectrum of the complex is shown in figure 32 and displays a seven line pattern which is characteristic of a mixed valence Cu(II)/Cu(I) complex. The seven line spectrum is indicative of

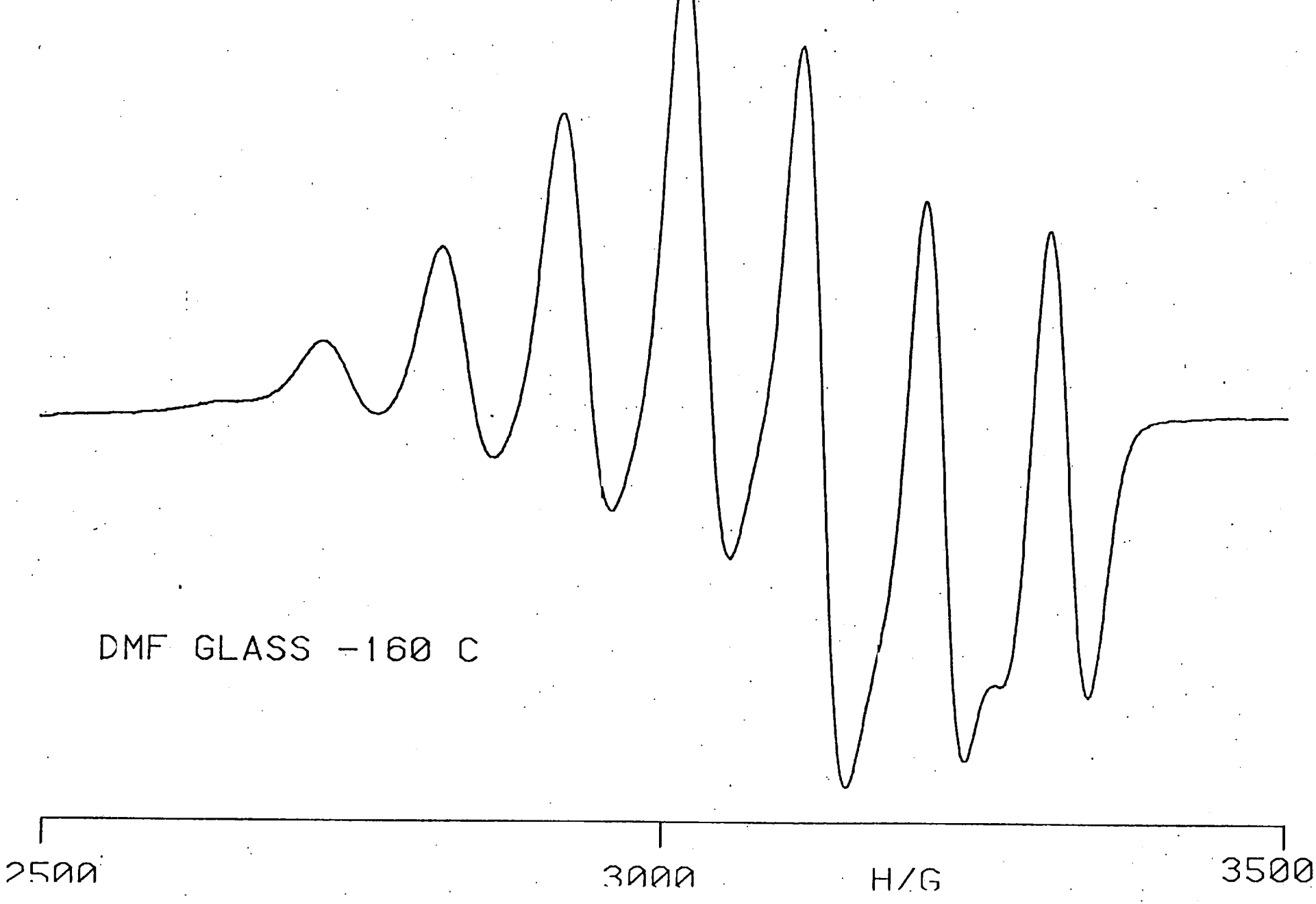

Figure 32 *The dmf glass esr spectrum of* $Cu_2GT(ClO_4)_4:4H_2O$

interaction of the odd electron with both copper centres (I = 3/2). The mixed valence species is valence detrapped down to 4K. The persistence of the seven line spectrum to such low temperatures indicates an unusual degree of valence delocalisation. The occurrence of seven-line esr spectra has been reported for mixed valence Cu(II)/Cu(I) complexes of phenoxo containing macrocycles shown in figure 33.[102] At reduced temperature the odd electron became localised and four line esr spectra resulted.

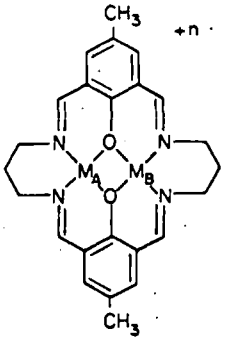

Figure 33 *Formation of a mixed valent Cu(II)/Cu(I) macrocyclic complex*

In the mixed valent complex shown above, the phenoxo bridges between the copper centres provide the pathway for delocalisation of the odd electron over the metal centres.[102,106] It is significant that seven-line esr spectra have only been obtained for the macrocyclic complexes that incorporate unsaturated nitrogen donors, saturation of the azomethine groups leads to four-line spectra.[106]

The seven-line spectrum observed for the dicopper GT complex may be due to direct metal-metal interaction between Cu(II) and Cu(I) if the metal ions are held within bonding distance within the cryptand. An intense near infrared band is observed in the electronic spectrum of the dicopper GT complex which we attribute to intervalence transfer (750nm ϵ = 5000 l $mol^{-1}cm^{-1}$). This decays rapidly in solution with a half-life of minutes in organic solvents and hours in water.

The solid state esr spectrum of the dicopper GT complex showed a seven line signal indicating that the complex is mixed-valence in the solid state. The CHN analysis figures however demonstrate the presence of four perchlorate counterions, therefore the Cu(II)/Cu(I) GT complex has to be protonated.

Copper was the only metal ion that was capable of forming dinuclear cryptates with the GT cryptand. The formation of a dinuclear cryptate of Cu(II) within GT may be a size effect. However crystal field stabilisation effects may also be involved. The Fe(II), Ni(II) and Co(II) ions may may strongly prefer the six-donor α-diimine binding site whereas the d^9 Cu(II) ion may be less destabilised by binding towards one end of the cryptand. The Cu(I) ion will like the tetrahedral site. The Mn(II) ion may be too large to form dinuclear cryptates with the GT cryptand.

The relatively facile unwrapping of the cryptand from Cu(II) to accommodate a second copper(II) ion suggested experiments in which $[CuGT]^{2+}$ is treated with a different transition metal ion with the aim of preparing hetrobinuclear complexes. The monocopper GT complex was refluxed with Ni(II), Zn(II) however only copper GT was obtained. Fab mass spectroscopy showed only clusters due to copper GT, there was no evidence of the presence of nickel or zinc.

ELECTROCHEMICAL STUDIES.

Appendix 1 outlines the electrochemical parameters which are used to interpret the results. Table 25 lists the results of cyclic voltammetry studies on the mononuclear transition metal complexes of GT. The cyclic voltammetry was performed by M. McCann of St. Patricks College, Maynooth. Figure 34 displays the cyclic voltammogram of $CoGT(BPh_4)_2$

Table 25 Electrochemical data for the GT cryptates

COMPLEX	E / mV					
	E½	ΔE	E½	ΔE	E½	ΔE
27 $CaGT(BPh_4)_2:2H_2O$	no electrochemical activity in this range					
30 $MnGT(BPh_4)_2:2H_2O$	+1350	irr	-987	76	-1276	76
31 $CoGT(BPh_4)_2:3H_2O$	+227	207	-847	87	-1402	87
32 $NiGT(BPh_4)_2:\frac{1}{2}H_2O$	+1166	irr	-1105	61	-1838	91
33 $FeGT(BPh_4)_2:2H_2O$	+714	irr	-962	61	-1332	77
35 $CuGT(ClO_4)_2:H_2O$	+740	irr	-815	61	-1371	77
38 $FeGT(ClO_4)_2:2H_2O$	+810	127	-983	61	-1349	61
39 $Cu_2GT(ClO_4)_4:2H_2O$	+1216	irr	+282	77	-1197	96

10^{-3}M in dmf, 0.1M Et_4NClO_4

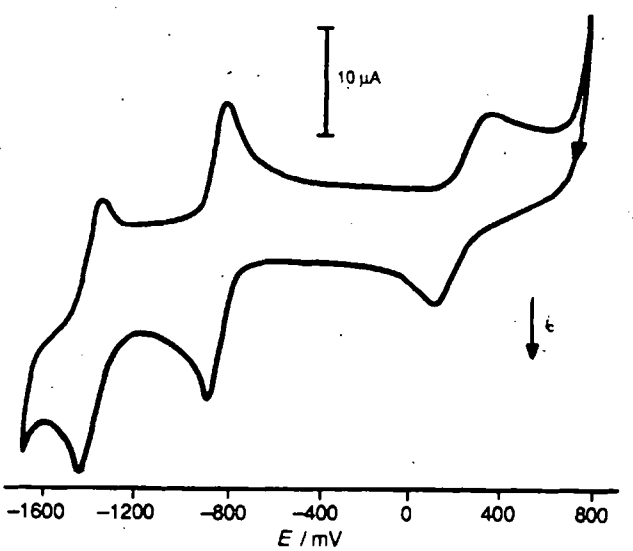

Figure 34 *The cyclic voltammogram of* $CoGT(BPh_4)_2$ *in dmf;*

scan rate 50mV/s vs Ag/AgCl

The ferrocene ferrocenium couple was used as a redox standard. This couple was observed at +0.362 *vs* Ag/AgCl and the peak to peak separation was 92mV. The difference in the anodic and cathodic peak potentials of the GT complex voltammograms exceeds the Nernstian requirement of 59mV for a reversible process, however by comparision with ferrocene which had a peak separation of 92mV the redox processes can be considered to be reversible or nearly so. An M(II) reversible reduction wave appears around -1.0V in the iron(II), nickel(II), cobalt(II) and manganese(II) cryptate cyclic voltammograms. The second reversible reduction process observed for the manganese, iron , cobalt and nickel cryptates may originate either in M(I) → M(0) reduction or a metal ion promoted M(I)L → M(I)L$^-$ ligand reduction. Esr experiments are required to distinguish between these alternatives. The calcium GT cryptate was found to be electroinactive, which suggests that the transition metal ion is involved to some extent in the redox processes observed for the transition metal cryptates.

Complexes of Co(III) with macrocyclic Schiff-base, dimethylglyoximato or vitamin B_{12} ligands exhibit two one-electron steps to produce Co(I) (d^8, square planar) complexes. Often no further reduction to cobalt metal is observed at accessible potentials. Limited electrochemical studies of the Co(II) α-diimine cryptate (structure 5, Chapter 1) were reported and electrochemistry comparable to that of $Co(bpy)_3$ (bpy = 2,2'-bipyridyl), which shows several reversible reductions, was observed. Unlike the electrochemistry found for complexes containing unsaturated ligands, the Co(II) sar and sep cryptates underwent a two-electron irreversible reduction at very negative potentials (< -2V), possibly involving cage rupture on generation of Co(I) and rapid reduction of the Co(I) transient to Co(0). The 3+/2+ couple for cobalt complexes of sar and sep is observed

at -200mV and -220mV respectively (vs SCE); which is approximately 470mV less positive than the analogous quasireversible couple in $CoGT(BPh_4)_2$ (adjusted to vs SCE for comparison) .

In contrast to Sargeson's hexamino cryptands, the hexaimino donor set of the GT cryptand stabilises low oxidation states of the metal ion. The enhanced stability of the Co(I) state in the GT cryptand is presumably a result of π back-donation of electron density from filled d-orbitals of Co(I) to empty π^* orbitals of the ligand.

The FeGT cryptate shows marked stabilisation of the Fe(I) state. Comparison of $E_{\frac{1}{2}}$ of Fe bipy and Fe terpy complexes with the $E_{\frac{1}{2}}$ of FeGT complexes demonstrates that the Fe(I) state is considerably stabilised within the GT cryptand. For bipy and 2,2': 6',2"-terpyridine (terpy) complexes of iron, the redox couples are as follows:

$Fe(bpy)_3^{2+} + e^- \quad Fe(bpy)_3^{+} \quad E_{\frac{1}{2}} = -1.34V$ *vs* SCE in CH_3CN

$Fe(bpy)_3^{+} + e^- \quad Fe(bpy)_3^{o} \quad E_{\frac{1}{2}} = -1.53V$

$Fe(terpy)_2^{2+} + e^- \quad Fe(terpy)_2^{+} \quad E_{\frac{1}{2}} = -1.25V$

$Fe(terpy)_2^{+} + e^- \quad Fe(terpy)_2^{o} \quad E_{\frac{1}{2}} = -1.42V$

$E_{\frac{1}{2}}\ FeGT^{2+/+} - E_{\frac{1}{2}}\ Fe(bpy)_3^{2+/+} = +0.38V$

More marked stabilisation of the Fe(I) state is found in the Fe catenate which was reported by Sauvage.[1ce-1e2]

$E_{\frac{1}{2}}\ Fe(cat)^{2+/+} - E_{\frac{1}{2}}\ Fe(bpy)_3^{2+/+} = +0.6V$

For the iron bpy and terpy complexes the redox orbitals involved are ligand localised, with the Fe catenate and the FeGT cryptate the redox process is likely to involve the metal centre as previously reported for other Fe(II)/Fe(I) couples. The metal-localised redox process $Fe(bpy)^{3+/2+}$

occurs at $E_{\frac{1}{2}}$ = + 1.012V whereas the redox process at + 0.810mV for FeGT may be due to $FeGT^{2+/3+}$. The Fe complex of the catenate could not be oxidised to the 3+ state at accessible potential.

The copper GT electrochemistry is difficult to interpret as a result of the reactivity of the complex. However, it seems that the product of decomposition which is probably dicopper(I)GT has reversible electrochemistry as discussed below.

The average of the potentials of the cathodic and the anodic peaks can be assumed as a good estimate of the formal electrode potential for the Cu(II)/Cu(I) couple and leads to a value of +282 mV *vs.* Ag/AgCl. The peak separation is 96mV which exceeds the Nernstian requirement of 59mV by 37 mV. and exceeds the peak separation found for ferrocene in the same experimental conditions by 4mV. It is likely that the quasireversibility of the process is largely due to the stereochemical changes accompanying the Cu(II)/Cu(I) redox process.[342,343] In addition, the anodic to cathodic peak currents are not equal and disproportionate loss of anodic current is observed. The reason for this is uncertain but may be due to a slow chemical reaction or rearrangement subsequent to electron transfer.

The second redox process observed may be due to a Cu(I)/Cu(O) redox change. If this is so the copper metal complex does not appear to undergo demetallation as there was no sign of a copper stripping reoxidation peak in the reverse scan of the cyclic voltammogram. The copper metal reoxidation usually occurs as a relatively sharp peak at *ca.* -0.3V *vs.* saturated calomel electrode. The Cu(I)/Cu(O) reduction has been observed in a series of N2S2 open chain ligands. The ligands stabilise the Cu(I) state and redox potentials ranging from +0.23 to +0.35 were observed. The Cu(I)/Cu(O) reduction occurred between -0.70 and -1.40 and rapid

demetallation resulted in an irreversible process, the characteristic stripping peak was observed in the reverse scan. The positive potential recorded for the 2+/1+ reduction is of interest as the potential lies in the range spanned by the type 1 sites of blue copper proteins (from +0.18 to +0.78V *vs* standard hydrogen electrode.)[345]

By contrast, the Cu(II) cryptate of Sargeson's amino substituted sar cage is irreversibly reduced to Cu(0) with full recovery of the cryptand.

The ease of reduction of the Cu (II) GT complex to Cu(I) suggests that the GT cryptand offers a coordination environment that favours tetrahedral geometry. The α-diimine groups of the GT cryptand are likely to contribute to the elevation of the Cu(II)/Cu(I) redox potential since they can exert effective withdrawal of electron density from the metal through the π system. Often positive redox potentials for the 2+/1+ Cu redox change are observed in systems incorporating 'soft' sulphur donor groups. Sulphur donor ligands are often oxidisable at the sulphur site and the redox instability of Cu(II)-thiolate bonding with respect to Cu(I) and disulphide is evident in a number of recent studies on copper(II) aliphatic thiolate complexes.[346]

LANTHANIDE ION GT COMPLEXES.

A series of lanthanide ion GT cryptates have been obtained by transmetallation of template GT tetraphenylborates. The barium GT cryptate was found to exchange the barium ion for the lanthanide ion on stirring in acetonitrile at temperature less than 50°C and crystalline product resulted on concentration of the filtrate to low volume. On stronger heating, only oils were obtained from the reaction mixture on reduction in volume. The strontium GT cryptate affords lanthanide ion cryptates on

transmetallation with lanthanide ion, however higher reaction temperatures are required to bring about the metal ion exchange. Product obtained from the SrGT transmetallation was less crystalline and did not analyse so well as that obtained from the barium GT starting material. Fab mass spectroscopy was required to verify that the metal exchange had occurred.

The differences observed on use of the different starting materials, BaGT and SrGT, may reflect their different stabilities. Strontium ion forms a more stable cryptate with GT than does the barium (II) ion. The barium exchange is also helped to proceed by the increased insolubility of the $Ba(NO_3)_2$ relative to $Sr(NO_3)_2$ in acetonitrile. It is possible that the differences may be due to differences in lability of the Ba and Sr cryptates, since increased temperature does cause exchange of strontium ion whereas unreacted SrGT is obtained at lower temperature.

Acetonitrile was the solvent of choice for the transmetallation reactions. Rare earth ions form quite stable solvates with polar solvents so that their complexes with neutral ligands are more readily isolated from from solvents with low to moderate donor strength, for example acetone or acetonitrile.[229] The fairly high solubility of the group 2 cryptate and the lanthanide nitrate in acetonitrile combined with the insolubility of the barium nitrate product of the exchange improves the likelihood of metal exchange.

The lanthanide ion cryptate is more soluble in acetonitrile than the group 2 metal cryptate and addition of ethanol and cooling was required to encourage crystallisation of the lanthanide cryptate at low volume. Crystals of lanthanide cryptate were only obtained at low volume by cooling on ice. Slow evaporation at room temperature did not give crystalline product, often oily material resulted.

The infrared spectra of the complexes show a medium intensity νC=N absorption at *ca.* 1610cm^{-1} and the absence of amine or carbonyl frequencies indicate that the cage ligand has remained intact on transmetallation. The imine absorption does not show the shift in position of *ca.* 10cm^{-1} that is observed on transmetallation with the transition metal ions. This suggests that the nature of the bonding of the imine to the lanthanide ion is similar to that found in the group (II) metal cryptates and relatively unlike the stronger coordinate type bond found in the transition metal cryptates. The combination tone at *ca.* 1650cm^{-1} is present in the spectra of the series of lanthanide cryptates.

Often the infrared spectrum shows the presence of nitrate counterion. The nitrate is likely to be coordinated to the metal ion. In principle ionic nitrate with D_{3h} symmetry, possesses three infrared-active modes at *ca* 1390cm^{-1} $\nu_3(A_1)$, 830cm^{-1} ν_2 and 720cm^{-1} ν_4. Upon coordination of the anion, the symmetry is lowered, and the ν_3 splits into two components at 1530-1480cm^{-1} and 1290-1250cm^{-1}. Six infrared absorptions should be observed,[220] ν_4 at 710, 740cm^{-1}, ν_2 at 820cm^{-1}, ν_1 at 1030cm^{-1}, ν_3 and ν_3 at 1500cm^{-1} and 1250cm^{-1}. The absorptions at ca. 1515cm^{-1} and *ca.* 1250cm^{-1} are clearly present in the infrared spectra of nitrate containing products, however the lower energy absorptions expected are masked by tetraphenylborate and GT absorptions. Although there was perchlorate present in the BaGT starting material this does not appear in the spectra of the lanthanide GT cryptate.

The n.m.r. spectra of the paramagnetic lanthanide cryptates showed strongly broadened and shifted signals, as expected for paramagnetic complexes.

TABLE 26 Infrared spectral data for lanthanide ion GT complexes.

COMPLEX	COLOUR	νC=N	νBPh$_4$	νNO$_3$	νOH
42 LaGT(BPh$_4$)$_2$(NO$_3$):H$_2$O	yellow	1605(m)	1577(m) 734(s) 706(s)	1520 1250	3439(br)
43 CeGT(BPh$_4$)$_2$(NO$_3$)	rust	1606(m)	1574(m) 734(s) 706(s)	1515 1249	3443(br)
44 PrGT(BPh$_4$)$_2$(NO$_3$)2H$_2$O	yellow	1607(m)	1575(m) 734(s) 706(s)	1516 1256	
45 EuGT(BPh$_4$)$_3$:4H$_2$O	yellow	1608(m)	1575(m) 733(s) 706(s)	-	
46 GdGT(BPh$_4$)$_2$(NO$_3$)	yellow	1607(m)	1575(m) 734(s) 705(s)	1518 1257	
47 TbGT(BPh$_4$)$_2$(NO$_3$):2H$_2$O	yellow	1606(m)	1575(m) 732(s) 705(s)	1516 1256	3437(br)

TABLE 27 Electronic spectral and magnetic data for $[LnGT]^{3+}$ complexes

COMPLEX	MAGNETIC DATA μ eff/BM 300K	65K	ELECTRONIC SPECTRAL DATA ν max/cm^{-1}	
42 $LaGT(BPh_4)_2(NO_3):2H_2O$	diamagnetic		25,700	CT
44 $PrGT(BPh_4)_2(NO_3):2H_2O$	3.58	2.82	25,600	CT
			23,809	f-f
			21,739	f-f
			20,833	f-f
			16,939	f-f
45 $EuGT(BPh_4)_3:4H_2O$	3.47	1.97	25,700	CT
46 $GdGT(BPh_4)_2(NO_3)$	8.49	8.32	25,700	CT
47 $TbGT(BPh_4)_2(NO_3):2H_2O$	9.73	9.58	25,700	CT
			20,534	f-f

CT = charge transfer

The formation of the lanthanide cryptates was confirmed by fab mass spectroscopy and magnetic measurements. Magnetic susceptibilities have been measured for the lanthanide complexes and the calculated paramagnetic moments, corrected for diamagnetic susceptibility contributions are displayed in table 27.

The fast atom bombardment mass spectrum of lanthanum GT cryptate shows clusters at m/e 496 (20%), 599 (5%) and 876 (10%) which are attributable to $[LaGT]^+$, $[LaGT(NO_3]^+$ and $LaGT(NO_3)(BPh_4)]^+$. However the starting material for the transmetallation was BaGT and the relative atomic masses of Ba and La are very similar, Ba = 137.33 and La = 138.91. the relative isotopic abundance of the isotopes of the two are quite different though, Ba has three isotopes 136(7.9%) , 137 (11.2%) and 138 (71.7%) whereas La

has two ; 138 (0.1%) and 139 (99.9%). The relative intensities of these are so different that probably only the more intense peak would be observed. The isotopic abundance pattern in the fab mass spectrum is similar to the pattern expected for LaGT. The NMR spectrum of a sample of LaGT shows three sets of resonances due to GT protons. The imine protons give rise to the signal at 8.01ppm, the methylene protons adjacent to the imine function give a triplet at 3.81 , the methylene protons next to the bridgehead nitrogens give the signal at 2.98ppm. The spectrum also shows strong resonances due to the tetraphenylborate counterion at 7.22m, 6.94t 6.75t , the tetraphenylborate signals integrate in the ratio 2:2:1. Signals due to coordinated ethanol appeared in the spectrum at 1.1t and 3.0q. Integration suggested the presence of three ethanol molecules per cryptate. The sample used for nmr was a different sample to that sent for CHN analysis and magnetic susceptibility measurements.

The formation of the gadolinium GT cryptate was verified by fab mass spectroscopy. Clusters due to $[GdGT]^+$ at m/e 515 (45%), $[GdGTNO_3]^+$ at m/e 577 (10%) and $[GdGT(BPh_4)]^+$ at m/e 835 (8%) were observed. Magnetic measurements and the presence of an esr spectrum for the complex provide further evidence that the Gd^{3+} ion is present. Magnetic measurements were taken in the range 300-80K and show a small decrease in magnetic moment from 8.49BM to 8.32BM. The esr spectrum of the complex was recorded as a dmf glass, a broad signal was observed.

Trivalent lanthanides have a $4f^n$ $5s^2$ $6p^6$ electronic configuration which results in weak crystal field and directional effects.[229,347,348] The forbidden *f-f* transitions are weak but with the exception of La^{3+}, Ce^{3+} and Yb^{3+} the trivalent lanthanides give line-like absorptions that resemble the lines of emission spectra more closely than the broad

absorptions of d-d type transitions. In the lanthanide GT series f-f transitions are superimposed on the much stronger charge transfer absorption at *ca.* 25,500cm^{-1}. Transitions (f-f) which occur on the tail of the charge transfer absorption are clearly visible, whereas transitions that appear to higher wavenumbers either form slight shoulders on the charge transfer absorption or are masked completely.

Fab mass spectroscopy of the europium GT cryptate shows a cluster at m/e 510 (40%) which is attributed to [EuGT]$^{+}$. The magnetic measurements for the complex verify that Eu^{3+} is present. The europium cryptate displays a large decrease in magnetic moment as the temperature is decreased, as expected. Eu^{3+} has a $^{7}F_{o}$ ground state and it's paramagnetism occurs as a result of population of low lying excited J states. The first second and third excited J states are sufficiently close to the ground state to be appreciably populated at room temperature. At reduced temperature a decrease in population of the excited states leads to marked reduction in the magnetic moment of the Eu^{3+} complex.

The europium cryptate was of particular interest in view of the possibility of luminescence from excited states of the cryptated europium ion. It was hoped that the GT cryptate might protect the europium ion from radiationless deactivation by solvent molecules, as reported for Lehn's europium cryptate.[240] Luminescence studies on the EuGT cryptate are underway, in collaboration with Prof. J. Kelly, Trinity College, Dublin.

In view of the cost of the europium salt and the low yield of europium cryptate obtained, attempts were made to improve the synthesis. It is known that lanthanide ions form insoluble lanthanide hydroxide precipitates in the presence of water, thus anhydrous conditions were employed in later preparations of the cryptate.

Gansow and Triplett have developed a synthesis of lanthanide polyether cryptates. Although the lanthanide cryptates of polyether cryptands are highly kinetically inert towards dissociation in aqueous solution, their formation constant is not large enough to allow their synthesis in such a polar solvent. The hydrated lanthanide salt solution in weakly coordinating organic solvent e.g. acetonitrile is treated with a dehydrating agent such as triethylorthoformate prior to complexation with an equimolar quantity of the cryptand. Crystallisation of the complex is induced by concentration of the solution and addition of a non-polar solvent.

A similar idea was applied to the synthesis of the EuGT complex. Dried solvents were used and 2,2-dimethoxypropane was added to scavenge water from the hydrated europium salt. Although the yield of cryptate was improved by use of anhydrous conditions and the presence of dehydrating agent, the yield was not dramatically increased. It is noticeable that the europium GT cryptate is the only member of the lanthanide cryptate series that can be obtained as tritetraphenylborate. All of the others retain some nitrate counterion.

It has been reported that the synthesis of 1:1 cryptates of lanthanide ions is usually easier when a good coordinating anion is provided, one that can coordinate to the metal ion through the strands of the cryptand. Nitrate is often chosen as the counterion due to its strong coordinating properties which make the complexes less sensitive to moisture and more readily crystallised. Perchlorate is also used and a bidentate perchlorate coordinates to europium through the strands of the 2:2:2 cryptand. However attempts to obtain a europium GT cryptate as a nitrate or a perchlorate failed. Initial attempts involved removal of tetaphenylborate anion from $EuGT(BPh_4)_3$ using silver perchlorate or silver

nitrate. The precipitate of silver tetraphenylborate was removed and the filtrate concentrated to low volume. Toluene was added to encourage crystallisation of the cryptate, however only oil resulted.

GROUP 1 CRYPTATES.

Cryptates of Na^+ and K^+ were obtained by transmetallation of barium GT using the group 1 metal sulphate. Sulphate was chosen as the counterion because barium sulphate, a product of the metal exchange, is practically insoluble in acetonitrile. The formation of barium sulphate should therefore assist in driving the metal exchange forward. The group 1 metal sulphate was dissolved in a minimum of hot water and added dropwise to barium GT in acetonitrile. A precipitate formed slowly and was filtered off after 2-3 hours. The infrared spectrum showed that this was a sulphate, presumably mainly barium sulphate. Transmetallation with Na^+ gave a mixture of pale yellow microcrystals and pale yellow powder at low volume. The infrared spectrum of the product showed that GT and the tetraphenylborate counterion was present. Fab mass spectroscopy verified that the sodium cryptate had been formed. The fab spectrum of $NaGT(BPh_4)$ showed a cluster at m/e 381 (15%) which is attributed to $[NaGT]^+$. A cluster at m/e 359 (25%) which is due to $[GT+H]^+$ was also observed. The fab spectrum showed no evidence of the presence of barium GT starting material.

Transmetallation of $BaGT(BPh_4)_2$ with K^+ gave pale yellow microcrystals which were surrounded by oil. The existence of the potassium cryptate was shown by fab mass spectroscopy. A strong cluster at m/e 397 (80%) due to $[KGT]^+$ was observed. In this case [GT+H] at m/e 359 was absent from the spectrum, as was evidence of the presence of barium GT

starting material. Acceptable CHN analysis was not obtained for this complex. Only oil resulted from attempted recrystallisation. The difficulty in isolating group 1 GT cryptates is not surprising in view of the 'hard' nature of the group 1 ions and the relatively soft nature of the α-diimine donor groups of the GT cryptand. The synthesis of sodium cryptates of macrobicyclic ligands containing bipiyridine and phenanthroline groups has been reported[26]. The sodium ion was found to be an effective template metal ion in the synthesis of the cryptand. The inclusive nature of the sodium cryptates was demonstrated by nmr.

ATTEMPTED REDUCTIVE DEMETALLATION OF GT COMPLEXES

A fairly large amount of time and effort was invested in attempted reduction of the GT cryptates. Various possible routes to the metal-free reduced GT ligand were investigated, including template of GT on Pb(II) followed by sodium borohydride reduction and synthesis of $PbGT(BPh_4)_2$ via transmetallation followed by sodium borohydride reduction. The lead GT complex $PbGT(BPh_4)_2$ was prepared by transmetallation of barium GT using lead nitrate. A precipitate was removed by filtration and infrared spectroscopy showed that this was a nitrate, probably barium nitrate. Fab mass spectroscopy showed clusters due to the lead GT cryptate, m/e 566 $[PbGT]^+$ (35%) and m/e 884 $[PbGT(BPh_4)]^+$ (8%)

The reduction attempts using lead GT starting material gave a black precipitate of lead metal on addition of $NaBH_4$, as expected, though the lead precipitate was solubilised again within minutes. Removal of the lead precipitate by filtration under vacuum was only partly successful. It appears that the reduced cryptand complexes lead avidly. The work-up procedure for the product of the borohydride reduction involves extraction

of the cryptand into chloroform, the metal complex does not dissolve in the chloroform layer and is lost in the work-up procedure.

As a result of the problems encountered in attempts to reductively demetallate PbGT, various metal ion cryptates were investigated as starting materials for the reduction. Attempted preparation of a silver cryptate for use in the reduction failed. Both attempts to synthesise a silver GT cryptate by template methods and transmetallation of the group (II) cryptates with Ag^+ were carried out. The manganese GT cryptate was used as starting material without success.

During the course of this work, the synthesis of the octaamino form of GT by traditional organic methods was published by Lehn and coworkers.[269]

ATTEMPTED SYNTHESIS OF A RUTHENIUM CRYPTATE

Fab mass spectroscopy showed that early attempts to transmetallate $SrGT(BPh_4)_2$ using $Ru(PC_6H_5)_3Cl_2$ failed. Cream crystals of unreacted starting material $SrGT(BPh_4)_2$ was obtained and the fab spectrum displayed $[SrGT]^+$ at m/e 446 as the base peak. A later attempt employing more vigorous conditions produced orange microcrystals. The infrared spectrum of the orange product indicated that the GT cryptand was present and intact. An imine absorption was observed at $1609cm^{-1}$ and amine and carbonyl frequencies were absent from the spectrum. Strong absorptions due to the tetraphenylborate counterion were observed in the infrared spectrum. The CHN analysis is not reliable as a means of determining if metal exchange has occurred as Ru and Sr have similar atomic mass. If the ruthenium ion remained Ru^{2+}, both RuGT and SrGT tetraphenylborates would give similar CHN analysis. Another possibility is that the ruthenium ion may oxidise to Ru(III). This need not affect the analysis to a great extent if the third anion was chloride.

The orange colour of the product was hopeful as the ruthenium cryptate of the large phenanthroline-based cryptand which was reported by de Cola was orange in colour.[214] The fab mass spectrum of the product showed no trace of $[RuGT]^+$. Despite the fact that the infrared spectrum clearly showed a complex of GT to be present, there was no evidence of $[SrGT]^+$ from the starting material or $[GT+H]^+$ in the spectrum.

ATTEMPTED SYNTHESIS OF CRYPTATES FROM ALIPHATIC DICARBONYLS

The success of the synthesis of GT from tren and glyoxal prompted attempts to extend the synthesis to reaction of other dicarbonyls with tren. The dicarbonyls pyruvic aldehyde, biacetyl and glutaraldehyde were used in attempted cryptate synthesis. Summaries of the synthesis attempts are presented in tabular form at the end of the experimental section. Pyruvic aldehyde and biacetyl contain one and two ketone groups respectively and it was expected that as a result these would be less reactive towards Schiff-base formation than a dialdehyde such as glyoxal. Early attempts concentrated on the use of more vigorous reaction conditions. Glutaraldehyde is a dialdehyde and should not cause problems in terms of reactivity. However the relatively long and flexible aliphatic chain of glutaraldehyde may make cryptand formation unfavourable in entropy terms. The aliphatic chain of glutaraldehyde is too long to give favourable five or six membered rings on coordination of imines around a metal ion. It may be more feasible to form binuclear complexes from reaction of tren with glutaraldehyde.

Two-three months was spent on the GT synthesis before marked progress was made, thus it is possible that these attempts are not totally hopeless. The infrared spectra showed some indications of imine formation and often the product did not appear to be polymeric.

CHAPTER 5

COMPLEXES OF 3Bp

There is interest in metal-ion complexes of small mono-nucleating cryptands because of their potential as redox reagents and their possible selectivity for metal-ions. Larger binucleating cryptands are of interest due to the possibility of coordination and activation of substrates between metal ions, or inclusion of small molecules or anions within the cryptand. The cryptand 3Bp is the largest of the series studied by us to date.

Tren, $N(CH_2CH_2NH_2)_3$, displays remarkable complexation properties towards transition metal cations.[249,250] The tren molecule is a convenient building block which permits a controlled arrangement of cations within a cryptand. The linkage of two tren subunits by reaction with three dicarbonyls provides Schiff-base cryptands which have potential for transition metal ion encapsulation. The internuclear separation of the metal ions can be controlled to some extent by choice of the bridging fragments.

The cryptand 3Bp contains para-substituted benzene in the bridging arms and is shown in figure 35.

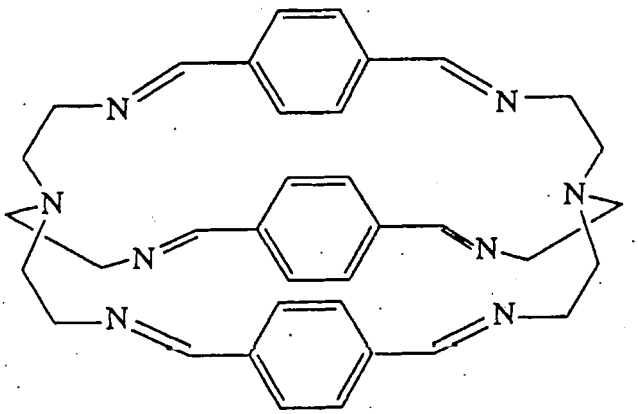

Figure 35 *The cryptand 3Bp*

Synthesis of the metal-free cryptand 3Bp and synthesis of the disilver and dilead cryptates by template methods was reported previously.[275]

The success of the synthesis of the 3Bp cryptand by a non-template method may reflect the rigidity of the dicarbonyl reactant and a possible internal hydrogen bonding template effect that tends to keep the amine in a suitable conformation for cryptand synthesis. The X-ray crystal structure of the metal-free cryptand has been determined[275] and is shown in figure 36. The X-ray structure shows that the cryptand adopts a divergent conformation and forms hydrogen bonds to six water molecules lying outside of the molecular cavity.

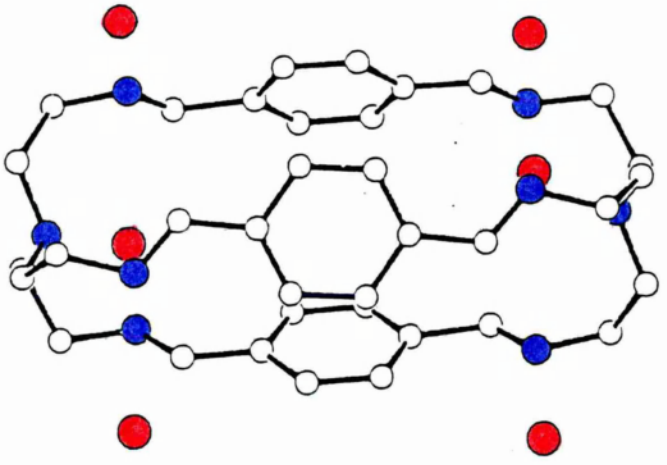

Figure 36 *The X-ray structure of 3Bp:6H₂O*

The water molecules are also hydrogen bonded to each other and link individual cryptands within the crystal.

Tasker has prepared a series of di-imine tetraaza macrocycles in metal-free form and has attributed the success of the synthesis to the formation of intramolecular hydrogen bonds in the product.[351] In this product the imine functions are in the trans trans conformation and this is the predominant conformation found in the reactant dialdehyde, thus a template ion is not required to hold this reactant in a suitable

conformation for reaction. Similarly, Fenton has noted that conformer distribution is related to whether a template ion is required for macrocyclisation.[352]

The work previously reported by D. Marrs has been extended here to the synthesis of transition metal ion cryptates of 3Bp. Both transmetallation of the templated disilver and dilead 3Bp complexes and metal ion insertion into the free 3Bp cryptand were investigated. The transition metal ion complexes of 3Bp and physical data for the complexes is listed in tables 28 and 29.

PHYSICAL DATA FOR TRANSITION METAL 3Bp COMPLEXES

TABLE 28 Infrared spectral data/cm^{-1}

COMPLEX	COLOUR	vC=N	vCF_3SO_3	vNCS	vOH
48 $Cu_2$3Bp$(CF_3SO_3)_2$	orange	1637ms 1620	1276 1222 1159 1026 635	-	-
49 $Cu_2$3Bp$(SCN)_2$:¼MeCN	yellow	1640ms 1625sh	-	2060 2048	-
50 $Co_2$3Bp$(NCS)_4$:$3H_2O$	blue	1642ms 1620br,sh	-	2066 2040sh	3400

Table 29 Magnetic, electronic spectral and conductivity data

COMPLEX	μ eff. /BM	Λ /S cm^2mol^{-1}	ELECTRONIC SPECTRAL DATA ν max /cm^{-1}	ϵ
48 $Cu_2$3Bp$(CF_3SO_3)_2$	diamagnetic	247	27500 35500	8000 70000
	300K 80K			
50 $Co_2$3Bp$(NCS)_4$:$3H_2O$	4.5 4.2	-	16050 7030	600 100

Many attempts were made to transmetallate dilead or disilver 3Bp complexes. Some of these attempts along with conditions employed, solvent and results are shown in table 2 in the experimental chapter. The only transition metal cryptate obtained by transmetallation was the dicobalt complex $Co_2$3Bp(NCS)$_4$. Fab mass spectroscopy verified that the product was a dicobalt complex of 3Bp, however acceptable CHN analysis was not obtained for the product formed by transmetallation.

Various strategies were used in attempted transmetallation. Anions were chosen so that insoluble silver or lead precipitates might form and improve the chances of metal exchange. Elevated temperatures were used in some cases to find if this would increase the rate of metal exchange, however this often led to ring opening which was apparent from the presence of amine and carbonyl frequencies in the infrared spectra of the products. Generally only anion exchange resulted when reactions were attempted at temperatures of around 55°C. It was noted that the thiocyanate anion was required for formation of the dicobalt cryptate, so this was used in some of the attempts with different transition metals to investigate if a good coordinating anion might stabilise cryptates of other transition metal ions. Despite the presence of thiocyanate, transmetallation attempts with metal ions apart from Co(II) were unsuccessful.

Metal insertion into the metal-free 3Bp ligand was more successful. Copper(I) and cobalt(II) formed binuclear cryptates of cryptand 3Bp. Attempted insertion of iron(II) or manganese(II) into the metal-free 3Bp cryptand gave protonated 3Bp. Attempted insertion of Ni(II), in the absence of thiocyanate, gave unreacted starting material or anion exchange

products. However a $[Ni_2 3Bp]^{4+}$ complex has since been obtained in the presence of thiocyanate ligand.

The dicobalt 3Bp complex $Co_2 3Bp(NCS)_4 : 3H_2O$ (50) was obtained by metal insertion into the metal-free 3Bp cryptand. The dicobalt complex (50) was insoluble in acetonitrile and precipitated out of solution on addition of a solution of cobalt thiocyanate to a solution of the starting material. Recrystallisation could only be achieved in low yield using a $DMA/Et_2O/MeOH$ solvent mixture. Fab mass spectroscopy verified that the dicobalt complex had formed. Fab mass spectroscopy showed clusters due to fragment ions containing $Co_2 3Bp$. A cluster at m/e 703 (50%) is due either to $[Co_2 3Bp]^+$ or to $[Co3Bp(NCS)]^+$ and another cluster observed at m/e 759 (55%) is assigned to either $[Co_2 3Bp(NCS)]^+$ or $[Co3Bp(NCS)_2]^+$. Cobalt and thiocyanate both have mass close to 58, therefore alternative assignments fit the peaks observed in the fab spectrum. The isotopic cluster pattern suggests the presence of two cobalt ions. There was no evidence of the presence of a $Co(NCS)_4$ counterion in the fab spectrum of the product.

The infrared spectrum of the dicobalt 3Bp complex (50) showed a strong ν(C=N) absorption at $1634cm^{-1}$ and absorptions attributable to amine or carbonyl functions were absent indicating that the 3Bp ligand had remained intact on metal insertion. A small shift in position of the ν(C=N), to *ca.* $10cm^{-1}$ lower than that of the 3Bp starting material, was observed on formation of the metal complex. A poorly resolved shoulder was observed on the low frequency side of the ν(C=N) absorption in the infrared spectrum of the cobalt complex which suggests either that not all of the imine nitrogens of the cryptand are coordinated to the cobalt ion or a low symmetry environment for the Co(II) ion. A strong thiocyanate

absorption was observed at 2066cm^{-1} in the infrared spectrum, suggesting N-terminal coordination of thiocyanate. The presence of a shoulder at *ca.* 2040cm^{-1} indicates that there are two different symmetry environments for the thiocyanate groups. The infrared spectrum of $HgCo(NCS)_4$ was taken to determine the position of the thiocyanate absorption for the cobalt tetrathiocyanate counterion and a strong absorption at 2095cm^{-1} was observed. Thus this observation provides further evidence that the cobalt tetrathiocyanate counterion is not present.

The electronic spectrum of complex (50) is typical of tetrahedrally coordinated Co(II), consisting of a fairly intense band at 16050cm^{-1} (ϵ = 600 l mol^{-1} cm^{-1}) and a less intense band at 7030cm^{-1} (100 l mol^{-1} cm^{-1}). The higher energy absorption is assigned to the transition $^4A_2 \rightarrow {}^4T_1$ (P) (in tetrahedral symmetry), while the lower energy band is assigned to the transition $^4A_2 \rightarrow {}^4T_1$ (F) The extinction coefficient, particularly of the higher energy band, is too high for octahedral coordination of the Co(II) ion and falls in the range expected for tetrahedral coordination.

Magnetic measurements for the complex provide further evidence of tetrahedral coordination of the Co(II) ion. A value for μ of 4.5BM per Co(II) ion at 300K was recorded. This value falls in the range expected for tetrahedrally coordinated Co(II) (4.2-4.8). The relatively low value of μ, for high-spin Co(II), suggests that there is little orbital contribution to the moment, as expected for tetrahedrally coordinated Co(II).

The thiocyanate ligand appears necessary to provide the tetrahedral binding site for Co(II) in the complex $Co_2$3Bp$(NCS)_4$:3H_2O. This factor combined with the observed splitting of the ν(C=N) absorption in the infrared spectrum suggests that the cobalt(II) ion may be coordinated by

two imine nitrogen donors of the cryptand and two N-terminal thiocyanate ligands in a tetrahedral arrangement.

Alternative counterions were used in an attempt to produce a more soluble dicobalt complex which might crystallise more slowly. On use of cobalt perchlorate, cobalt triflate or cobalt nitrate, only pale brown solutions resulted and brown oils were obtained at reduced volume. The brown colour of the solution suggests that the Co(II) ion is attempting to find six donors in solution. It appears that a small or linear coordinating anion is required to provide a suitable tetrahedral coordination site for the cobalt (II) ion within the 3Bp cryptand.

The potentially bridging anions, azide and cyanate, were investigated in an attempt to form $Co_2$3Bp complexes. Addition of an aqueous solution of azide to a pale brown solution of 3Bp and cobalt triflate, did not produce green colour. An oily rust-brown mixture was obtained on reduction in volume. Addition of NaN_3 as a solid to a solution of 3Bp produced green colouration, however the product obtained was impure. Addition of a solution of cyanate to a pale brown solution of 3Bp and cobalt triflate gave instant green colour however only a green oily mixture was obtained on reduction in volume.

Attempted insertion of Cu(II) into the metal-free cryptand 3Bp as described in the experimental section, gave a green solution from which orange crystals of the dicopper(I) complex $Cu_2$3Bp$(CF_3SO_3)_2$ were obtained on slow evaporation. The infrared spectrum of the dicopper(I) cryptate is shown in figure 37. A strong and split νC=N absorption was observed at *ca.* 1637cm^{-1} and absorptions attributable to amine or carbonyl functional groups were absent from the spectrum, indicating that the cryptand had remained intact on metal insertion. A shift in the frequency of the imine

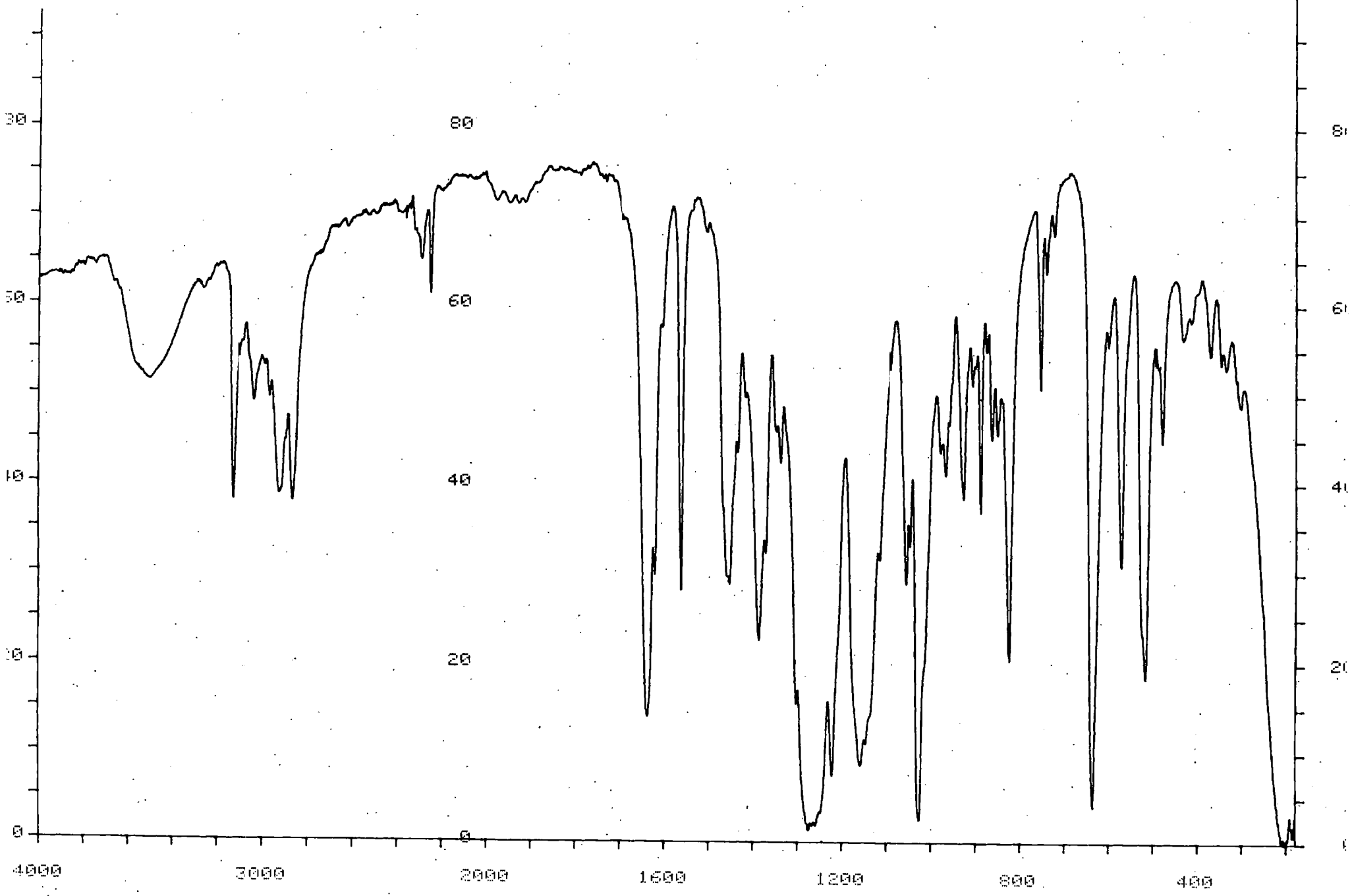

Figure 37 *The infrared spectrum of* $Cu_2 3Bp(CF_3SO_3)_2$

absorption was observed on coordination to the Cu(I) ion, from 1643cm^{-1} in the metal-free 3Bp cryptand to 1637cm^{-1} in the complexed cryptand. The splitting of the imine absorption suggests either a low symmetry binding site for Cu(I) or that not all of the six imines are involved in coordination of the Cu(I) ion.

The electronic spectrum of the complex shows a strong charge transfer absorption at 27,500cm^{-1} (ϵ = 8000 l mol^{-1} cm^{-1}) which accounts for the intense orange colour of the complex. This is presumably a Cu(I) → imine charge transfer transition. A stronger absorption was observed at 38,500cm^{-1} (ϵ = 70.000 l mol^{-1} cm^{-1}), which is possibly a π-π^* absorption of the ligand. The conductivity measurement for the complex in acetonitrile falls in the range expected for a 2 : 1 electrolyte which indicates that the triflate anions do not coordinate the metal ions of the complex in acetonitrile solution.

Crystals of suitable size and quality for X-ray structural analysis were obtained and the complex was found to be isomorphous with the disilver 3Bp complex $Ag_2$3Bp$(CF_3SO_3)_2$. The X-ray structure of the disilver 3Bp complex was solved previously[275] and is shown in figure 38.

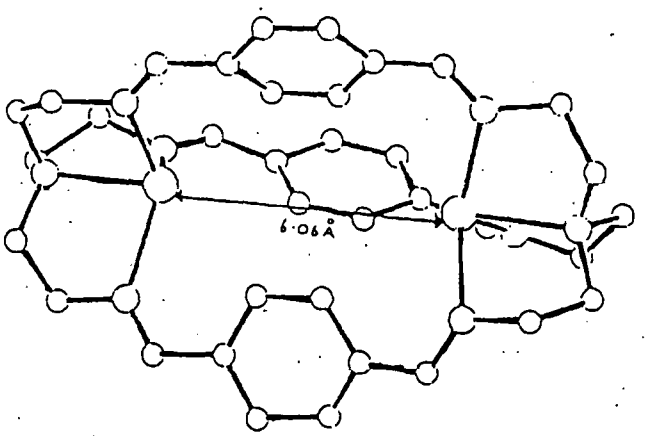

Figure 38 *The X-ray crystal structure of* Ag_2*3Bp*$(CF_3SO_3)_2$

In the metal ion cryptate the lone pairs point into the molecular cavity and coordinate to the metal ions which are bound inside the cryptand cavity. The imine nitrogens are in a mutually cis relationship in the metal complex. The bridgehead N-C bonds are eclipsed in the complex but are staggered in the free ligand. Each silver ion is four coordinate and is bonded to the bridgehead nitrogen and to three imine nitrogen donors of the tripodal tren based subunits located at either end of the cryptand. The silver ion lies outside the tetrahedron formed by the four nitrogens towards the centre of the cavity.

Complexation of the metal ion within 3Bp induces drastic conformational change in the cryptand. The X-ray structure of the metal-free 3Bp cryptand (figure 36) shows a divergent conformation with the imine nitrogens involved in hydrogen bonding to water molecules lying outside the molecular cavity. The imine nitrogens are trans to each other in the free ligand. On complexation, transformation to a convergent binding conformation is achieved(figure 38). In the metal-free and complexed forms of the 3Bp cryptand, the orientation of the benzene rings differ. The benzene rings of the silver complex are tilted so that hydrogen atoms on one side of each ring point towards the molecular cavity. Each silver ion has contacts with three hydrogens from the bridging benzene rings.

Lehn has reported a crystal structure of a dicopper(I) complex of a Schiff-base cryptand which is shown in figure 39.[23]

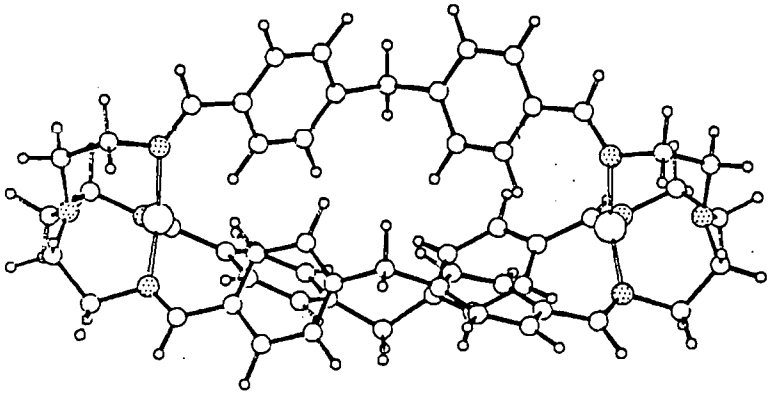

Figure 39 *The X-ray crystal structure of Lehn's dicopper(I) cryptate*

The crystal structure of Lehn's dicopper(I) cryptate showed that each copper(I) cation is tetracoordinate and lies 0.2Å outside the tren based subunit to which it is bound. In Lehn's cryptate too, hydrogen atoms of the benzene rings are directed towards the copper (I) ions (figure 39). It is unclear why the ν(C=N) is split in the dicopper(I) complex. The infrared spectrum of the complex $Ag_2$3Bp$(CF_3SO_3)_2$ whose crystal structure is shown in figure 38 exhibits a sharp and unsplit ν(C=N) absorption at 1639cm^{-1} in the infrared spectrum. It may be that the Cu(I) binding site is more irregular, perhaps the Cu(I)-N imine bond lengths are not equivalent. Crystallographically isomorphous complexes need not necessarily be precisely isostructural[174] and there may be slight differences in the coordination sphere of Cu(I) and Ag(I).

The dicopper(I) 3Bp complex (**48**) has been obtained by an alternative route involving metal ion insertion into 3Bp using $Cu(MeCN)_4CF_3SO_3$. The orange product obtained by this method was not so crystalline as that obtained by use of $Cu(CF_3SO_3)_2$. The strong green colour which formed on stirring 3Bp with a Cu(II) salt in acetonitrile suggested that a copper (II) complex formed initially and could possibly be obtained as a solid if isolated quickly. However rotary evaporation of the green solution gave

only yellow Cu(I) containing products. Attempts to precipitate a copper(II) 3Bp complex by mixing a solution of 3Bp in methylene chloride with a solution of $Cu(CF_3SO_3)_2$ in ethanol gave a pale green precipitate containing protonated 3Bp salt. It is probable that the 3Bp cryptand cannot provide a square-based coordination site which would stabilise Cu(II), whereas the tren-based subunits at either end of the 3Bp cryptand offer a coordination site which is acceptable to the Cu(I) ion. In addition the unsaturation of the cryptand will tend to stabilise the lower oxidation state further.

The complex $Cu_2$3Bp$(SCN)_2$ was prepared by metal insertion into 3Bp using $Cu(CF_3SO_3)_2$ and a solution containing an excess of sodium thiocyanate was added to the filtrate. This caused an instant colour change of the reaction mixture from green to a deep orange-red colour and product started to crystallise out on stirring. The infrared spectrum of the product shows νC=N at 1640cm^{-1} and absorptions attributable to amine or carbonyl are absent from the spectrum. The presence of a shoulder on the low frequency side of the imine absorption, at *ca.* 1625cm^{-1} suggests either a low symmetry environment or that not all of the imines are coordinated to the Cu(I) ions.

Infrared spectral evidence suggests that the thiocyanate anions are coordinated. A strong absorption at 2084cm^{-1} and a shoulder at 2060cm^{-1} indicate that the thiocyanates exist in two different environments. The ν(NCS) absorptions fall at the low frequency end of the range expected for S-bonding of the thiocyanate ligand. Coordination of the Cu(I) by S-bonded thiocyanate is expected in view of the soft nature of Cu(I). Each copper(I) ion may be coordinated by two imine nitrogens and a thiocyanate ligand.

Attempted insertion of Fe(II) or Mn(II) into the metal-free 3Bp cryptand gave protonated 3Bp. The pale cream colour of the product suggested that the metal ion had not been inserted into the cryptand yet the infrared spectra showed strong absorptions due to the counterion, suggesting that the cryptand had become protonated. Fab mass spectroscopy of the product obtained from the manganese insertion attempts showed a peak at m/e 587 as the base peak which could be attributed to 3Bp or protonated 3Bp. However, higher mass peaks that might have shown protonated ligand/anion combinations were not observed in the fab mass spectrum. The crystalline nature of the cream product obtained from the manganese insertion attempt combined with the very strong nitrate absorptions in the infrared spectrum suggest that this was a pure sample of protonated ligand nitrate, as opposed to a mixture of 3Bp and manganese nitrate.

In the 3Bp series, there appears to be competition between the formation of the metal complex and formation of the protonated ligand. Proton n.m.r. shows that there is a strong hydrogen bond in the protonated ligand complex. This is probably intramolecular.

Intramolecular hydrogen bonding within a small cryptand has been reported by Ciampolini *et al.*[29] The cryptand behaves as a very strong base in the first protonation step. The exceptionally high basicity for the amine led to the proposal of a structure for the monoprotonated cryptand in which two NH hydrogens are involved in hydrogen bonds with tertiary nitrogens within the cyclic framework. The proposed structure is shown in figure 40.

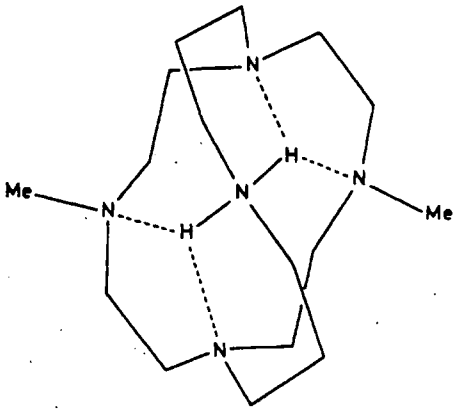

Figure 40 *The proposed structure of Ciampolini's protonated cryptand*

Alternatively, it may be that it is the small size of the coordination site in 3Bp that interferes with the ligand's ability to complex a wider range of transition metal ions. In the Co(II) and Ni(II) complexes the thiocyanate ligand was required to provide an acceptable coordination site. Copper(I) and silver(I) ions may be more willing to tolerate coordination on one face of the ion and close approach of the benzene hydrogen atoms to the other face. The unusual geometry of the coordination site occupied by silver or copper (I) in the 3Bp complexes may not be acceptable to more stereochemically demanding transition metal ions.

TRANSITION METAL ION COMPLEXES OF THE CRYPTAND R3Bp.

The cryptand R3Bp was obtained by reductive demetallation of $Pb_2$3Bp$(NCS)_4$ with sodium borohydride in ethanol, by modification of the method previously reported.[275]

The infrared spectrum of the reduced ligand R3Bp shows a strong absorption due to ν(N-H) stretching at 3231cm^{-1}. The strong sharp signal of the 3Bp parent imine at 1640cm^{-1} is absent. A broad and weak absorption at *ca.* 1620cm^{-1} which appears in the spectrum of the reduced

form, R3Bp, is attributed to δ(N-H) bending. The parent ion peak was observed in the mass spectrum at m/e 598 corresponding to $[3Bp + 12H]^{+}$, which is the octaamino derivative.

The metal-free R3Bp cryptand was used in complex formation with a range of transition metal ions. A series of binuclear transition metal ion cryptates was obtained and the infrared spectral data for the complexes is shown in tables 30 and 31.

PHYSICAL DATA FOR R3Bp COMPLEXES

Table 30 Infrared spectral data

	COMPLEX	COLOUR	νNH	νOH	νCF_3SO_3	νClO_4
51	Cu_2R3Bp$(CF_3SO_3)_2:H_2O$	cream	3253(s)	3450(w,br)	1256(s) 1157(s) 1028(s) 639(s)	-
52	Cu_2R3BpμOH$(ClO_4)_3$:MeCN:$3H_2O$	green	3297(m)	3583(m,sp)	-	1091(s) 1040(s) 623(m)
53	Co_2R3BpμOH$(ClO_4)_3:2H_2O$	green	3278(m) 3242(m)	3578(m,sp)	-	1092(s) 1075(s) 1017(m) 622(m)
54	Co_2R3BpμOH$(CF_3SO_3)_3$	green	3271(m) 3230(m)	3585(m,sp)	1272(s) 1258(s) 1028(s) 636(m)	-
55	[R3Bp+4H+]$(CF_3SO_3)_4$	colourless	3248(s,br)	-	1234(s) 1163(s) 1025(s) 639(m)	

Infrared spectra of the cryptates show a weak δ(N-H) at *ca* 1620cm^{-1}.
sp = sharp absorption

Table 31 Infrared spectral data

COMPLEX	COLOUR	ν NH	ν OH	νNO_3	νNCS
57 Ni_2R3Bp$(NO_3)_4$	turquoise	3202(m)	3450(br)	1479(s) 1445(s) 1322(s)	-
58 Co_2R3Bp$(NCS)_4$	petrol-blue	3235(m)	3400(br)	-	2067(s br)

The infrared spectra of the cryptates show a weak δ(N-H) at *ca.* 1620cm^{-1}.

Table 32 Magnetic, electronic spectral and conductivity data

COMPLEX	μ eff. 300K	μ eff. 80K	Λ	ELECTRONIC SPECTRAL DATA ν max	ϵ
50 Cu_2R3Bp$(CF_3SO_3)_2:H_2O$	diamag.	241		-	
52 Cu_2R3BpμOH$(ClO_4)_3$:MeCN:3H_2O	1.87	1.34	319	15400(sh) 11500	 213
53 Co_2R3BpμOH$(ClO_4)_3$:2H_2O	-	-	-	21200 15800	151 84
54 Co_2R3BpμOH$(CF_3SO_3)_3$	4.3	4.0	-	21200 15500	131 70

ν max in cm^{-1}
μ per transition metal ion in BM.
Λ in S cm^2 mol^{-1}

The infrared spectra of the metal complexes of R3Bp showed one or two fairly strong bands between 3200 and 3300cm^{-1} which are attributable to ν(N-H) vibrations. The dicobalt complexes exhibited two absorptions in the NH stretching region presumably symmetric and asymmetric stretching modes, whereas the copper complexes showed only one absorption due to

ν(NH) stretching. A weak band at *ca.* 1620cm^{-1} is assigned to the NH bending mode, the OH bending mode may also contribute to this absorption in complexes containing water of crystallisation. The infrared spectra of the complexes formulated as containing bridging OH^- (52), (53) and (54) exhibited a sharp ν(OH) absorption in the range 3550-3600cm^{-1}. The sharp nature of the absorption suggests that the hydroxo is not hydrogen bonded and is possibly protected within the cryptand cavity.

Various dicopper cryptates of R3Bp were synthesised. The dicopper(I) cryptate Cu_2R3Bp$(CF_3SO_3)_2$(51) analysed as the monohydrate. Both the analysis of the % copper in the product and the fast atom bombardment mass spectrum of the cream product verify that this is a copper cryptate and not just protonated R3Bp with triflate counterion. Figure 41 shows the infrared spectrum of complex (51). The fab mass spectrum showed a strong cluster around m/e 873 (90%) which is due to $[Cu_2$R3Bp$(CF_3SO_3)]^+$. Clusters due to other copper containing R3Bp ions were evident in the spectrum. The fab mass spectral data is listed in the experimental section. The conductivity measurement for the complex is typical of a 2 : 1 electrolyte and indicates that the triflate anions are not coordinated in solution in acetonitrile. The complex as a solid showed a slight tendency to surface oxidation and a solution of the complex showed a more marked green colour on exposure to air. This observation contrasts with that for the dicopper(I) 3Bp complexes which show no tendency to oxidise. Cyclic voltammetry was carried out on the dicopper(I) R3Bp complex, however the electrochemical processes observed were irreversible. A copper stripping peak was observed.

The conductivity measurement taken for the dicopper(II)μOH complex (51) falls in the range expected for 3 : 1 electrolytes, which suggests

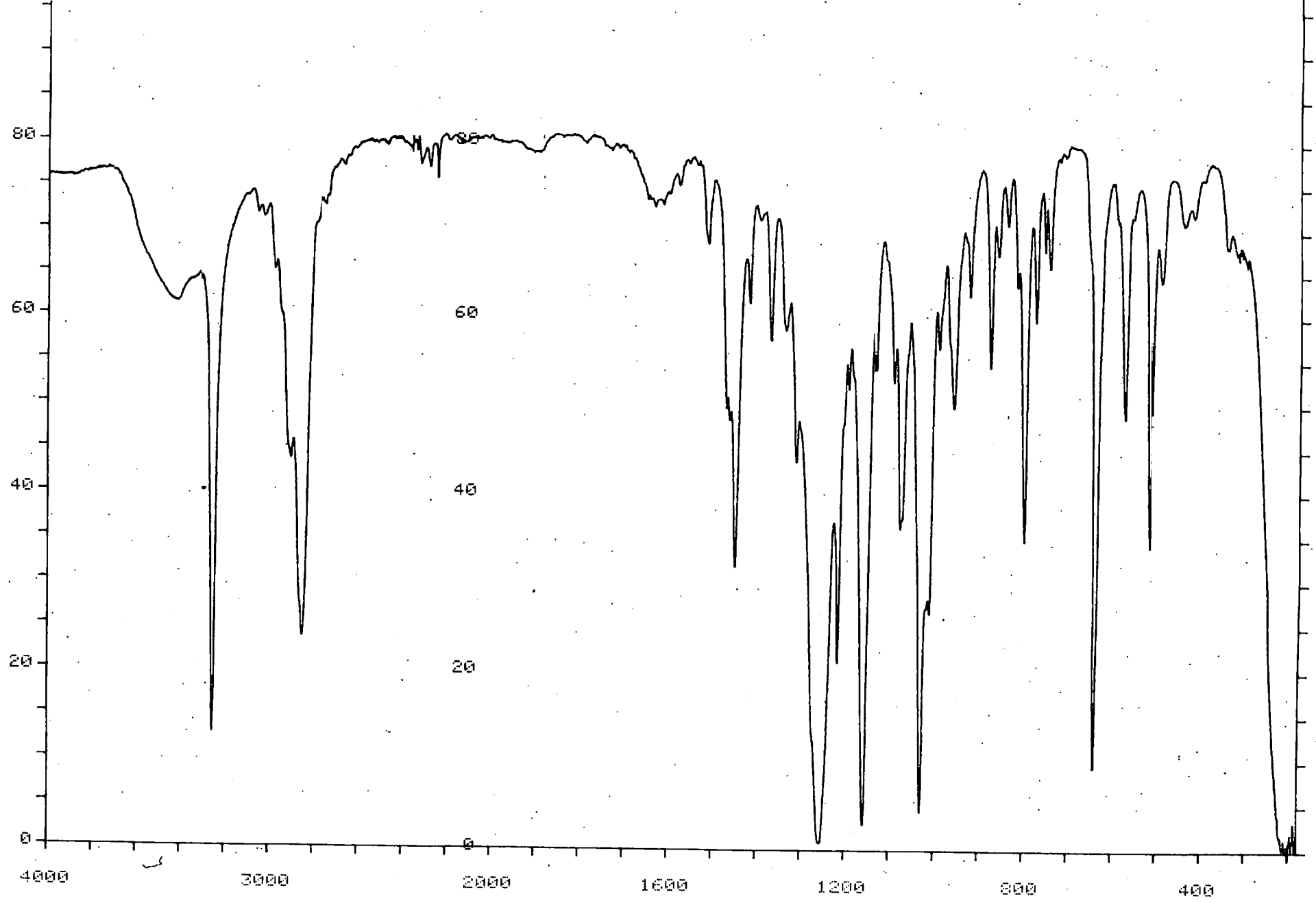

Figure 41 *The infrared spectrum of* $Cu_2R3Bp(CF_3SO_3)_2.H_2O$

that the hydroxo ligand remains coordinated to the metal ions in acetonitrile solution and the perchlorate anions are ionic. Variable temperature magnetic susceptibility measurements on the hydroxo-bridged dicopper complex showed a reduction in moment with temperature, indicating the presence of weak interaction between the copper(II) centres, presumably via the hydroxo bridge. The electronic spectrum shows a broad d-d band at *ca.* 11,500cm^{-1} which is consistent with tetragonal coordination. The presence of a slight shoulder at 15,400cm^{-1} may indicate some reduction in symmetry.

Lehn has reported the dicopper(II) cryptate of the bistren ligand (figure 18, Chapter 1) and it was observed that addition of water to a solution of the cryptate Cu_2Bistren$(ClO_4)_4$ in acetonitrile led to a strong decrease in the intensity of the esr signal.[96] This was attributed to strong antiferromagnetic coupling of the two Cu(II) ions via a hydroxo bridge. Martell found that the coordination of μ hydroxo group stabilised the binuclear cryptates of the bistren cryptate.[97] The binding of the hydroxo group was considerably greater than that of the chloride anion. It was suggested that this was an indication of much stronger coordinate bonding and perhaps more favourable steric factors for hydroxide binding. In addition, hydrogen bonding of the hydroxo hydrogen to an ether oxygen of the cryptand may further stabilise the hydroxo complex within the polyether cryptand.[97]

The infrared spectra of the dicobalt R3Bp complexes (53) and (54) show a sharp absorption at *ca.* 3585cm^{-1} which is attributed to the bridging hydroxo ligand. The fast atom bombardment mass spectrum of the complex (54) shows a strong cluster at m/e 1178 (90%) which is presumably due to $[Co_2$R3BpμOH$(CF_3SO_3)_3]^+$. The magnetic susceptibility measurements

indicate that the metal centres are weakly antiferromagnetically coupled. The electronic spectra of complexes (53) and (54) show two bands at 21,200cm^{-1} and *ca.* 15,600cm^{-1} and suggests that the cobalt ion isfive coordinate.[89,320]

The synthesis of a dicobalt R3Bp thiocyanate was attempted to discover if a bridging mode of thiocyanate could be accomodated between the cobalt ions. However the infrared spectrum of the product Co_2R3Bp(NCS)$_4$ indicated that the thiocyanate was N-terminal. It is possible that steric hindrance between the aromatic rings of the cryptand and the thiocyanate ligand prevents bridging. The thiocyanate absorption was strong and relatively broad and may indicate slightly different environments for the thiocyanate ligands.

Attempted insertion of Mn(II) into R3Bp initially produced a strong yellow coloured solution which suggested that Mn(II) had been inserted into the cryptand, but gradually the solution became brown and on reduction in volume a brown solid came out of solution. The infrared spectrum of the solid showed that it was inorganic and probably a Mn(III) hydroxide, with some triflate anion also present. On slow evaporation the colourless filtrate gave colourless crystals of protonated R3Bp triflate which were were of suitable quality and size for X-ray structural analysis.

The infrared spectrum of the crystals showed a broad absorption over the ν(N-H) region of the spectrum. The broadening of the N-H stretching band may be a result of hydrogen bonding as well as overlapping of the individual N-H stretching bands. Several individual N-H stretching bands were present on the high frequency side of the broad absorption. Hydrogen bonding weakens the N-H bond and results in a shift of the N-H stretching absorption to lower frequencies.[320] In addition, strong absorptions due to

the triflate anion were observed in the infrared spectrum. The CHN analysis of the product suggested the presence of four triflate anions to one cage molecule implying tetraprotonation of the R3Bp cage. This was later confirmed by X-ray structural analysis.

THE CRYSTAL STRUCTURE OF [R3Bp + $4H^+$] $(CF_3SO_3)_4$

The X-ray crystal structure of [R3Bp+$4H^+$] $(CF_3SO_3)_4$ is displayed in figure 42. The structure shows that there are four triflate anions to one cation, the tetraprotonated R3Bp ion. The bridgehead nitrogens are not protonated and the lone pair points into the molecular cavity. Two of the six secondary nitrogen atoms have hydrogen atoms which are hydrogen bonded to triflate anions. Two other secondary nitrogen atoms have each got two hydrogens which are hydrogen bonded to an oxygen atom of a triflate and to the remaining two nitrogen atoms of the cryptand. There is one intramolecular hydrogen bond at each end and one external hydrogen bond to a triflate anion. The cation has twofold symmetry.

Protonation of the R3Bp ligand was expected to occur on the secondary nitrogen sites of the bridges. Tren itself forms a triprotonated species $N(CH_2CH_2NH_3^+)_3$ [155] and the crystal structure of the tren trichloride complex has been determined. Equilibrium constants for the reaction of tren with HCl have been determined. At 20°C $\log K^1$ for the first protonation step was 10.15, $\log K^2$ was 9.26 and $\log K^3$ was 7.96, which is in accordance with expectations since the attraction for succeeding protons is decreased by electrostatic repulsion of those already bonded to the molecule. The basicity of the tertiary tren nitrogen is much lower than that of the primary amines.

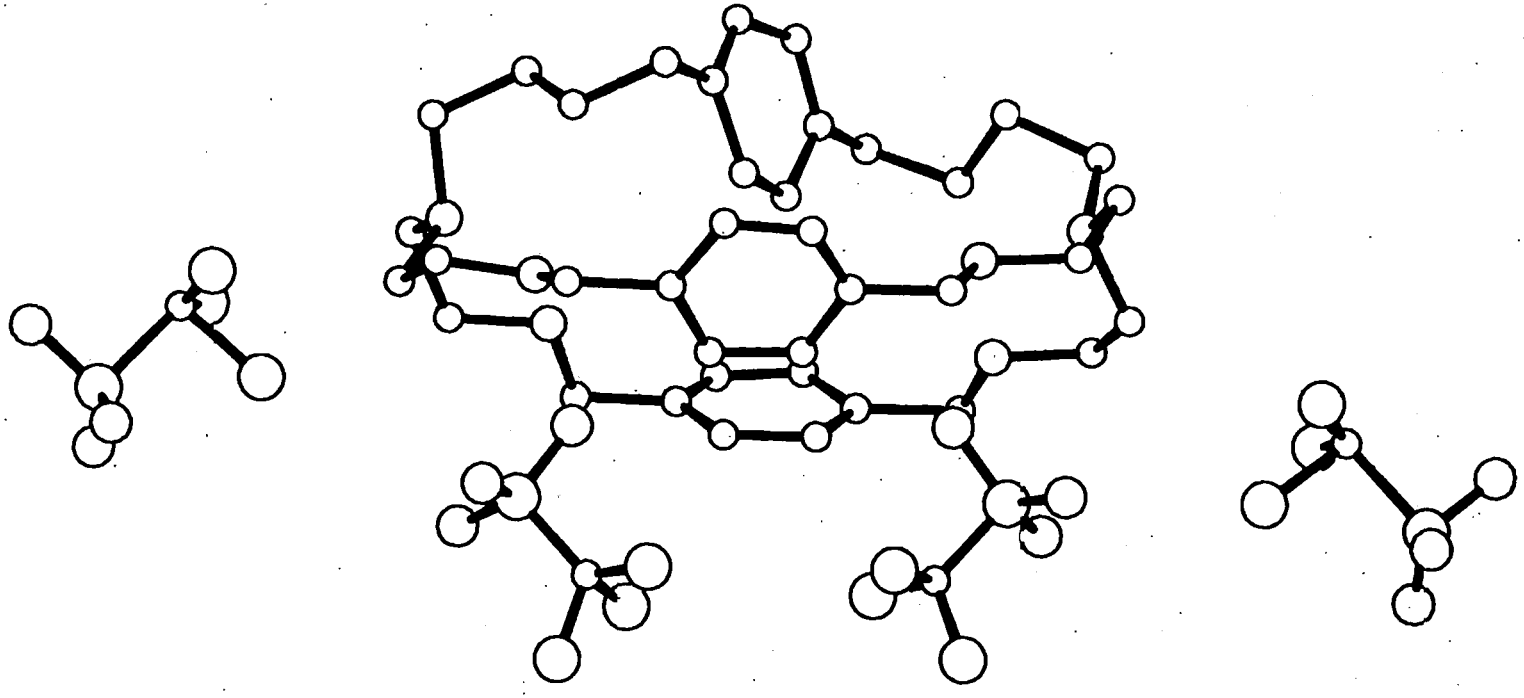

Figure 42 *The X-ray crystal structure of [R3Bp +4H^{+}](CF$_3$SO$_3$)$_4$*

Similarly the hexaprotonated bis-tren cryptand is protonated at the six secondary nitrogen sites and the bridgehead nitrogens are much more difficult to protonate. Lehn's fluoride anion sequestering cryptand (structure 104, Chapter 1) makes use of protonation of the secondary nitrogen sites to retain fluoride within the cryptand.[269] The bridgehead nitrogens were not protonated.

We hope to be able to accomodate anions within the protonated R3Bp ligand. The reduced cryptand R3Bp was found to form a wider range of metal-ion complexes than the hexaimine cryptand 3Bp. The presence of the imine groups adjacent to the aromatic rings in 3Bp leads to a more rigid macrobicyclic framework and accompanying steric constraint. The increased flexibility of the reduced cryptand, relative to the hexaimine, enables the cryptand to provide a wider range of coordination geometries.

COMPLEXES OF LIGAND 3Bm

Ligand 3Bm was synthesised by 2+3 Schiff-base condensation of tren with isophthalaldehyde in methanol. The infrared spectrum of the white crystalline product showed a strong imine absorption at 1643cm^{-1} and frequencies attributable to amine or carbonyl were absent from the spectrum indicating that Schiff-base condensation was complete.

The X-ray crystal structure of the 3Bm ligand has been determined previously and is shown in figure 43.[275]

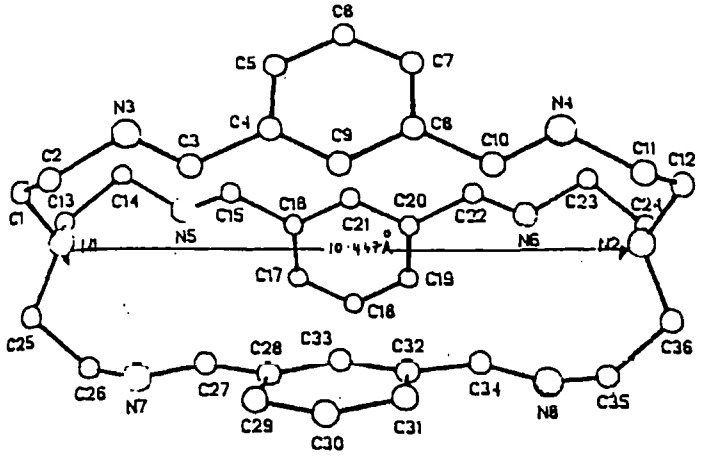

Figure 43 *The X-ray crystal structure of the 3Bm ligand*

The bridgehead N-C bonds are eclipsed as the view of the structure along the bridgehead N,N axis demonstrates. In this conformation there is little free space inside the molecule and the nitrogen donor atoms are divergent. However the 3Bm cryptand can adopt other conformations and complex formation with Cu(I), Cu(II) and Ag(I) has been described.[275] Thus in the presence of a suitable metal ion it is energetically favourable for the cryptand to adopt the convergent conformation which is required to form metal ion cryptates.

Cryptate formation from 3Bm and other transition metal ions was not previously investigated.

Attempted insertion of Ni(II) into the 3Bm cryptand gave purple microcrystalline solid. On addition of a solution of nickel nitrate in acetonitrile to a solution of 3Bm in ethanol a deep green coloured solution results which gradually becomes blue. Purple microcrystals were obtained on reduction in volume. The infrared spectrum of the purple product showed strong absorptions at *ca.* 3360cm^{-1} due to the presence of amine. In addition to the imine absorption at 1630cm^{-1}. A relatively weak peak at 1720cm^{-1} was observed and was attributed to the presence of the carbonyl function. The fab mass spectrum verified that ring opening of the 3Bm cryptand had occurred and displayed strong peaks due to the dinickel complex of the diamino pendant arm macrocycle, 2Bm, which is showm in figure 44.

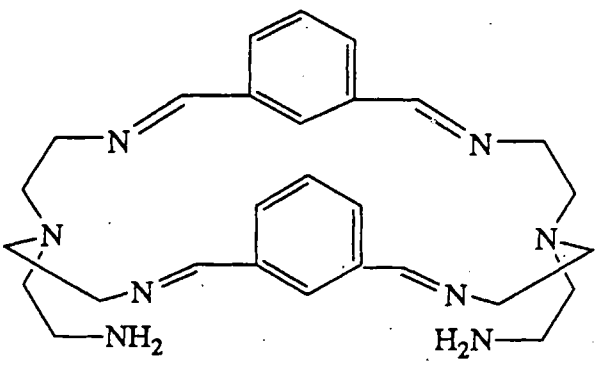

Figure 44 *The pendant arm macrocycle 2Bm*

Clusters due to [$Ni_2$2Bm$(NO_3)_3$]+ at m/e 790 (70%) and [$Ni_2$2Bm$(NO_3)_2$]+ at m/e 845 (5%) were observed in the fab spectrum. In addition a weak cluster due to a complex of 3Bm which had opened at one imine function was present [Ni_2L$(NO_3)_3$]+ at m/e 908 (15%). The colour change which occurred during the reaction may signify a change in coordination geometry about

the Ni(II) ion on ring opening of the cryptand. It is probable that 3Bm cannot fulfill the stereochemical requirements of the Ni(II) ion and the cryptand undergoes ring opening as a consequence. Perhaps strain generated on trying to provide a suitable coordination sphere for Ni(II) activates the ligand towards hydrolysis. Ligand rearrangement is often observed in cases where a ligand cannot provide an acceptable coordination geometry to a metal ion.[50,85] Attempted metal ion insertion into 3Bm using Fe(II) and Mn(II) were not successful and led to protonation of the cryptand.

The 3Bm ligand has been reduced to the octaamino form by reflux with sodium borohydride in ethanol. A prolonged reflux with an excess of borohydride, followed by stirring for 48hrs at room temperature. The infared spectrum of the product showed a strong N-H stretching absorption at 3298cm^{-1} and the absence of the strong and sharp ν(C=N) absorption of the parent imine 3Bm. However a broad and weak absorption around 1630cm^{-1} which is mainly attributed to δ(N-H) may mask the presence of residual ν(C=N) absorption. Mass spectroscopy was used to characterise the product and showed that the 3Bm ligand was difficult to reduce thoroughly. Although the base peak was m/e 598 [3Bm+12H]+ , weak peaks were also observed at m/e 597 and 595.

The product from the reduction was used in transition metal ion complex formation. Binuclear complexes of Co(II), Ni(II) and Cu(II) were obtained.

PHYSICAL DATA FOR R3Bm COMPLEXES

Table 34 Infrared spectral data

COMPLEX	COLOUR	νNH	νClO_4	νNO_3	νOH
59 Cu_2R3Bm$(ClO_4)_4$:$2H_2O$	green	3258(s)	1098(s) 622	-	3514(br)
60 Ni_2R3Bm$(NO_3)_4$:$4H_2O$	turquoise	3268(s) 3212(s)	-	1449(br)	3414(br)
61 Co_2R3Bm$(ClO_4)_4$:EtOH	green	3246(s)	1094(s) 622	-	3587(br)
62 [R3Bm +2H+]$(NO_3)_2$	colourless	3020(s)	-	1353(br)	3442(br)

The infrared spectra of the R3Bm complexes showed a broad δ(N-H) absorption at *ca.*1630cm^{-1}.

The fab mass spectrum of the dinickel complex Ni_2R3Bm$(NO_3)_4$: $4H_2O$ showed peaks due to nickel complexes of R3Bm. Clusters were observed at m/e 901 (60%) which was attributed to [Ni_2R3Bm $(NO_3)_3$]$^+$, successive loss of nitrate produced the peaks at m/e 838, 775 and 654. The infrared spectrum of the dinickel product showed two sharp ν(N-H) absorptions at 3268 and 3212cm^{-1} which may be due to symmetric and asymmetric (N-H) stretching modes. A broad and strong ν(O-H) stretch was observed at 3514cm^{-1} which supports the presence of $4H_2O$ as suggested by the analytical figures. A broad absorption at *ca.* 1630cm^{-1} in the infrared spectrum was attributed to δ(N-H) combined with δ(O-H) bending. The electronic spectrum of the complex in solution showed three bands at 28,000cm^{-1} (ϵ = 52 l mol^{-1}cm^{-1}), 17,100 (ϵ = 28 l mol^{-1}cm^{-1}), 10,600cm^{-1} (49 l mol^{-1}cm^{-1} as expected for Ni(II) in octahedral symmetry. The bands are assigned to the transitions $^3A_{2g} \rightarrow {}^3T_{1g}$(P) , $^3A_{2g} \rightarrow {}^3T_{1g}$ (F), and $^3A_{2g} \rightarrow {}^3T_{2g}$ respectively. The relatively low intensity of the bands provide further

evidence of octahedral coordination. The mull electronic spectrum shows absorption bands in similar positions to the solution spectrum (28,000sh, 16,800 w, 10,200cm^{-1} w,) suggesting that coordination geometry in the solid state is similar to that in solution. The Ni(II) ion may achieve octahedral geometry by coordination of the four tren based donors and two water molecules. It is interesting that the Ni(II) ion can be accomodated within the R3Bm ligand whereas ring opening was observed in attempted insertion into 3Bm. Presumably the increased flexibility of the R3Bp ligand permits accomodation of the Ni(II) ion.

The infrared spectrum of the dicopper (II) cryptate Cu_2R3Bm$(ClO_4)_4$ shows a sharp ν(N-H) absorption at 3258cm^{-1} and a broad δ (N-H) absorption at 1632cm^{-1}. The absorptions due to the perchlorate counterion were typical of ionic perchlorate, ν_3 and ν_4 were unsplit and were observed at 1098 and 622cm^{-1}. The electronic spectrum of this complex displays a broad d-d band at 10,900cm^{-1} (ϵ = 230 l mol^{-1} cm^{-1}), a slight shoulder at 14,300cm^{-1} was observed in addition to a stronger charge transfer transition at 33,900cm^{-1}, ϵ = 7900. The electronic spectrum is consistent with a tetragonal coordination. The presence of a shoulder on the high energy side of the d-d band maximum may indicate some reduction in symmetry.

Surprisingly, and in contrast to the behaviour of R3Bp with Cu(I), attempted insertion of Cu(I) into the R3Bm cryptand gave oxidised Cu(II) containing products despite the use of dry and deoxygenated solvents and nitrogen protection from the atmosphere.

The infrared spectrum of complex Co_2R3Bm$(ClO_4)_2$:EtOH (61)showed a sharp ν(N-H) absorption at 3246cm^{-1}. The absorptions due to the perchlorate counterion were observed at 1098 and 622cm^{-1} and are typical

of ν_3 and ν_4 of ionic perchlorate, respectively. A broad absorption at 1625cm^{-1} may be attributed to δ(N-H) bending, but may also include contributions from imine functions in the product. The fab mass spectrum displayed several clusters. A cluster at m/e 656 (35%) is attributed to $[Co_2R3Bm]^{+}$ and m/e 813 (75%) to $[CoR3Bm(ClO_4)]^{+}$ however peaks due to complexes of partially reduced 3Bm (ie 3Bm + xH) ligand were also observed. A strong cluster at m/e 1003 (95%) corresponds to $[Co_2R3Bm-7H(ClO_4)_3]^{+}$ which suggests that there are imine functions remaining in the ligand. A less intense peak corresponding to $[Co_2R3Bm-4H]^{+}$ m/e (35%) was also observed. The complex analysed correctly for the proposed structure however the presence of some of the partially reduced complex is not likely to affect the CHN analysis.

As the same batch of R3Bm was used for synthesis of both the nickel and the cobalt cryptates, it is probable either that the ligand was not fully reduced and that the Ni(II) ion selects the fully reduced R3Bm in preference to the partially reduced ligand or that Co(II) may be capable of introducing unsaturation into the R3Bp ligand. With the redox active metals, cobalt and copper, there appears to be the possibility that oxidative dehydrogenation has occurred. It is necessary to repeat the synthesis of the dicobalt complex using ligand that is certain to be fully reduced. A new batch of R3Bm has been prepared and proton n.m.r. was used to verify the absence of imine proton signals.

As observed in the 3Bp /R3Bp series reduction of the imine groups of the Schiff-base 3Bm cryptand enables complexation of a wider range of transition metal ions. The 3Bm ligand appeared to be unable to provide an acceptable coordination site for the Ni(II) ion yet a dinickel(II) R3Bm complex was obtained. The increase in flexibility obtained on reduction of

the imines may account for the reduced ligands ability to provide an acceptable coordination geometry to the Ni(II) ion. The binuclear complexes of R3Bm do not appear to bind hydroxo as do the R3Bp series.

CONCLUSIONS

The aim of this project was to prepare a range of metal ion complexes of macrocycles and cryptands and to investigate their properties and structure. The binucleating macrocycles P and MC provided a range of homobinuclear and heterobinuclear complexes which were capable of binding small bridging ligands. It was hoped that the cyclohexyl groups of the MC macrocycle would provide additional steric protection to the binding site, however this hope was not realised.

The macrobicyclic ligands 3Bp, R3Bp, 3Bm and R3Bm provide a more sterically protected binding site. The 3Bp ligand appears to leave the divalent transition metal ions coordinatively unsaturated and other small ligands are required to stabilise Co(II) and Ni(II) complexes. This suggests the possibility of formation of bridged binuclear assemblies within 3Bp, possibly with ligands such as imidazolate that may give a stabilising stacking interaction with the substituted benzene of the cryptand.

The R3Bp cryptand has proven useful as a host for the hydroxo-bridged binuclear assembly. The protonated R3Bp ligand may be capable of forming anion cryptates and should provide a linear cavity suitable for binding linear anions such as azide for example.

The 3Bm ligand may be capable of forming a wider range of metal complexes if a small coordinating ligand such as thiocyanate is provided.

As was observed with in the 3Bp/R3Bp series the reduced ligand produces metal complexes readily, presumably due to the increase in flexibility resulting from reduction of the imine functions.

The work on the GT series has been productive, and a wide range of transition metal ion, lanthanide ion and group(1) cryptates have been obtained. Many interesting and potentially useful properties have been uncovered for the cryptates. The reversible electrochemistry found for the transition metal cryptates suggests potential use as redox reagents, whereas the kinetic and aqueous stability of some of the cryptates may enable uses in MRI, labelling or metal ion transport. An investigation of the possible luminescence of the europium cryptate, in collaboration with Prof. Kelly is underway. Nevertheless there are many areas worthy of development. A ^{23}Na nmr study is planned for the NaGT cryptate. Further work on the copper GT cryptates is likely to be worthwhile, particularly on the mixed valence dicopper complex.

Further attempts at preparation of the reduced GT ligand would be desirable, particularly as this ligand appears to complex lead avidly and could have potential in detoxification.

APPENDIX 1 **Fundamentals of cyclic voltammetry.**

Cyclic voltammetry has become a popular technique in the study of electrochemical reactions during the last twenty years.[354-359] The technique has been extended to the field of inorganic chemistry, where it is used to evaluate the effect of ligands on the oxidation-reduction potentials of metal ions in metal complexes and multinuclear clusters.

Cyclic voltammetry involves cycling the potential of the working electrode between the initial E_i, and final E_f potential, at a constant scan rate, while measuring the current. The current response is plotted as a function of the applied potential to give a current-voltage curve or cyclic voltammogram, which indicates the potentials at which electrochemical processes (oxidation-reduction) occur. Since the experiment is performed at stationary electrodes in an unstirred solution over a short time interval, diffusion is the principal mode of moving the electroactive species to the electrode surface.

Figure 45 shows a typical cyclic voltammogram showing the important parameters that will be used to interpret the results.

The fundamental thermodynamic quantity assigned to an electrode process is the standard E° or formal ($E^{\circ\prime}$) electrode potential.[360] The formal electrode potential, $E^{\circ\prime}$ is related to the cell potential, E_{cell} by an equation in which activities of the species taking part are replaced by any composition variable, (e.g. concentration), with the electrode reaction and reaction medium being clearly specified.

$$E_{cell} = E^{\circ\prime} - \left(\frac{RT}{nF}\right) \sum_1 \nu_i \ln C_i \quad ; \quad a_i \text{ replaced by concentration.}$$

The electrochemical oxidation of ferrocene provides the basis for judging electrochemical reversibility and permits a quantitative comparison of

electrode potentials obtained using different reference electrodes or different solvents.[361,362] The redox potential of ferrocene is accepted as a reference for reporting electrochemical oxidation-reduction systems.

Three main types of electrochemical processes have been identified, namely, reversible, quasireversible and irreversible processes. These are briefly described below.

Reversible processes are those in which the rate of electron transfer is greater than the rate of mass transport and both the oxidisable and the reducible species rapidly exchange electrons with the working electrode. The reaction is therefore fast enough to maintain the concentration of the oxidised (O) and reduced (R) forms in equilibrium with each other.

$$O + e^- \rightleftharpoons R$$

The Nernst equation gives the equilibrium concentration ratio of O and R at the electrode surface, at a given potential.

$$E = E^{o'} + \frac{RT}{nF} \ln \frac{[C_O]}{[C_R]}$$

The peak currents (ip^a and ip^c) obtained from cyclic voltammograms are described by the Randles-Sevcik equation:

$$i_p = (2.69 \times 10^5)\, n^{3/2} D^{1/2} C v^{1/2}$$

Where: n = number of electrons involved

D = diffusion coefficient

C = concentration of electroactive species

v = scan rate

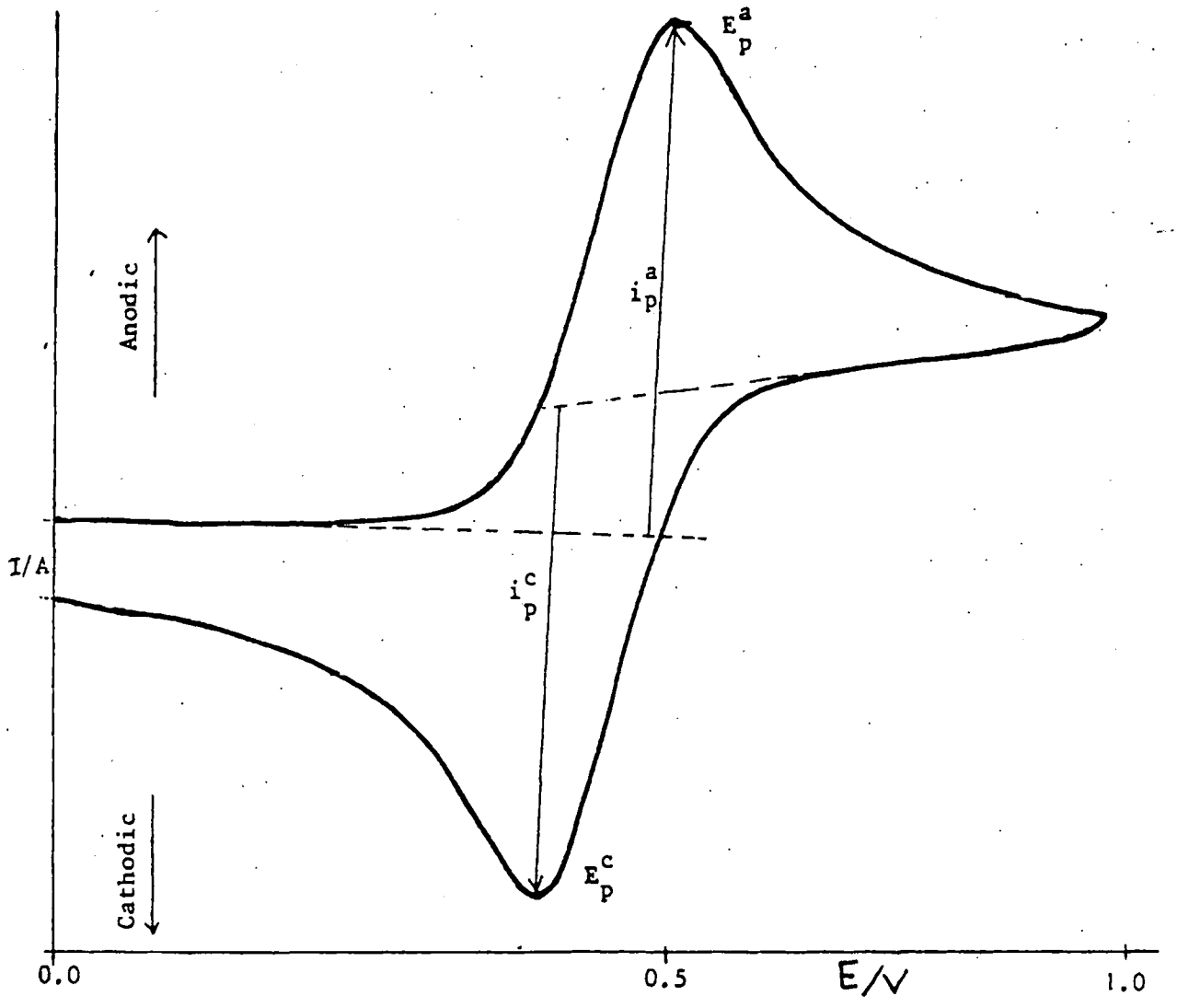

Figure 45 *Cyclic voltammogram for 10^{-3}M ferrocene in CH_2Cl_2/0.2M nBu_4NPF_6*

versus Ag/AgCl reference electrode, Pt wire working electrode and Pt auxiliary electrode. Scan rate = 100mV s^{-1}.

$E^a p$ = Anodic (oxidation) peak potential.

$E^c p$ = Cathodic (reduction) peak potential.

$i^a p$ = Anodic peak current.

$i^c p$ = Cathodic peak current.

$\Delta E = E^a p - E^c p$ = Peak potential separation.

$\Delta E = \frac{0.059}{n}$ for a reversible *n* electron system.

$\frac{i^a}{i^c}$ = Peak current ratio = 1 for a reversible reaction.

Plots of i_p versus $v^{1/2}$ and i_p are straight lines for reversible electrochemical systems. For a quasireversible process, the anodic and

cathodic peak potentials shift further apart with increasing scan rate. The reverse peak may be shorter than the forward peak, probably as a result of an accompanying chemical reaction.[357,358]

When the reaction is totally irreversible, the rate of electron transfer is much less than the rate of mass transport, resulting in a slow exchange of electrons at the working electrode. This results in either a complete separation of the forward and reverse peaks, or a complete disappearance of the reverse peak probably due to chemical reaction accompanying the electron transfer process.[358,366,357].

Two problems have been identified in cyclic voltammetry. As a result of charge transfer across the solution interface, there is often an accumulation of charges on both sides of this double layer which then behaves as a capacitor. Since the potential is continually changing, a double layer charging current I_d always flows in addition to the faradaic current, $I_{faradaic}$. This double layer charging current distorts cyclic voltammograms recorded, especially at high scan rates. Secondly, as a result of the internal resistance drop, iR_u, caused by the solution and cell resistance between the reference and working electrodes, the applied voltage is often changed from the desired value, E,to $E + iR_u$. This results in a decrease in peak current heights, and an increase in peak potential seperation.

These problems associated with cyclic voltammetry are often suppressed by using a supporting (or backing) electrolyte in the electrolyte solution. The supporting electrolyte therefore increases the conductivity of the solution, thus reducing the resistance between the working and reference electrodes, and hence eliminating migration as a mode of mass transport for the electroactive species. The suppo rting

electrolyte also suppresses the double layer effect on kinetics by minimising the variation of the double layer charging potential with the applied potential.

ELECTROCHEMICAL STUDIES

The catalytic activity of many metalloproteins is associated with redox change of the metal ion, either in electron transfer processes or in oxidation or reduction of a substrate. The redox potential of the metal ion is obviously of fundamental importance and is highly dependant on the nature of its binding site within the protein. Complexes of synthetic macrocycles and cryptands have provided convenient systems for the evaluation of the dependance of oxidation reduction properties on the detailed structure of the ligand while imposing an approximately constant coordination geometry on a given metal ion. The complexes of tetraaza tetradentate macrocycles have featured widely in such studies. Attention is focused on oxidation reduction processes involving the central metal ion and not involving redox changes of the ligand. Variation of macrocyclic structure while maintaining relatively fixed stereochemistry and constant donor set, has allowed the redox potential of the Ni^{2+}/Ni^{3+} to be varied over a two volt range.[368] Figure 46 shows selected macrocycles and their effect on the nickel (II)/(III) redox couple.

Sargeson and coworkers have investigated the effect of cage ligand structure on redox potential of the (II)/(III) couple for the encapsulated cobalt ion.[199,369] The use of cryptands in such studies prevents the metal ion binding different axial ligands or moving out of the plane of the ring, as is possible in the macrocyclic studies. Various types of change in cryptand structure have been investigated, different bridgehead atoms

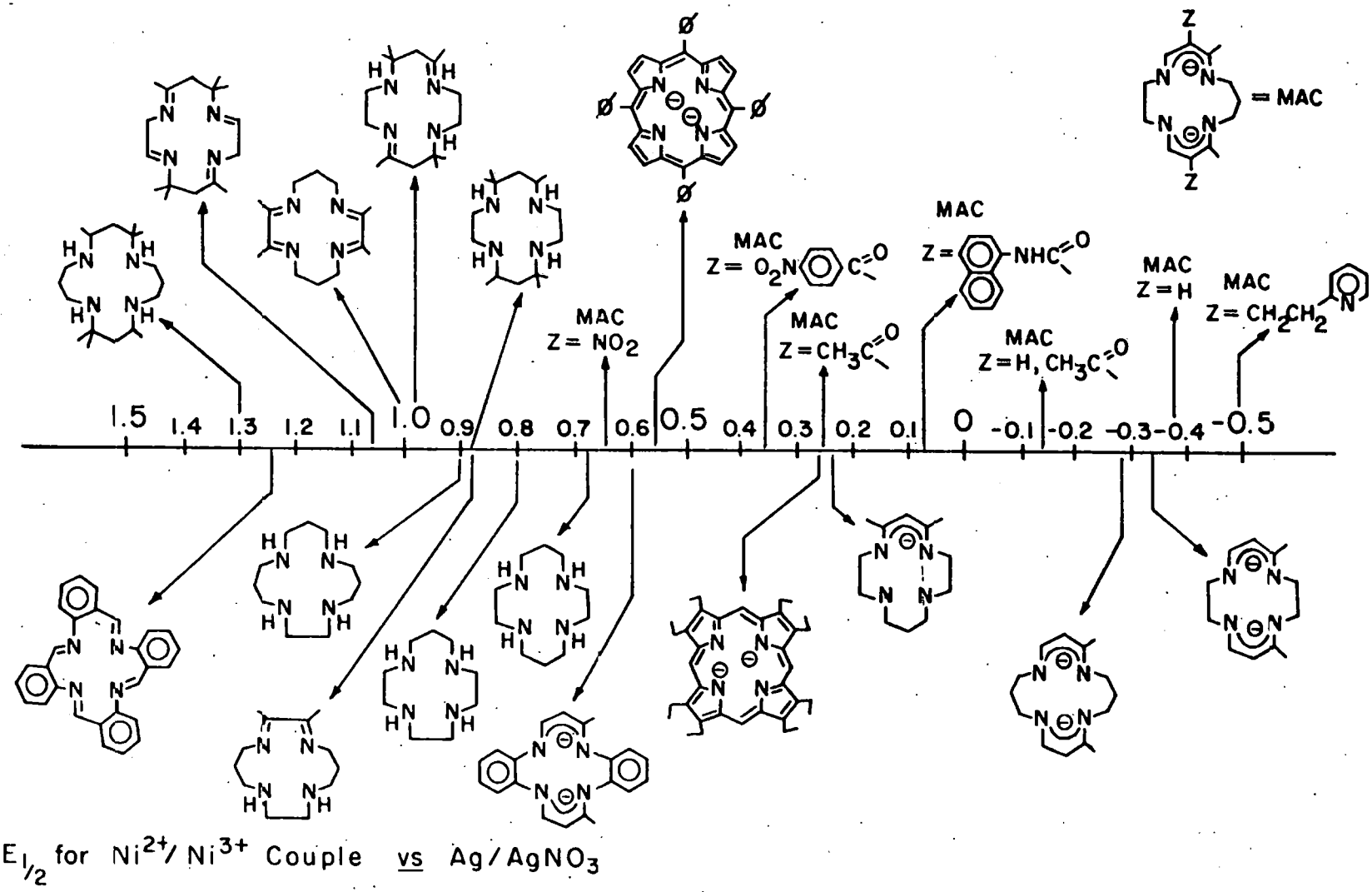

Figure 4b $E_{1/2}$ for the Ni^{2+}/Ni^{3+} couple in tetraaza macrocyclic complexes vs. $Ag/AgNO_3$, 0.1 M, reference electrode in CH_3CN.

(N or C),substituents on the bridgehead carbon atom, charged cages, cavity sizes, various degrees of unsaturation or ring strain in the cage. The factors influencing redox potential are summarised below.

(a) Negative charges in the ligand favour the higher oxidation state of the metal ion.

(b) Electron withdrawing substituents destabilise the higher oxidation state.

(c) Increase of cavity size favours the lower oxidation state.

(d) Strong δ-donor ligands favour high oxidation states.

(e) Strong π-acceptor ligands, or introduction of unsaturation into the ligand favours low oxidation states.

(f) Ring strain effects operate either way and favour the state in which strain is released.

APPENDIX 2 **Electron spin resonance**

The relative low symmetry of copper(II) coordination environments often makes interpretation of electronic spectra difficult. In such cases electron spin resonance (esr) spectroscopy can be used to provide information about the electronic ground state and the coordination geometry.

In electron spin resonance the magnetic dipoles of unpaired electrons are normally aligned with the applied field causing the degeneracy of the spin states of the electron to be removed (Zeeman effect). The energy difference between the two states is gBH, where g is the gyromagnetic ratio, B is the Bohr magneton and H the applied field strength. For a free electron the value of g is 2.0023.

If the electron is associated with a nucleus possessing spin then the energy of the electron will depend on which of the possible nuclear spin states it is coupled to (Nuclear Zeeman Effect). This gives rise to hyperfine structure consisting of 2I +1 (I = nuclear spin quantum number) lines of equal intensity.

The d^9 configuration of the copper(II) cation means that one of the d orbitals contains an unpaired electron. When radiation of frequency v is applied to a copper(II) complex in a magnetic field a net absorption occurs when hv = gBH. This results in an absorption peak and it is the first derivative of this peak that the esr records. Figure 47 shows how the esr signal arises for magnetically dilute copper(II). For the axially symmetric copper(II) ion only one transition is possible which obeys the selection rule $\Delta_{MS} = \pm 1$. The $g_{\parallel}$ signal is obtained when the magnetic field is oriented along the axial direction, the z-axis, and the $g_{\perp}$ signal is obtained when the field is in the equatorial x,y plane. Since in the

Figuee 47.

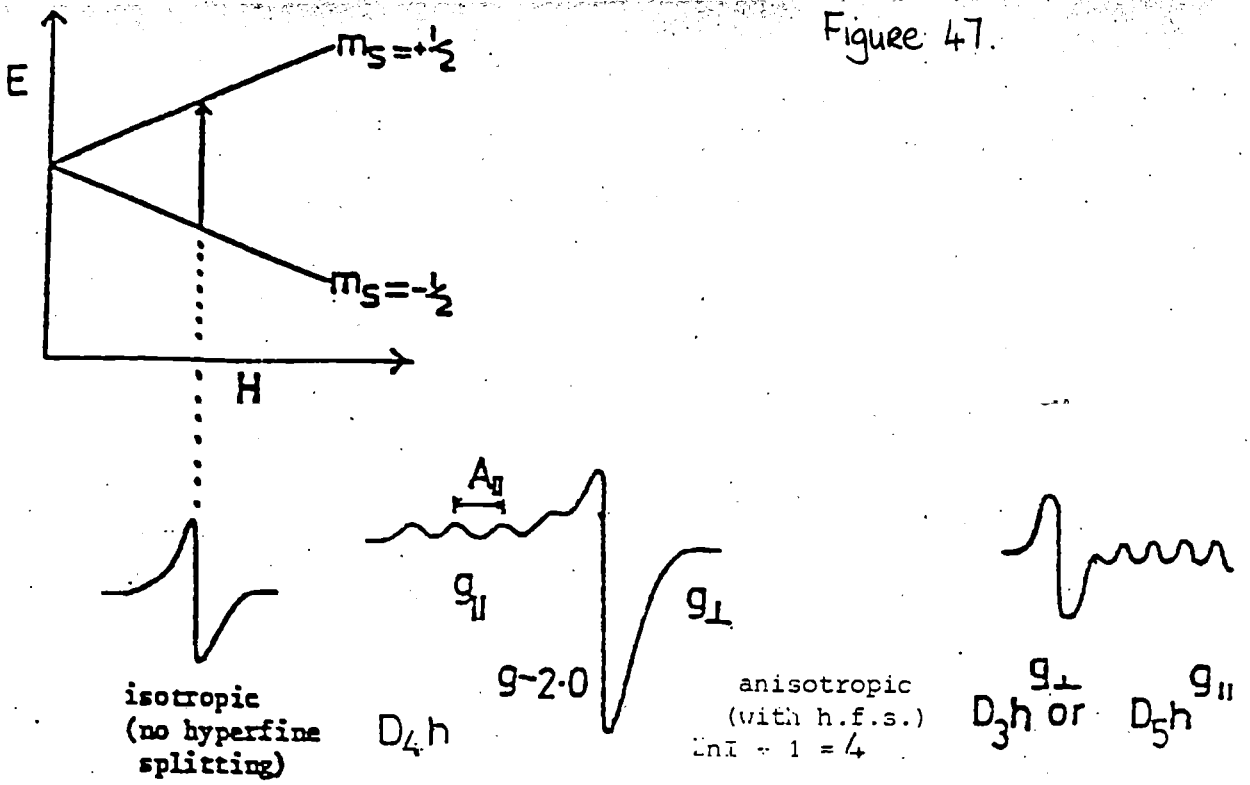

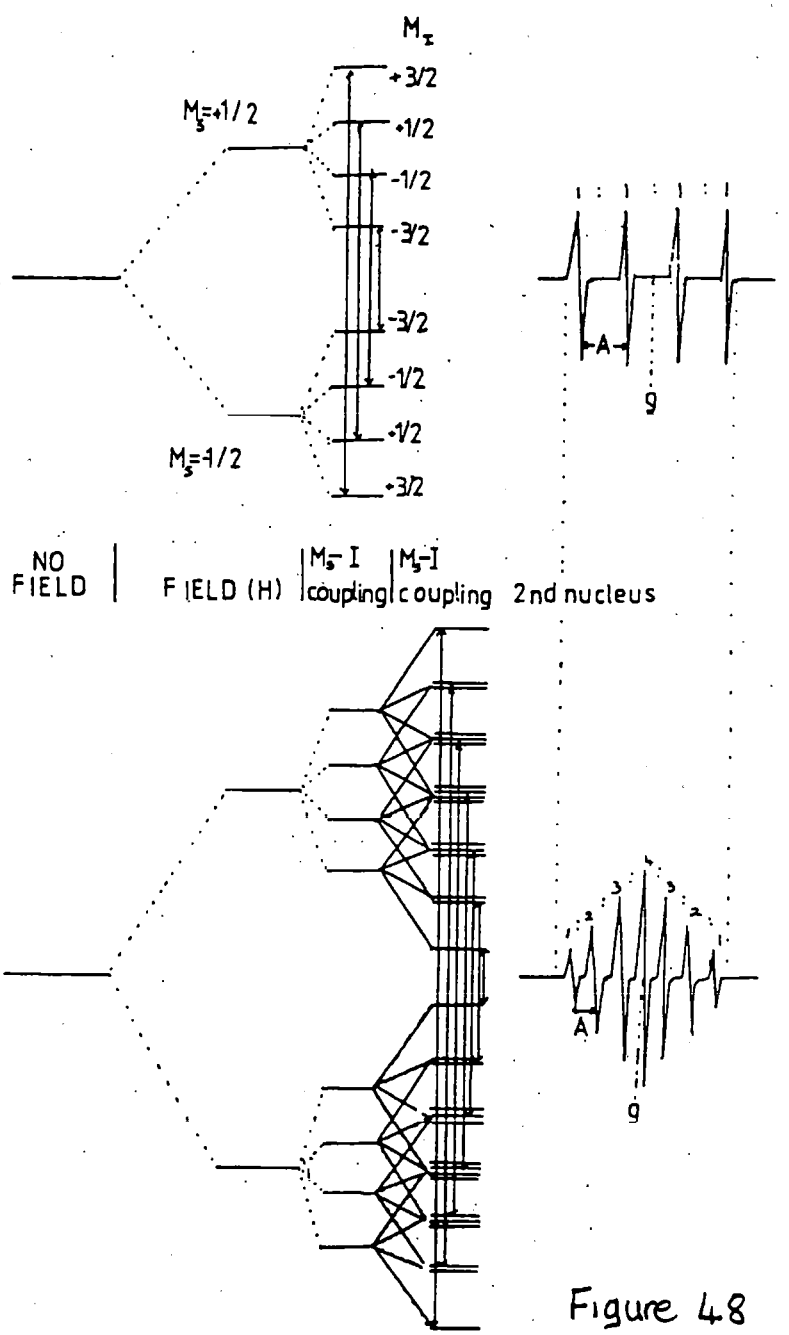

Figure 48

situation of axial symmetry, the $\perp$ axes are doubly degenerate, the probability of transition is twice that in the ll and hence the $g_{\perp}$ signal has approximately double the intensity of the g_{11} signal.

When the unpaired electron couples to the copper nucleus, spin I = 3/2, a hyperfine pattern of four equally intense lines is produced. The hyperfine is usually observed in the g_{11} region $\langle A_{11} \rangle$ 130 x $10^{-4}cm^{-1}$ but is often unresolved in the $g_{\perp}$ region.[370] For rhombically symmetric copper(II) the x and y axes are not equivalent and therefore three signals, g_x, g_y and g_z are observed. The type of esr spectrum of copper(II) complexes will be determined by several factors including the nature of the electronic ground state and the coordination geometry of the copper(II) ion.[371] Copper(II) complexes with square based geometry, have a d x^2-y^2 electronic ground state. When the applied magnetic field is along the z-axis, the d x^2-y^2 orbital can commute into the dxy orbital. Thus there will be spin orbit coupling and

$$g11 = g\ elec + \frac{8\lambda}{dx^2-y^2 - dxy}$$

where λ is the spin orbit coupling constant.[372] Rotation of dx-y about the x or y axis when the applied field is in an equatorial direction can lead to rotation of dx^2-y^2 into d_{xz} or d_{yz}, and

and

$$g_{\perp} = g\ elec + \frac{2\lambda}{dx^2-y^2 - dxz\ yz}$$

Thus for copper(II) complexes with square based geometry $g_{11} > g_{\perp} > g_{electron} = 2.0023$ as the spin orbit coupling constant is positive. The g values are smaller for square planar complexes than for other square

based geometries.[373] The hyperfine splittings, A_{11} , are large for complexes with square based geometries and $A_{\perp}$ is often unresolved.

For trigonal bipyramidal[374,375] and seven-coordinate pentagonal bipyramidal copper(II) geometries, the dz^2 orbital contains the unpaired electron.An axial field (Z direction) cannot commute dz^2 into any other orbital geometry and so g_{11} will equal the free electron value of 2.0023.[370] When the applied magnetic field is in the equatorial (x,y) direction, dz^2 can rotate into dxy or dyz with

$$g_{\perp} = 2.0023 + \frac{6\lambda}{dx2\text{-}y2 \; -dxy \; yz}$$

and therefore $g_{\perp} > g11 = 2.0023$. The A_{11} hyperfine splittings are usually lower than observed for complexes with a $dx^2\text{-}y_2$ electronic ground state[371,375] in copper(II). Thus ESR may be used to determine the ground state in copper(II) complexes.

For binuclear copper(II) complexes in which the copper centres are magnetically coupled through a bridging ligand, a zero -field splitting of the triplet state occurs. As a result of the splitting the forbidden 'half-band' $\Delta M = 2$ signal is observed in addition to the stronger $\Delta M = 1$ signal. The half-band signal may be resolved into a relatively isotropic seven line pattern (2nI+1) due to hyperfine interaction. The intensity ratios of the line are often as simple as the expected 1:2:3:4:3:2:1 pattern. The hyperfine spacing of about 75G is approximately half of that found in mononuclear copper(II) spectra. The $\Delta M = 1$ region of the spectrum is often complicated by distortions from regular geometries and by hyperfine splitting patterns on components of the $\Delta M = 1$ transition. The intensity of the esr signal is dependant on the degree of electron pairing due to interaction between Cu(II) centres via the bridging ligand. As a result

strongly antiferromagnetically coupled Cu(II) centres may be esr silent. When there is no bridging ligand present between (Cu(II) centres and the ions are not directly bonded, the only means of interaction is by dipolar coupling. The esr spectrum reflects the internuclear separation of two Cu(II) ions as the zero-field splitting is inversely proportional to r^3 , where r is the internuclear separation. For r > 7A , D is of the order of $0.01cm^{-1}$ and a single transition is observed. At smaller internuclear distance, the zero-field splitting can dominate producing a split and broadened $\Delta M = 1$ signal and a narrower $\Delta M = 2$ half-band transition. The $\Delta M = 1$ signal can extend over a wide magnetic field range.

Figure 48 shows isotropic hyperfine coupling for mono copper(II) and binuclear Cu(II)

APPENDIX 3 **Electronic spectra**

Electronic transitions in copper (II) complexes give two main types of absorption, d-d transitions and charge transfer transitions. Transitions within the d subshell are Laporte forbidden, ($\Delta L = 0$). Several mechanisms for the breakdown of this selection rule exist and have the effect of enhancing the intensity of absorption due to d-d transitions.[376,377] These mechanisms include :-

1 d-p mixing in non-centrosymmetric systems.

2 vibronic coupling in which strong metal ligand coupling allows coupling of a vibrational mode of the molecule with the electronic excited state.

3 intensity borrowing from an energetically near allowed transition (usually charge transfer in nature). This leads to extinction coefficients for a Cu(II) ion d-d transition in the range 50-200$M^{-1}cm^{-1}$.

Copper (II) has a d^9 electronic configuration and is subject to Jahn Teller distortions if placed in a field of cubic symmetry. The distortions lead to tetragonal splitting of the e_g level so that dz^2 lies below $d_{x^2-y^2}$ as shown in figure 49. Thus for tetragonally distorted six coordinate Cu(II) complexes, three bands are expected due to the transitions, $dz^2 \rightarrow d_{x^2-y^2}$, $dxy \rightarrow d_{x^2-y^2}$ and $dxz,yz \rightarrow d_{x^2-y^2}$. The three bands generally overlap giving one broad band.

Square planar Cu(II) complexes are assigned to the D_{4h} point group and three transitions are expected from dz^2, dxz,yz and dyz to dx^2-y^2. Charge transfer processes are both Laporte allowed and spin allowed and are therefore much more intense ($\epsilon \simeq 10^3 M^{-1}cm^{-1}$) than d-d transitions. Figure 51 shows the splitting pattern for d^8 Ni^{2+} and d^7 Co^{2+}in octahedral and tetrahedral fields.

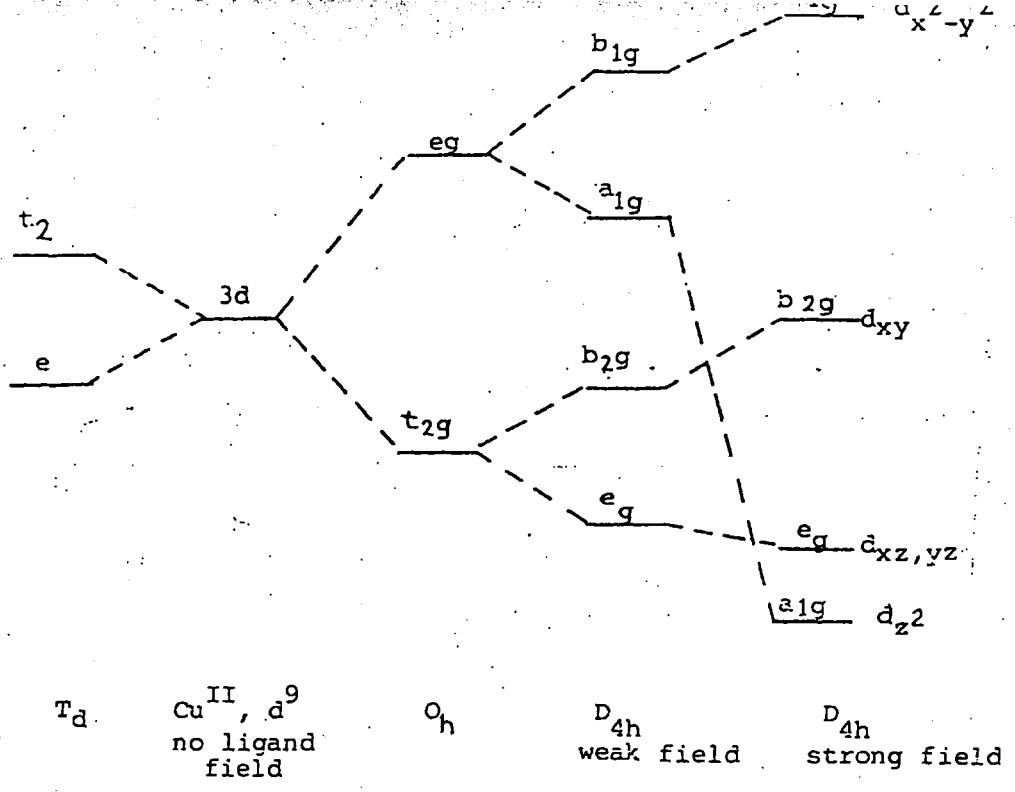

Figure 49 *d-orbital splitting for Cu(II) in T_d, O_h and D_{4h} symmetries*

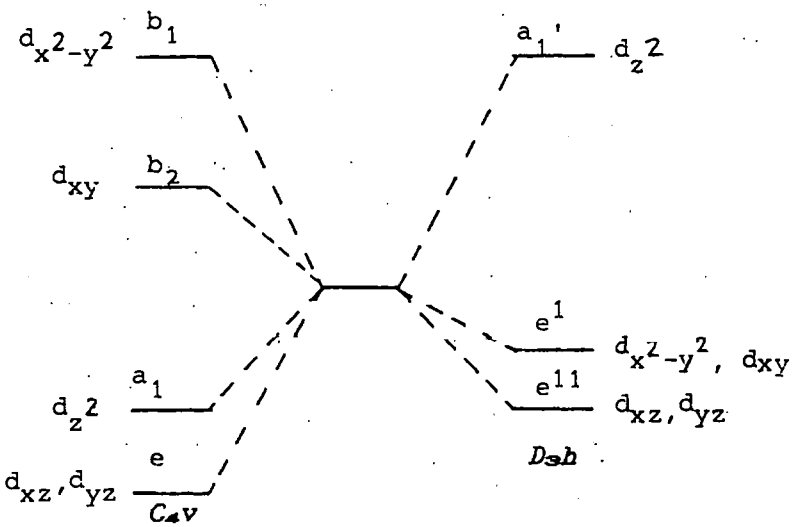

Figure 50 *d-orbital splitting for Cu(II) in C_{4v} and D_{3h} symmetries*

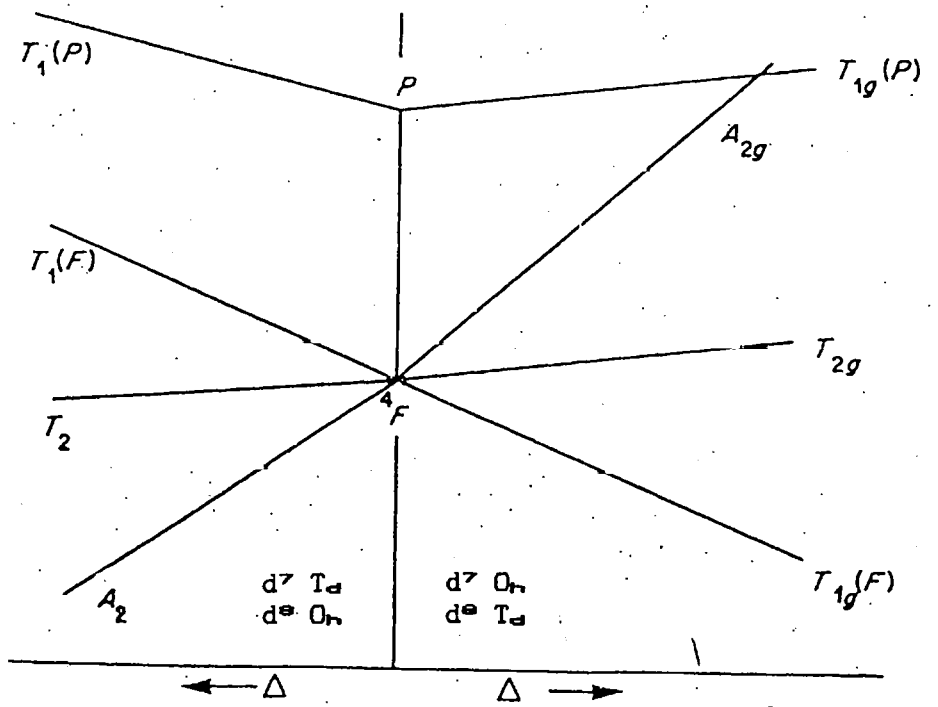

Figure 51 *Orgel diagram for d^7 and d^8 ions in T_d and O_h ligand fields*

In lanthanide complexes f-f bands are often observed.[378,379] The electronic absorption spectrum of the tripositive ions (except La^{3+}, Ce^{3+} and Yb^{3+}) contain several sharply defined bands. Unlike the d-d bands observed in transition metal complexes, the bands resulting from transitions within the f subshell are not sensitive in position. This is a result of the f electrons being inner electrons which are sheilded from ligand effects. In contrast, the absorption bands of the Ce^{3+} and Yb^{3+} ions result from $4f \rightarrow 4f^{n-1}5d^1$ or $4f \rightarrow 4f^{n-1}5g^1$ or a similar configuration, are broad and altered by complexing groups. The principal absorption bands of relevant Ln^{3+} ions are shown in Table 35 .

Table 35 Principal f-f absorption bands

Ion	Wavelength/nm
La^{3+}	none
Ce^{3+}	210, 222, 238, 252
Pr^{3+}	444, 469, 482, 588
Eu^{3+}	375, 394
Gd^{3+}	273, 273, 275, 276
Tb^{3+}	369, 378, 487

APPENDIX 4 Intramolecular antiferromagnetism

In magnetically dilute systems the paramagnetic metal centres are isolated from each other and do not interact. However, paramagnetic metal centres may interact with each other either directly, when the distance between them is small, or through bridging ligands, as illustrated in figure 50.

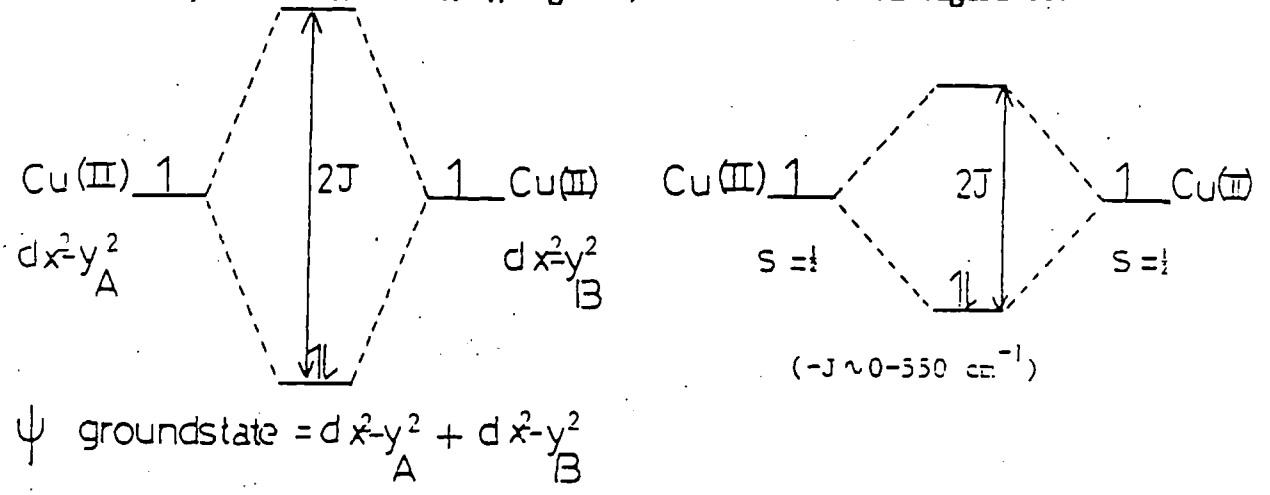

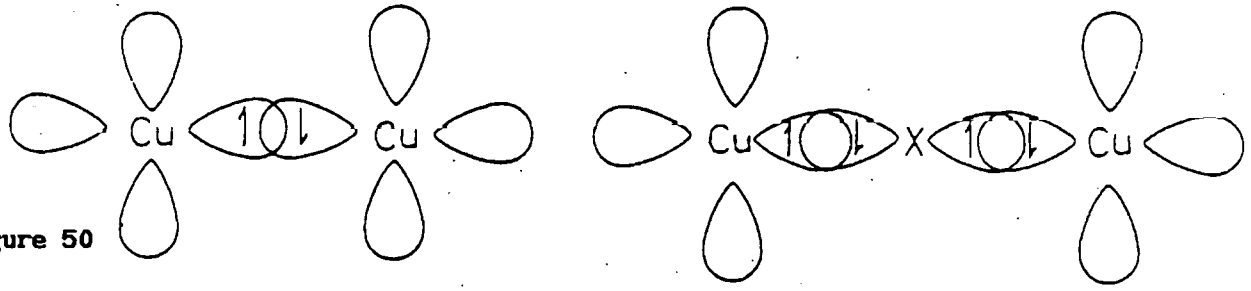

Figure 50

Interaction may be of a ferromagnetic (S = 1) or an antiferromagnetic (S = 0) nature. If the interaction is antiferromagnetic in nature a decreased magnetic moment is observed, and diamagnetism can result at low temperatures. Unpaired electrons from adjacent metal centres pair up by superexchange through a bridging ligand, or by covalent bond formation in the case of metal-metal bonds.

Antiferromagnetic behaviour can be confirmed by magnetic measurements taken over a range of temperatures and is shown by the presence of a maximum, termed the Neel point, in the plot of susceptibility against temperature. Below this temperature antiferromagnetic behaviour is

observed. As temperature is raised, thermal energy overcomes the magnetic interaction, resulting in normal paramagnetic behaviour and the Curie-Weiss law is followed. This differs from the normal Curie law. Although the plot of $1/\chi$ versus temperature is linear, there is a non-zero intercept on the temperature axis. The singlet-triplet separation is given by the exchange coupling parameter, 2J, which is defined by the Hamiltonian operator $H = -2JS_1 S_2$ where S_1 and S_2 are the spins of the two nuclei involved. The value of J is negative for antiferromagnetic coupling and positive for ferromagnetic coupling as illustrated below.

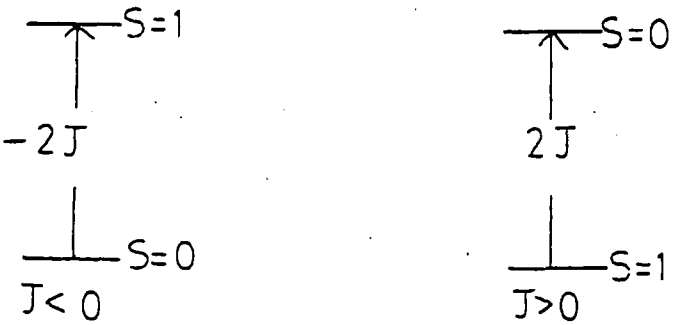

Antiferromagnetic Ferromagnetic

Magnetic susceptibility varies with temperature as a function of -J and the magnitude and sign of the coupling constant, J, is calculated from magnetic susceptibility χ_m *vs.* temperature data, using the Bleaney Bowers equation.[2].

MAGNETIC CHARACTERISTICS OF LANTHANIDE ION COMPLEXES

Paramagnetism in lanthanide complexes arises as a result of the presence unpaired 4f electrons. As the 4f orbitals are shielded from the influence of external forces by $5s^2$ and $5p^6$ shells, magnetic moments of the lanthanide series are only slightly affected by their surroundings.[378,379] The states of the $4f^n$ configurations are given by the Russell-Saunders coupling scheme. Because the 4f electrons are sheilded both their orbital

and spin motions contribute, and the observed moment results from coupling of these. The spin orbit coupling constants are quite large (order of 1000 cm^{-1}).

The lanthanides, with the exception of Eu^{3+} and Sm^{3+}, have ground states with a single well defined value of the total angular momentum J, with the next lowest J state at energies many times *kT* above.

For Eu^{3+} and Sm^{3+} excited states are close to the ground state and are appreciably populated at room temperature, thus the observed magnetic moments for Eu^{3+} and Sm^{3+} are higher than those calculated by considering the ground states only. The theoretical (Van Vleck) value is determined by the magnitudes of separation between the energy levels (produced by coupling of spin and orbital motion) and the term *kT*. The theoretically calculated values match observed values well. Magnetic moments and electronic ground states for selected tripositive cations of the lanthanides are tabulated below.

ION	GROUND STATE	THEORETICAL (Van Vleck)	OBSERVED $Ln_2(SO_4)_3:8H_2O$	OBSERVED $Ln(C_8H_8)_3$
La^{3+}	$^1S_0$	0	-	0
Ce^{3+}	$^2F_{5/2}$	2.56	-	2.46
Pr^{3+}	$^3H_4$	3.62	3.47	3.61
Eu^{3+}	$^7F_0$	3.40-3.51	3.54	-
Gd^{3+}	$^8S_{7/2}$	7.94	7.9	7.98
Tb^{3+}	$^7F_6$	9.7	9.6	-

APPENDIX 5 Instruments

Infrared spectra were recorded in the range 4000-300cm^{-1} as KBr discs or nujol mulls using a Perkin-Elmer 983G infrared spectrophotometer.

Electronic spectra were recorded as solution or mull spectra using a Perkin-Elmer Lambda 9 UV/VIS/NIR spectrophotometer.

Conductivity measurements[200] were obtained using a Metrohm Herisau conductometer E518 or a conductivity cell with a cell constant 0.0352, constructed from bright platinum electrodes, in conjunction with a conventional resistance/capicitance bridge.

$$K = \frac{0.0352}{R}$$ (where R = resistance reading)

$$K_{corr} = K - K_s \quad \text{(where } K_s = \frac{0.0352}{\text{resistance of MeCN}}\text{)}$$

Molar conductivity = $1000K_{corr}/c$ (where c = molar concentration.)

Ranges in MeCN:

1:1 electrolyte	120-160 S cm^2 mol^{-1} (92-199)
1:2 electrolyte	220-300 S cm^2 mol^{-1} (145-336)
1:3 electrolyte	340-420 S cm^2 mol^{-1} (variable)

Mass spectra were recorded at an ionising voltage of 70eV using either an AEI or an Ms902 mass spectrometer. Fast atom bombardment mass spectroscopy was carried out by the SERC mass spectrometry service, Swansea. ^{1}H NMR spectra were run using a Bruker WM250 MHz Fourier transform NMR spectrometer or a 300MHz General electric QE300 spectrometer. Magnetic results were obtained either by the Gouy method using a Newport Instruments variable temperature (93-300K) magnetic balance or by use of an Oxford instruments resistance susceptibility balance, which provides results in the temperature range (65-300K).

Esr spectra were obtained as undiluted powders or as the frozen glass, using a Varian E10 instrument.

1 G.A. Melson, "Coordination Chemistry of Macrocyclic Compounds." Plenum Press, New York, 1979.

2 J. Van Alpen, *Rec. Trav. Chim. Pays-Bas*, 1936, **55**, 835.

3 R.P. Linstead and M. Whalley, *J. Chem. Soc.*, 1952, 4839.

4 G.E. Ficken and R.P. Linstead, *J. Chem. Soc.*, 1952, 4846.

5 J.A. Elvidge and R.P. Linstead, *J. Chem. Soc.*, 1952, 5008.

6 J.A. Elvidge and J.H. Golden, *J. Chem. Soc.*, 1957, 700.

7 N.F. Curtis, *J. Chem. Soc.*, 1960, 4409.

8 M.C. Thompson and D.H. Busch, *J. Am. Chem. Soc.*, 1964, **86**, 3651.

9 C.J. Pederson, *J. Am. Chem. Soc.*, 1967, **89**, 2495.

10 C.J. Pederson, *J. Am. Chem. Soc.*, 1967, **89**, 7017.

11 A.C.L. Su and J.F. Weiher, *Inorg. Chem.*, 1968, **7**, 176.

12 D.R. Boston and N.J. Rose, *J. Am. Chem. Soc.*, 1968, **90**, 6859.

13 D.H. Busch, *Record Chem. Prog.*, 1964, **25**, 107.

14 B. Dietrich, J.M. Lehn and J.P. Sauvage, *Tetrahedron Lett*, 1969, 2885, 2889.

15 J. Rebek Jr., *Acc. Chem. Res.*, 1984, **17**, 258.

16 D.J. Cram and K.N. Trueblood, Topics in Curr. Chem., 1981, **98**, 43.

17 W.H. Watson, J. Galloy, D.A. Grossie, F. Vogtle and W.M. Muller, *J. Org. Chem.*, 1984, **49**, 347.

18 K.B. Mertes and J.M. Lehn in 'Comprehensive Coordination Chemistry' ed. G. Wilkinson, R.D.Gillard and J.A. McCleverty, Pergamon Press, Oxford, 1987, Vol.2, p.915.

19 E.K. Barefield, *Inorg. Chem.*, 1972, **11**, 2273.

20 E.K. Barefield and F. Wagner, *Inorg. Chem.*, 1973, **12**, 2435.

21 J.E. Richman and T.J. Atkins, *J. Am. Soc.*, 1974, **96**, 2262.

22 S. Ogawa, T. Yamaguchi and N. Gotoh, *J. Chem. Soc., Chem. Commun.*, 1972, 557.

23 J. Zagwinski, J.M. Lehn, R. Merric and J.P. Vigneron, *Tetrahedron Lett.*, 1987, **28**, 3489.

24 D. Mc Dowell and J. Nelson, *Tetrahedron Lett.*, 1988, **29**, 385.

25 S.M. Nelson, *Pure Appl. Chem.*, 1980, **52**, 2461.

26 M.C. Thompson and D.H. Busch, *J. Am. Chem. Soc.*, 1962, **84**, 1762.

27 B. Deitrich, M.W. Hosseini, J.M. Lehn and R.B. Sessions, *Helv. Chim. Acta*, 1985, **68**, 289.

28 J, Jazwinski, J.M. Lehn, D. Lilienbaum, R. Ziessel, J. Guilhem and C. Pascard, *J. Chem. Soc., Chem. Commun.*, 1987, 1691.

29 M. Ciampolini, M. Micheloni and F. Vizza, *J. Chem. Soc., Dalton Trans.*, 1986, 505.

30 R.J. Geue, T.W. Hambley, J.M. Harrowfield and A.M. Sargesen, *J. Am. Chem. Soc.*, 1984, **106**, 5478.

31 A.M. Sargeson, *Chem.Br.*, 1979,**15**, 23.

32 N.F. Curtis, *Coord. Chem. Rev.*, 1968, **3**, 3.

33 L.F. Lindoy and D.H. Busch, *Prep. Inorg. React.*, 1971, **6**, 1.

34 E.J. Jager, *Z. Chem.*, 1968, **8**, 30.

35 N.F. Curtis in 'Comprehensive Coordination Chemistry' ed. G. Wilkinson, R.D.Gillard and J.A. McCleverty, Pergamon Press, Oxford, 1987, Vol.2, p.899.

36 G.A. Melson and D.H. Busch, *Proc. Chem. Soc.*, 1963, 223.

37 V. Katovic, S.G. Vertes and D.H. Busch, *Inorg. Chem.*, 1977, **16**, 1716.

38 P. Comba, N.F. Curtis, G.A. Lawrance, A.M. Sargeson, B.W. Skelton and A.H. White, *Inorg. Chem.*, 1986, **25**, 4260.

39 D.K. Cabbiness and D.W. Margerum, *J. Am. Chem. Soc.*, 1970, **92**, 2151.

40 D.K. Cabbiness and D.W. Margerum, *J. Am. Chem. Soc.*, 1969, **91**, 6540.

41 D.H. Busch, K. Farmery, V. Goedken, V. Katovic, A.C. Melnyk, C.R. Seperati and N. Tokel, Bioinorganic Chemistry, Adv. Chem. Ser., 1971, **100**, 44.

42 J.M. Lehn and J.P. Sauvage, *J. Am. Chem. Soc.*, 1975, **97**,6700.

43 J.M. Lehn, *Acc.Chem.Res.*, 1978, **11**, 49.

44 F.P. Hinz and D.W. Margerum, *J. Am. Chem. Soc.*, 1974, **96**, 4993.

45 F.P. Hinz and D.W. Margerum, *Inorg. Chem.*, 1974, **13**, 294.

46 A. Anchini, L. Fabbrizzi, P. Paoletti, and R.M. Clay,
J. Chem. Soc., Dalton Trans., 1978, 577.

47 L. Fabbrizzi, P. Paoletti and R.M. Clay,
Inorg. Chem., 1978, 17, 1043.

48 R.M. Clay, M. Micheloni, P. Paoletti and W.V. Steele,
J. Am. Chem., 1979, 101, 4119.

49 D.H. Busch, *Acc. Chem. Res.*, 1978, 11, 392.

50 D.E. Fenton, *Pure Appl. Chem.*, 1986, 58, 1437.

51 S.M. Nelson in 'Copper Coordination Chemistry, Biochemical and inorganic perspectives', Ardenine Press, New York, 1983.

52 E.L. Blinn and D.H. Busch, *Inorg. Chem.*, 1968, 7, 820.

53 M.C. Thompson and D.H. Busch, *J. Am. Chem. Soc.*, 1962, 84, 1762.

54 M.C. Thompson and D.H. Busch, *J. Am. Chem. Soc.*, 1964, 86, 213.

55 D.E. Fenton and P.A. Vigato, *Chem.Soc.Rev.*, 1988, 17, 69.

56 L. De Cola, D.L. Smailes and L.M. Vallarino,
Inorg. Chim. Acta, 1985, 110, L1.

57 D.H. Cook and D.E. Fenton,
J. Chem. Soc., Dalton Trans., 1979, 266.

58 D.H. Cook and D.E. Fenton,
J. Chem. Soc., Dalton Trans., 1979, 810.

59 D.H. Cook, D.E. Fenton, M.G.B. Drew, A. Rodgers, M. McCann and S.M. Nelson, *J. Chem. Soc., Dalton Trans.*, 1979, 414.

60 N.A. Bailey, D.E. Fenton, P.B. Roberts and A.M. Walford,
J. Chem. Soc., Dalton Trans., 1987, 1865.

61 N.A. Bailey, D.E. Fenton, R.J. Good, R. Moody and C.O.Rodriguez de Barbarin, *J. Chem. Soc., Dalton Trans.*, 1987, 207.

62 S.M. Nelson, F.S. Esho and M.G.B. Drew,
J. Chem. Soc., Dalton Trans., 1983, 1857.

63 M.G.B. Drew, A. Rodgers, M. McCann and S.M. Nelson,
J. Chem. Soc., Chem. Commun., 1978, 415.

64 M.G.B. Drew, J. Nelson and S.M. Nelson,
J. Chem. Soc., Dalton Trans., 1981, 1678.

65 L.F. Lindoy, *Quart.Rev.*, 1971, 25, 379.

66 N.A. Bailey, D.E. Fenton, M.G. Williams and D.J. Winter, *J. Chem. Soc., Dalton Trans.*, 1989, 1727.

67 C.J. van Staveren, D.E. Fenton, D.N. Reinhoudt, J. van Eerden and S. Harkema, *J. Am. Chem. Soc.*, 1987, **109**, 3456.

68 A. Bashall, M. McPartlin, B.P. Murphy, D.E. Fenton, S.J. Kitchen and P.A. Tasker, *J. Chem. Soc., Dalton Trans.*, 1990, 505.

69 N.A. Bailey, D.E. Fenton and D.J, Winter, *J. Chem. Soc., Dalton Trans.*, 1990, 15.

70 D. Christodoulou, M.G. Kanatzidis and D. Coucouvanis, *Inorg. Chem.*, 1990, **29**, 191.

71 S.M. Nelson, *Inorg. Chim. Acta*, 1982, **62**, 39.

72 M.F. Cabral, B. Murphy and J. Nelson, *Inorg. Chim. Acta*, 1984, **90**, 169.

73 M.G.B. Drew, M. McCann and S.M. Nelson, *J. Chem. Soc., Dalton Trans.*, 1981, 1868.

74 M.G.B. Drew, J. Nelson, F. Esho, V. McKee and S.M. Nelson, *J. Chem. Soc., Dalton Trans.*, 1982, 1837.

75 S.M. Nelson, F. Esho and M.G.B. Drew, *J. Chem. Soc., Dalton Trans.*, 1857.

76 M.G.B. Drew, F. Esho and S.M. Nelson, *J. Chem. Soc., Dalton Trans.*, 1983, 1653.

77 V. McKee, K.P. McKillop, S.M. Nelson and J. Nelson, *J. Chem. Soc., Chem. Commun.*, 1988, 387.

78 U. Castellato, D. Fregona, S. Sitran, S. Tamburini, P.A. Vigato and D.E. Fenton, *Inorg. Chim. Acta*, 1985, 181.

79 S.M. Nelson, C.V. Knox, M. McCann and M.G.B. Drew, *J. Chem. Soc., Dalton Trans.*, 1981, 1669.

80 N.A. Bailey, M.M. Eddy, D.E. Fenton, S. Moss, A. Mukhopadhyay and G. Jones, *J. Chem. Soc., Chem. Commun.*, 1981, 628.

81 N.A. Bailey, M.M. Eddy, D.E. Fenton, S. Moss, A. Mukhopadhyay and G.Jones, *J. Chem. Soc., Dalton Trans.*, 1984, 2281.

82 A.M. Arif, J.D.J. Backer-Dirks, C.J. Gray, F.A. Hart and M.B. Hursthouse, *J. Chem. Soc., Dalton Trans.*, 1987, 1665.

83 J.C. Dutton, G.D. Fallon and K.S. Murray, *J. Chem. Soc., Chem. Commun.*, 1990, 64.

84 P. Zanello, S. Tamburini, P.A. Vigato and G.A. Mazzochin, *Coord. Chem. Rev.*, 1987, **77**, 165.

85 C. Cairns, S.G. McFall, S.M. Nelson and M.G.B.Drew, *J. Chem. Soc., Dalton Trans.*, 1979, 446.

86 D.E. Fenton, V. Castellato, P.A. Vigato and M. Vidali, *Chem. Soc. Rev.*, 1979, **8**, 199.

87 J.M. Lehn, *Pure Appl.Chem.*, 1980, **52**, 2441.

88 M.W. Hosseini, J. Comarmond and J.M. Lehn, *Helv.Chim.Acta*, 1989, **72**, 1066.

89 M.G.B. Drew, F.S. Esho, A. Lavery and S.M. Nelson, *J. Chem. Soc., Dalton Trans.*, 1984, 545.

90 P.K. Coughlin, J.C. Dewan, S.J. Lippard, E.I. Wanatabe and J.M. Lehn, *J. Am. Chem, Soc.*, 1979, **101**, 265.

91 R.J. Motekaitis, A.E. Martell, B. Deitrich and J.M. Lehn, *Inorg. Chem.*, 1984, 23.

92 P.K. Coughlin, J.C. Dewan, S.J. Lippard, E. Watanabe and J.M. Lehn, *J. Am. Chem. Soc.*,1979, **101**, 265.

93 A.E. Martell and R.J. Motekaitis, *J. Am. Chem. Soc.*, 1988, **110**, 8059.

94 A.E. Martell and R.J. Motekaitis, *J. Chem. Soc., Chem. Commun.*, 1988, 915.

95 M.G. Basallote and A.E. Martell, *Inorg.Chem.*, 1988, **27**, 4219-4224.

96 J.M. Lehn, S.H. Pine, E. Watanabe and A.K. Willard, *J. Am. Chem. Soc.*, 1977, **99**, 6766.

97 R.J. Motekaitis, A.E. Martell, J.M. Lehn and E. Watanabe, *Inorg.Chem.*, 1982, 21, 4253.

98 R.J. Motekaitis, A.E. Martell, B. Dietrich and J.M. Lehn, *Inorg. Chem.*, 1984, **23**, 1588.

99 R.J. Motekaitis, A.E. Martell, I. Murase, J.M. Lehn and M.W.Hosseini, *Inorg.Chem.*, 1988, **27**, 3630.

100 A.E. Martell, *Acc.Chem.Res.*, 1982, **15**, 155.

101 R. Menif, D. Chen and A.E. Martell, *J. Chem. Soc., Chem. Commun.*, 1989, 1521.

102 S.M. Nelson, F. Esho, A.Lavery and M.G.B.Drew, *J. Am. Chem. Soc.*, 1983, **105**, 5693.

103 R.R. Gagne, L.M. Henling and T.J. Kistenmacher, *Inorg. Chem.*, 1980, **19**, 1226.

104 S.K. Mandal, L.K. Thompson, K. Nag, J.P. Charland and E.J. Gabe, *J. Am. Chem. Soc.*, 1987, **26**, 1391.

105 S.K. Mandal, L.K. Thompson, M.J. Newlands and E.J. Gabe, *Inorg. Chem.*, 1989, **28**, 3707.

106 J.M. Lehn and M.E. Stubbs, *J. Am. Chem. Soc.*, 1974, **96**, 4011.

107 J.M. Lehn and J. Simon, *Helv.Chim.Acta*, 1977, **60**, 141.

108 R. Louis, Y. Agnus and R. Weiss, *J. Am. Chem. Soc.*, 1978, 3604.

109 A. Carroy and J.M. Lehn, *J. Chem. Soc., Chem. Commun.*, 1986, 1232.

110 F. Fages, J.P. Desvergne, H.B. Laurent, J.M. Lehn, J.P. Konopelski, P. Marsau and Y. Barrans, *J. Chem. Soc., Chem. Commun.*, 1990, 655.

111 N.H. Pilkington and R. Robson, *Aust.J.Chem.*, 1970, **23**, 2225.

112 R. Robson, *Aust.J.Chem.*, 1970, **23**, 2217.

113 S.S. Tandon and V. McKee, *J.Chem. Soc., Dalton Trans.*, 1989, 19.

114 B.F. Hoskins, R. Robson and P. Smith, *J. Chem. Soc., Chem. Commun.*, 1990, 488.

115 V. McKee and W.B. Shepard, *J. Chem. Soc., Chem. Commun.*, 1985, 185.

115(b) S. Brooker, V. McKee, W.B. Shepard and L.K.Pannell, *J. Chem. Soc., Dalton Trans.*, 1987, 2555.

116 V. McKee and S.S. Tandon, *J. Chem. Soc., Chem. Commun.*, 1988,385.

116(b) V. McKee and S.S. Tandon, *J. Chem. Soc., Chem. Commun.*, 1988, 1334

117 V. McKee and S.S. Tandon, *Inorg. Chem.*, 1989, **28**, 2901.

118 M. Bell, A.J. Edwards, B,F. Hoskins, E.H. Kachab and R. Robson, *J. Chem. Soc., Chem. Commun.*, 1987, 1852.

119 M. Bell, J.A. Edwards, B,F. Hoskins, E.H. Kachab and R. Robson, *J. Am. Chem. Soc.*, 1989, **111**, 3606.

120 J.B. Vincent and C. Christou, *Inorg. Chim. Acta.*, 1987, **136**, L41.

121 J. Comarmond, B. Deitrich, J.M. Lehn and R.Louis, *J. Chem. Soc., Chem. Commun.*, 1985, 74.

122 T. Tomohiro, K. Uoto and H. Okuno, *J. Chem. Soc., Chem. Commun.*,

1990, 194.

123 A. Messerschmidt, A. Rossi, R. Ladenstein, R. Huber, M. Bolognesi, G. Gatti, A. Marchesini, T. Petruzzelli and A. Finazziagra, *J. Mol. Biol.*, 1989, **206**, 513.

124 R.R. Gagne, C.L. Spiro, T.J. Smith, C.A. Hamann, W.R. Thies and A.K. Shiemke, *J. Am. Chem. Soc.*, 1981, **103**, 4073.

125 R.R. Gagne and C.L. Spiro, *J. Am. Chem. Soc.*, 1980, **102**, 1443.

126 U. Castellato, *Inorg. Chim. Acta*, 1985, 181.

127 U. Castellato, *Coord. Chem. Revs.*, 1977, **23**, 31.

128 J. Nelson, B. Murphy, M.G.B. Drew, P.C. Yates and S.M. Nelson, *J. Chem. Soc., Dalton Trans.*, 1988, 1001.

129 M.G.B. Drew, M. McCann, S.M. Nelson, *J.Chem.Soc., Dalton Trans.*, 1981, 1868.

130 F.C.J.M. van Veggel, S. Harkema, M. Bos, W. Verboom, C.J. van Staveren, G.J. Gerritsma and D.N. Reinhoudt, *Inorg. Chem.*, 1989, **28**, 1133.

131 C.J. van Stavern, D.E. Fenton, D.N. Reinhoudt, J. van Eerden and S Harkema, *J. Am. Chem. Soc.*, 1987, **109**, 3456.

132 P. Chadhuri and K. Weighardt, *Prog. Inorg. Chem.*, 1987, **35**, 33.

133 P. Paoletti, *Pure Appl. Chem.*, 1980, **52**, 2433.

134 E. Kimura, *Pure Appl.Chem.*, 1986, **58**, 1461.

135 L. Fabrizza, *Pure Appl. Chem.*, 1989, **61**, 1569.

136 E. Kimura, *Pure Appl. Chem.*, 1989, **61**, 823.

137 D. Parker, J.R. Morphy, K. Jankowski and J. Cox, *Pure Appl. Chem.*, 1989, **61**, 1637.

138 R. W. Hay, M. P. Pujari, W. T. Moodie, S. Craig, D.T. Richens, A. Perotti and L. Ungaretti. *J. Chem. Soc., Dalton Trans.*, 1987, 2605.

139 D. Parker, *J. Chem. Soc., Chem. Commun.*, 1989, 127.

140 J.R. Morphy, D. Parker, R. Kataky, A. Harrison, M.A.W. Eaton, A. Millican, A. Phipps and C. Walker, *J. Chem. Soc., Chem. Commun.*, 1989, 792.

141 A.S. Craig, I.M. Helps, K.J. Jankowski, D. Parker, N.R.A. Beeley, B.A. Boyce, M.A.W. Eatom, A.T. Millican, K. Millar, A. Phipps, S.K. Rhind, A. Harrison and C. Walker, *J. Chem. Soc., Chem. Commun.*, 1989, 794.

142 D.A. Moore, P.E. Fanwick and M.J. Welch, *Inorg. Chem.*, 1990, **29**, 672.

143 P.L. Anelli, M. Grandi, F. Uggeri and P. Paoli, 7-123, XXVIII International Conference on Coordination Chemistry 1990.

144 R.B. Laufer, *Chem. Rev.*, 1987, **87**, 901.

145 J.F. Desreux and F.F. Barthelemy, *Nucl. Med. Biol.* 1988, **15**, 9.

146 P.S. Pallavicini, A. Perotti, A. Poggi, B. Seghi and L. Fabbrizzi, *J. Am. Chem. Soc.*, 1987, **109**, 5139.

147 R.W. Hay, M.P. Pujari, B. Korybut-Daszkiewicz, G. Ferguson and B.L. Ruhl, *J.Chem. Soc.,Dalton Trans.*, 1989, 85.

148 E. Kimura, S. Wada, M. Shionoya, T. Takahashi and Y. Litaka, *J. Chem. Soc., Chem. Commun.*, 1990, 397.

149 M. Ciampolini, L. Fabbrizzi, A. Perotti, A. Poggi, B. Seghi and F. Zanobini, *Inorg. Chem.*, 1987, **26**, 3527.

150 M. Ciampolini, M. Micheloni, N. Nardi, F. Vizza, A. Buttafava, L. Fabbrizzi and A. Perotti, *J. Chem. Soc., Chem. Commun.*, 1984, 998.

151 L. Fabbrizzi, L. Mortagne, A. Poggi, T.A. Kaden and L. Siegfried, *Inorg. Chem.*, 1986, **25**, 2671.

152 E.K. Barefield, K.A. Foster, G. Freeman and K.D. Hodges, *Inorg. Chem.*, 1986, **25**, 4663.

153 A. Mc Auley, S. Subramanian and T.W. Whitcombe, *J. Chem. Soc., Chem. Commun.*, 1987, 537.

154 A. Bencini, A. Bianchi, E. Garcia-Espana, M. Micheloni and P. Paoletti, *Inorg. Chem.*, 1988, **27**, 176.

155 S.C. Rawle, R. Yagbasan, K. Prout and S.R. Cooper, *J. Am. Chem. Soc.*, 1987, **109**, 6181.

156 A. Blake, A. Holder, T. Hyde, Y. Roberts, A. Lavery and M. Schroder, *J. Org. Chem.*, 1987, 261.

157 L. Casella, M. Gullotti, A. Pintar, F. Pinarolli, R. Vigano and P. Zanello, *J. Chem. Soc., Dalton Trans.*, 1989, 1161.

158 D. Parker, J.M. Lehn and J. Rimmer, *J.Chem. Soc.,Dalton Trans.*, 1985, 1517.

159 B.A. Boyce, A. Carroy, J.M. Lehn and D. Parker, *J. Chem. Soc., Chem. Commun.*, 1984, 1546.

160 C. Deitrich-Buchecker, J.P. Sauvage, *Tetrahedron*, 1990, **46**, 503.

161 C. Deitrich-Buchecker, J.P. Sauvage and J.M. Kern, *J.Am.Chem.Soc.*, 1989, **111**, 7791.

162 C. Deitrich-Buchecker, J. Guilhem, A.K. Khemiss, J.P. Kintzinger, C. Pascard and J.P. Sauvage, *Agnew. Chem. Int. Ed.*, 1987, **26**, 661.

163 L.F. Lindoy, 'The chemistry of Macrocyclic Ligand Complexes', Cambridge University Press, Cambridge, U.K. 1989.

164 L.F. Lindoy and D.S. Baldwin, *Pure Appl. Chem.*, 1989, **61**, 909.

165 L.F. Lindoy, *Pure Appl. Chem.*, 1989, **61**, 1575.

166 D.R. Boston and N.J. Rose, *J.Am.Chem.Soc.*, 1973, **95**, 4163.

167 G.A. Zakrzewski, C.A. Ghilardi and J. Lingafelter, *J.Am.Chem.Soc.*, 1971, 4411.

168 E. Larsen, G.N. LaMar, B.E. Wagner, J.E. Parks and R.H. Holm. *Inorg.Chem.*, 1972, **11**, 625.

169 S.C. Jackels, S.S. Duerdorf, N.J. Rose and J. Zekter, *J.Chem.Soc., Chem.Commun.*, 1972, 1291.

170 S.C. Jackels and N.J. Rose, *Inorg.Chem.*, 1973, **12**, 1232.

171 J.E. Parks, B.E. Wagner and R.H. Holm, *J. Am. Chem. Soc.*, 1970, **92**, 3500.

172 J.E. Parks, B.E. Wagner and R.H. Holm, *Inorg.Chem.*, 1971, **10**, 2472.

173 M.R. Churchill and A.H. Reis Jr., *Inorg.Chem.*, 1972, **11**, 1811.

174 M.R. Churchill and A.H. Reis Jr., *Inorg.Chem.*, 1973, **12**, 2280.

175 M.R. Churchill and A.H. Reis Jr., *Inorg.Chem.*, 1972, **11**, 2299.

176 M.R. Churchill and A.H. Reis Jr., *J.Chem.Soc., Chem.Commun.*, 1970, 879.

177 M.R. Churchill and A.H. Reis Jr., *J.Chem.Soc., Dalton Trans.*, 1973, 1570.

178 E. Larsen, G.N. La Mar, B.E. Wagner, J.E. Parks and R.H. Holm, *Inorg. Chem.*, 1972, **11**, 2652.

179 M.R. Churchill and A.H. Reis Jr., *J.Chem.Soc., Chem.Commun.*, 1971, 1307.

180 V.L. Goedken and S.M. Peng, *J.Chem.Soc., Chem.Commun.*, 1973, **62**.

181 I.I. Creaser, J.MacB. Harrowfield, A.J. Herlt, A.M. Sargeson, J. Springborg, R.J. Geue and M.R. Snow, *J.Am.Chem.Soc.*, 1977, **99**, 3181.

182 A.M. Sargeson, *Pure Appl. Chem.*, 1978, **50**, 905.

183 I.I. Creaser, R.J. Geue, J.MacB. Harrowfield, A.J. Herlt, A.M. Sargeson, M.R. Snow and J. Springborg, *J.Am.Chem.Soc.*, 1982, **104**, 6016.

184 R.V. Dubs, L.R. Gahan and A.M. Sargeson, *Inorg. Chem.*, 1983, **22**, 2523.

185 I.I. Creaser, A.M. Sargeson and A.W. Zanella, *Inorg.Chem.*, 1983, **22**, 4022.

186 J.MacB. Harrowfield, A.J. Herlt, P.A. Lay, A.M. Sargeson, A.M. Bond, W.A. Mulac and J.C. Sullivan, *J.Am.Chem.Soc.*, 1983, **105**, 5503.

187 H.A. Boucher, G.A. Lawrance, P.A. Lay, A.M. Sargeson, A.M. Bond, D.F. Sangster and J.C. Sullivan, *J.Am.Chem.Soc.*, 1983, **105**, 4652.

188 K.S. Hagen, P.A. Lay and A.M. Sargeson, *Inorg.Chem.*, 1988, **27**, 3424.

189 R.J. Geue, T.W. Hambley, J.MacB. Harrowfield, A.M. Sargeson and M.R. Snow, *J.Am.Chem.Soc.*, 1984, **106**, 5478.

190 A.M. Sargeson, *Pure Appl. Chem.*, 1984, 1603.

191 A. Hammershøi and A.M. Sargeson, *Inorg.Chem.*, 1983, **22**, 3554.

192 P.A. Lay and A.M. Sargeson, *Inorg.Chem.*, 1986, **25**, 4802.

193 D.J. Bull, I.I. Creaser, A.M. Sargeson, B.W. Skelton and A.H. White, *Inorg.Chem.*, 1987, **26**, 3040.

194 R.J. Geue, M.G. McCarthy and A.M. Sargeson, *J.Am.Chem.Soc.*, 1984, **106**, 8282.

195 A.J. Hendry, K.J. Naidoo and D.A.Thornton, *J.Chem.Soc. Chem.Commun.*, 1989, 998.

196 R.J. Geue, M.G. McCarthy, A.M. Sargeson, E. Horn and M.R. Snow, *J.Chem.Soc. Chem.Commun.*, 1986, 848.

197 R.J. Geue, M.G. McCarthy, A.M. Sargeson, B.W. Skelton and A.H. White, *Inorg.Chem.*, 1985, **24**, 1607.

198 G.J. Gainsford, R.J. Geue and A.M. Sargeson, *J. Chem.Soc., Chem.Commun.*, 1982, 233.

199 A. Hammershøi, G.A. Lawrance and A.M. Sargeson, *Aust.J.Chem.*, 1986, **39**, 2183.

200 L.R. Gahan, T.W. Hambley, A.M. Sargeson and M.R. Snow, Inorg.Chem., 1982, **21**, 2699.

201 L.R. Gahan, T.M. Donlevy and T.W. Hambley, Inorg.Chem., 1990, **29**, 1451.

202 L.R. Gahan, A.A. Achilleos, K.A. Nicolaidis and T.W. Hambley, *J.Chem.Soc. Chem.Commun.*, 1988, 912.

203 B Korybut-Daszkiewiez, R.M. Hartshorn and A.M. Sargeson, *J. Chem. Soc.,Chem. Commun.*, 1989, 1375.

204 M.P. Suh, W. Shin, K. Kim and S. Kim, *Inorg.Chem.*, 1984, **23**, 618.

205 R.J. Geue, T.W. Hambley, J.M. Harrowfield, A.M. Sargeson and M.R.Snow, *J.Am.Chem.Soc.*, 1984, **106**, 1.

206 P. Comba, L.M. Engelhardt, J.MacB. Harrowfield, G.A. Lawrance, L.L. Martin, A.M. Sargeson and A.H. White, *J.Chem.Soc. Chem.Commun.*, 1985, 174.

207 P. Bernhard and A.M. Sargeson, Inorg.Chem., 1987, **26**, 4122.

208 P. Comba, A.M. Sargeson, L.M. Engelhardt, J.MacB. Harrowfield, A.H. White, E. Horn and M.R. Snow, *Inorg. Chem.*, 1985, **24**, 2325.

209 V. Houlding, T. Geiger, U. Kolle and M. Gratzel, *J.Chem.Soc. Chem.Commun.*, 1982, 681.

210 A.M.Sargeson *Pure Appl. Chem.*, 1986, **58** 1511.

211 P. Bernhard and A.M. Sargeson, *J.Chem.Soc. Chem.Commun.*, 1985, 1516.

212 P. Bernhard, A.M. Sargeson and F.C. Anson, *Inorg. Chem.*, 1988, **27**, 2754.

213 P. Bernhard and A.M. Sargeson, *J.Am.Chem.Soc.*, 1989, **111**, 597.

214 L. DeCola, F. Barigelletti, V. Balzani, P. Belser, A. von Zelewsky, F. Vogtle, F. Ebmeyer and S. Grammenudi. *J.Am.Chem.Soc.*, 1988, 7210.

215 A. Bianchi, E. Garcia-Espana, M. Micheloni, N. Nardi and F.Vizza, *Inorg. Chem.*, 1986, 4379.

216 T.J. McMurray, S.J. Rodgers and K.N. Raymond, *J.Am.Chem.Soc.*, 1987, **109**, 3451.

217 T.J. McMurry, M.W. Hosseini, T.M. Garrett, F.E. Hahn, Z.E. Reyes and K.N. Raymond, *J.Am.Chem.Soc.*, 1987, **109**, 7196.

218 K.N. Raymond, M.E. Cass and S.L. Evans, *Pure Appl. Chem.*, 1987, **59**, 711.

219 P. Stutte, W. Kiggen and F. Vogtle, *Tetrahedron*, 1987, **43**, 2065.

220 W. Kiggen and F. Vogtle, *Angew.Chem.*, 1984, **23**, 714.

221 Y. Sun and A.E. Martell, *Tetrahedron*, 1990, **46**, 2725.

222 J.M. Lehn and F. Montavon, *Helv.Chim. Acta*, 1978, **61**, 67.

223 J.D.T. Backer Dirks, C.J. Gray, F.A. Hart, M.B. Hursthouse and B.C. Schoop, *J.Chem.Soc., Chem.Commun.*, 1979, 774.

224 W. Radecka-Paryzek, *Inorg. Chim. Acta*, 1980, **45**, L147.

225 L. DeCola, D.L. Smailes and L.M. Vallarino, *Inorg. Chem.*, 1986, **25**, 1729.

226 A.M. Arif, J.D.T. Backer Dirks, C.J. Gray, F.A. Hart and M.B. Hursthouse, *J. Chem. Soc. Dalton Trans.*, 1987, 1665.

227 R.W. Hay and N. Govan, *J.Chem.Soc.Chem.Commun.*, 1990, 714.

228 W. Radecka-Paryzek, *Inorg. Chim. Acta*, 1981, **52**, 261.

229 J.C.G. Bunzli and D. Wessner, *Coord.Chem.Rev.*, 1984, **60**, 191.

230 G. Bombieri, F. Benetollo, A. Polo, L. DeCola, D.L. Smailes and L.M. Vallarino, *Inorg. Chem.*, 1986, **25**, 1127.

231 F.A. Hart in 'Comprehensive Coordination Chemistry' ed. G. Wilkinson, R.D.Gillard and J.A. McCleverty, Pergamon Press, Oxford, 1987, Vol.3, p.1059.

232 K.K. Abid and D.E. Fenton, *Inorg Chim.Acta*, 1984, **95**, 119.

233 F. Benetolo, G. Bombieri, L. De Cola, A. Polo, D.L. Smailes and L.M. Vallarino, *Inorg. Chem.*, 1989, **28**,, 3447.

234 G. Bombeiri, *Inorg. Chim. Acta*, 1987, **139**, 21.

235 K.K. Abid and D.E. Fenton, *Inorg Chim.Acta*, 1984, **82**, 223.

236 P. Guerriero, U. Castellato, S. Tamburini, P.A. Vigato and R. Graziani, *Inorg.Chim.Acta*, 1987, **129**, 127.

237 P. Guerriero, P.A. Vigato, J.G. Bunzli and E. Moret, *J.Chem.Soc.Dalton Trans.*, 1990, 647.

238 D.E. Fenton, S.J. Kitchen, C.M. Spencer, S. Tamburini and P.A.Vigato, *J.Chem.Soc. Dalton Trans.*, 1988, 685.

239 O.A. Gansow, A.R. Kausar, K.M. Triplett, M.J. Weaver and E.L.Yee, *J.Am.Chem.Soc.*, 1977, 7087.

240 I. Marolleau, J.P. Gisselbrecht and M. Gross, *J.Chem.Soc.Dalton Trans.*, 1989, 367.

241 E.L. Yee, O.A. Gansow and M.J. Weaver, *J.Am. Chem. Soc.*, 1980, 2278.

242 E.L. Yee, J.T. Hupp and M.J. Weaver, *Inorg. Chem.*, 1983, **22**, 3468.

243 O.A. Gansow, A.R. Burke and G.N. LaMar, *J.Chem.Soc. Chem. Commun.*, 1972, 457.

244 F. Arnaud-Neu, E.L. Loufouilou and M.J. Schwing-Weill, *J.Chem.Soc. Dalton Trans.*, 1986, 2629.

245 M.C. Almasio, F. Arnaud-Neu and M.J. Schwing-Weill, *Helv. Chim. Acta*, 1983, **66**, 1296.

246 J.H. Burns and C.F. Baes, *Inorg.Chem.*, 1981, **20**, 616.

247 R. Pizer and R. Selzer, *Inorg.Chem.*, 1983, **22**, 1359.

248 G. Gillian, P. Barthelemy, F. Arnaud-Neu, E.L. Barthelemy, J. Massaux and J.F. Desreux, *J.Chem.Soc. Dalton Trans.*, 1986, 2629.

249 J. Tabib, J.T. Hupp and M.J. Weaver, *Inorg.Chem.*, 1986, **25**, 1916.

250 F.A. Hart, M.B. Hursthouse, K.M.A. Malik and S. Moorhouse, *J.Chem.Soc. Chem.Commun.*, 1978, 549.

251 M. Ciampolini, P. Dapporto and N. Nardi, *J.Chem.Soc. Dalton Trans.*, 1979.

252 J.H. Burns, *Inorg.Chem.*, 1979, 3044.

253 F. Benetollo, *Inorg. Chim. Acta*, 1985, **110**, 7.

254 K.N. Raymond and P.H. Smith, *Pure Appl. Chem.*, 1988, **60**, 1141.

255 J.C. Rodriguez-Ubis, B. Alpha, D. Plancherel and J.M. Lehn, *Helv.Chim.Acta*, 1984, **67**, 2264.

256 J.M. Lehn and J.B. Regnouf de Vains, *Tett.Lett.*, 1989, **30**, 2209-2212.

257 O. Juanes, J. de Mendoza and J.C. Rodriguez-Ubis, *J.Chem.Soc. Chem. Commun.*, 1985, 1765.

258 B. Alpha, E. Anklam, R Deschenaux, J.M. Lehn and M. Pietraszkiewicz, *Helv. Chim. Acta*, 1988, **71**, 1042.

259 J.M. Lehn, *Angew. Chem.*, 1988, **27**, 89.

260 B. Alpha, J.M. Lehn and G. Mathis, *Angew.Chem. Int.Ed.*, 1987, 266.

261 J.M. Lehn, M. Pietraszkiewicz and J. Karpiuk, *Helv.Chim.Acta*, 1990, **73**, 106.

262 R.J. Motekatis, A.E. Martell, I. Murase, J.M. Lehn and M.W. Hosseini, *Inorg. Chem.*, 1988, **27**, 3630.

263 J. Jazwinski, J.M. Lehn, R. Merc, J.P. Vigneron, M. Cesario, J.Guilhem and C. Pascard, *Tett.Lett.*, 1987, **28**,3489.

264 A. Bencini, A. Bianchi, E. Garcia-Espana, M. Giusti, S. Mangani, M.Micheloni, P. Orioli and P. Paoletti, *Inorg.Chem.*, 1987, **26**, 3902.

265 P.G. Potvin and J.M. Lehn in 'Synthesis of macrocycles: The design of Selective Complexing Agents,' Ed. R.M. Izatt and J.J. Christensen, John Wiley and Sons, New York 1987, p167.

266 J.M. Lehn, E. Sonveaux and A.K.Willard, *J.Am.Chem.Soc.*, 1978, 4914.

267 B. Dietrich, J. Guilhem, J.M. Lehn, C. Pascard and E. Sonveaux, *Helv. Chim.Acta*, 1984, **67**, 91.

268 M.W. Hosseini, J.P. Kintzinger, J.M. Lehn and A. Zahidi, *Helv.Chim.Acta*, 1989, **72**, 1078.

269 B. Deitrich, J.M. Lehn, J. Guilhem and C. Pascard, *Tetrahedron Lett.*, 1989, **30**, 4125.

270 B. Metz, J.M. Rosalky and R. Weiss, *J.Chem.Soc. Chem.Commun.*, 1976, 533.

271 U. Luning, R. Baumstark, M. Muller, C. Wangnick and F. Schillinger, *Chem. Ber.*, 1990, **1**, 221.

272 P. Hemmerich and C. Sigwart, *Experimenta*, 1963, 19, 448.

273 M. McCann, Private communication.

274 B.P. Murphy Ph.D. Thesis 1984 Open University.

275 D. Marrs Ph.D. Thesis 1990 Open University.

276 R.W. Hay, 'Bioinorganic chemistry' Ellis Harwood, Chichester 1984.

277 M.N. Hughes, 'The inorganic chemistry of biological processes' Second edition, John Wiley and Sons, 1981.

278 R. Malkin and B.G. Malstrom, *Adv. Enzm.*, 1970, **33**, 177.

279 E.I. Solomon, J.W. Hare and H.B. Gray, Proc.Natl.Acad. Sci. USA, 1970, **73**, 1389.

280 W.P.J. Gaykema, A. Volbeda and W.G. Hol, *J.Mol. Biol.*, 1985, **187**, 255.

281 A. Volbeda and W.G. Hol, *J.Mol. Biol.*, 1989, **209** 249.

282 J. Sanders-Loehr, T.B. Freedman and T.M. Loehr, *Biophys. Res. Commum.*, 1974, **56**, 510.

283 J.A. Tainer, E.D. Getzoff, K.M. Beem, J.S. Richardson and D.C. Richardson, *J.Mol.Biol.*, 1982, **160**, 181.

284 D.E. Wilcox, J.A. Long and E.I. Solomon, *J.Am.Chem.Soc.* 1984, **106**, 2186.

285 G.L. Woolery, L. Powers, M. Wrinkler, E.J. Solomon and T.G. Spiro, *J. Am. Chem. Soc.*, 1984, **106**, 86.

286 J.M. Brown, L. Powers, B. Kincaid, J.A. Larabee and T.G.J. Spiro, *J. Am. Chem. Soc.*, 1980, **102**, 4210.

287 D.J. Spira-Solomon and E.I. Solomon, *J.Am.Chem.Soc.* 1987, **109**, 6421.

288 C.A. Reed, M.G. Patch, H. Choi, D.R. Chapman, R. Bau and V. McKee, *Inorg. Chem.* 1990, **29**, 110.

289 D.J. Spira-Solomon, M.D. Allendorf and E.I. Solomon, *J. Am. Chem. Soc.*, 1986, **108**, 5318.

290 J.A. Fee, *Struct Bonding*, 1975, **23**, 1.

291 R. Huber, Angew. Chem. Int.Ed., 1989, **28**, 84.

292 J.M. Gussaud and H.C. Freeman, *J.Mol.Biol.*, 1983, **169**, 521.

293 E.I. Solomon in "Copper proteins", T.G. Spiro Ed. John Wiley and Sons 1981

294 E.R. Amudsen, J. Whelan and B. Bosnich, *J. Am. Chem. Soc.*, 1977, **99**, 6730.

295 C. Akers, S.W. Peterson and R.P. Willet, *Acta Cryst.*, 1968, **B24**, 1125.

296 G.A. Melson and D.H. Busch, *Proc. Chem. Soc.*, 1963, 223.

297 K. Vreise and G.V. Koten in 'Comprehensive Coordination Chemistry' ed. G. Wilkinson, R.D.Gillard and J.A. McCleverty, Pergamon Press, Oxford, 1987, Vol.2, p.189.

298 S.M. Nelson, F.S. Esho and M.G.B. Drew, *J.Chem.Soc., Chem Commun.*, 1981, 388.

299 L.M. Engelbert, B.M. Furphy, J.MacB. Harrowfield, J.M. Patrick, B.W. Skelton and A.H. White, *J.Chem.Soc., Dalton Trans.*,, 1989, 595.

300 F.A. Cotton, A. Davidson, W.H. Ilsey and H.S. Trop, *Inorg. Chem.*, 1979, **18**, 2719.

301 L.R. Groenveld, G. Vos, G.C. Vershar and J. Reedijk, *J.Chem.Soc., Chem Commun.*, 1982, 620.

302 M.G.B. Drew, F.S. Esho and S.M. Nelson, *Inorg. Chim. Acta*, 1983, 76, L269.

303 M.G.B. Drew, A. Lavery, F.S. Esho and S.M. Nelson, *J.Chem.Soc Dalton Trans.*, 1984, 545.

304 P. Harding, K. Hendrick, L.F. Lindoy, M. McPartlin and P.A. Tasker, *J.Chem.Soc., Chem Commun.*, 1983, 1300.

305 J.L. Burmeister, in 'Chemistry and Biochemistry of thiocyanic acid and its derivatives.' Ed. A.A. Newman, Academic press, 1975.

306 S. Raghunathan, C. Stevenson, C. Harding, D. McDowell, J. Nelson, M.G.B. Drew and P. Yates, *J.Chem.Soc., Dalton Trans.*, 1990,

307 J. Nelson, B.P. Murphy, M.G.B. Drew, P. Yates and S.M. Nelson, *J.Chem.Soc., Dalton Trans.*, 1988, 1001.

308 B.P. Murphy, J. Nelson, M.G.B. Drew, P. Yates and S.M. Nelson, *J.Chem.Soc., Dalton Trans.*, 1987, 123.

309 K.R. Adam, A.J. Leong, L.F. Lindoy, B.J. McCool, A. Ekstrom, L. Leipa, P.A. Harding, K. Hendrick, M. McPartlin and P.A. Tasker, *J.Chem.Soc., Dalton Trans.*, 1987, 123.

310 S. Raghunathan, C. Stevenson, J. Nelson and V. McKee, *J.Chem.Soc., Chem. Commun.*, 1989, 5.

311 G.A. van Albada, R.A.G. de Graff, G.A. Haasnoot and J. Reedijk, *Inorg. Chem.*, 1984, **23**, 1404.

312 R.A. Bailey, S.L. Kozak, T.W. Michelson and W.N. Mills, *Coord. Chem. Rev.*, 1971, **6**, 407.

313 F.A. Cotton, A. Davidson, W.H. Isley and H.S. Trop, *Inorg Chem.* 1979, **18**, 2719.

314 P.A. Lay, R.H. Magnuson and H.J. Taube, *J. Am. Chem. Soc.*, 1982, **104**, 7658.

315 C.A. Salata, M.T. Youinou and C. J. Burrows, *J. Am. Chem. Soc.*, 1989, **111**, 9278.

316 W. Stratton and D.H. Busch, *J. Am.Chem. Soc.*, 1960, **82** 4834.

317 R.A. Palmer and T.S. Piper, *Inorg. Chem.*, 1966, **5**, 864.

318 M.G.B. Drew, M. McCann and S.M. Nelson, *J. Chem. Soc Dalton Trans.*, 1981, 1868.

319 M.G.B. Drew, C. Cairns, S.G. McFall and S.M. Nelson, *J. Chem. Soc Dalton Trans.*, 1980, 2020.

320 K. Nakamoto, 'Infrared spectra of inorganic and coordination compounds' Second edition, 1970, Ed. J. Wiley N.Y.

321 P. Krumholz, *J.Am.Chem.Soc.*, 1953, **75**, 2163.

322 P. Krumholz, *Struct Bonding (Berlin)*, 1971, **9**, 139.

323 C. Stoufer and D.H. Busch, *J.Am.Chem.Soc.*, 1960, **82**, 3491.

324 W.R. McWhinnie and J.D. Miller, *Adv. Inorg.Chem.Radiochem.*, 1969, **12**, 135.

325 L.F. Lindoy and S.E. Livingstone, *Coord.Chem.Rev.*, 1967, **2**, 173.

326 W.W. Brandt, F.P. Dwyer and E.C. Gyarfas, *Chem. Rev.*, 1954, **54**, 959.

327 C. Mahon and W.L. Reynolds, *Inorg.Chem.*, 1967, **6**, 1927.

328 S. Herzog, R. Klausch and J. Lantos, *Z. Chem.*, 1964, **4**, 150.

329 P.E. Figgins and D.H. Busch, *J.Phys.Chem.*, 1961, **65**, 2236.

330 S.P. Sinha, *Spectrochim. Acta*, 1964, **20**, 879.

331 B. Martin, W.R. McWhinnie and G.M. Waind, *J.Inorg.Nucl.Chem.*, 1961, **23**, 207.

332 T. Ito and N. Tanaka, *J.Inorg.Nucl.Chem.*, 1970, **32**, 155.

333 E. Konig, *Z. Naturforsch*, 1964, **194**, 1139.

334 R. Pappalardo, *Inorg.Chim. Acta*, 1968, **2**, 209.

335 P. Krumholz, *Inorg. Chem.*, 1965, **4** , 612.

336 E. Konig, *Coord. Chem. Rev.*, 1968, **3**, 471.

337 D.H. Cook and D.E. Fenton, *J. Chem. Soc Dalton Trans.*, 1979, 266.

338 P.E. Figgins and D.H. Busch, *J. Am. Chem. Soc.*, 1960, **82**, 820.

339 S.M. Nelson, M. McCann, C. Stevenson and M.G.B. Drew, *J. Chem. Soc. Dalton Trans.*, 1979, 1477.

340 W.O. Gillum, R.A.D. Wentworth and R.F. Childers, *Inorg. Chem.* 1970, **9**, 1825.

341 P.C, Yates, M.G.B. Drew, J. Trocha-Grimshaw, K.P. McKillop, S.M. Nelson, P.T. Ndifon and C.A. Mc Auliffe, *J. Chem. Soc. Dalton Trans.*, in press, paper reference 1/00091/H/DAP.

342 W.E. Geiger, *Prog. Inorg. Chem.*, 1985, **33**, 275.

343 H. Yokoi and A.W. Addison, *Inorg. Chem.*, 1977, **16**, 1341.

344 E.W. Ainscough, A.M. Brodie, J.M. Husbands, G.J. Gainsford, E.J. Gabe and N.F. Curtis, *J. Chem. Soc Dalton Trans.*, 1985, 151.

345 B. Reilhammer and B.G. Malstrom, 'Blue Copper containing oxidases.'

346 J. Whelan and B. Bosnich, *Inorg. Chem.*, 1986, **25**, 3671.

347 T. Moeller,'The chemistry of the lanthanides.' Reinhold N.Y.

348 J.C. Bunzli in 'Handbook on the Physics and chemistry of the rare earths', eds. K.A. Gschneider and L. Eyring, Elsevier Science Publishers, Amsterdam, 1987.

349 S.E. Rasmussen and R. Gronbaek, *Acta Chem. Scand.* 1963, **17**, 832.

350 J.M. Lehn, E. Sonnveaux and A.K. Willard, *J. Am. Chem. Soc.*, 1978, 4916.

351 P.G. Owston, R. Peters, E. Ramsammy, P.A. Tasker and J. Trotter, *J. Chem. Soc., Chem. Commun.*, 1980, 1218.

352 D.E. Fenton in 'Biological and Inorganic Copper Chemistry' Volume 2, Ed. K.D. Karlin, J. Zubieta, Adenine Press N.Y. 1984 p191.

353 S.G. Zipp, A.P. Zipp and S.K. Madan, *Coord. Chem. Rev.*, 1974, **14**, 29.

354 R. Greef, R. Peat, L.M. Peter, D. Pletcher and J. Robinson, 'Instrumental Methods in Electrochemistry,' Ellis Horwood Ltd., Chichester, 1985.

355 J.J.Van Benschoten, J.Y. Lewis, W.R. Heineman, D.A. Roston and P.T. Kissinger, *J. Chem. Ed.*, 1983, **60**, 772.

356 D.H. Evans, K.M. O'Connell, R.A. Petersen and M.J. Kelly, *J. Chem. Ed.*, 1983, **60**, 290.

357 Z. Galus, H.Y. Lee and R.N. Adams, *J. Electroanalyst. Chem.*, 1963, **5**, 17.

358 P.T. Kisinger and W.R. Heineman, *J. Chem. Ed.*, 1983, **60**, 702.

359 G.A. Mabbott, *J. Chem. Ed.*, 1983, **60**, 697.

360 R. Parsons, *Pure and Appl. Chem.*, 1974, **37**, 499.

361 J.A. Page and G. Wilkinson, *J. Am. Chem. Soc.*, 1952. **74**, 6149.

362 J.G. Mason and M. Rosenblum, *J. Am. Chem. Soc.*, 1960, **82**, 4206.

363 G. Gritzner and J. Kuta, *Pure and Appl. Chem.*, 1982, **54**, 1527.

364 R.R. Gagne, C.A. Koval and G.C. Lisensky, *Inorg. Chem.*, 1980, **19**, 2854.

365 R. Nicolson, *Analyst. Chem.*, 1965, **37**, 1351.

366 R.S. Nicolson and I. Shain, *Analyst. Chem.*, 1964, **36**, 706.

367 D.H. Evans, *Acc. Chem. Res.*, 1977, **10**, 313.

368 D.H. Busch, *Acc. Chem. Res.*, 1978, **11**, 392.

369 A.M. Bond, G.A. Lawrance, P.A. Lay and A.M. Sargeson, *Inorg. Chem.*, 1983, **22**, 2010.

370 J.E. Wertz and J.R. Bolton, "Electron Spin Resonance", Chap.10, Chapman and Hall, London 1986.

371 T.D. Smith and J.R. Pilbrow, *Coord. Chem. Rev.*, 1974, **13**, 178.

372 R.R. Adams and J.B. Raynor, *Adv. Inorg. Radiochem.*, 1970, **13**, 135.

373 A. Longo and T. Buch, *Inorg. Chem.*, 1967, **6**, 556.

374 P.J.M. Birker, J. Hedler, G. Henkel, B. Krebs and J. Reedijk, *Inorg. Chem.*, 1982, **21**, 2637.

375 B.J. Hathaway and D.E. Billing, *Coord. Chem. Rev.*, 1970, **5**, 231.

376 D. Sutton, 'Electronic Spectra of Transition Metal Complexes, an introductory text.' McGraw-Hill London, 1986.

377 H. Beinhart, *Coord. Chem. Rev.*, 1980, **55**, 33.

378 A.E. Earnshaw, 'Introduction to magnetochemistry' London Academic press, 1968.

379 F.A. Cotton and G. Wilkinson, 'Advanced Inorganic Chemistry', J. Wiley and Sons. New York, fourth edition, 1980.

380 W.J. Geary, *Coord. Chem. Rev.*, 1983, **22**, 2010,